Developing and Utilising a Mouse Mammary Organoid Model

Mairian Thomas

Thesis presented to Cardiff University for the award of
Doctor of Philosophy (Ph.D)

2012 - 2016

Acknowledgements

I would first like to thank my PhD supervisor Prof Trevor Dale, for his continued guidance and support throughout this project in his lab, and also Dr Matt Smalley, for his valued scientific input throughout the years.

I am indebted to Dr Thierry Jardé and Dr Bethan Lloyd-Lewis, without whom this project would not have come about, whose support and advice (across the time zones!) has been invaluable. Thank you to the whole of the Dale lab (past and present!) for their help and advice, particularly to Anika Offergeld and Luned Badder, for being great friends, providing creative discussions and listening to my complaints when needed! My PhD experience wouldn't have been the same without the wonderful people in the 3rd Floor East contingent of Biosciences; constant sources of not only scientific know-how, but also much needed laughter and entertainment, home baking, crosswords and very occasionally, glitter catapults. A special thank you to my fellow TMNTs, Mark and Claris, for providing essential (and mostly hilarious) motivation throughout the writing process.

There are many people who have helped me technically; I am particularly grateful to Howard Kendrick, for offering his time and expertise to perform (and teach) mouse experiments, lentiviral work, and also for his commitment to enduring hours of monotonous cell sorting with me. Mark Bishop and Kirsty Richardson have also provided huge help with running FACS experiments over the years. I also acknowledge Eleanor Cawthorne and Sarah Stanley for their valued contributions to this thesis during their undergraduate lab projects, and Bleddyn Williams for help given during his MSc studies. Work performed in the latter part of this thesis would not have been possible without tumour material provided by Dr Jeff Rosen (Baylor College of Medicine, Houston) and novel compounds offered by Dirk Wienke of Merck Serono (Darmstadt, Germany), so I thank them both equally.

Finally, I dedicate this thesis to my parents. I couldn't have made it to this point without their constant support and unwavering belief in me. I'm especially thankful to them for letting me move back home to write this thesis, putting up with my stresses and supplying me with coffee, cake and chocolate to get me through it. To my Dad, the reason I chose to purse a career in science from the age of 9 (and again at 18, and 24!) thank you. To my Mum, thank you for everything; your bravery in your own experience of breast cancer in recent months has been more than inspiring.

Table of Contents

List of Figures

List of Tables

Abbreviations

Symbols

°C	Degrees Celsius
µg	Microgram
µm	Micrometer
µM	Micromolar

A

ABC	Avidin Biotin Complex
APC	Adenomatous Polyposis Coli
Axin	Axis Inhibitor

B

BMP	Bone Morphogenic Protein
BrdU	Bromodeoxyuridine (5-bromo-2'deoxyuridine)
BSA	Bovine Serum Albumin

C

c-Myc	Celular-Myelocytomatosis oncogene
CDK8	Cyclin Dependent Kinase 8
cDNA	Complementary Deoxyribonucleic Acid
CI	Combination Index
CRISPR	Clustered regularly interspaced short palindromic repeats
CSC	Cancer stem cell

D

DAB	3,3'-diaminobenzidine
ddH_2O	Double distilled water
dH_2O	Deionized water
Dkk1	Dickkopf-1
DMSO	Dimethyl sulfoxide
DMEM	Dulbecco's Modified Eagle Medium
DMEM/F12	Dulbecco's Modified Eagle Medium, nutrient mix F12
DNA	Deoxyribonucleic acid
DNase	Deoxyribonuclease
Dsh	Dishevelled

E

ECM	Extracellular matrix
EDTA	Ethylenediaminetetraacetic acid
EGF	Epidermal Growth Factor
EMT	Epithelial-mesenchymal transition
ER	Estrogen receptor
Erk	Extracellular regulated Map kinase
EtOH	Ethanol

F

FACS	Fluorescence Activated Cell Sorting
FBS	Fetal bovine serum
FGF	Fibroblast growth factor
Fzd	Frizzled

G

GFP	Green Fluorescent Protein
GSK-3	Glycogen Synthetase kinase 3

H

H&E	Haematoxylin and Eosin
H_2O_2	Hydrogen peroxide
HBSS	Hank's balanced salt solution
HGF	Hepatocyte Growth Factor
HRP	Horseradish peroxidase

I

IGF-1	Insulin-like-Growth-Factor 1
IF	Immunofluorescence
IHC	Immunohistochemistry

K

K5	Keratin 5
K8	Keratin 8
K14	Keratin 14
KCl	Potassium Chloride

L

L	Litre
L-15/FBS/PSG	Leibovitz's L-15 medium with 10% FBS, 1% Penicillin /Streptomycin/GlutaMAX
LEF	Lymphoid Enhancer-Binding Factor 1
Lgr5	Leucine-rich repeat-containing G-protein coupled receptor 5
LRP	Low density lipoprotein receptor-related protein

M	
M	Molar/Moles
mAb	Monoclonal antibody
MAPK	Mitogen activated Protein Kinase
MaSC	Mammary stem cell
MEC	Mammary epithelial cell
mg	Milligram
ml	millilitre
mM	millimolar

N	
NFκB	Nuclease Factor of kappa light polypeptide gene enhancer in B-cells
nM	Nanomolar
Nog	Noggin
Nrg	Neuregulin

O	
o/n	Over night

P	
pAb	Polyclonal antibody
PBS	Phosphate Buffered Saline
PCR	Polymerase Chain Reaction
PFA	Paraformaldehyde
PI3K	Phosphatidylinositol 3-kinase
PKA	Protein Kinase A
pM	Picomolar
PR	Progesterone receptor
PTEN	Phosphatase and Tensin Homolog deleted on Chromosome ten

R	
RNA	Ribonucleic acid
Rpm	Revolutions per minute
R-Spo1	R-spondin 1
RT	Room Temperature

S	
SMA	Smooth muscle actin
SoC	Standard of Care

T	
TA	Transit amplifying
TBS	Tris buffered saline
TBS/T	Tris buffered saline with 0.1% Tween-20
Tcf	T-cell specific transcription factor
TEB	Terminal End Bud
tetO	Tet Operon
TGF- β	Transforming Growth Factor-β

W	
w/v	Weight per Volume

X	
x g	Times gravity

Abstract

The mammary gland is a complex organ, relying upon multiple cell types and signalling pathways to orchestrate its predominantly postnatal development. To obtain a detailed understanding of such development, and also the mechanisms whose deregulation lead to mammary tumourigenesis, a physiologically relevant, quantifiable and qualitative model system is required. *In vitro*, currently available mammary culture systems have allowed studies into prospective stem cell populations, cell-cell interactions, differentiation, proliferation, paracrine networks and hormonal responses, but are limited in the degree to which they can truly recapitulate *in vivo* mammary biology. Three dimensional organoid culture systems from many tissues have recently been shown to concurrently allow sustained stem-cell maintenance, proliferation and functional differentiation; however, no such recapitulative *in vitro* model currently exists for the mammary gland.

This thesis therefore details the development of a novel murine mammary organoid culture system. Culture conditions described, including R-Spondin1 and Neuregulin1, enable the development and expansion of mammary epithelial organoids for up to 2.5 months in culture. Organoids possess distinct basal and luminal compartments - functional steroid receptors in the latter allowing hormonal responses - and regenerative cell populations enabling mammary gland reconstitution *in vivo*. Additional conditions are also described promoting the growth of abnormal, tumour-like organoids.

Utilisation of the organoid model allowed the study of key signalling pathways associated with mammary development; most notably revealing the critical importance of the Wnt signalling pathway in regulating normal development, its role in mammary tumourigenesis and demonstrating its potential as a target in anti-tumour therapy. Cell-cell signalling, individual cell populations and behaviours, and tumour organoid growth were studied, the latter offering a platform in which to study potential therapeutic compounds. Evidence provided furthers the understanding of mammary biology and supports that the organoid model comprises a suitable physiologically relevant tool for use in mammary research and drug discovery.

1 Introduction

1.1 Mammary gland biology

The mammary gland functions as a producer and secretor of milk, as a key nutrient source for offspring, and is highly specialised to do so. It is one of the only organs able to both undergo the majority of its development after birth and adapt during different stages of growth, highlighting its highly plastic nature.

1.1.1 Development of the mammary gland

During embryonic development, which in the mouse begins at embryonic day 10.5, early epithelial structures grow outward from each of the nipples, branching to become basic ductal trees that invade each of the five pairs of mammary fat pads by embryonic day 18.5 (Figure 1.1). Cell rich 'terminal end buds' (TEBs) form at the tips of these epithelial branches (Figure 1.2).

The mammary epithelium then remains quiescent until the next stage of development initiates at around post-natal day 21, whereby the primitive structures within the mammary fat pad begin to respond to hormonal cues as part of the onset of puberty (Figure 1.1). The TEBs, comprising precursors of the adult mammary epithelial cells - 'body' epithelial cells surrounded by an outer layer of 'cap' epithelial cells (Figure 1.2B) - at this point proliferate extensively, and the mammary gland undergoes its highest rate of ductal growth, invading further into the mammary fat pads to form secondary and tertiary branches that by approximately post-natal week 12 fill the fat pad entirely. Highly orchestrated signalling processes determine the extent to which branching is allowed to occur, with Transforming Growth Factor-β (TGF- β) acting as a key inhibitor (Nelson *et al.* 2006).

In virgin mice, the mammary epithelium changes in response to the estrus cycle, with both proliferation and apoptosis occurring. The final stage of development occurs during pregnancy. Hormonal changes during pregnancy induce ductal branch proliferation and finally vast alveolar differentiation, such that by the end of the pregnancy the majority of the gland is filled with secretory alveolar structures primed for milk production. Once offspring are weaned, milk production comes to an end, and the alveoli regress to their pre-pregnancy state by a carefully orchestrated programmed cell death program, known as involution (Richert *et al.* 2000; Dale 2011).

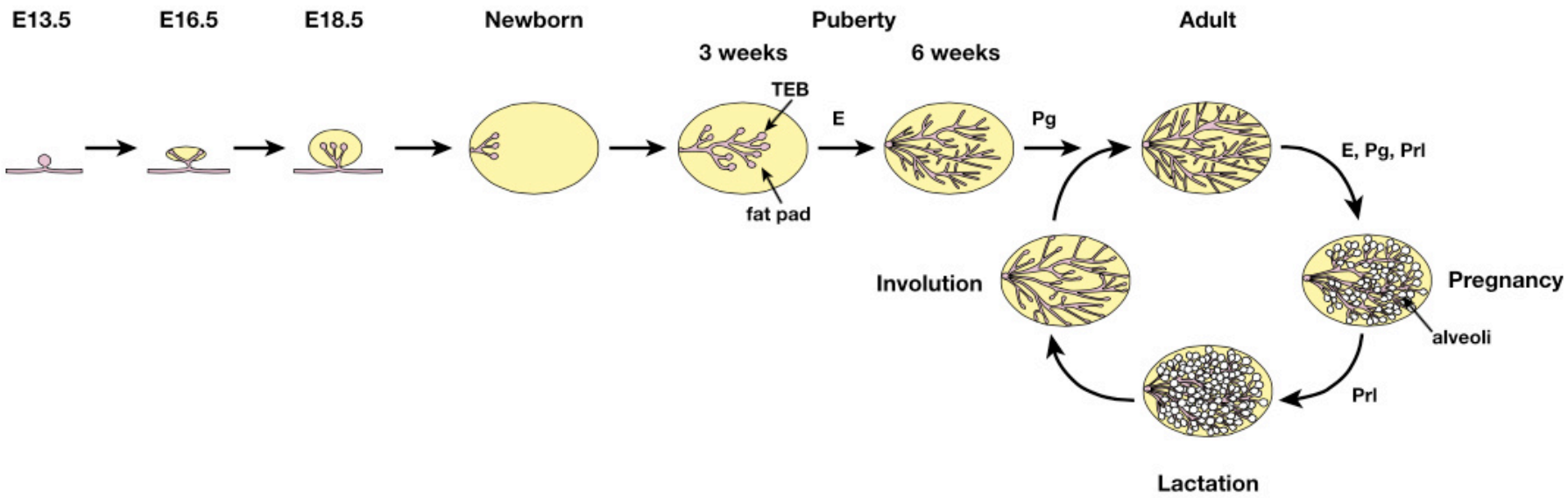

Figure 1.1 Phases of mammary gland development are carefully orchestrated, embryonically and postnatally.

Basic ductal structures grow during the first 18.5 days of embryonic development, with cell rich terminal end buds forming the bulk of the cells within the primordial gland. Postnatally, pubertal growth of the gland begins around day 21, with the TEBs proliferating profusely to form more intricate developed ductal branches. By 6-8 weeks, a fully adult mammary gland exists within each mammary fat pad, and is subject to cyclical changes in estrogen (E) and progesterone (P) during estrus. During pregnancy, E, P and prolactin (Prl) all perform key functions in inducing alveolar proliferation and differentiation to generate milk-producing cells. After weaning of pups, an involution process occurs and the gland cycles back it's pre-pregnancy state. These cyclical changes can occur multiple times. Image from (Visvader and Stingl 2014).

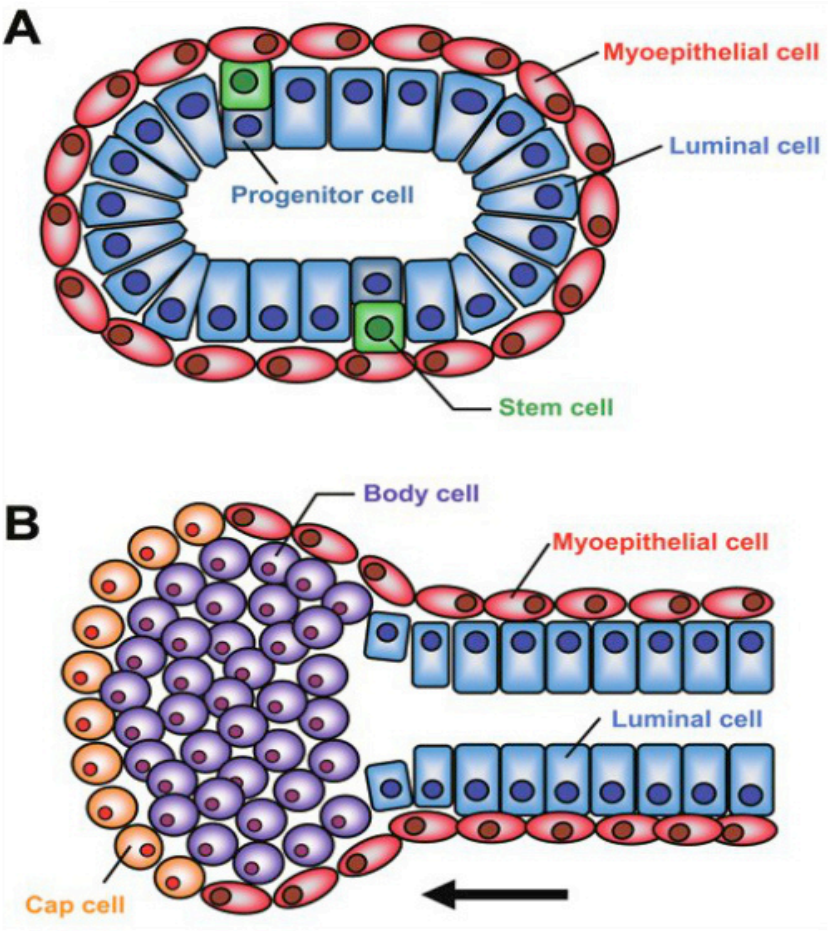

Figure 1.2 Mouse mammary epithelial cell populations and tissue architecture.

(A) Distinct basal and luminal cell layers exist within the mammary gland, such that basal, myoepithelial cells are located around the outer edges of ducts, while luminal estrogen receptor negative or positive cells line ducts and face into the lumen. **(B)** During mammary gland development, terminal end buds become sites of vast proliferation, and elongation and branching of ducts is performed through these structures. Reprinted by permission from Macmillan Publishers Ltd: [Cell Research] (Tiede and Kang, 2011), copyright (2011).

1.1.2 Cellular anatomy of the mammary gland epithelium

At a cellular level, broadly speaking the normal mammary gland epithelium consists of two main cell layers (Figure 1.2A). Firstly, an inner, luminal cell population comprising the bulk volume of the ductal and lobular structures seen in the gland. These can be identified through their expression of several keratin subtypes (8, 11, 18), and further subdivided based on expression of the progesterone and estrogen receptor-α steroid hormone receptors. Luminal cells are responsible for the synthesis and release of milk into the alveolar lumen. A basal cell population can be found in contact with the basement membrane and surrounding the luminal cell layer. This contains both contractile myoepithelial cells, responsible for physically promoting milk secretion in response to oxytocin stimulation, and the widely reported and debated 'stem/progenitor' population (Sleeman *et al.* 2007). The basal layer is phenotypically characterised by expression of keratins 5 and 14, in addition to smooth-muscle actin and the p53 transcription factor family member p63.

1.1.3 Signalling pathways implicated in mammary gland development and homeostasis

The many developmental stages detailed above are carefully orchestrated by the signalling of a combination of systemic hormones and local endogenous growth factors, overviews of which are given here.

1.1.3.1 Hormonal regulation

Female reproductive hormones including estrogen, progesterone and prolactin control the majority of postnatal mammary gland development. The levels of the ovarian hormones vary throughout the estrus cycle and pregnancy, the mammary gland responding accordingly, owing to the downstream signalling of several growth factor pathways.

1.1.3.1.1 Estrogen

Estrogens act through signalling at Estrogen receptor alpha or beta (ERα/ERβ), intracellular transcription factors able to regulate hormone responsive genes. Deletion of ERβ abates terminal differentiation, but has little other developmental effect (Förster *et al.* 2002), while ERα is shown to be more important for the production of the simple ductal structures early on in development, as well as side branching and alveologenesis

(Bocchinfuso and Korach 1997; Mallepell *et al.* 2006). Paracrine signalling to steroid receptor negative stromal cells via Amphiregulin is thought to be responsible for the proliferative effects of estrogen (Ciarloni *et al.* 2007) (Figure 1.3).

1.1.3.1.2 Progesterone

Progesterone regulates the formation of side branches, and has been shown to activate mammary stem cell proliferation, through a paracrine mechanism involving the luminal hormone receptor positive cell population, and their release of the intermediate effectors Wnt4 and Receptor activator or nuclear factor kappa-B ligand (RANKL) (Brisken, *et al.,* 2000; Joshi, *et al.,* 2015) (Figure 1.3). Progesterone receptor (PR) is detected within the gland later than ER (usually at 7 weeks) (Bocchinfuso and Korach 1997), with PR-B demonstrated as essential for mammary gland development such that loss of the receptor halts development at the simple ductal stage (Brisken *et al.* 1998; Mulac-Jericevic *et al.* 2000).

1.1.3.1.3 Prolactin

Prolactin signalling provides a stimulus for alveogenesis and the differentiation of the milk producing cells within the mammary gland, with deletion of the Prolactin receptor causing total absence of lobuloalveolar development (Brisken *et al.* 1999).

1.1.3.2 Growth factor signalling pathways

1.1.3.2.1 Wnt signalling pathway

The Wnt gene was discovered in mice as int-1, a gene which was commonly found to hold an insertion site for the Mouse Mammary Tumour Virus (MMTV) and as such was highly overexpressed, leading to mammary tumour formation (Nusse and Varmus 1982), and later identified to be identical to a gene known as Wingless, found to exist in Drosophila as a segment polarity gene (Rijsewijk *et al.* 1987). Canonical Wnt signalling via the Wnt family of small, lipid modified glycoproteins plays a pivotal role in multiple tissues, commonly associated with the control of stem cell proliferation and maintenance throughout embryogenesis and postnatal development and tissue homeostasis (Holland *et al.* 2013). Regulation of such processes occurs at the gene level, through the Wnt-dependent control of the transcriptional co-activator β-catenin, also known for its participation in junctional complexes.

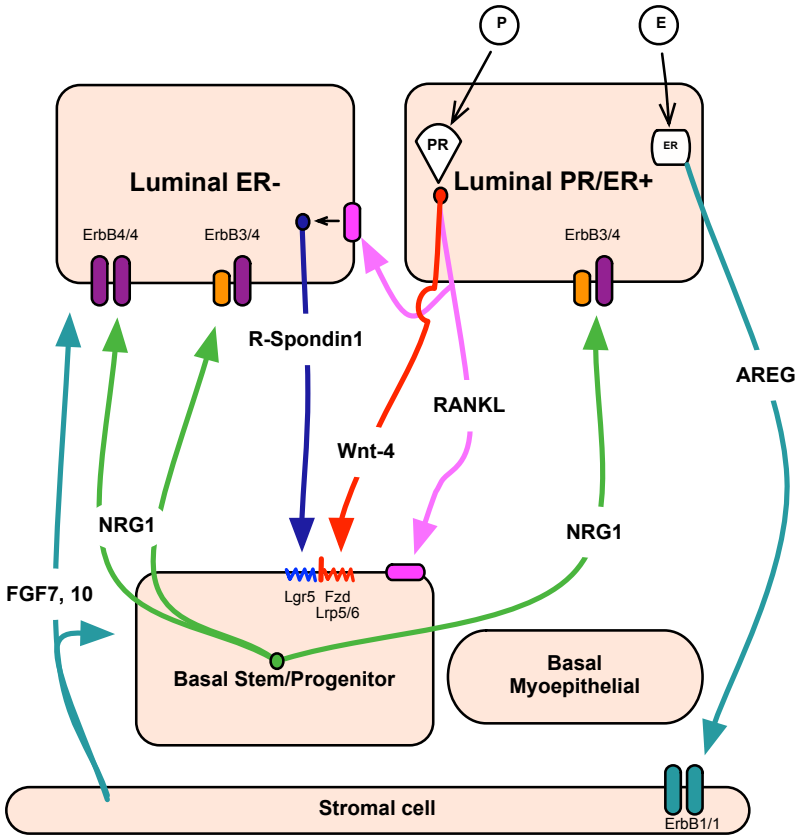

Figure 1.3 Hormonal signalling pathways in mammary gland development and regulation.
Steroid hormone action activated in hormone receptor positive luminal epithelial cells occurs through intricate paracrine signalling networks. Estrogen stimulation of the luminal ER+ cell population caused the release of amphiregulin (AREG), which in turn activates growth factor (FGF family) release from stromal cells. These factors are thought to upregulate proliferation of multiple mammary epithelial cell types. Progesterone signalling to PR+ luminal cells induces expression of Wnt4 and RANKL; RANKL induces R-Spondin1 release from luminal ER- cells, which co-operates with Wnt4 and RANKL to induce expansion of the basal stem/progenitor population. Activation of the p63+ basal subset induces Nrg1 release, which feeds back to luminal populations and induces their lobulo-alveolar like differentiation.

In the absence of an extracellular Wnt ligand, the canonical pathway is in an 'off-state' (Figure 1.4BA). A β-catenin destruction complex exists within cells, consisting of proteins including the main scaffold protein Axin, Adenomatous polyposis coli (APC) and the serine/threonine kinases CK1 and Glycogen Synthase Kinase-3 (GSK-3), serving to regulate levels of β-catenin, with Ser/Thr phosphorylation and ubiquitination targeting the protein for proteolysis.

However, Wnt ligand binding in a trimeric complex with the extracellular cysteine rich domain of its receptor (a member of the Frizzled (Fzd) family of seven-transmembrane receptors) and a co-receptor (lipoprotein receptor related protein 5/6 (LRP5/6) switches the canonical pathway to an 'on-state' and enables the release of the intracellularly bound scaffolding protein Dishevelled (Dvl) (Figure 1.4). This protein can,

in turn, recruit the Axin component of the destruction complex, preventing the targeting of β-catenin for degradation. This enables the accumulation of β-catenin in the nucleus of Wnt-responsive cells, displacement of transcriptional repressor Groucho, and the co-activation of T-cell specific transcription factor or Lymphoid enhancer-binding Factor-1 (TCF/Lef1) dependent transcription of Wnt target genes, with the aid of the Mediator complex (MacDonald *et al.* 2009; Kim *et al.* 2006). Such genes include, but are not limited to; cyclin D1, axin2 and the mitogenic c-myc, and are commonly associated with cell survival and proliferation. Wnt signalling can be further potentiated by a secreted protein family, the R-Spondins, which bind Lgr5 receptors situated within the heterodimeric Fzd/LRP receptor complexes themselves, with high affinity, to enhance the Wnt ligand signal (de Lau *et al.* 2011). R-Spondins are reported to elicit their Wnt enhancing effect via inhibition of the E3 ubiquitin ligase ZNRF3, inhibiting the removal of Fzd and Lrp receptors from the cell surface (Hao *et al.* 2012).

Given the importance of the pathway in development, it is unsurprising that it can be tightly regulated at various stages. In the first instance, Wnt ligand secretion can be controlled by the need for its post-translational palmitoylation in the endoplasmic reticulum by the membrane bound O-acyltransferase (MBOAT) enzyme Porcupine (Porcn)(Rios-Esteves et al., 2014)(Figure 1.5A).

Extracellularly, negative Wnt pathway regulators exist naturally, including Dickkopf 1 (Dkk), which binds LRP6 with high affinity, preventing receptor complex formation (Yonghe Li *et al.* 2010). Another inhibitor of Wnt signalling is the secreted Frizzled-related protein 1 (sFRP1), a protein with a homologous cysteine rich domain to that found in the Fzd receptor, such that free Wnt ligand can be sequestered from binding and signalling, and its family member Wnt inhibitory factor-1 (WIF-1)(Gauger *et al.* 2012).

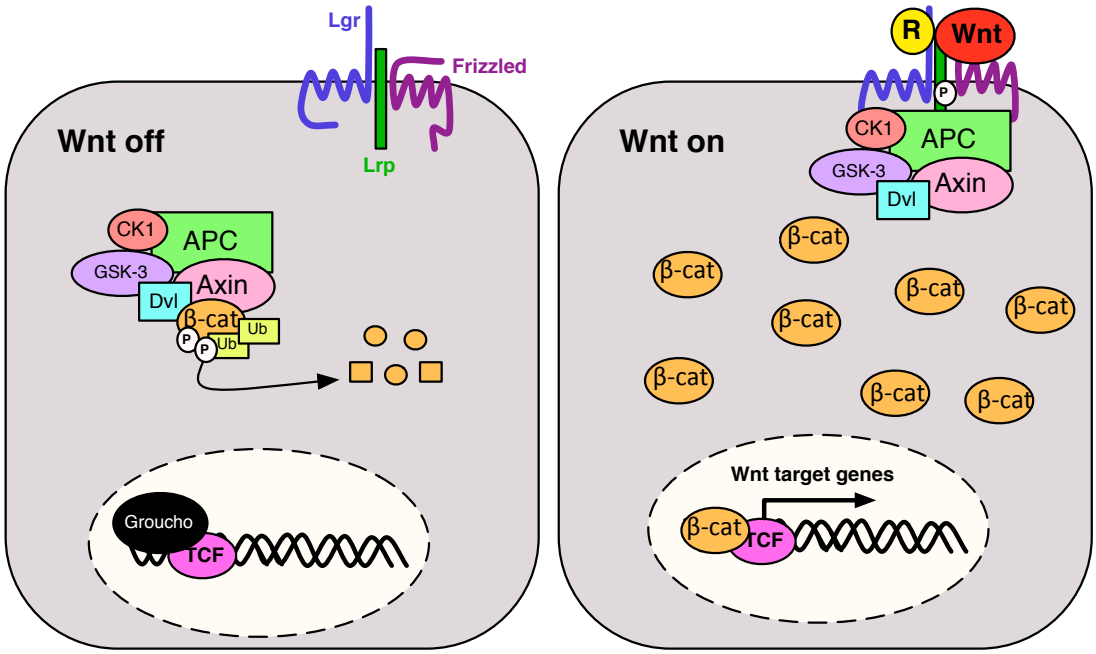

Figure 1.4 The canonical Wnt pathway.

(A) In the absence of Wnt ligand, a multi-protein 'destruction' complex composed of the tumour suppressor proteins Axin and APC, glycogen synthase kinase 3 and casein kinase-1, targets β-catenin for degradation by ubiquitination. **(B)** Wnt ligand binding to Frizzled recruits low density lipoprotein receptor-related proteins 5/6, and intracellular recruitment of Axin to the receptor-ligand complex occurs. This renders the destruction complex unable to target β-catenin for degradation, leaving the protein free to induce TCF dependent Wnt target gene expression. R-Spondins are able to promote Wnt activity, via binding to the Lgr receptors as part of the Wnt-receptor complex**.**

Intracellularly, relative Axin levels and stability of the protein can be up or down-regulated, as required, thus down or upregulating Wnt signalling, respectively. In terms of pathway downregulation, a feedback loop exists in physiologically normal cells whereby increased β-catenin dependent gene transcription by the TCF complex leads to an upregulation of AXIN2 gene transcription, causing a subsequent rise in the level of Axin protein available for destruction complex assembly. Conversely, a family of poly-ADP-ribosylase enzymes, consisting of Tankyrases 1 and 2 (Huang *et al.* 2009) exist to promote the ubiquitination and degradation of Axin, through it's PARsylation and subsequent interaction with the RING ubiquitin E3 ligase RNF146, allowing increased B-catenin accumulation and Wnt responsive gene expression. Under normal physiology, this activity is limited by RNF146 tagging itself and the Tankyrases themselves for proteasome-mediated degradation (Figure 1.5B).

Wnt signalling has been widely implicated in the development and regulation of the mammary gland. Lef1, a transcription factor downstream of the Wnt pathway, is essential for development of mammary limb buds during embryogenesis (van Genderen *et al.* 1994), when Wnt10b is also reportedly expressed (Veltmaat *et al.* 2004). Post-natally, while Wnt-1 has been shown under the control of the MMTV to increase terminal end bud branching, the mammary gland does not express this ligand endogenously (Tsukamoto *et al.* 1988). However, Wnt-2, Wnt-4, Wnt 5a, Wnt5b, Wnt6 and Wnt7b are all expressed at various levels during TEB development, implicating the pathway strongly in this process. In pregnancy, studies by Brisken et al. (2004) have shown hormone induced increases in Wnt4 expression, as part of a paracrine signalling pathway between distinct cell populations to induce lobular development prior to lactation. In addition, LRP5 knockout in a mouse model resulted in branching abnormalities, with reduced numbers of TEBs (Lindvall *et al.* 2006).

Wnt responsive, Lgr5 positive cells located in the basal cell compartment of the mammary gland, have been reported to be the stem population within the gland responsible for the vast regeneration, growth and adaptation of the gland. They transplant highly successfully in mammary gland regeneration assays, while in contrast, cells null for the Lgr5 receptor have demonstrated little stem cell activity in such assays (Shackleton *et al.* 2006; Ashworth and Smalley 2006; Stingl *et al.* 2006). Mammary stem cells will be discussed further in section 1.1.4.

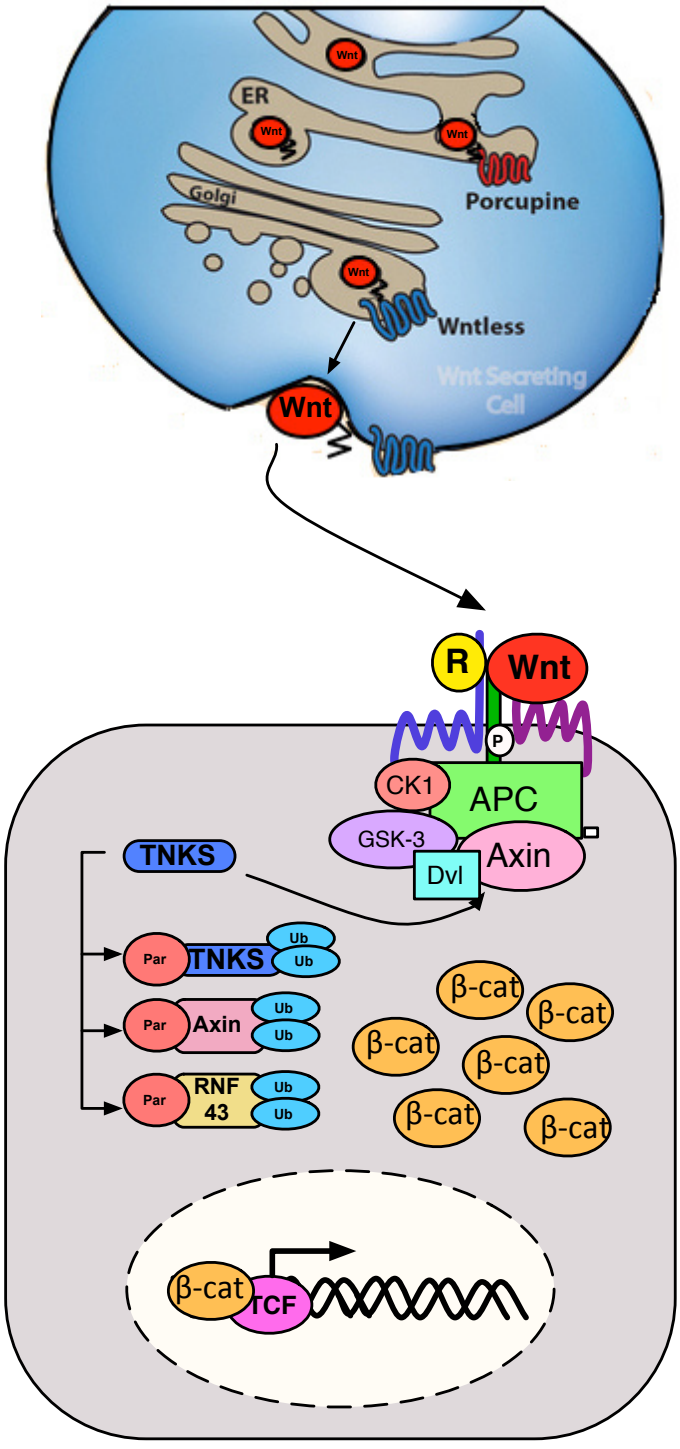

Figure 1.5 Regulation of the Wnt pathway occurs at multiple levels.

Wnt release from Wnt secreting cells is regulated by palmitoylation in the endoplasmic reticulum. The membrane bound O-acyltransferase enzyme Porcupine post translationally modifies Wnt protein for release. Intracellularly, tankyrases (TNKS) are responsible for the ubiquitination of Axin through interaction with RNF43, leading to a β-catenin accumulation and overall increase in Wnt pathway activity.

Adapted by permission from Macmillan Publishers Ltd: Bone Research, (Maupin *et al.* 2013), copyright (2013).

1.1.3.2.2 Receptor tyrosine kinase ligands

The extensive family of receptor tyrosine kinases is comprised of several subgroups, each with similar structural properties and signalling mechanisms. Each receptor possesses an extracellular domain, available for specific ligand binding, and an intracellular, tyrosine kinase-containing signalling domain, connected by a single transmembrane domain. Binding of ligand extracellularly initiates the tyrosine kinase domain activity and phosphorylation of designated signalling molecules intracellularly, usually as the first of many steps in a kinase signalling cascade resulting in transcriptional changes within the cell.

1.1.3.2.2.1 Fibroblast growth factor (FGF) family

The extensive fibroblast growth factor (FGF) family consists of a range of signalling molecules designed to transduce mitogenic signals via receptor tyrosine kinases. In addition to their commonly known role in inducing fibroblast proliferation, several FGF ligands are found in multiple stages of mammary gland development. The FGF receptor FGFR2-IIIb, is known to be essential for embryonic development of the tissue (De Moerlooze *et al.* 2000), regulated by expression of FGF10 from the mesenchyme (Howard and Lu 2014). Postnatally, this receptor is found highly expressed in the terminal end buds of developing mammary glands, and is crucial for the proliferation of the luminal epithelium (Parsa *et al.* 2008). The ligands FGF7, and FGF10 are known to be expressed during this stage of development (Spencer-Dene *et al.* 2001; Parsa *et al.* 2008; Hynes and Watson 2010). Overexpression of FGFR2, or FGF10, is associated with breast cancer development, indicating a key role of the pathway in regulating mammary development and proliferation (Theodorou *et al.* 2004; Meyer *et al.* 2008). Pond et al. (2013) have also recently successfully demonstrated the role of FGF signalling in mammary stem cell maintenance and normal development, using conditional FGFR1 and FGFR2 mutants.

1.1.3.2.2.2 Epidermal growth factor (EGF) family

The EGF family signal through the ErbB family of receptor tyrosine kinases, of which there are four specific subtypes (ErbB1/EGFR, ErbB2/HER2, ErbB3 or ErbB4). Particular members can homo- or hetero-dimerise with varying ligand specificity, to activate downstream pathways including the Mitogen activated protein kinase (MAPK) and phosphatidyl inositol 3 kinase (PI3K) cascades (Prenzel *et al.,* 2001).

EGF

Epidermal growth factor binds the Epidermal Growth Factor receptor (EGFR) or ErbB1/HER1, and has been used extensively in studies of mammary gland growth in both 2 and 3-dimensional *in vitro* assays. However, it is not widely understood to be the key EGFR ligand for mammary gland development *in vivo*. While exogenous addition of the ligand to the growth halted mammary glands of ovariectomised mice reinstated ductal branching morphogenesis in previous studies (Coleman *et al.* 1988), deletion of EGF ligand actually proved to have limited effect on postnatal mammary gland development, suggesting that other EGFR ligands actually play a more prominent role in the process (Luetteke *et al.* 1999).

Neuregulin

Embryonically, Neuregulin 3 (NRG3), which binds ErbB4, is expressed in the lateral plate mesoderm, directly before the mammary buds develop, regulating the grouping of epithelial cells for placode formation. Reduced levels of NRG3 activity as assessed by mutant mouse lines demonstrates failure or reduced ability to form placode number 3 (the first of the 5 to form), while ectopic expression of the ligand in the basal layer leads to a larger than normal number of glands forming (Howard *et al.* 2005; Panchal *et al.* 2007). Other family members, NRG1, 2 and 4 are also expressed during embryonic stages and although this has not been fully evaluated, it could be that they too have roles in early mammary development (Wansbury *et al.* 2008).

Postnatally, Nrg1 is important in the mammary gland, recently having been shown to be a basally-expressed factor required for luminal progenitor maturation, in a paracrine fashion (Forster *et al.* 2014) (Figure 1.3). This correlates with recent data from the Dale lab describing Nrg1 and its receptors ErbB3 and ErbB4 to be expressed reciprocally, such that Nrg1 is predominantly expressed in basal cells over luminal, while the receptors are expressed most highly in the luminal ER- cell population (Jardé *et al*. 2016).

Amphiregulin (AREG)

During puberty, AREG is the most prevalent RTK ligand, released in response to hormonal cues (namely estrogen) and binding specifically to EGFR/ErbB1 to induce vast expansion of epithelial cells, with a key role particularly in ductal elongation. This elongation is significantly reduced in AREG deficient mice, along with a reduction in TEB

formation. It is however thought that AREG induced epithelial expansion occurs as an indirect effect, such that AREG induces release of mitogenic factors from the stroma (Ciarloni *et al.* 2007)(Figure 1.3).

1.1.3.2.2.3 Hepatocyte growth factor (HGF)

HGF, first discovered as a mitogenic factor for hepatocytes, has multiple functions, including stimulation of cell growth, morphogenesis and motility, on a broad number of epithelial cell types. Due to its role in cell migration, it has also historically been termed scatter factor, and is known to bind the RTK c-Met.

In the mammary gland, HGF was originally termed mammary growth factor, and was found to be produced by the surrounding stromal fibroblasts of the gland, acting on mammary epithelial cells in paracrine fashion (Sasaki *et al.* 1994). In very early studies, human breast cells embedded in collagen gel produced structures which displayed extensive branching upon treatment with HGF, highlighting a role for the factor in mammary morphogenesis, while in 2-dimensional studies, human mammary epithelial cells demonstrate increased motility and proliferation in response to HGF treatment (Niranjan *et al.* 1995).

Overexpression of HGF or its receptor have, in *in vivo* mouse studies, proved tumourigenic postnatally, suggesting the signalling pathway to be highly important for the homeostasis of the already established gland (Kamalati *et al.* 1999), while developmental studies indicate a role for the growth factor in the proliferation of terminal end buds (Yant *et al.* 1998).

More recently, a study by Di-Cicco et al (2015) demonstrated expression of the ligand from both stromal and basal cells, with c-Met receptor expression in both luminal and basal cell populations themselves. This study highlighted particular effects of continued HGF treatment on luminal cells, such that they appear the main effectors of the paracrine signal, increasing their proliferation in response to ligand stimulation. In addition, luminal cells under HGF stimulation have been shown to acquire basal-like properties, with increased stem cell potential and reduced luminal gene expression.

1.1.4 Mammary stem cells

The constant remodelling and obvious regenerative capacity of the mammary gland has led to an extensive, on-going search for a definitive stem-cell population, which many believe to be the target of malignant transformations leading to cancer. However, current methods for the study of mammary gland development have not yet allowed the conclusive identity of a multipotent mammary stem cell (MaSC) population within the adult mammary gland.

In vivo, transplantation of either gland fragments or mammary epithelial cells (MECs) into the cleared fat pads of mice – currently the 'gold standard' mammary stem cell assay – and consequent full gland regeneration, has repeatedly demonstrated the existence of a stem population (DEOME *et al.* 1959; Kordon and Smith 1998; Shackleton *et al.* 2006; Stingl *et al.* 2006). Transplantation of single cell populations possessing surface markers indicative of a broad basal phenotype ($Lin^{-}CD29^{hi}CD24^{+}$, or $CD24^{med}CD49f^{hi}$) assessed this subtype to contain the key multipotent MaSCs present in adult mammary glands (Shackleton *et al.* 2006; Ashworth and Smalley 2006; Stingl *et al.* 2006). A quiescent stem population within this basal subset has been prospectively identified, expressing the cell surface glycoprotein CD1d, and conferring a 5.5 fold increase in mammary repopulating ability (Santos *et al.* 2013). Moreover, similar purification of basal cells indicates a distinct Wnt-responsiveness of MaSC populations; sorting cells based on the novel Wnt target gene protein C receptor (ProcR) further enhances both repopulating frequencies (1 in 12 Procr+ cells compared to 1 in 69 total basal cells), and colony formation (1 in 3 Procr+ compared to 1 in 15 total basal cells) (Wang *et al.* 2014), while Lgr5 positivity also confers increased regenerative ability (1 in 4.2 Lgr5+ cells compared to 1 in 90 total basal cells)(Plaks *et al.* 2013). Transplantation experiments however have been questioned in terms of their true reflection of *in vivo* stem cell potential; results can be altered by the presence or absence of extracellular matrix substitutes (Spike *et al.* 2012), while the non-physiological conditions of a cleared mammary fat pad, in which wound healing or stress signals are likely prominent, have been suggested to reveal unusual potentials of cells that would otherwise not exist in a normal, functional glands, leading to the use of *in vivo* models for stem cell studies in an appropriate context.

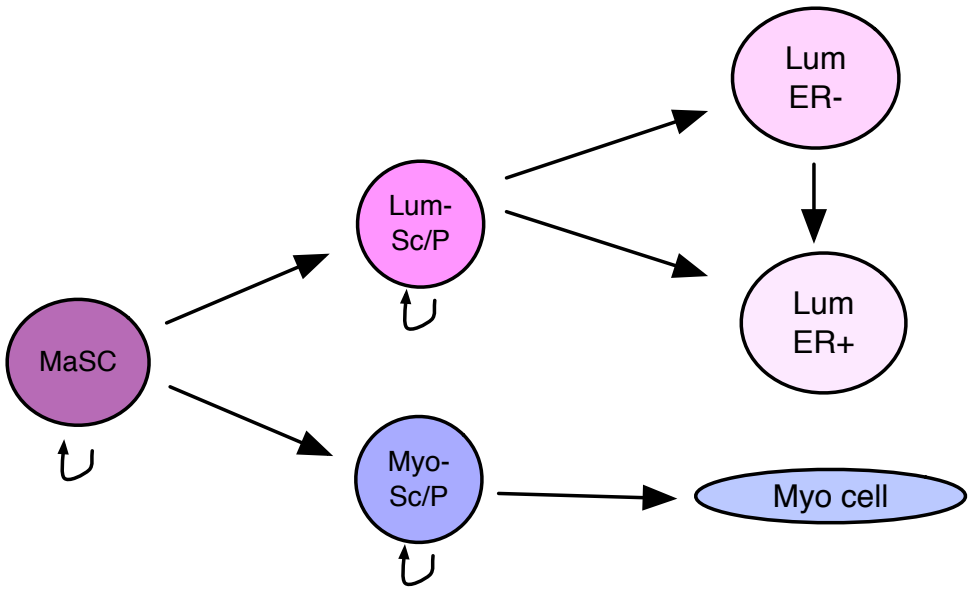

Figure 1.6 Summary hierarchy model based on currently published evidence
A consensus hierarchy model in which an initial basal MaSC population forms either luminally (Lum) or myopithelially restricted stem cells (Sc), or progenitors (P), which each serve to repopulate their individual lineage, is shown, based on findings from various in vivo lineage tracing studies.

Conflicting evidence for hierarchies of stem and progenitors cells (Figure 1.5) from *in vivo* lineage tracing studies has further complicated our understanding of such populations (Smith 1996; Van Keymeulen *et al.* 2011). Van Keymeulen *et al.* (2011) indicated that normal adult mammary gland development relies purely on unipotent luminal and myoepithelial stem cells derived from a common MaSC during embryonic development. Indeed, several studies agree with the presence of unipotent adult stem cells that self-sustain their individual lineage (Tao *et al.* 2014; Wuidart *et al.* 2016). van Amerongen et al. (2012), also similarly indicated the presence of Wnt responsive unipotent stem cells within the mammary gland during puberty, but also further demonstrated a bipotent stem cell reserved for proliferation associated with pregnancy. Interestingly, this work also identified that Axin2+ (and therefore Wnt responsive) cells to vary in their differentiation potential depending on developmental stage; in the mammary placode at embryonic days 12.5 to 17.5 becoming luminal lineages and in the prepubescent gland forming basal populations. Evidence from the Visvader lab (Rios *et al.* 2014) provides strong evidence for the existence of bipotent MaSCs, and long lived progenitor cells. Such discrepancies in evidence from different experimental models demonstrate the sensitivity of cells to their environment, and the critical need for a system in which to study such cellular dynamics.

1.2 Breast cancer

Breast cancer is the most common cancer in the UK, affecting around more than 50,000 women a year, with approximately 12,000 women dying each year as a result of the disease (Breast Cancer Now, 2016). Breast cancer on the whole is highly heterogeneous - it can be ductal or lobular in nature, histologically, while at the clinical level it is often classed dependent on expression levels of estrogen, progesterone and HER2/ErbB2 receptors: Luminal A estrogen receptor positive; Luminal B ER and HER2 positive; Claudin low, receptor negative tumours; HER2 overexpressing tumours with mainly luminal features; basal-like tumours, triple negative for ER, PR and HER2; and finally the normal-like subtype (Perou *et al.* 2000; Sørlie *et al.* 2001). At the molecular level, the disease has most recently been divided into at least 10 different subgroups, based on integrated clustering of copy number alterations and gene expression data from over 2000 breast cancer samples (Curtis *et al.* 2012).

Each diverse breast cancer subtype has uniquely associated properties and contributing factors, some of which provide targeted treatment options for the successful ablation of tumours. ER positive tumours, for example, are by far the lowest risk breast cancer subtype, given their critical hormone dependence and susceptibility to anti-estrogen (Tamoxifen) or aromatase inhibitor (Letrozole) treatment; the former significantly reducing tumour recurrence and mortality rates over 15 years, when used as an adjuvant to surgery for 5 years (Early Breast Cancer Trialists' Collaborative Group (EBCTCG) *et al.* 2011). HER2 positive tumours result from the overexpression of the ErbB2/HER2 receptor in subpopulation of cells, accounting for around 20% of breast cancers. As such, they are uniquely targetable by Herceptin (Trastuzumab) - an antibody able to competitively bind the overexpressed receptor and prevent ligand induced signalling - and consequently show moderate survival rates. Other subtypes however do not yet have such targeted therapies; critical to the identification of potential targets is the understanding of the biology of the cancer.

1.2.1 Basal breast cancer

The basal-like breast cancer subtype lacks hormone receptor expression or HER2 overexpression and often includes ‘Triple Negative’ breast cancers (TNBCs), and accounts for around 15% of invasive ductal breast cancers (Badve *et al.* 2011). Phenotypically, as the name would suggest, basal breast cancers predominantly exhibit basal/myoepithelial

cell-like properties: they lack steroid hormone receptors, while keratins 5, 14 and 17 are highly expressed. Importantly, upregulation of the MaSC associated Wnt pathway has been widely associated with basal breast cancers; Increased active β-catenin (cytoplasmic and nuclear) is frequently observed, correlating with an enrichment of stem/progenitor cells (Khramtsov *et al.* 2010).

The presence of such an increased stem cell like population is thought to be the cause of this subtype having one of the worst prognoses of any breast cancer subtype. Although a high mitotic index renders basal breast cancers initially susceptible to so called 'standard of care' (SoC) chemotherapeutics such as Taxol - a microtubule stabilising compound designed to inhibit the division of rapidly dividing cells - they invariably exhibit the highest rates and severities of tumour relapse, due to a residual subpopulation of slowly dividing, and thus treatment resistant cells.

This corresponds with the long-standing 'cancer stem cell' (CSC) hypothesis, which says that much like a normal tissue is maintained by tissue specific stem cells, a tumour is derived from and maintained by the self renewal and expansion of a cell with stem-like properties (also known as a tumour initiating cell), also responsible for metastasis and tumour recurrence. Indeed, such a population capable of initiating tumour growth in mouse transplantation assays has been identified in the human breast (Al-Hajj *et al.* 2003). Under such a CSC theory, successful cancer treatment relies on the removal of the CSC population; even if 95% of tumour cells have been killed by a broad spectrum, cytotoxic chemotherapeutic, the persistence of a slowly dividing CSC population confers recurrence potential (Figure 1.7). Conversely, the specific targeting of a feature supporting CSC survival leaves only more differentiated cell types behind, often resulting in tumour regression. The safest chemotherapeutic regime is in fact the combination of both approaches, thus removing the possibility of non-CSC to CSC conversion in absence of a true CSC population (Chaffer *et al.* 2013).

Importantly, CSCs often utilise known SC associated pathways, offering potential targets for therapy; given the clear aberrant activity of the Wnt pathway in basal breast cancers, and the known link between Wnt and stem cell activity, strategies to target a prospective CSC population in this subtype with inhibitors of Wnt activity have emerged as exciting possibilities in basal breast cancer research.

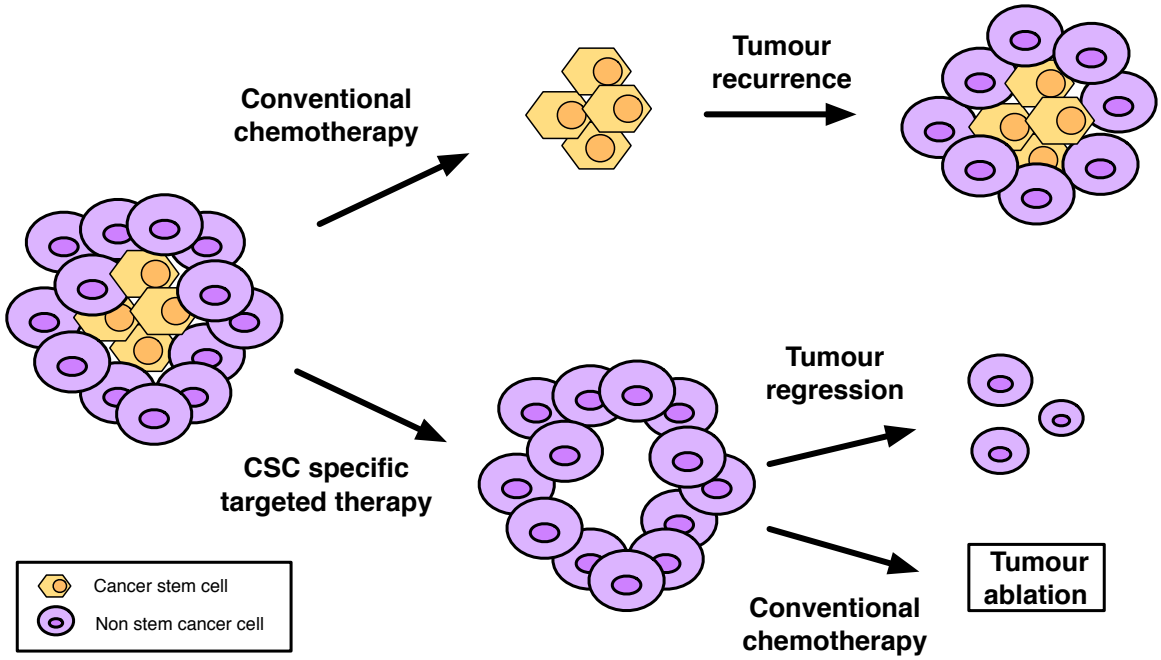

Figure 1.7 The roles of cancer stem cells in cancer treatment.

A tumour comprising of CSCs and non stem cancer cells can be treated with conventional therapy to remove rapidly dividing cells from the bulk tumour. Although this is effective in reducing tumour size, over time residual, slowly dividing CSCs can repopulate the tumour. Alternatively, a CSC targeting therapy can remove the source of the tumour, leaving behind more differentiated cell types eventually vulnerable to necrosis, leading to tumour regression. Moreover, CSC specific therapy combined with conventional chemotherapy can aid the total ablation of tumour cells.

1.2.1.1 The Wnt pathway as a prospective therapeutic target in basal breast cancers

Connections between Wnt signalling and breast cancers were first made with the discovery of mammary hyperplasia and tumourigenesis upon Wnt1 overexpression under the MMTV promoter in the mouse (Tsukamoto *et al.* 1988). In a similar phenomenon to that observed in the basal subtype, Wnt1 overexpression caused a significant expansion of MaSC and progenitor populations (Yi Li *et al.* 2003; B. Y. Liu *et al.* 2004). Importantly, knockout of the LRP receptor characteristic of a Wnt responsive cell prevented this expansion (Lindvall *et al.* 2006), lending support for the inhibition of Wnt signalling in the treatment of basal breast cancers.

Of course, inhibiting Wnt signalling may not be simple, since deregulation of the pathway is not confined to a single mutation or mechanism in basal breast cancers. Aberrant Wnt receptor activation or expression has been demonstrated by Liu et al (2010), with LRP6 overexpression in around 30% of human breast cancers, most of which were triple negative, ER-negative or HER2-negative subtypes (C.-C. Liu *et al.* 2010). Upregulation of Dishevelled or loss of inhibitory Wnt regulators can also be linked to β-

catenin upregulation; while it is fairly uncommon for APC or Axin oncogenic mutations to occur in breast cancer (deregulations reviewed extensively by (Incassati *et al.* 2010)), breast cancer cell lines demonstrate silencing or down-regulation of several Dickkopf protein family members (DKK2, 3 and 4)(Xiang *et al.* 2013). In contrast, DKK1 is overexpressed in several TNBC cell lines and is associated with nuclear B-Catenin accumulation, while its expression level in patients correlates with poor prognosis. As DKK1 is itself a Wnt target gene, it is thought that its overexpression is a result of activated Wnt signalling, despite it's usual role as a Wnt inhibitor in the cell (Xu *et al.* 2012; Zhou *et al.* 2014; Forget *et al.* 2007).

In humans, a high expression level of the basally associated ΔNp63 transcription factor has been found prevalent within the basal like breast cancer subtype, linked with an increased expression of the Fzd7 receptor (Chakrabarti *et al.* 2014). Increased Tankyrase expression, and consequently increased Wnt signalling activity, has also been detected in hormone receptor negative breast cancers in particular (Gelmini *et al.* 2004).

Given that alterations in Wnt activity may be induced at any level of the pathway, inhibitors may be required for a broad range of Wnt pathway related factors; from Wnt ligand itself, to receptors, and even proteins responsible for Wnt related gene expression. Several such inhibitors are currently in development.

1.2.1.1.1 Inhibitors of Wnt release

An inhibitor of Wnt production (IWP-2) has been demonstrated to act via it's highly specific inactivating effects on Porcn function (Chen *et al.* 2009), suggesting that it may be useful as a therapeutic compound. Several other Porcn inhibitors, including LGK974 and Wnt-C59, have also shown high efficacy in inhibiting Wnt signalling in multiple cancer types, including MMTV-Wnt1 mouse models (J. Liu *et al.* 2013; Proffitt *et al.* 2013), with the former currently in use in a Phase I clinical trial (Clinicaltrials.gov, 2016).

1.2.1.1.2 Inihbitors of Wnt-receptor binding

Wnt signalling occurs through a receptor complex, such that Frizzled and Lrp6 are both potential targets of inhibtion. Several compounds altering receptor levels have been identified; niclosamide, a derivative of salicylic acid, has been indicated to promote Frizzled internalisation (M. Chen *et al.* 2009) and Lrp6 degradation (W. Lu *et al.* 2011),

while the small molecule inhibitor salinomycin, shown in high throughput screening to selectively target breast cancer stem cells (Gupta *et al.* 2009), inhibits expression of the Lrp6 receptor (W. Lu and Yonghe Li, 2014). Notably, the latter compound reduced CSCs over 100 fold compared to the SoC treatment, Taxol (Gupta *et al.* 2009). Importantly, a recombinant human monoclonal antibody to the Frizzled7 receptor, Vantictumab (OMP18R5), has shown success in patient derived xenograft models, reducing the tumorigenicity of human tumour cells (Gurney *et al.* 2012), and has been shown to be well tolerated in a Phase I clinical trial by OncoMed Pharmaceuticals, with work now on-going to determine dosing (OncoMed Pharmaceuticals, 2016).

1.2.1.1.3 Regulators of intracellular Wnt signalling pathway components

As discussed in detail in 1.1.3.1, the intracellular Wnt pathway comprises a consortium of proteins that are responsible for the control of β-catenin levels in the cell, many being prime targets for inhibition of the Wnt pathway; inhibitors of TNKS1 and/or TNKS2 activity have shown promise in this respect. XAV939, originally identified to be able to inhibit β-catenin mediated transcription through inhibition of TNKS1/2 by Huang et al (2009), has clearly been demonstrated to promote axin stability, preventing cell migration and colony formation in breast cancer cell lines, while Inhibitor of Wnt response-1 (IWR-1), has been indicated to work similarly (Bao *et al.* 2012).

1.2.1.1.4 Inhibitors of Wnt target gene expression

Merck Serono have recently developed an inhibitor of the Mediator complex kinases CDK8 and CDK19 (Dale *et al.* 2015). The compound, CCT251545, initially reported by a high throughput cell-based reporter assay to have inhibitory effects on the Wnt pathway (Mallinger *et al.* 2015) acts via competitive ATP inhibition, and works at the level of, or downstream of, T cell Factor (TCF), thus regulating Wnt dependent gene transcription (Dale *et al.* 2015).

In vivo experiments performed on an animal model of β-catenin dependent intestinal hyperplasia indicated that the compound could successfully reduce crypt proliferation and overall length, while in MMTV-Wnt1 induced mouse breast cancer allografts, inhibitor treatment reduced tumour growth rate, and caused a reduced Wnt target gene signature (Dale *et al.* 2015). Moreover, *in vitro* experiments on MMTV-Wnt1

tumour organoids previously showed successful response to the compound (Ewan; Unpublished).

The range of inhibition routes and clear biological promise of the compounds described here makes the Wnt pathway an exciting target for the treatment of basal breast cancers. The development and validation of such targeted therapies however, relies on the availability of relevant models in which to study effects on overall tumour growth, stem cell compartments both alone and in combination with SoC therapy.

1.3 *In vitro* systems for study of the mammary gland

1.3.1 2D culture

The study of the mammary gland, including the search for a MaSC population, cell signalling pathways and breast cancer characteristics amongst other aspects, has extended past in vivo work into 2 dimensional *in vitro* studies, none of which have thus far been able to fully recapitulate a physiologically relevant system, despite their independent contributions to the knowledge of breast biology. Immortalised cell lines, cultured on tissue culture treated plastic, have been frequently used in studies of the breast. The human MCF-7 breast tumour cell line, for example, enabled the first elucidation of the sensitivity of estrogen receptor positive cancers to anti-estrogen treatment Tamoxifen, and has been used as a key model for understanding the mechanisms used by estrogen to stimulate breast cells to proliferate (Levenson and Jordan 1997). While primary MECs can also be cultured, they often lose their differentiation ability upon contact with the two dimensional plastic surface, and have been demonstrated to adapt genetically over long periods of culture (Neve *et al.* 2006).

2-D mammary colony forming cell assays, in which mammary cells seeded in adherent culture with 'feeder' fibroblasts are assayed for ability to form clonal populations of cells, are useful in detecting possible progenitor cells, but culture conditions used do not allow for the differentiation of all cell types, and may not support stem cell survival (Stingl 2009).

1.3.2 3D culture

Attempts to translate *in vitro* mammary gland studies into 3D culture, and therefore better mimic the true microenvironment of the mammary gland have also been made. However, the degree to which these systems can fully recapitulate *in vivo* mammary gland biology is somewhat limited.

The mammosphere assay, where serum free non-adherent culture conditions allow the growth of spherical structures comprised of undifferentiated cells with self-renewal abilities, are routinely used to identify and quantify stem-like cells, and under different culture conditions, demonstrate their differentiation capacity (Dontu *et al.* 2003); culture conditions allowing both traits simultaneously have not yet been found. This method can also be used to produce tumourspheres for the study of so called 'cancer-stem cells' from tumour material. However difficulties exist in the distinction between MaSC and progenitor involvement during formation of these spheroids, and evidence has suggested that most mammospheres are in fact a result of aggregations of cells in suspension, rather than clonal outgrowths, thus limiting the certainty of 'stem cell' conclusions using such assays (Stingl 2009).

Strong evidence has shown the retained or increased expression of mammary specific genes such as β-casein when primary cells are cultured on floating collagen membranes or in basement membrane-like substrates (Emerman *et al.* 1977; M L Li *et al.* 1987). As such, newer 3D systems have introduced an extracellular matrix substitute, such as collagen I or Matrigel, (derived from Engelbreth Holm Swarm mouse sarcoma, comprising mainly laminin and collagen IV) to promote the maintenance of normal cell signalling, and tissue architecture (Campbell and Watson 2009). Such assays have typically demonstrated growth of acinar structures, possessing the architecture of the in-vivo gland, but structures formed are often growth arrested and therefore not maintainable in long-term culture (Debnath et al. 2003; Campbell and Watson, 2009).

Recent approaches have identified factors enabling the formation of polarised epithelial cells of basal and luminal phenotype, organised with a central lumen, for a short period (Ewald *et al.* 2008; Pasic *et al.* 2011; Obr *et al.* 2013). Such structures can retain steroid hormone receptor expression in culture, but for a limited period of 14 to 21 Days (Obr *et al.* 2013).

The ideal *in vitro* 3-dimensional mammary gland culture system would combine the best features of each of these assays to fully recapitulate the *in vivo* mammary gland; concomitantly enabling stem cell maintenance and proliferation, and biologically relevant, functional differentiation, in a tissue specific architecture.

1.3.3 Organoid culture systems

1.3.3.1 Introduction

An organoid, defined most simply, is a structure closely resembling an organ. More specifically, it is a collection of cell types derived from a specific tissue, grown in a 3-dimensional, in-vitro environment, closely resembling the in-vivo tissue in structure or function. Such organoid culture systems differ from previously established 3D culture models, in that they retain functioning stem cells, enabling long-term cultures that can be expanded at great magnitude to enable high throughput analysis, from a small amount of starting material. In general, stem-cell containing organoid cultures also exhibit a full complement of functioning differentiated cell types of the tissue from which they originated, arranged in a organ specific architecture, communicating through physiologically relevant cell-cell signalling mechanisms (Figure 1.8).

Toshiro Sato and Hans Clevers initially defined the stem-cell containing organoid culture system (Sato *et al.* 2009). It took the form of a 3D, matrigel based model supporting growth of complex intestinal organoids recapitulating basic crypt physiology: from their 3D architecture, to Lgr5+ stem cell self-renewal and capacity for differentiation of all epithelial cell types (Sato *et al.* 2009). The key to this breakthrough was the control of the Wnt signalling pathway, known to be essential for crypt proliferation (Pinto *et al.* 2003), using the Lgr5 ligand R-spondin1. This protein potentiates Wnt signalling, forming a complex with Lgr5 receptors and the Frizzled receptor and preventing their removal from the cell surface, and is shown to regulate intestinal organoid formation in a concentration dependent manner (de Lau *et al.* 2011). Other minimum requirements in this culture system included epidermal growth-factor (EGF) for intestinal cell proliferation, and the transforming growth factor-β (TGF-β) pathway inhibitor Noggin (Nog) (Sato *et al.* 2009). Investigations based around the paracrine interactions that constitute the 'stem-cell niche' of the small intestine have since enabled whole crypt culture from as little as a single cell in culture (Figure 1.9)(Sato, van Es, *et al.* 2011).

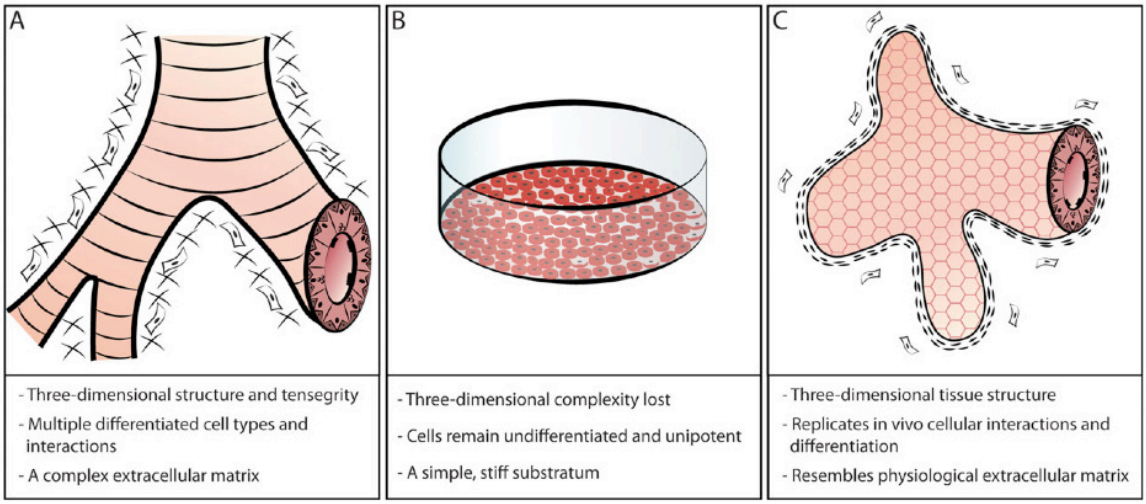

Figure 1.8 Organoid models have advantages over 2D culture systems.

(A) In vivo tissue composition and architecture. Multiple cell types build up a heterogenous, functioning tissue. **(B)** In 2 dimensional culture, cells oftern lack heterogeneity, and artificial 2D nature prevents important physiological interactions between cell subtypes. **(C)** 3D cultures permit physiological relevant cell signalling, recapitulation of tissue architecture and structure, and maintained cell heterogeneity. Reprinted by permission from Macmillan Publishers Ltd: [Stem Cells] (Hynds et al., 2013), copyright (2013).

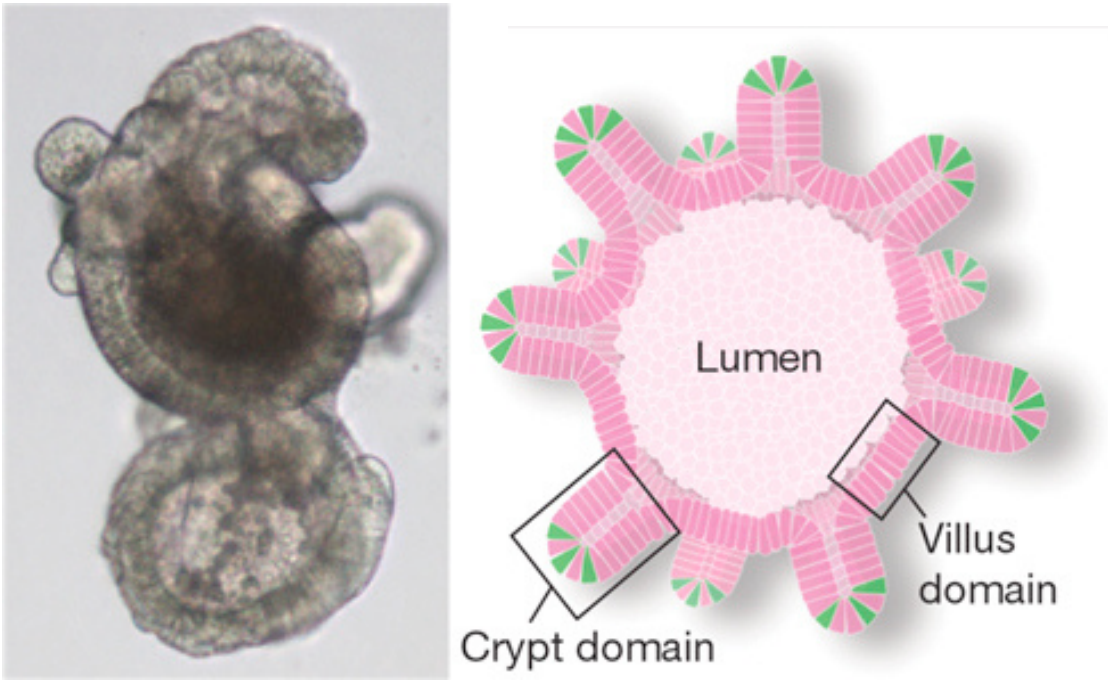

Figure 1.9 Intestinal organoid cultures recapitulate in vivo gut morphology.

Culture conditions generated by Sato *et al.* (2009) allow the generation of intestinal organoids with functional and distinct crypt and villus domains, with full complement of differentiated and stem cell types. Reprinted by permission from Macmillan Publishers Ltd: Nature, (Sato et al., 2009), copyright (2009).

1.3.3.2

The utilities of the intestinal culture system are extensive. The roles and growth dependencies of individual cell populations during development can be monitored, the effects of growth factors and inhibitors development can be studied, while organoids derived from genetically modified mouse models enable the study of disease mechanisms and can aid early stage drug discovery (Jardé *et al.* 2012). Furthermore, human organoid culture can now be achieved using similar culture conditions (Sato, Stange, *et al.* 2011), and has taken a role in the field of translational medicine.

To date, organoid systems have been created for growth of tissue from the liver (Huch *et al.* 2013), lung (Rock *et al.* 2009), prostate (Karthaus *et al.* 2014), pancreas (Boj *et al.* 2015), and various sections of the gastrointestinal tract including the stomach and colon(Bartfeld *et al.* 2014) (Sato, Stange, *et al.* 2011), to name but a few.

1.3.3.3 Mammary organoid culture

As in the intestine, and indeed multiple other organ systems, Wnt signalling has been shown to be important in the development of the mammary gland (Zeng and Nusse 2010). With this knowledge, early work in the Dale lab began generating media conditions based on those described by Sato *et al.* (2009), with the aim of enabling the long-term growth and expansion of fully differentiated, self-renewable mammary organoids recapitulating *in vivo* tissue architecture, from primary murine tissue.

Initial experiments used the defined, EGF, Noggin, R-Spondin1 conditions published by Sato et al. (2009). While these conditions supported the long-term culture of many mammary organoids, phenotypical analysis demonstrated that structures were 'abnormal' in their differentiation, containing no luminal cells, but an abundance of basal, Wnt-responsive cells, leading to highly keratinous, squamous structure development (Jardé et al. 2016). R-spondin1 controlled cell viability, and was absolutely essential for the correct development of the basal layer (the continuous expression of smooth muscle actin, for example), and the maintenance and renewal of mammary organoids. However, similarities of structures to that of MMTV-Wnt1 driven tumours highlighted that R-Spondin1 levels were far too high; conditions only enabling the generation of abnormal organoids that may be useful in the investigation of tumour development (Appendix I-1). This led to the belief that an optimal or 'just-right' level of

Wnt signalling exists in the mammary gland for normal mammary development; too little and organoids fail to thrive, and too much and tumour-like basal differentiation is favoured.

EGF, key in intestinal culture conditions, is an important and commonly implemented growth factor in normal two-dimensional mammary cell culture (Nandi *et al.* 1984). However, evidence provided by Jardé et al. (2016) demonstrated that unlike the intestinal system, in the mouse mammary organoid culture system, the alternative EGF family member Nrg1 more efficiently generated lobular, organised mammary structures resembling the in-vivo mammary gland, when used in combination with Noggin (Appendix I-2). Further to this, and in agreement with a recent study by Forster et al., (2014), luminal cell populations were assessed to express the Nrg1 receptors ErbB3 and ErbB4 at high levels, while transcripts of the ligand were most prevalent in the basal population (Appendix I-2).

In depth characterisation of organoid growth under conditions combining Nrg1, Noggin and R-Spondin1 was initiated by Jardé et al (2016), with culture conditions showing promise in the generation of complex, lobular structures recapitulating the *in vivo* physiology of the mammary gland.

1.4 Aims and objectives

The mechanisms orchestrating mammary gland development are extensive and as yet not fully understood. Ultimately, it is the failure or deregulation of these processes that underlies the progression of normal mammary tissue to malignancy. As such, a detailed knowledge of normal mammary gland developmental requirements is essential to understand mechanisms potentially driving breast cancer initiation and progression, and consequently, to indicate potential targets for breast cancer treatment. For this, a suitable system in which to perform studies is required.

The first aims of this thesis were therefore to develop, optimise and evaluate the mammary organoid system initiated by Dr Jardé further, such that it fully represented the *in vivo* mammary gland, and could subsequently be exploited for more detailed investigation of normal mammary gland biology and factors or pathways altering normal development or potentially driving progression to malignant phenotypes. During this work, a particular focus was placed on the role of the Wnt pathway in mammary organoid development. This is described in Chapters 3, 4 and 5.

Following on from this, a second key objective was the utilisation of the mammary organoid system for the culture of tumour derived organoids, and the subsequent evaluation of the potential for Wnt inhibition in the treatment of basal breast cancers in an appropriate pre-clinical model, assessing both initial treatment responses, and effects on prospective CSC populations.

2 Materials and Methods

2.1 Experimental Animals

The mouse was used as a model to obtain all primary material and to perform *in vivo* experiments in this thesis. Strain information will be provided where appropriate.

2.1.1 Husbandry

All animals were obtained commercially from Harlan or Charles River, or bred in-house. Mice were housed under UK Home Office regulations. Mice were all given access to a standard diet (Special diets Service UK, expanded diet) and water *ad libitum.*

2.1.2 Breeding

Animals bred in house were done so using the standard cage format of two females and one male. Pups were weaned and sexed at four weeks of age, unless weaning at an earlier time point of 19 days was specifically required by experimental protocol. In this case, weaned mice were given access to HydroGel to ensure their hydration, and solid food softened in water.

2.1.3 Genetic mouse models

The majority of the experiments performed in this thesis were done so using the wild-type, FvB mice. However, the transgenic Tet-ODN89β-catenin mouse model described in (Jardé et al. 2012) was also used for indicated experiments. Under doxycycline induction, mice/tissues derived from this model constitutively express a truncated, stabilised form of β-catenin.

2.2 Experimental procedures

All experimental procedures were carried out by licensed individuals with the appropriate training, under the regulations of the UK Home Office, under the project license codes 30/2571 (pre-2014) and 30/3022 (2014 onward).

2.2.1 Cleared mammary fat pad transplantation

Transplantation of organoids or organoid derived cells was carried out into the cleared fourth mammary fat pads of 21-day-old, female FvB mice, according to the standard procedure described in detail by Alvi et al (2003). For this, organoid (50 per fat pad) or cell suspensions (60,000 per fat pad) were resuspended in 50% PBS and 50%

Matrigel, and injected at 10µl. Following transplantation, mice were checked daily for tumour development by palpation, and fat pads were harvested after 8 weeks for analysis.

2.2.2 Tumour fragment transplantation

For expansion of material, T1 tumour fragments of approximately $1mm^3$ were transplanted into the cleared mammary fat pads of 21-day-old female Balb/C mice, following a similar protocol to that described above. Due to the rapid nature of tumour development, animals were checked daily for tumour growth by palpation, and tumours removed before exceeding 1cm in diameter, usually within two weeks, according to the Rosen laboratory protocol and Home Office Regulations.

MMTV-Wnt1 tumour fragments were implanted heterotopically by subcutaneous trocar into nude mice by Howard Kendrick, and tumour growth monitored as above.

2.3 Primary cell preparation for 3D culture

2.3.1 'Normal' cell preparation

Unless stated otherwise, 'normal' mouse mammary organoid culture studies were carried out using tissue gathered from female virgin FvB mice, of 8-12 weeks of age.

2.3.1.1 Tissue dissection

Mice were culled by CO_2 inhalation according to Schedule 1 protocols of Home Office Licence procedures. Each mouse was surface sterilised with a spray of 70% ethanol to the abdomen, before incision to the abdominal skin, taking care not to rupture the abdominal cavity. The tissue was blunt dissected to expose the mammary tissue, and the 2^{nd}, 3^{rd}, 4^{th} and 5^{th} mammary fat pads harvested. The lymph nodes from the 4^{th} fat pads were removed prior to cell preparation, to improve purity of epithelial populations.

2.3.1.2 Epithelial fragment preparation

Epithelial preparations were achieved using protocols described by Sleeman *et al.* (2006) and Smalley (2010). Harvested mammary gland epithelial tissue was placed in Leibowitz L-15 medium (Invitrogen), supplemented with 10% Heat inactivated, filtered Fetal bovine serum (Invitrogen), 1% Penicillin/Streptomycin (Invitrogen) and 1% GlutaMax (Invitrogen) (L-15/10%FBS/PSG), before being chopped at 100 µm intervals using the McIlwain Tissue Chopper (Mickle Laboratory Engineering Company, Gomshall,

Surrey, UK). The chopped tissue was then placed in shaking incubation at 37°C for one hour in a digestion mix comprised of Leibowitz L-15 medium, 3 mg/ml Collagenase A (Sigma) and 1.5 mg/ml trypsin from porcine pancreas (Sigma). The resulting mixture was centrifuged at 350 x g for 5 minutes, and washed in L-15/10%FBS/PSG, before incubation for 5 minutes in red blood cell lysis buffer (Sigma). The cell mixture was then washed again before pre-plating for 1 hour and 30 minutes at 37°C/5%CO2 in Dulbecco's Modified Eagle's medium (Invitrogen), supplemented with 10% Heat inactivated, filtered Fetal bovine serum (Invitrogen), 1% Penicillin/Streptomycin (Invitrogen) and 1% GlutaMax (Invitrogen), to allow fibroblasts within the preparation to adhere to the tissue culture plastic. After incubation, the non-adherent mammary epithelial cells/organoids were taken from the plate in the media and washed in fresh L-15/10%FBS/PSG. At this stage, mammary epithelial organoids were either counted and plated, or digested further to single cells as described below.

2.3.1.3 Single mammary epithelial cell isolation

Following primary organoid isolation, cells were washed in Joklik's Modification of Minimal Essential Medium for Suspension Culture (Sigma) and incubated in a water bath at 37°C for 15 minutes. Digestion to single cells was carried out through addition of Trypsin-EDTA 0.05% (Invitrogen) for 2 minutes at 37°C, and encouraged by gentle trituration by pipette. Cell clumping following cell damage induced DNA release during trypsinisation stage was reduced by treatment with 5 µg/ml DNase I in serum-free L-15 medium for 5 minutes on ice, before addition of 20 ml L-15/10% FBS-PSG. Single cells were strained through a 70 µm cell strainer, pelleted at 265 x g for 5 minutes, and suspended in fresh L-15/10% FBS-PSG, counted, and plated at the desired density.

2.3.1.4 Flow cytometry and cell sorting

FACS was performed according to protocols defined by Sleeman *et al.* 2006. Single mammary epithelial cells were counted and resuspended at 10^6 cells per ml in L-15/10% FBS/PSG medium. Fluorescent antibody staining was performed on ice for 45 minutes, using antibodies detailed in Table 2.1. Stained cells were pelleted at 265 x g for 5 minutes, and resuspended in 1.5ml L-15/10%FBS-PSG medium containing 0.01% DAPI. Due to a degree of spectral overlap between the fluorophores used, compensation controls of each of the individual stains, and an unstained control were also created, in

order to automatically determine the contribution of each fluorophore to the signal in a given detector and calibrate the sorter. Cells were sorted using a BD FACSAria II, or BD FACSAria III (BD Biosciences) fitted with a 100 um nozzle, at 70 psi, using gating detailed in Figure 2.1. Briefly, cell doublets were excluded from the sort based on forward and side scatter area profiles (Figure 2.1B, C), dead cells by selection of DAPI-negative cells ($<10^3$), and epithelial only cells selected based on negative CD45-Cy7 staining ($<10^3$). Mammary epithelial populations were further subdivided based on their expression of CD24 (Luminal-CD24^{high} or Basal CD24^{low}), and Sca1 (Luminal ER negative^{Sca1-} or Luminal ER positive^{Sca1+}).

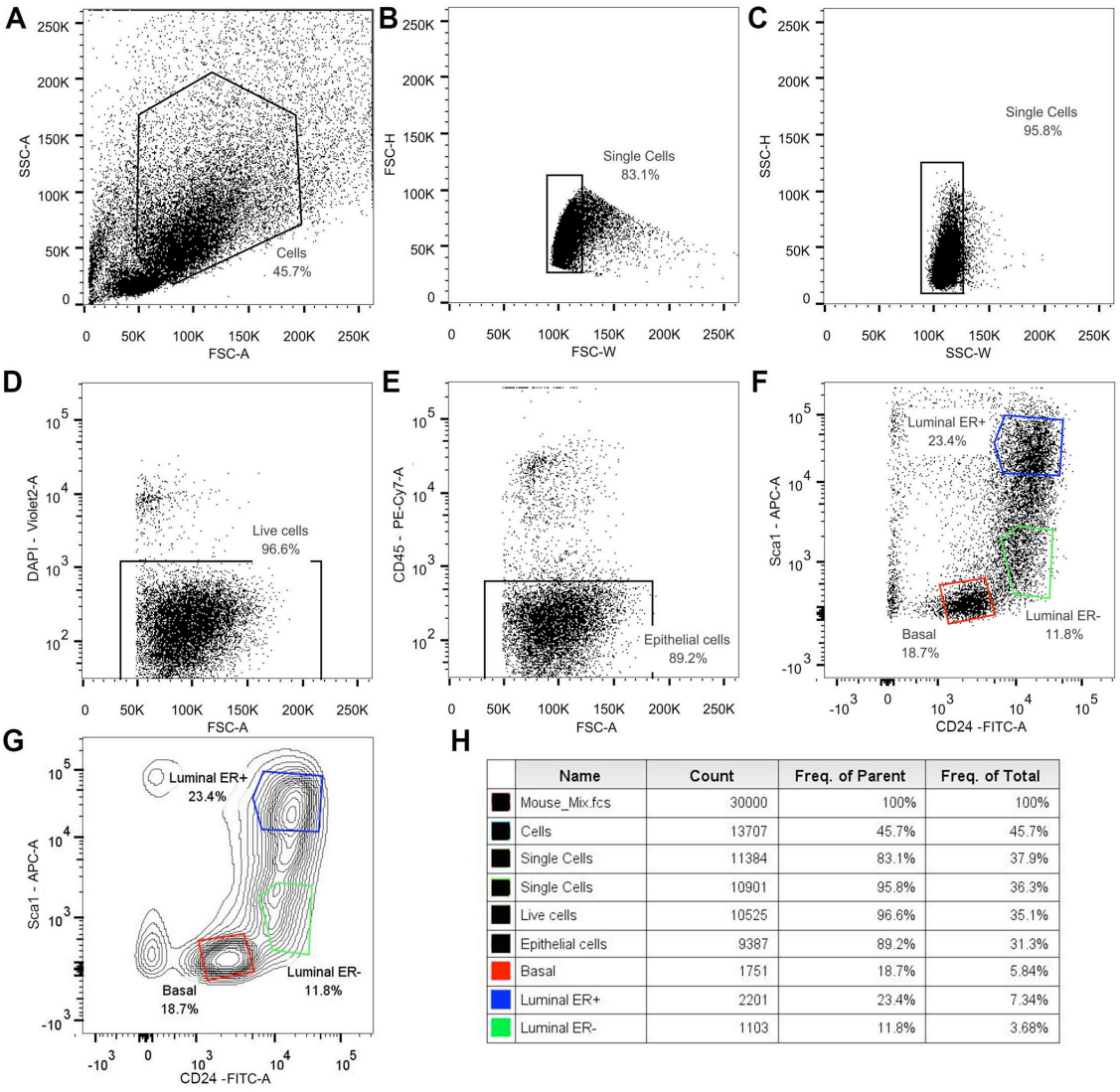

	Name	Count	Freq. of Parent	Freq. of Total
	Mouse_Mix.fcs	30000	100%	100%
	Cells	13707	45.7%	45.7%
	Single Cells	11384	83.1%	37.9%
	Single Cells	10901	95.8%	36.3%
	Live cells	10525	96.6%	35.1%
	Epithelial cells	9387	89.2%	31.3%
	Basal	1751	18.7%	5.84%
	Luminal ER+	2201	23.4%	7.34%
	Luminal ER-	1103	11.8%	3.68%

Figure 2.1 Fluorescence activated cell sorting of the three main mammary epithelial cell types.

Using the gating steps originally described by Sleeman et al (2006, 2007), primary mammary epithelial cells from 8-12 week old FvB mice were sorted into three distinct populations: basal ($CD24^{low}Sca\text{-}1^{-}$), luminal estrogen receptor negative ($CD24^{high}Sca\text{-}1^{-}$) and luminal estrogen receptor positive ($CD24^{high}Sca\text{-}1^{+}$). **(A)** Cells were first gated based on forward and side scatter to exclude clumps and debris. **(B)** Individual forward and **(C)** Side scatter-based gating to enable the sorting of only single cells. **(D)** Dead cells were excluded based on a higher intensity of DAPI staining. **(E)** Leukocytes gated out of the sorted population by selection of only CD45-negative cells. **(F)** Final gates were set based on the CD24 and Sca1 marker profiles of the three epithelial cell populations. **(G)** In cases where distinct populations could not be clearly seen using dot plots, a contour map was used to enable visualisation of discreet groups of cells. To ensure efficiency, output samples were purity tested, and sorting routinely shown to be >99% accurate. **(H)** Representative population percentages from a single FvB mammary epithelial FAC sort.

2.3.2 Tumour cell preparation

Tumour cells were obtained from two different tumour models, the T1, p53 null, and the MMTV-Wnt1 model, grown as described in 2.2.2. There were minor differences in preparation between the two, as indicated in the following sections.

2.3.2.1 Tumour harvesting

Mice were culled by CO_2 inhalation according to Schedule 1 protocols of Home Office Licence procedures, at a time point designated by the conditions set in 2.2.2. Tumours were harvested from their respective sites of transplantation and dissected into small ($1mm^3$) chunks, and frozen in cryovials, in 1ml homemade freezing medium (50% DMEM/F-12, 40% FBS, 10% DMSO).

2.3.2.2 Tumour cell isolation

2.3.2.2.1 T1 tumour cell isolation

Frozen T1 tumour fragments were thawed in a 37°C water bath, and freezing media washed out by addition of 10ml Hanks Buffered Saline Solution (Invitrogen) with centrifugation at 100 x g for 3 minutes, according to protocols provided by the Rosen laboratory. This wash was repeated and tumour chunks chopped manually into smaller fragments. Red cell lysis buffer (Sigma) was then applied for 5 minutes, and tissue washed thoroughly in DMEM/F-12 media. Digestion of tissue was performed using 1.5 ml Trypsin-0.05%-EDTA at 37°C for 2 minutes. After neutralisation of trypsin with equal volumes of heat-inactivated fetal bovine serum, the remaining suspension was strained at 100 µm and cells counted using a haemocytometer.

2.3.2.2.2 MMTV-Wnt1 tumour cell isolation

Frozen tumour fragments were thawed in a 37°C water bath, and freezing media washed out by addition of 10ml Leibowitz L-15 medium (Invitrogen), supplemented with 10% Heat inactivated, filtered fetal bovine serum (Invitrogen), 1% Penicillin/Streptomycin (Invitrogen) and 1% GlutaMax (Invitrogen) (L-15/10%FBS/PSG) and centrifugation at 100 x g for 3 minutes. This wash was repeated, and larger tumour chunks cut manually into smaller pieces, before finer processing using the McIlwain Tissue Chopper (Mickle Laboratory Engineering Company, Gomshall, Surrey, UK), set at 100 µm chopping

intervals. Digestion and fibroblast removal of the minced tissue was then performed as described for normal mammary epithelial tissue (2.3.1.1).

The resulting suspension was spun at 350 x g for 5 minutes, and the pellet digested further using gentle trituration and incubation at 37°C in 200µl Trypsin-EDTA 0.05% (Invitrogen) for two minutes. Trypsin was then inactivated with equal volume FBS, and 400 µl DMEM-F12 added before filtering of the final suspension through a 70µm cell strainer. A final 200µl DMEM-F12 wash through the strainer brought the total volume to 1ml, for cell counting using a haemocytometer.

2.4 'Normal' mammary organoid culture

2.4.1 Organoid culture and maintenance[1]

Epithelial fragments (50 per well) or single cells (1000 cells per µl, to a total of 25µl) were suspended in growth-factor reduced Matrigel (BD Biosciences) in tissue culture standard 48 well plates, and following polymerisation of the Matrigel at 37°C for 15 minutes, overlaid with 300µl stock mammary organoid culture medium of DMEM/F12 (Phenol Red free) (Invitrogen), 1% Penicillin/Streptomycin (Invitrogen), 1% Hepes (Invitrogen), 1% GlutaMax (Invitrogen), 1% progesterone free N2 supplement (homemade, Table 2.2) and 2% progesterone free B27 (homemade, Table 2.3) based on Brewer et al. (1993) and adapted from Chen et al. (2008), respectively, supplemented with Neuregulin1 (100 ng/ml), Noggin (100 ng/ml), R-Spondin1 (2.7 ng/ml), and Y-27632 (10 µM) for the first 5 days in culture (Table 2.4). Media changes were carried out every 3 to 4 days. All incubator conditions were standard throughout this thesis, at 37°C, 5% CO_2 and 90-95% humidity.

2.4.1.1 Organoid passage

Trypsin-based dissociation was carried out when necessary (when organoids become large and dense), usually at around 14 to 18 days in culture. Growth media was discarded from wells and ice cold PBS or DMEM/F12 was added to the contents of 4-6 wells, before mechanical trituration of Matrigel through an FBS-coated P1000

[1] Given that a key aim of this thesis was to optimise culture conditions for the growth of mammary epithelial cell populations, and tumour cell populations, many conditions were trialled and described in the text. For clarity, this section describes only the most recent optimised methods and conditions for culture.

Antigen	Label	Source	Name/Clone; Catalogue n^{o}	Final concentration
CD24	FITC	BD Pharmingen^{TM}	M1/69; 553261	0.5 µg/ml
CD45	Cy-7	BD Pharmingen^{TM}	30-F11; 552848	0.5 µg/ml
Ly6-A/E; Sca1	APC	eBioscience	D7;17-5981-81	0.2ug/ml

Table 2.1 Fluorescent antibodies used in staining for FACS.

Reagent	Supplier, catalogue number	Concentration (µg/ml)
Holo-transferrin	Calbiochem, 616242	10,000
Insulin	Sigma-Aldrich, I1882	500
Putrescine	Sigma-Aldrich, P5780	1,611
Sodium selenite	Sigma-Aldrich, S9133	0.52

Table 2.2 Composition of homemade N2 Supplement (In DMEM/F-12).

Reagent	Supplier, catalogue number	Concentration (µg/ml)
Albumin	Gift from Dr Tess Saltmarsh	2500
Catalase	Sigma-Aldrich, C41	2.5
Glutathione (reduced)	Sigma-Aldrich, G6013	1
Insulin	Sigma-Aldrich, I1882	4
Superoxide dismutase	Sigma-Aldrich, S5395	2.5
Holo-transferrin	Calbiochem, 616242	5
Triiodo-L-thyronine (T3)	Sigma-Aldrich, T6397	0.002
L-carnitine	Sigma-Aldrich, C7518	2
Ethanolamine	Sigma-Aldrich, E9508	1
D-galactose	Sigma-Aldrich, G0625	15
Putrescine	Sigma-Aldrich, P5780	16.1
Sodium selenite	Sigma-Aldrich, S9133	0.01435
Corticosterone	Sigma-Aldrich, C2505	0.02
Linoleic acid	Sigma-Aldrich, L1012	1
Linolenic acid	Sigma-Aldrich, L2376	1
α-tocopherol	Sigma-Aldrich, 95240	1
α-tocopherol acetate	Sigma-Aldrich, T3001	1
Biotin	Sigma-Aldrich, B4639	0.1

Table 2.3. Composition of homemade B27 supplement (In DMEM/F-12).

Factor	Supplier, catalogue number	Concentration tested
Noggin	Peprotech, 250-38	100ng/ml
Neuregulin	R&D systems, 5898-NR-050	100 ng/ml
R-Spondin 1	Peprotech, 120-38	2.7 – 85 ng/ml
Y-27632 dihydrochloride	Tocris, 1254	10µM
Epidermal Growth Factor	Sigma, E4127	50 ng/ml
Fibroblast growth factor 2	R&D systems, 233-FB-025/CF	25 – 100 ng/ml
Fibroblast growth factor 7	R&D systems, 251-KG-010	25 – 100 ng/ml
Fibroblast growth factor 10	Peprotech, 100-26	25 – 100 ng/ml
Hepatocyte Growth Factor	Peprotech, 100-39	12.5 – 100 ng/ml
Wnt3a	R&D systems, 5036-WN-010/CF	25-200 ng/ml
Wnt4	R&D systems, 475-WN-005/CF	100 ng/ml

Table 2.4. Supplementary growth factors used in culture media

pipette tip and pooling of contents in a 15 ml falcon. The suspension then underwent several cycles of washing in ice cold PBS or DMEM/F-12, with chilled (4°C) centrifugation at 350 x g for 5 minutes. Enzymatic digestion was carried out through addition of 300µl Trypsin-EDTA 0.05% (Invitrogen) at 37°C for 5 minutes, followed by mechanical trituration and neutralisation by addition of an equal volume of FBS. Larger structures were allowed to settle in the falcon, and supernatant was strained through a 100 µm cell strainer. This process was repeated as necessary on remaining structures, up to a maximum of three times to ensure maximum trypsinisation efficiency. Cells were centrifuged at 265 x g for 5 minutes before suspension at the desired density in growth factor reduced Matrigel, as above.

2.4.2 Organoid assays

2.4.2.1 Growth factor, hormone, or inhibitor assays.

For general testing of growth factors, hormones or inhibitors, cells were seeded in 10µl growth factor reduced Matrigel, in 96 well, black tissue culture treated plates, and overlaid with 100µl total media, as indicated in individual experiments. For OcellO assays, organoids were seeded in 14.5 µl growth factor reduced Matrigel in 384 well, black tissue culture plates and overlaid with 25µl culture media. In this case, media was added cumulatively. All additional factors and their tested concentrations are summarised in Table 2.4.

2.4.2.2 Doxycycline induction of mutant β-catenin expression in Tet-OΔN89-β-Catenin organoids

Epithelial cells were obtained as described above, from mice previously described by Jardé *et al.* (2012). Mice were untreated and tissue therefore considered wild-type prior to dissection and experiment start point. For activation of the transgene, cells were treated once with doxycycline (2µg/ml) upon seeding, in combination with the various growth factors detailed in text.

2.4.2.3 EdU incoroporation assays

Organoids cultured for 14 days were treated three hours prior to fixing with 10µM EdU (5-ethynyl-2'-deoxyuridine). Such a time point was chosen to allow sufficient incorporation of the thymidine analogue into newly synthesized DNA.

EdU detection was performed using a Click-iT® EdU Alexa Fluor® 488 Imaging Kit (Invitrogen), under a protocol optimised for 3D wholemount cultures. Following 20 minutes fixation in 4% paraformaldehyde at RT, wells were washed twice in PBS-BSA (3%) and incubated in a 0.5% Triton® X-100 PBS solution for 20 minutes. After this incubation, wells were washed twice with PBS-BSA (3%) and then given 50µl per well of a reaction cocktail composed according to the manufacturer's protocol, for 30 minutes at RT in the dark. Wells were then washed with PBS-BSA (3%) and immunofluorescence staining performed as detailed in 2.6.4.

2.4.2.4 Lentiviral infection of organoids with shRNA

shRNAs were developed using the Block-It shRNA system (Thermo Fisher) against both Erbb3 and Erbb4 cloned into a Gateway modified pSEW vector (Groner Lab). Lentiviral pseudo-virus was produced using the psPAX2 and PMD.G2 lentiviral packaging plasmids (Trono lab). Lentivial titre was established and test cells were infected at an MOI of >3. This work was kindly performed by Howard Kendrick.

For infection, freshly isolated single mammary epithelial cells were resuspended in an equal mix of Matrigel and lentiviral suspension, and plated over a pre-set thin layer of 100% Matrigel in 48-well plates. Each well was then overlaid with standard culture media and after 24 hours for cells to settle into the Matrigel and

infection to occur, media was replaced. This process was repeated every two days. Plates were fixed after 10 days and counterstained with DAPI, and images taken with an Olympus IX73 microscope, with a 10X objective.

2.5 Tumour organoid culture

2.5.1 Tumour organoid culture and maintenance

T1 tumour cells were seeded at a density of 1000 cells per µl growth factor reduced Matrigel (to a total of 25µl) in 48 well plates and overlaid with media containing Neuregulin1 (100 ng/ml), Noggin (100 ng/ml) and R-Spondin1 (2.7 ng/ml), **or** media containing EGF (50 ng/ml), Noggin (100 ng/ml) and R-Spondin1 (42.5 ng/ml), to be replaced every 3-4 days.

MMTV-Wnt1 cells were seeded at a density of 750 per µl growth factor reduced Matrigel (to a total of 25 µl) in 48 well plates and overlaid with media containing Neuregulin (100 ng/ml) and Noggin (100 ng/ml) for routine maintenance.

2.5.1.1 Tumour organoid passage

T1 tumour organoids were passaged at a rate of approximately once per week; MMTV-Wnt1 organoids every 10 days, with on-going culture and passage carried out in 48 well tissue culture treated dishes. Passaging was performed in a similar way to that described in 2.4.1.1, but with 750µl Trypsin added to account for an increased number of organoid per well, and cells filtered through a 40µm strainer. Cells were replated each time at a density of 1000 per µl growth factor reduced Matrigel, and overlaid with media as described above.

2.5.1.2 Tumour organoid freezing and thawing

Organoids at early passage grown for 3-4 days were recovered whole from their Matrigel matrix as described for passage (2.4.2.3) and resuspended in 1.5 ml homemade freezing medium (50% DMEM/F-12, 40% FBS, 10% DMSO), at an approximate density of 1.5 wells per cryovial, and stored at -80°C.

Cryovials of organoids were thawed rapidly in a 37°C water bath, and freezing media washed away thoroughly by repeated resuspension in 10 ml DMEM/F-12 and centrifugation at 125 x g for 4 minutes. The contents of each cryovial were resuspended in 300µl Matrigel, and overlaid with media corresponding to their original growth

condition, supplemented with Y-27632 for the first 3 days in culture. After a recovery period of 3-5 days, organoids were then passaged according to protocol 2.4.2.3.

2.5.2 Tumour organoid assays

2.5.2.1 Single inhibitor assays

Trypsinised tumour cells were seeded at a density of 1000 per µl (T1) or 750 per µl (MMTV-Wnt1) growth factor Reduced Matrigel, in NunC clear round-bottomed 96 well plates (12µl Matrigel per well). Following polymerisation of Matrigel at 37°C, each well was treated with 100µl complete media (Nrg1 (100 ng/ml), Noggin (100 ng/ml), R-Spondin1 (2.7 ng/ml) or EGF (50 ng/ml), Noggin (100 ng/ml), R-Spondin1 (42.5ng/ml)), supplemented with either control substance (% matched DMSO or PBS, relevant to corresponding inhibitor composition) or inhibitor of known concentration, diluted from 10µM stocks Table 2.5.

For 7 day treatment assays, media and inhibitors were replaced on the fourth day in culture. At least 3 replicate wells per condition were created in each case, and at least 9 titration points, plus control included.

2.5.2.2 Chou Talalay drug combination assay

Following single inhibitor titrations, IC50s were determined for each drug (Taxol and CCT251545). The ratio of IC50s was used to calculate combinatorial fixed ratio (1:1) two fold dilutions of the inhibitors. Three clear, round-bottomed 96-well plates were then seeded with T1 tumour cells as described in 2.5.2.1, one for each single inhibitor, and one for their combination. Cultures were then overlaid with media containing Nrg1 (100 ng/ml), Noggin (100 ng/ml) and R-Spondin1 (2.7 ng/ml), and one of the drug conditions detailed in Table 2.6. Nine titration points were created, plus a control, with at least 3 replicate samples per plate. All three plates, individual and combination, were assayed simultaneously as recommended by Chou (2006), for optimal comparison.

2.5.2.3 Replating assays

T1 tumour cells were seeded at 1000 per µl growth factor reduced Matrigel in NunC clear round-bottomed 96 well plates (12µl per well) and overlaid with media

Compound	Source	Diluted in	Dilution range (nM)	Fold dilution
Taxol	Merck Serono	DMSO	160 – 0.625	2
IWP-2	Sigma (I0536)	DMSO	2000 – 7.8	2
IWR-1	Sigma (I0161)	DMSO	1200 – 4.7	2
MSC2526550A	Merck Serono (Test compound)	DMSO	8000 – 31.25	2
MSC2501490A-5	Merck Serono (Test compound)	DMSO	8000 – 31.25	2
MSC2504877-A	Merck Serono (Test compound)	DMSO	8000 – 31.25	2
MSC2504070	Merck Serono **(Tool compound)**	DMSO	8000 – 31.25	2
CCT251545	Merck Serono (Test compound)	DMSO	8000 – 31.25	2
Anti-Lrp6 Tetrabody	Merck Serono (Test compound)	PBS	1000 – 0.051	3
Anti-Lrp6 SEED	Merck Serono (Test compound)	PBS	1000 – 0.051	3
Anti-Frizzled	Confidential source	PBS	1000 – 0.051	3

Table 2.5. Inhibitors used in organoid assays

Concentration (nM)		
CCT251545	**Taxol**	**Combination**
8000	133.33	8133.33
4000	66.67	4066.67
2000	33.33	2033.33
1000	16.67	1016.67
500	8.33	508.33
250	4.17	254.17
125	2.08	127.08
62.5	1.04	63.54
31.25	0.52	31.77
15.63	0.26	15.89
7.81	0.13	7.94
3.91	0.07	3.97
1.95	0.03	1.99
0.98	0.02	0.99

Table 2.6. Concentrations of CCT and Taxol used in combination assays

containing Nrg1 (100 ng/ml), Noggin (100 ng/ml) and R-Spondin1 (2.7 ng/ml) for 72 hours, to establish small structures. Culture media was then changed as described for each individual experiment, and culture maintained for a further 24, 48 or 72 hours. At this point, tumour organoids were retrieved and trypsinised according to protocol 2.5.1.2, and replated at 1000 cells per µl growth factor reduced Matrigel under the conditions indicated in each individual experiment, for a further 7 days.

2.6 General organoid analysis techniques

2.6.1 Morphological analysis

Organoids were monitored and representative images were taken routinely using a Leica DM IL inverted contrasting microscope, with a Moticam 2000 camera attached, at 4X magnification. Motic Images Plus was used for this purpose, and ImageJ used to apply scale bars and prepare images for figures.

2.6.2 Growth analysis

In order to track a variety of parameters (organoid number, diameter, optical density, etc.) of the cultures under study, plates were scanned periodically using GelCount™ technology (Oxford Optronix). Data obtained from these images was analysed using a defined charm* setting, in which parameters were set such that individual organoids could be detected. These settings were unique to either normal or tumour organoid measurement (Table 2.7).

Data collected in this way was further analysed using Microsoft Excel and/or GraphPad Prism. In general, the average of at least three wells was taken for each condition under study in a single biological repeat. Where possible, the average of more than a single biological repeat was taken.

2.6.3 Phenotypical analysis: standard immunohistochemistry

2.6.3.1 Sample processing

Organoids still embedded in growth factor reduced Matrigel (BD Biosciences) were fixed overnight in 10% Formalin at 4°C, and subsequently removed from the Matrigel through several washes in cold phosphate buffered saline (PBS), and centrifugation at 265 x g. Organoids were then suspended in equal volumes of cold PBS and 4% Low melting agarose (Sigma) prior to paraffin block embedding and sectioning.

2.6.3.2 Dewaxing, rehydration and antigen retrieval of slides

Slides were de-waxed through three 5 minutes washes in xylene, before rehydration in decreasing concentrations of ethanol (2x5 minutes in 100%, 2x5 minutes in 95% EtOH). Rehydration was completed by a minute wash in tap water, followed by a minute wash in dH_20. Slides were then placed in Citrate Buffer (DAKO) at 95°C for 20 minutes for antigen retrieval.

2.6.3.3 Prevention of endogenous staining

Slides were washed in PBS (pre-heated in microwave for 1 minute) for 5 minutes, RT PBS for a further five minutes, and placed in a 2.5% hydrogen peroxide solution (H_2O_2 (Millipore) in PBS) for 5 minutes. Slides were then washed twice for 5 minutes, in PBS.

2.6.3.4 Blocking and antibody staining

2.6.3.4.1 Vector Mouse on Mouse (MOM) Elite Peroxidase kit adapted protocol

Blocking serum provided by Vector was diluted in PBS, added to slides and incubated in a humidified chamber at RT for 1 hour. Slides were washed twice in PBS, before addition of MOM diluent for 5 minutes. Anti-mouse antibodies detailed in Table 2.8 were applied to slides, diluted in MOM diluent, and incubated overnight in a humidified chamber at 4°C.

Any excess, unbound primary antibody was removed by three 5 minute washes in PBS, before application of a 0.4% biotinylated secondary antibody solution (secondary antibody provided by Vector, diluted in MOM diluent), and incubation at RT for 30 minutes in a humidified chamber. Unbound secondary antibody was removed through three 5-minute washes in PBS. In order to see a signal from the secondary antibody, avidin-biotin complexes were formed through addition of the ABC solution supplied by Vector. This solution possesses both avidin (A), a strong binding protein of biotin, and a biotinylated enzyme (B), (in this case peroxidase) and was prepared 30 minutes before use, by mixing 2 drops of each of the A and B reagents in 2.5 ml PBS. This was incubated on the slides for 15 minutes in the dark at RT, and washed away with three 5 minute washed in PBS.

Charm* setting	Normal organoids	Tumour organoids
Edge detection sensitivity	30.1	62
Centre detection sensitivity	34.6	58.1
Soft colony lower diameter (µm)	45	30
Soft colony upper diameter (µm)	375	375
Minimum center to center separation	45	30
Smoothing	3	1
Circularity factor	2	2
Edge distance threshold	0.74	0.74
Number of spokes	32	32
Shape filtering	3	3
Shape processing	Best fit circle	Best fit circle
Colony diameter minimum (µm)	45	30
Colony diameter maximum (µm)	375	375
Colony minimum intensity (optical density)	0.01	0.01
Colony maximum intensity (optical density)	10	10
Good edge factor	0.06	0.06

Table 2.7. GelCount charm* settings for normal and tumour organoid analysis

Antigen	Source	Name/Clone; Catalog n°	Dilution
Luminal markers			
ERα	Daco	Clone (Mouse) C-1D5; M7047	1/100
PR	Thermo SCIENTIFIC	Clone SP2 (Rb^2) RM-9102	1/40
K8	Abcam	Polyclonal (Rb^2) C-04; ab735	1/100
Basal markers			
K14	Covance	Polyclonal (Rb^2) PRB-155P	1/500
P63	BD Transduction laboratories™	Clone (Mouse) C-04; ab735	1/40
K5	Covance	Polyclonal (Rb^2) PRB-160P	1/100
SMA	Abcam	Ab5694 Rabbit	1/200
Other markers			
Ki67	Millipore	Polyclonal (Rb^2) ab9260	1/500
E-cadherin	Abcam	Clone (Mouse) 36; 610182	1/400
β-catenin	BD Transduction laboratories™	Clone (Mouse) 14; 610154	1/500

Table 2.8. Primary antibodies used in IHC and immunofluorescence staining.

2.6.3.4.2 Vectastain ABC Kit (Rabbit IgG) adapted protocol

Blocking serum provided in the kit was diluted in PBS, added to slides and incubated in a humidified chamber at RT for 1 hour. Blocking solution was removed, and primary antibodies detailed in Table 2.8 were applied to slides, diluted in PBS/1%BSA, and incubated overnight in a humidified chamber at 4°C. Any excess, unbound primary antibody was removed by three 5-minute washes in PBS, before application of a 0.5% biotinylated secondary antibody solution (secondary antibody provided by Vector, diluted in PBS/1%BSA), and incubation at RT for 1 hour in a humidified chamber. ABC solution supplied in the kit was prepared 30 minutes before use, by mixing 1 drop of each of the A and B reagents in 5 ml PBS. This was incubated on the slides for 30 minutes in the dark at RT, and washed away with three 5-minute washes in PBS.

2.6.3.5 Visualisation of staining localisation

3,3'-diaminobenzidine (DAB), is a susbtrate of the biotinylated enzyme peroxidase. Peroxidase activity on DAB creates a colour change that allows visualisation of the location of antibody staining within the sample. Hence, DAB tablets (Sigma) were dissolved in dH20 and applied to the slides for 30-60 seconds, until staining could be detected. Slides were then washed in tap water, followed by distilled water, each for three minutes.

2.6.3.6 Counterstaining, dehydration and mounting of slides

Slides were counterstained in Mayer's Haematoxylin solution for 60-90 seconds, washed in tap water until excess stain removed, and dehydrated in increasing concentrations of ethanol (2x1 minute in 90%, 2x1 minute in 100%). Slides were then placed in xylene (3x3minutes), before mounting using DPX (Sigma).

2.6.3.7 Imaging of slides

Slides were imaged using a standard inverted microscope.

2.6.4 Phenotypical analysis: whole-culture immunostaining

Cells or organoids of interest plated and cultured on Nunc™ MicroWell™ 96-Well Optical-Bottom Plates in 10 ul of growth factor reduced Matrigel (BD Bioscience) were fixed by application of 4% paraformaldehyde at RT for 30 minutes.

Each well was then washed with PBS-Glycine, three times for 10 minutes, and left overnight at 4°C in 10% horse serum (Gibco), diluted in immunofluorescence (IF) buffer (Table 2.9). Primary antibodies, as detailed in Table 2.8, were then applied diluted in IF buffer, overnight at 4°C and removed by washing three times in IF buffer, lastly overnight at 4°C. Secondary fluorescent antibodies, as detailed in Table 2.10, were applied overnight at 4°C. Following three further washes in IF buffer, Hoechst counterstain was applied for 30 minutes, and washed out with PBS, before imaging. This protocol was adapted from Lee et al. (2007).

2.6.4.1 Confocal microscopy

Immunofluoresence staining was identified using confocal microscopy, performed using a Leica TCS SP2 AOBS spectral confocal microscope, by the 20X objective. Images were then processed using FIJI software.

2.6.4.2 InCell 6000

Several images were acquired using the InCell 6000, in agreement with GE Healthcare, with the aid of Bleddyn Williams, an MSc Biophotonics student.

2.6.5 OcellO analysis

Organoids were cultured as detailed above (2.4.2.1) for 12 days. A 5X concentrated proprietary OcellO stain-fixative containing simple nuclear and cytoskeletal stains was then applied to each well, and the plate left on a gently rocking platform overnight at RT. Each well was then topped up with PBS and the plate sealed before shipping to OcellO for in-depth morphometric analysis.

Reagent	Supplier, catalogue number	Final % in PBS (Invitrogen)
Albumin	Gift from Dr Tess Saltmarsh	0.1
Triton X-100	Sigma-Aldrich, T9284	0.2
Tween 20	Sigma-Aldrich, P1379	0.05

Table 2.9. Immunofluorescence buffer composition.

Antigen	Label	Source	Name/Clone; Catalogue n^{o}	Dilution
Rabbit IgG	AlexaFluor® 568	Life Technologies	A11011	1/500
Mouse IgG	AlexaFluor® 488	Life Technologies	A11029	1/500
Mouse IgG	AlexaFluor® 568	Life Technologies	A11031	1/500

Table 2.10. Secondary fluorescent antibodies used in IF staining.

2.6.6 Karyotype analysis

Organoids grown under defined conditions were treated with 0.05 µg/ml Colcemid (Gibco, Invitrogen) for 16 hours in order to inhibit microtubule and therefore spindle formation, arresting cells in metaphase. Organoids were then washed and trypsinised according to previously described protocols, before treatment with a hypotonic solution of potassium chloride (56mM), to cause osmotic cell swelling. Briefly, cells were kept in suspension using a vortex, while 1ml of hyptotonic solution was gradually added. A further 6 ml KCl was then added, and cells left in this suspension for 10 minutes. Following centrifugation at 225 x g for 4 minutes, cells were fixed in 3:1 MeOH:Acetic acid, again by slow addition over vortex. Cells were then washed two further times in fixative solution, before plating onto slides to create chromosome spreads. Slides were aged overnight at 55° C, before staining of chromosomes with 4', 6-diamidino-2-phenylindole dihydrochloride (DAPI). Images were obtained using an Olympus IX73 40X microscope, with a 40X objective. Chromosome spreads were counted manually using the ROI manager plugin of ImageJ software.

2.6.7 Gene expression analysis: Quantitative Reverse Transcription – Polymerase Chain Reaction (qRT-PCR)

2.6.7.1 RNA extraction

Plates were placed on ice before media was removed from each well and replaced with 400µl Trizol reagent (Invitrogen) treated with 125 µg/ml glycogen co-precipitant (Life technologies). The Trizol/Matrigel/organoid mix was mechanically disrupted with a P1000 pipette and transferred to a 1.5ml centrifuge tube and the well washed with a further 400 µl Trizol reagent. Organoids were lysed by vortexing the solution for 30 seconds, and 20 µl glycogen added to each tube. To enable phase separation, 160 µl chloroform/isoamyl alcohol 49:1 solution (Sigma Aldrich) was added each tube and the mixture vortexed for 15 seconds until emulsified, and held at RT for 2 minutes before centrifugation at 12,000g for 15 minutes at 4°C. The upper, aqueous layer of approximately 400 µl was then transferred to a new 1.5ml centrifuge tube, mixed with 400 µl isopropanol and left at RT for 5 minutes. The mixture was then centrifuged at 12,000g for 10 minutes at RT, leaving a small pellet visible. The pellet was washed twice with 75% ethanol at 7,500g, RT, and then allowed to air dry for 10 minutes. To remove DNA contaminants, Turbo DNase (Life technologies) was made up in a master mix (29.6 µl H_20, 3.4 µl 10x buffer and 1 µl DNAse per sample) and 34 µl applied to each RNA/glycogen pellet for 30 minutes at 37°C. The DNase was then inactivated using beads supplied in the kit, and the resulting mixture spun at 10,000g for 1 minute before transfer of supernatant to a labelled tube for quantification using the Nanodrop spectrometer.

2.6.7.2 cDNA synthesis

The RNA obtained from organoids was used as a template for cDNA synthesis, using the ImpromII kit from Promega. For this, starting masses of RNA were standardised to 450 ng per sample in the presence of 2 µl Random Hexamer primers made up to a final volume of 10µl in nuclease free water, and denatured at 70°C for 5 minutes, before cooling to 4°C. A No Template Control (NTC) was also created.

A Reverse Transcriptase reaction mastermix was made from components of the kit as detailed in Table 2.11, along with a No Reverse Transcriptase control mix, and 5µl of the contents of the denatured tubes added to 15 µl of each mix, in PCR strip tubes. The mixtures were then put through a 5 minute, 25°C annealing step, a 60 minute, 42°C

extension step and a 15 minute, 70°C enzyme inactivation step, before cooling to 4°C and 1/10 dilution in nuclease free water.

2.6.7.3 Gene Expression Analysis

qRT-PCR was carried out using MicroAmp fast optical 96-well reaction plates (Applied Biosystems), on a Step One Plus real-time PCR system (Applied Biosystems), using the SensiFAST SYBR Hi-ROX kit (Bioline) for detection and measurement of relative mRNA abundance. A mastermix of 10 µl SensiFAST SYBR Hi-ROX 2x, 0.1 µl forward primer, 0.1 µl reverse primer, and 6.8 µl nuclease free water was combined with 3 µl cDNA in each well, with each reaction carried out in triplicate. House-keeping genes ß-2 microglobulin (B2M), ribosomal protein L13A (RPL13A) and hypoxanthine phosphoribosyltransferase (HPRT) were analysed for each cDNA sample to normalise the expression levels of target genes (Table 2.12). Sealed plates were subjected to analysis under thermocycler conditions of: 95°C for 2 minutes followed by 40 cycles of 95°C for 5 seconds, 60°C for 10 seconds and 72°C for 20 seconds. StepOne software automatically recorded data and individual threshold cycle (C_T) values per well.

Analysis was performed on the average of triplicate C_T values, normalised by subtraction of the average of the triplicates of the three housekeeping gene C_T values, generating a ΔC_T value. The 2-ΔΔCT method, whereby the average of the ΔC_T values of the control condition is subtracted from the average of the ΔC_T value of the treatment condition to generate a $\Delta\Delta C_T$ value, was used to calculate fold expression changes by the equation fold change = $2^{-\Delta\Delta C_T}$. Statistical analysis was performed using a paired, two-tailed student T-test, on n=3 biological repeats.

	RT reaction (ml)	No RT control (ml)
Reverse Transcription Mix	1x	1x
Nuclease-Free Water (to a final volume of 15µl)	6.1	7.1
ImProm-II™ 5X Reaction Buffer	4	4
MgCl2 (6 uM final from 25 uM stock)	2.4	2.4
dNTP Mix (final concentration 0.5mM each dNTP)	1	1
Recombinant RNasin®Ribonuclease Inhibitor (optional)	0.5	0.5
ImProm-II™ Reverse Transcriptase	1	0

Table 2.11. Reverse transcription reaction mastermix.

Gene	Sequence	
	Forward	Reverse
PR	GCTTGCATGATCTTGTGAAACAGC	GGAAATTCCACAGCCAGTGTCC
RankL	GCAGATTTGCAGGACTCGACT	CCCCACAATGTGTTGCAGTT
Wnt4	GTCAGGATGCTCGGACAACAT	CACGTCTTTACCTCGCAGGA
B2M	CTTTCTGGTGCTTGTCTCACTG	AGCATTTGGATTTCAATGTGAG
HPRT	CCTAAGATGAGCGCAAGTTGAA	CCACAGGACTAGAACACCTGCTAA
RPL13A	CACTCTGGAGGAGAAACGGAAGG	GCAGGCATGAGGCAAACAGTC

Table 2.12. Primers used in qRT-PCR reactions.

2.7 Tumour organoid inhibitor assay analysis

2.7.1 Growth curve analysis

Responses to inhibitor were calculated using GelCount™ technology and software as previously described. Measurements were taken daily, from the earliest time point at which organoids could be detected by the software (T1, day 3; MMTV-Wnt1, day 2). "Total volume per well" data was used as the readout for this analysis, and was converted to fold vs control, untreated total volume per well and expressed as a log growth curve.

2.7.2 Cell viability analysis using Cell Titer Glo 3D

Organoids grown in single inhibitor titration experiments in 96-well round-bottomed plates were transferred to Costar 96 well white plates in their surrounding Matrigel, along with their current media (50µl). 50 µl Cell Titer Glo 3D reagent was then applied to each well, and the plate agitated in the dark on a Rickman shaker for 5 minutes at high speed to induce cell lysis and ATP release to enable the luciferase

reaction. Luminescence signal was allowed to stabilise for 1 hour, while the plate was slowly agitated in the dark, to keep cells in suspension. Luminescence was then recorded using a BMG Fluostar plate reader. For analysis, blank control media wells were included in each plate, and subtracted from the final values to account for background signal. For each condition, four technical repeats were used. Data was expressed as fold vs control untreated wells for each experiment.

2.7.3 Single inhibitor IC50 calculation

Inhibitor response curves were calculated using "Total volume per well" data from the GelCount™ system, and analysis based on principles set out by Chou & Talalay (1984). A template Excel spreadsheet was used to calculate the average "total volume per well" under control conditions, and from this, the fraction affected (f_a) and fraction unaffected (f_u) under each of the treatment conditions.

A linear regression analysis was then performed, in which the fraction affected (f_a) and fraction unaffected (f_u) at each dose was calculated, based on average total organoid volume per well, from at least 3 wells. Taking the f_u values between 0.9 and 0.1, a median effect line was generated by plotting of the log[(1/fu)-1] against the log(Drug concentration). The line was then used to calculate the log(IC_{50}), at the x intercept of the line, and the slope, m, indicating the sigmoidicity of the original dose-response curve. From this, the median effect equation:

$$\frac{f_a}{f_u} = \left(\frac{D}{D_m}\right)^m \text{, or rearranged to } D = D_m[fa/(fu)]^{1/m}$$

where D is a given dose of an inhibtor and d_m is the dose producing the median effect (IC_{50}), was used to calculate inhibitor IC50 (Chou & Talalay 1984). Where possible, the average IC50 from 2 or 3 biological repeats was calculated. Appendix II shows representative dose response curves.

2.7.4 Chou Talalay drug combination analysis

As previously described (2.5.2.2), and based on the 'Median effect principle', the ratio of the two individual IC_{50}s was used to generate a constant-ratio two-fold dilution range of the two inhibitors with several points either side of their IC_{50}s, and an assay performed in which each individual drug titration was carried out alongside an additional combination titration (Table 2.6).

Linear regression analysis was then performed using the method outlined in 2.7.3. As an assessment of synergy, an isobologram consisting of a line connecting two points (one on the y axis, depicting the concentration of drug A required to reach the IC_{50} for combination of drug A+B in absence of drug B, the other on the x axis, depicting the concentration of Drug B required to reach the IC_{50} for combination of drug A+B in the absence of drug A) was constructed to predict the required drug dose pairs at a constant ratio to produce the combined IC_{50}, assuming an additive effect. A third point was then plotted, the coordinates of the concentration of each drug required to reach the same effect (the IC_{50}) in combination. Any point to the left of the additive line represents a synergistic response to the two compounds – ie. a lower concentration of each of the compounds in combination is required to produce the same IC_{50}. Conversely, a point on the right represents an antagonism – a greater concentration of one or both drugs is necessary for the same effect (Foucquier & Guedj 2015).

Similarly, using the above equation principle, a combination index was then algebraically calculated as:

$$CI = \frac{(D)_1}{(D_x)_1} + \frac{(D)_2}{(D_x)_2}$$

for mutually nonexclusive drug interactions, where $(D)_1$ and $(D)_2$ were the concentrations of each drug in a combination to produce *x* survival, while $(D_x)_1$ and $(D_x)_2$ were the concentrations of each drug alone to produce the same *x* survival. Here, a final result equal to 1 (=1) signified an additive chemotherapeutic effect, while synergistic CI values would be below 1 (<1), and antagonistic CI values exceeding 1 (>1).

Full details of this combination analysis are described in Chou & Talalay (1984).

2.8 Mammary gland transplantation analysis

Whole 4th mammary fat pads were carefully dissected from transplanted mice and each spread across a microscope slide. Slides were placed for fixation into 4% neutral buffered formalin for 4 hours, in Coplin jars. After three 10 minute washes with PBS, whole mounts were stained overnight in Carmine solution at room temperature (RT). This was made by dissolving 1g Carmine and 2.5g Aluminium Potassium Sulphate in 500 ml deionised water, boiling for 20 minutes, adjusting to 500ml total volume and filtering the solution through Whatman Filter paper, before finally adding 50-100mg Thymol for

preservation of the solution. Following 3 thorough 10-minute washes in PBS, slides were next dehydrated in a series of increasing concentrations of ethanol (50% overnight, 70%, 90%, 100% for at least one hour each), at RT. Fat clearance was carried out in Methyl Salicylate (Sigma) within a fume hood for at least 1 hour, until the stained mammary structures were clearly visible. Wholemounts were examined on a binocular microscope (Zeiss, Stemi SV11). Images were captured with a Canon PC1089 camera and Canon Zoom Browser software (with white balance set to fluorescent, and auto exposure activated).

A negative score was assigned if no mammary structures were present, while a 'failed clear' exhibited intrusion of the original mammary epithelial network into the fat pad. In the case of a failed clear, numbers were not included in final scoring. Successful transplantation was judged by the organization of the epithelial networks, and their origin. Each successful take was also rated on the percentage of mammary gland repopulated by the new epithelial structures, as depicted by pie charts in individual figures.

2.9 General data analysis

Raw data obtained from the GelCount™ analysis of organoid assays was inputted into Microsoft Excel spreadsheets built to calculate means from individual experiments. For biological repeats, means and standard deviations were calculated and used for graphical representation of the data.

All statistical analysis was performed using GraphPad Prism for Mac. Comparison of two means was performed using a two-tailed T-test, or a Mann-Whitney U test for non-normally distributed data. Comparisons between multiple means were performed using analysis of variance analysis (ANOVA), with Dunnett's (comparison against one control) or Tukey's (comparison between all means) post-hoc analysis.

3 Optimisation and characterisation of a mammary epithelial organoid model.

3.1 Introduction

The recent advances in the use of representative organoid models from various organs (Sato et al. 2009) have set a precedent indicating the potential for the similar use of a mammary organoid model in the study of both normal developmental signalling pathways in the mammary gland and those driving malignancy and tumour behaviour, in addition to as a pre-clinical tumour model for drug discovery.

In order to be considered a truly representative model, and therefore useful in achieving any of these outcomes, any mammary organoid model system must firstly be fully refined and characterised to definitively meet three key criteria concurrently:

1) *In vitro* recapitulation of the *in vivo* mammary gland architecture;
2) Differentiation, maintenance and functionality of all MEC populations for extended periods.
3) Extended repopulating cell capacity, and thus significant expansion capability.

While previous publications by other groups have offered simple 3-D *in vitro* mammary culture systems that have expanded our knowledge of various aspects of mammary biology, including cell proliferation and differentiation, paracrine signalling, hormonal regulation and the identity of the stem cell population and it's niche, no such systems have yet met these criteria simultaneously. Many systems grow primary material for a short time only in culture – the longest currently published culture duration for organoids with well organised, heterogenous cell populations and maintained hormone responsiveness is 14-21 days (Obr et al. 2013), while longer term cultures in which mammary stem cells are able to be expanded are associated with small, disorganised colonies (Zeng and Nusse 2010). Looking prospectively at the system as a model for investigation of normal biological responses or as a pre-clinical therapeutic model, there is a need for physiologically relevant mammary organoids to be grown in large quantities with high efficiency (in terms of both speed and output) from small quantities of starting material, if they are to be used in medium to high throughput studies. Initial data generated in the Dale lab by Dr Jardé, using the intestinal culture conditions as a starting

point, was able to demonstrate the basic ability to grow 'mammary organoids' from primary murine tissue.

As previously described in Chapter 1, the Wnt signalling pathway has long been implicated in mammary gland development and maintenance processes. In support of this, preliminary mammary organoid culture data from the Dale group based on original conditions set out by Sato *et al* (2009) indicated that mammary organoids, more so than intestinal or liver organoids, were extremely sensitive to the concentration of the Wnt signal potentiator R-Spondin1 applied to them. Too high a concentration was shown to drive the development of abnormal, highly keratinous mammary organoids resembling the phenotype of the MMTV-Wnt1 tumour (Appendix I-1), while no R-Spondin1 stimulation at all led to fewer, smaller structures forming. It was therefore proposed that a 'just right' level of Wnt/R-Spondin1 stimulation may be required to encourage the desired mammary organoid phenotype and morphology to develop, while still stimulating organoid formation efficiency.

Furthermore, while EGF has historically been widely used in *in-vitro* mammary cell cultures and is the RTK ligand of choice in formative organoid studies by Hans Clevers and Toshiro Sato, there have to date been no extended cultures of mammary cells *in vitro* in which EGF has successfully been able to maintain concurrently cell proliferation, differentiation, and normal tissue architecture. In early exploration of alternative RTK ligands relevant to mammary development, qRT-PCR experiments by Jardé *et al*. (2016) indicated that MECs, particularly luminal populations, express ErbB3/4 receptors typically used in Neuregulin1 (Nrg1) signalling (Appendix I-2). In addition, basal cells express high levels of Nrg1 mRNA transcripts, suggesting a paracrine Nrg1 signalling network between cell types within the mammary gland. In support of this, Nrg1 (100 ng/ml), in combination with Noggin (100 ng/ml), was shown in basic organoid culture experiments by *Jardé et al.* (2016) to improve organoid formation efficiency and size, producing a 3 fold increase in cell viability in a direct comparison with EGF (50 ng/ml) in culture (Appendix I-3) with further increases in viability with increased concentration of Nrg1.

The work detailed in this chapter therefore builds upon this early data, further investigating the 'just-right' hypothesis of R-Spondin1 stimulation and the use of Nrg1 signalling in mammary organoid development and growth, to enable the generation and

optimisation of a utilisable, physiologically relevant system allowing expansion of organoid numbers over 2.5 months in culture.

3.2 Results

3.2.1 Optimisation of mammary organoid culture conditions

3.2.1.1 R-Spondin1 is a crucial regulator of mammary organoid formation efficiency, size and differentiation status

As a starting point for this project, early findings described above were first reconfirmed using a new source of R-Spondin1 (Peprotech), at a concentration comparative to previously used levels of R-Spondin1 (R&D Systems). R-Spondin1 (85 ng/ml) was applied to cultures in combination with the original receptor tyrosine kinase ligand provided in the intestinal culture conditions, EGF (50 ng/ml), and the TGF-β pathway inhibitor, Noggin (100 ng/ml). Organoids grown for 14 days under these conditions were observed to grow profusely, as large, round structures possessing highly squamous cores, exhibiting what was termed an 'abnormal' phenotype. These structures were lacking in both the expected mammary hormone receptors and luminal keratin 8 expression, while expressing at high levels the known basal cell markers Keratin 14 and p63 (Figure 3.1).

Furthermore, the previously proposed alternative RTK ligand Nrg1, in combination with a high R-spondin1 concentration, generated structures nearly identical to those grown under EGF stimulation, that is, lacking in normal phenotypic expression markers while containing a highly keratinous, squamous core (Figure 3.2). This implied that while choice of RTK ligand may play a part in determining organoid growth efficiency and development, it was the Wnt activity within structures that inferred the majority of their phenotypic development. In order to investigate this hypothesis further, titrations of R-Spondin1 were performed, and analysis of effect on organoid formation efficiency, diameter (µm) morphology and phenotype carried out, with the aim of finding the optimal R-Spondin1 concentration for mammary development.

Cells obtained through the trypsinisation of primary mammary epithelial fragments were seeded at an approximate density of 1000 per µl growth-factor reduced Matrigel, and overlaid with basic mammary organoid culture media

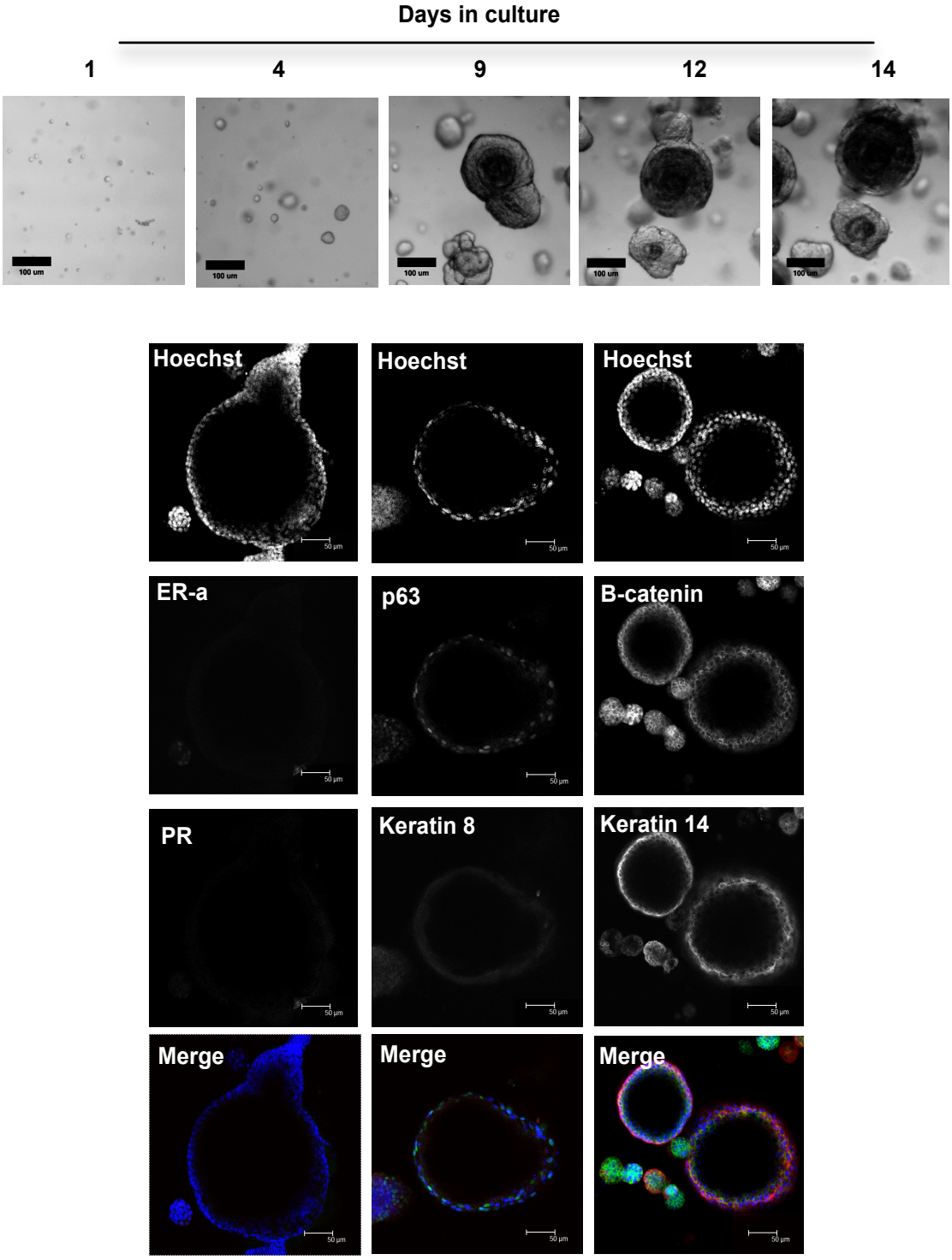

Figure 3.1 Characterisation of organoids grown in EGF and noggin media supplemented with a high concentration of R-Spondin1.

Primary MECs were isolated, seeded in growth factor reduced Matrigel and cultured for 14 days in media containing EGF (50 ng/ml), noggin (100 ng/ml) and R-Spondin1 (85 ng/ml). **(A)** Representative images of organoid morphology over 14 days in culture. Scale 100 µm. **(B)** Wholemount immunostaining of organoids fixed at day 14. Organoids were co-stained for: luminal markers ER and PR; basal p63 and luminal Keratin 8; basal Keratin 14 and β-catenin, and counterstained with Hoechst. Scale 50 µm.

supplemented with Neu (100 ng/ml) and Nog (100 ng/ml). A two-fold dilution range of R-spondin1 between 21.3 ng/ml and 85 ng/ml was applied to cultures alongside a no R-Spondin1 control (Figure 3.3). It was clearly evident after 12 days that structures treated with all concentrations of R-Spondin1 possessed an 'abnormal' keratinous core, and as a result further titrations were performed using the same method.

Between a range of 2.7 and 21.3 ng/ml R-Spondin1, the number of organoids formed was seen to positively correlate with increasing R-Spondin1 concentration (Figure 3.4C), as did the size of organoids formed (Figure 3.4D), as determined by analysis performed using GelCount^{TM} technology based on a fixed organoid detection (charm*, see Methods Table 2.7) setting. Morphologically, organoids grown for 15 days under R-Spondin1 concentrations higher than 5.3 ng/ml were restricted to the abnormal, highly keratinous appearance (Figure 3.4A) previously associated with a lack of differentiation of luminal cell types. Phenotypic analysis confirmed this to be the case - such structures were observed to lack hormone receptor expression, while showing extremely strong expression of basal keratin 14 expression (Figure 3.4B).

In cultures grown at 5.3 ng/ml R-Spondin1, structure morphology was no longer homogeneously considered abnormal, such that around 50% of the structures possessed a highly keratinous core and thin outer layer of basal cells, while the remaining structures better resembled those of the desired morphology, and expressed both luminal and basal cell markers, in an architecture similar to that of the *in vivo* mammary gland (Figure 3.4A, B, F). At the lowest R-Spondin1 concentration assessed (2.7 ng/ml), while a minority of structures (<5%) developed keratinous cores, most remained at a morphology and phenotype recapitulating that found *in vivo* (Figure 3.4A, B) making this concentration the most suited to mammary organoid culture. Staining performed on this condition to assess PR and SMA expression was deemed inconclusive (Figure 3.4B, D, F), warranting further, in depth analysis of this condition.

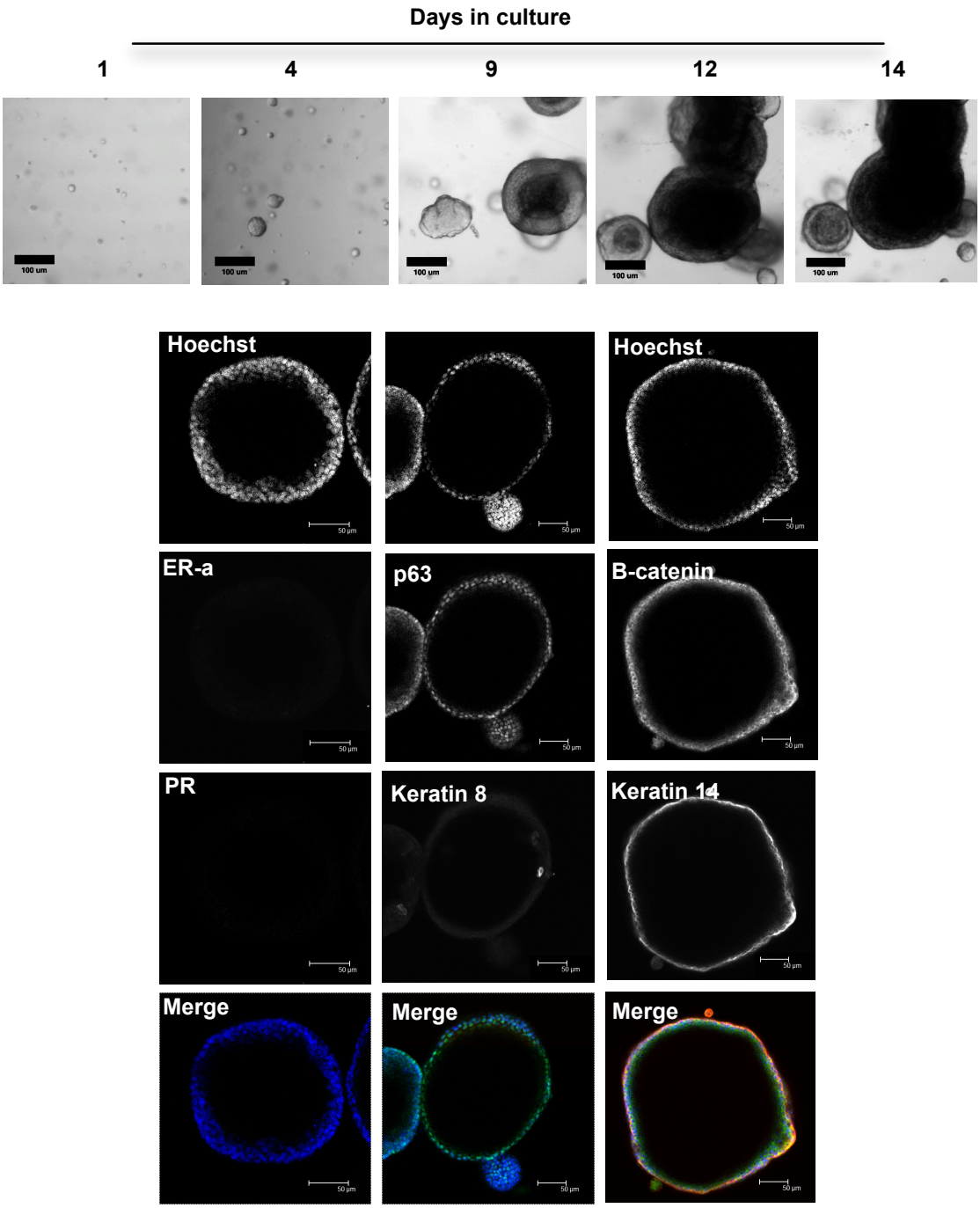

Figure 3.2 Characterisation of organoids grown in Nrg1 and noggin media supplemented with a high concentration of R-Spondin1.

Primary MECs were isolated, seeded in growth factor reduced Matrigel and cultured for 14 days in media containing Nrg1 (100 ng/ml), noggin (100 ng/ml) and R-Spondin1 (85 ng/ml). **(A)** Representative images of organoid morphology over 14 days in culture. Scale 100 µm. **(B)** Wholemount immunostaining of organoids fixed at day 14. Organoids were co-stained for: luminal markers ER and PR; basal p63 and luminal Keratin 8; basal Keratin 14 and β-catenin, and counterstained with Hoechst. Scale 50 µm.

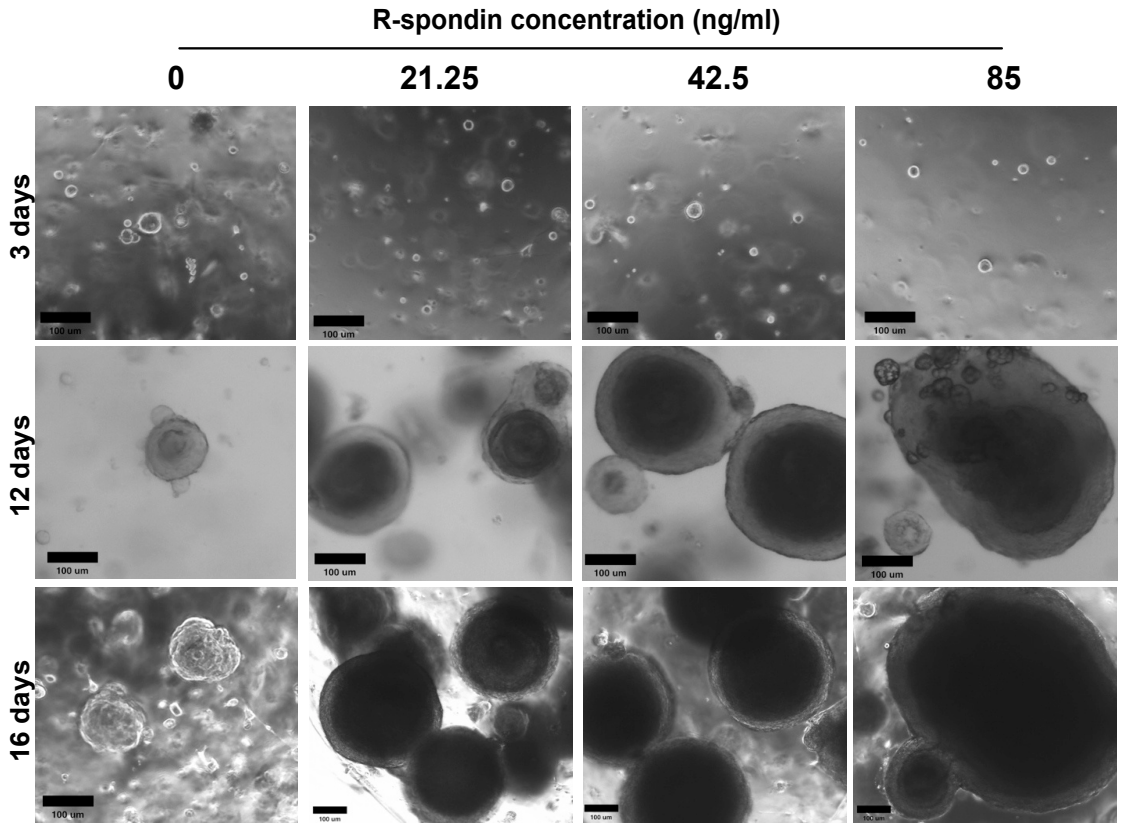

Figure 3.3 Morphology of mammary epithelial organoids grown under a titration of R-Spondin1 concentrations over a 16 day period.

Unsorted, 'single' cells were seeded at a density of 1000 per µl growth-factor reduced Matrigel, and overlaid with DMEM/F12 based media supplemented with Nrg1 (100 ng/ml), noggin (100 ng/ml) and either 0, 21.25, 42.5 or 85 ng/ml R-Spondin1 (Peprotech), and images taken over a 16 day period. Scale 100 µm.

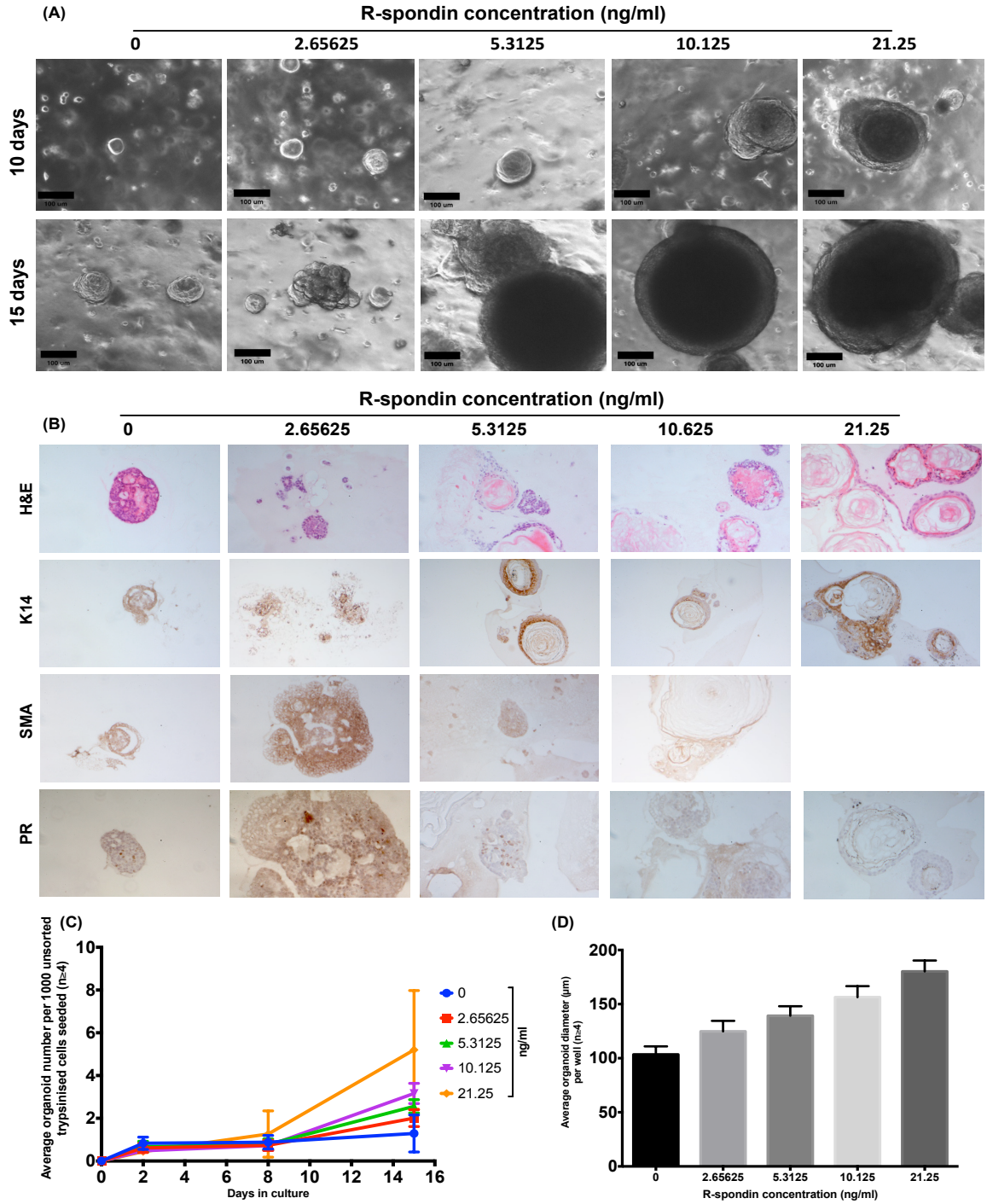

Figure 3.4 Analysis of mammary epithelial organoids grown under a titration of R-Spondin1 concentrations over a 15 day period.

Unsorted, trypsinised single cells were seeded at a density of 1000 per µl growth-factor reduced Matrigel, and overlaid with DMEM/F12 based media supplemented with Nrg1 (100 ng/ml), noggin (100 ng/ml) and either 0, 2.7, 5.3, 10.1 or 21.3 ng/ml R-Spondin1 (Peprotech). **(A)** Morphology of organoids after 10 and 15 days in culture. Scale bars 100 µm. **(B)** Histological analysis of organoids after 15 days in culture. Slides were stained with Haematoxylin and eosin (H&E), and antibodies against basal markers Keratin 14 and smooth muscle actin (SMA), and luminal marker Progesterone receptor (PR). **(C)** Average organoid number per 1,000 unsorted, trypsinised single cells seeded over a 15 day period (n≥4)**.(D)** Average organoid diameter (µm) after 15 days in culture. Data points shown as mean ± standard deviation.

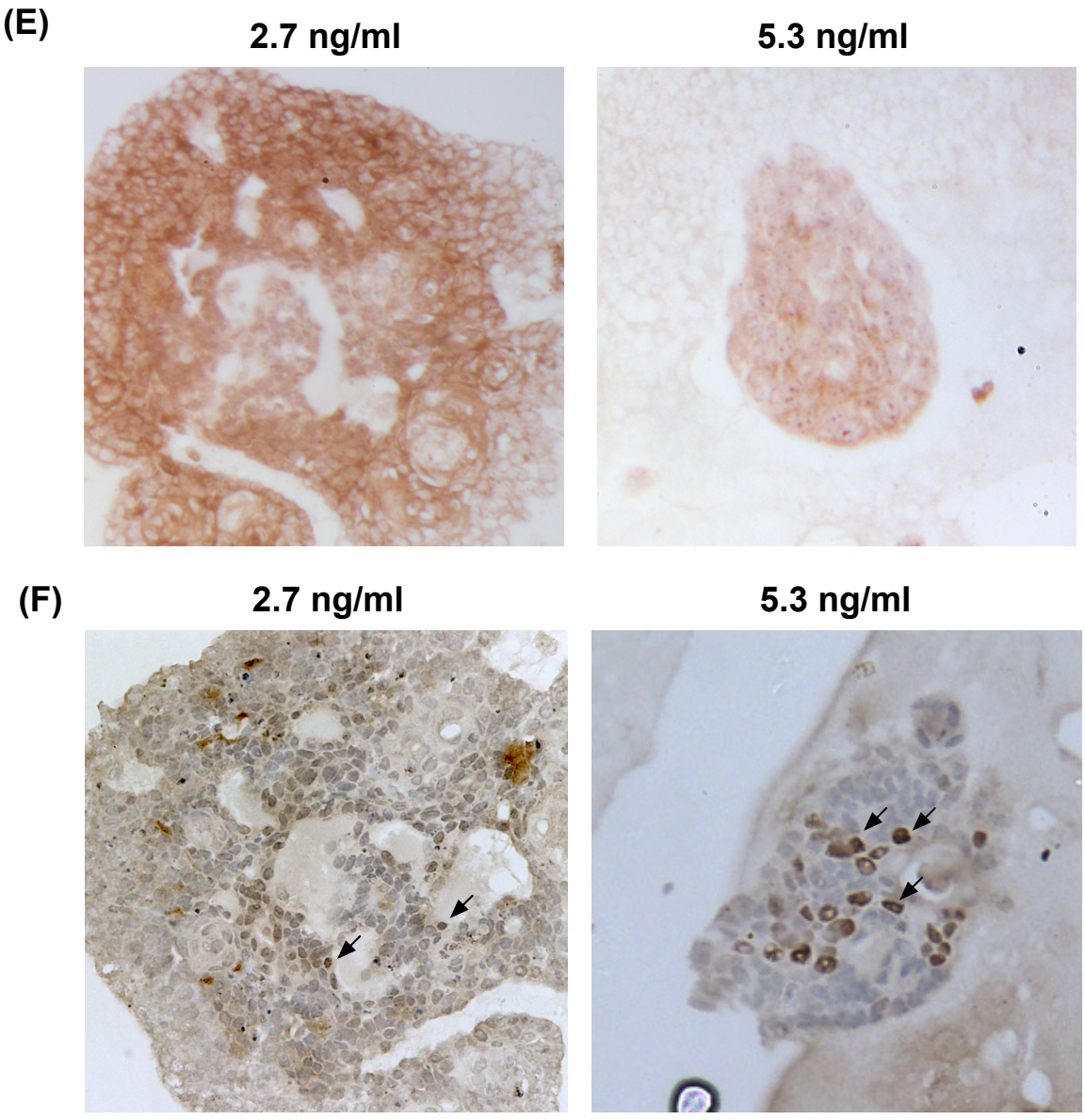

(E) High magnification SMA staining of organoids grown under 2.7 ng/ml or 5.3 ng/ml R-Spondin1. SMA staining was deemed inconclusive at these concentrations of R-Spondin1. **(F)** High magnification PR staining of organoids grown under 2.7 ng/ml or 5.3 ng/ml R-Spondin1. Arrows indicate positive staining.

In order to ensure that the GelCount™ readouts of organoid formation efficiency per 1000 cells plated or organoid diameter were not inappropriately skewed by the presence of cell doublets, or larger aggregations of cells in plated populations, fluorescence-activated cell sorting (FACS) was implemented. Trypsinised epithelial cells were stained with DAPI and anti-CD45 and sorted to remove any epithelial cell clumps, doublets, or dead cells, in addition to any stromal or non-epithelial cells (CD45+) (See Materials and methods, Figure 2.2).

After 15 days, sorted, live, single cells plated at 1000 per ul Matrigel under conditions where a two-fold titration range of 2.7 ng/ml to 21.3 ng/ml R-spondin1 was applied showed results consistent with what had been seen previously, again indicating the use of the lowest R-Spondin1 concentration of 2.7 ng/ml, and demonstrating a dose dependent increase in organoid formation, diameter and squamous morphology with R-Spondin1 (Figure 3.5).

3.2.1.1.1 Organoid formation efficiency can be further increased using the Rho-Kinase inhibitor Y-27632

In addition to determining conditions for the production of phenotypically 'normal' mammary organoids, this work aimed to maximise the organoid output from a small mass of starting material. As already demonstrated, to generate morphologically and phenotypically normal mammary organoids, R-Spondin1 concentration had to be limited, thus compromising on the improvements in growth rate and plating efficiency gained by adding high levels of the factor. The solution to this problem however, came as the result of an unexpected finding following the FACS based titration detailed above.

It was noted that compared to previous results using unsorted cells, consistently lower organoid formation efficiencies were observed from sorted cells at each R-Spondin1 concentration (6.3, 5.4, 3.4 and 4 fold lower, respective to increasing concentrations), with most strikingly, an 18.4 fold reduction in organoid formation under control conditions (Figure 3.5). The degree to which this was observed was somewhat surprising given that the process refined cell populations, excluding dead and non-epithelial cells, thus theoretically increasing the proportion of cells likely to grow into organoids. The stresses put upon cells during FACS can drastically decrease viability, and in single cell populations loss of cell-cell contacts is known to activate signalling cascades

leading to programmed cell death (Kurosawa, 2012). As such, many publications in which FACS has been performed for the purpose of single cell investigations detail the use of the Rho associated coiled-coil protein kinase (ROCK) inhibitor Y-27632 after sorting. Y-27632 has previously been demonstrated to promote the survival of cell types susceptible to anoikis upon dissociation to single cells, including human induced pluripotent stem cells (Park et al. 2008) and human embryonic stem cells (Watanabe et al. 2007), with the latter specifically being shown to benefit from ROCK inhibition following FACS (Emre et al. 2006). Sato et al. (2009) also detail the use of the inhibitor in their intestinal crypt culture system following cell sorting to benefit crypt growth.

As such, a titration was performed on sorted, single epithelial cell cultures in which Y-27632 (10 μM) was supplemented into the media for the first 5 days. Results after 15 days showed substantial increases in organoid formation efficiency per 1000 cells plated at all R-Spondin1 concentrations trialled (9.2, 9.3, 6.2, 2.3 fold with increased concentrations), to a range similar to that seen in cultures of unsorted, trypsinised cells without the inhibitor (Figure 3.6). Interestingly, average organoid diameter at each R-Spondin1 concentration was also seen to increase in comparison to its untreated counterpart (1.5, 1.4, 1.3, 1.6 fold, respectively) (Figure 3.6C).

Moreover, this result was not specific to post-FACS organoid culture; unsorted, trypsinised cells grown with the support of Y-27632 for the first 5 days of culture also showed improved organoid formation efficiency, albeit not to the same magnitude as sorted cell populations (1.9, 2.2, 2.3, 1.7 fold, Figure 3.7B). This may in fact confirm that most cells within these populations are not definitively single, and therefore do not require the support from the inhibitor to the same extent. Y-27632 treatment also caused a larger average organoid diameter under all R-Spondin1 conditions (1.3, 1.3, 1.3, 1.1 fold, Figure 3.7C), suggesting that a level of apoptosis may occur even in established organoids.

With the advantages of ROCK inhibition clear, it was instated as a standard early culture media component within the mammary organoid system alongside Neuregulin, Noggin and R-Spondin1 (2.7 ng/ml), even for organoids derived from epithelial fragments, in order to enhance organoid formation efficiency. However, as the exact mechanism of Y-27632 is not yet confirmed, it was not used continually throughout culture in order to avoid potential unwanted effects to growth and differentiation.

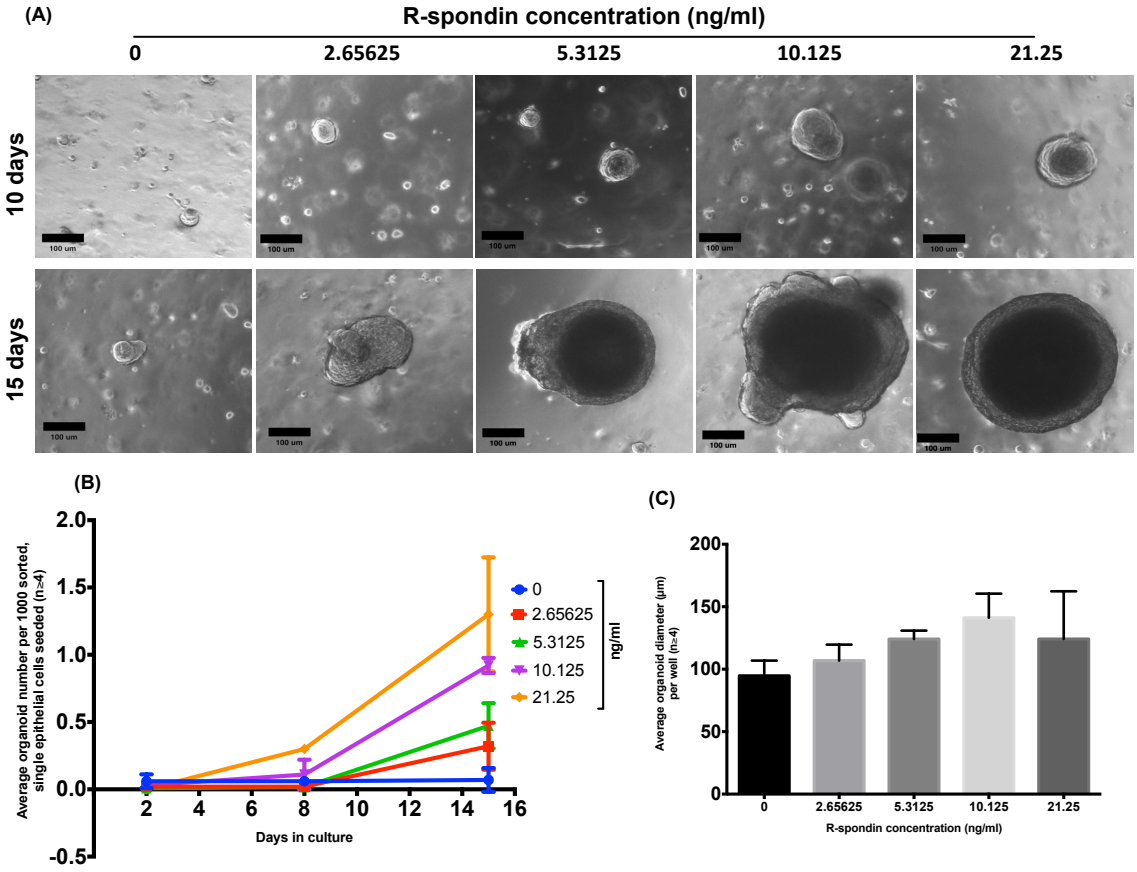

Figure 3.5 Analysis of mammary epithelial organoids grown from single, sorted cells under a titration of R-Spondin1 concentrations over a 15 day period.

Sorted, single epithelial cells were seeded at a density of 1000 per µl growth-factor reduced Matrigel, and overlaid with DMEM/F12 based media supplemented with Nrg1 (100 ng/ml), noggin (100 ng/ml) and either 0, 2.7, 5.3125, 10.125 or 21.25 ng/ml R-Spondin1 (Peprotech). **(A)** Morphology of organoids grown after 10 and 15 days in culture. **(B)** Average organoid number per 1,000 sorted single epithelial cells seeded, over a 15 day period (n≥4). **(C)** Average organoid diameter (µm) after 15 days in culture. Data points shown as mean ± standard deviation. Scale bars 100 µm.

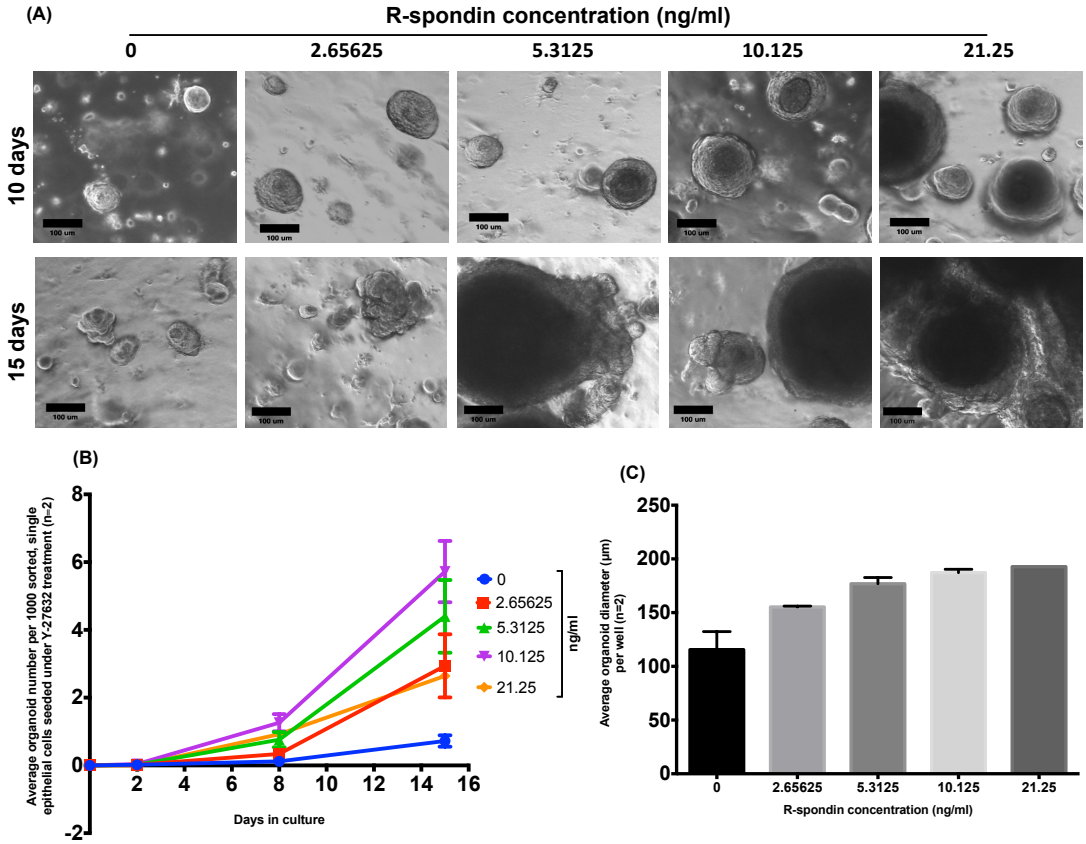

Figure 3.6 Analysis of ROCK inhibitor treated mammary epithelial organoids grown from single, sorted cells under a titration of R-Spondin1 concentrations over a 15 day period.

Sorted, single epithelial cells were seeded at a density of 1000 per µl growth-factor reduced Matrigel, and overlaid with DMEM/F12 based media supplemented with Nrg1 (100 ng/ml), noggin (100 ng/ml) and either 0, 2.7, 5.3125, 10.125 or 21.25 ng/ml R-Spondin1 (Peprotech). The Rock inhibitor Y-27632 was also applied for the first 5 days of culture (10µM). **(A)** Morphology of organoids after 10 and 15 days in culture. Scale bars 100 µm. **(B)** Average organoid number per 1,000 single epithelial cells seeded over a 15 day period, following Y-27632 treatment (n≥4). **(C)** Average organoid diameter (µm) after 15 days in culture following Y-27632 treatment. Data points shown as mean ± standard deviation.

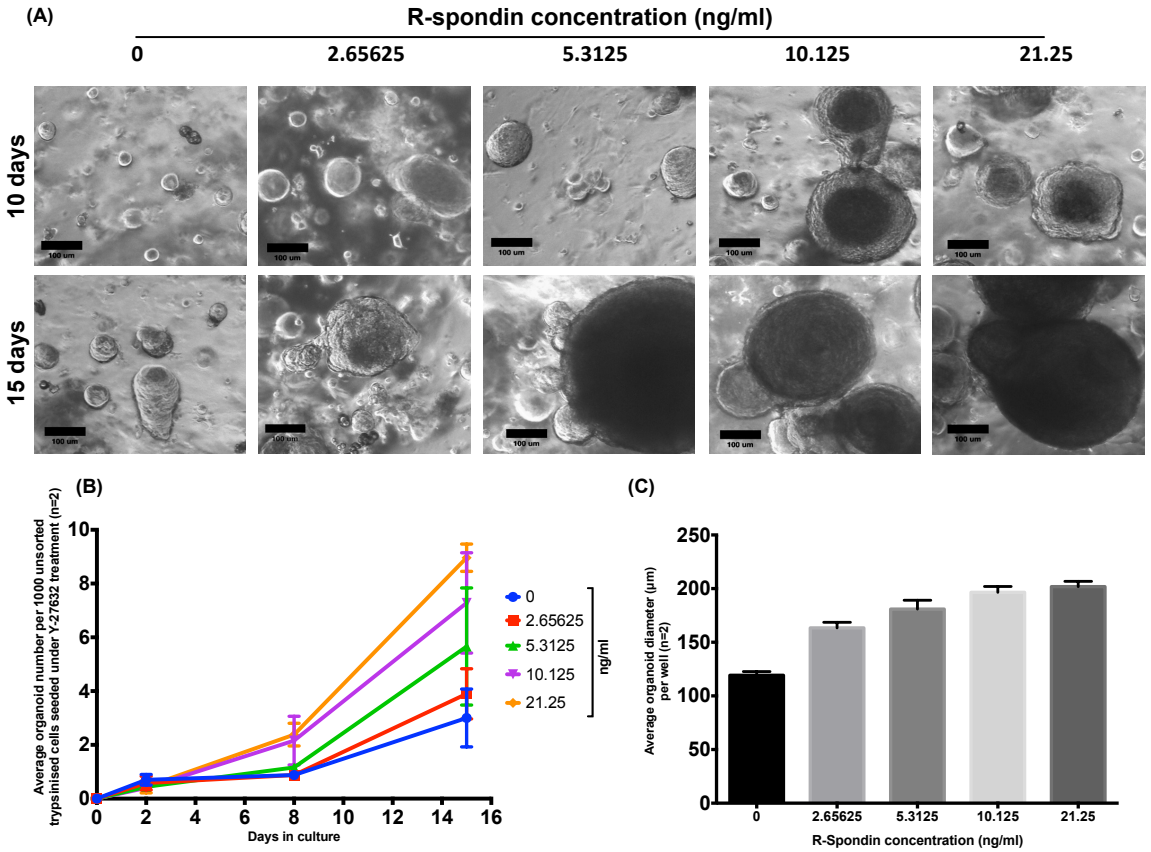

Figure 3.7 Analysis of ROCK inhibitor treated mammary epithelial organoids grown under a titration of R-Spondin1 concentrations over a 15 day period.

Unsorted, trypsinised single cells were seeded at a density of 1000 per µl growth-factor reduced Matrigel, and overlaid with DMEM/F12 based media supplemented with Nrg1 (100 ng/ml), noggin (100 ng/ml) and either 0, 2.7, 5.3125, 10.125 or 21.25 ng/ml R-Spondin1 (Peprotech). The Rock inhibitor Y-27632 was also applied for the first 5 days of culture (10µM). **(A)** Morphology of organoids after 10 and 15 days in culture. Scale bars 100 µm. **(B)** Average organoid number per 1,000 unsorted, trypsinised single cells seeded over a 15 day period, following Y-27632 treatment (n≥4). **(C)** Average organoid diameter (µm) after 15 days in culture following Y-27632 treatment. Data points shown as mean ± standard deviation.

3.2.1.1.2 High content imaging and analysis of organoids reveals detailed effects of R-spondin1 in culture

Although R-Spondin1 stimulation was shown likely to be key in increasing the plating efficiency and size of organoids, the extent to which GelCount™ measurements could be interpreted biologically was limited for several reasons. For example, a larger organoid could reflect increased cell proliferation and remodelling inside the structure, or cell death and an accumulation of debris. In order to analyse in greater detail the effects of R-Spondin1 on organoid morphology, a new high throughput 3D screening, imaging and profiling system, available through collaboration with a company called OcellO , was utilised. Using this technology, up to 900 parameters, many of which would be otherwise impossible to analyse, can be measured and compared. In this study, only a select number were chosen for analysis.

Mammary epithelial organoids were grown in 384 well format from trypsinised single epithelial cells for 14 days, under Nrg1 (100 ng/ml) and Noggin (100 ng/ml) supplemented conditions alone, or in combination with the determined optimal concentration of R-Spondin1 (2.7 ng/ml) or a proven 'high' concentration of 42.5 ng/ml R-Spondin1. In addition, the original intestinal ERH conditions deemed unfavourable for mammary organoid growth were used in comparison. Organoids were fixed and stained at the end of culture using a proprietary OcellO fixative solution, containing simple cytoskeletal (Phalloidin) and nuclear stains (Hoechst) (described in (Di et al. 2014)).

The four culture conditions were clearly observed to induce differential effects on many parameters, as shown by heat mapping across the plate (Figure 3.8A). Four key parameters were chosen by OcellO and studied in further detail (Figure 3.8B). Consistent with previous GelCount™ analysis, OcellO data confirmed that increasing R-Spondin1 concentration increased organoid size, in a concentration dependent manner, when in combination with Nrg1 and Noggin (Figure 3.8C). Analysis also highlighted novel data showing a concentration dependent reduction in lumen roundness and increase in lumen complexity, and a decrease in the fraction of apoptotic cells within the organoids.

Interestingly, under direct comparison, ERH treated organoids grown for the same time were on average smaller than NRH treated organoids, and were characterised to contain a higher proportion of apoptotic cells and display both increased lumen

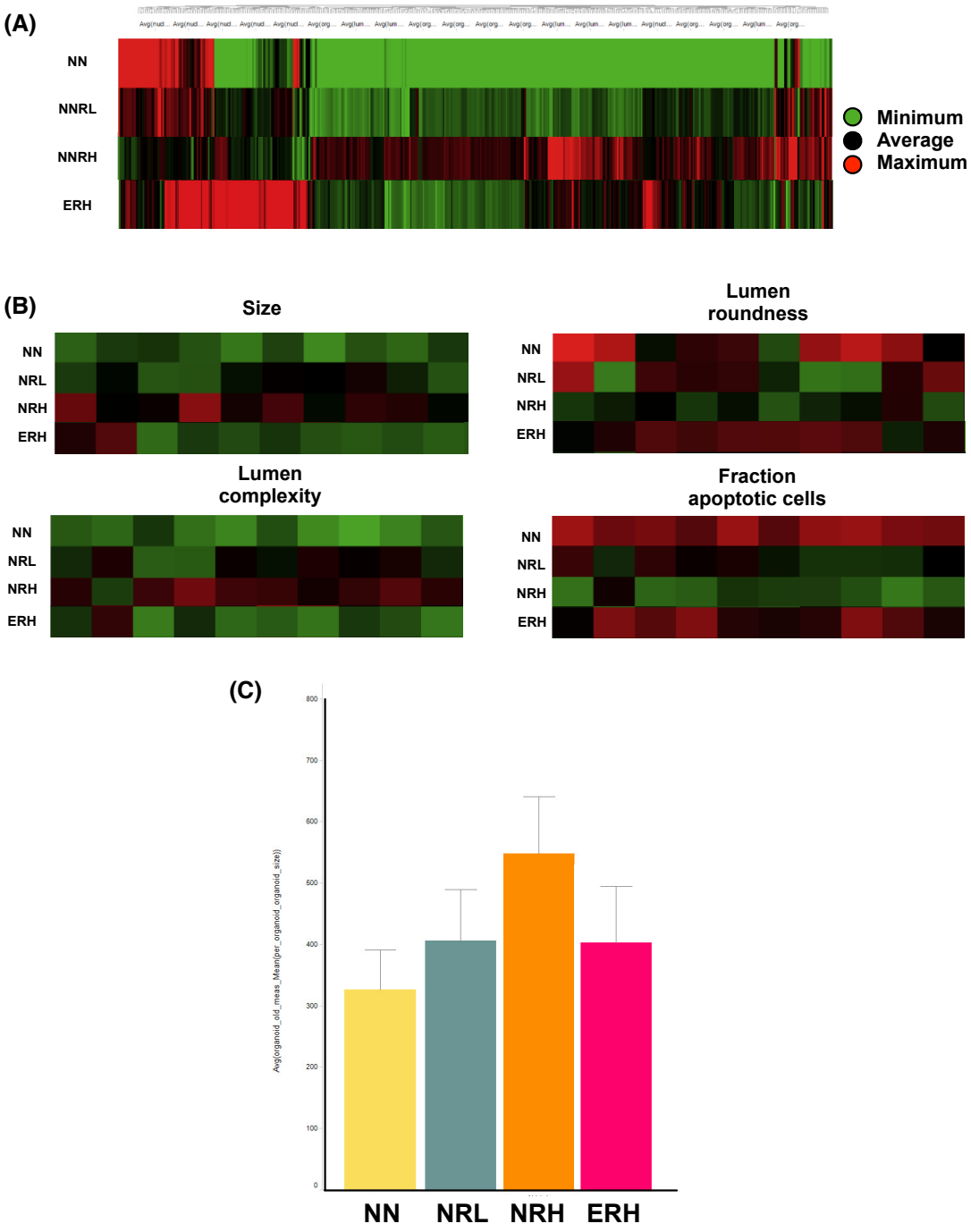

Figure 3.8 In depth OcellO analysis of organoids grown under specific culture media conditions reveals distinct effects of culture components.

Freshly isolated MECs were seeded in 384 well format in growth factor reduced Matrigel and grown for 14 days under conditions containing either: Nrg1 (100 ng/ml) and noggin (100 ng/ml) alone **(NN)**; Nrg1 and noggin in combination with R-Spondin1 (2.7 ng/ml) **(NRL)** or R-Spondin1 (42.5 ng/ml) **(NRH);** or EGF (50 ng/ml), noggin (100 ng/ml) and R-spondin1 (42.5 ng/ml). Organoids were then fixed in OcellO proprietary stain and analysed by OcellO. **(A)** Feature cluster heat map indicating variation in multiple organoid properties between each culture condition. Over 400 parameters are summarized here. **(B)** Heat maps indicating variation in organoid size, lumen roundness, lumen complexity and fraction of apoptotic cells per organoid between culture conditions. **(C)** Bar chart indicating average organoid size under each culture condition.

roundness and decreased lumen complexity, thus supporting the use of Nrg1 as the main RTK ligand in mammary organoid culture.

3.2.1.2 R-Spondin1 elicits effects in the mammary organoids through regulation of the Wnt pathway

Although R-Spo1 is known to up-regulate canonical Wnt signalling (de Lau et al. 2011), members of the R-Spondin1 family have also been associated with non-canonical Wnt signalling, specifically through the Wnt/Planar cell polarity (PCP) pathway (Ohkawara et al. 2011). As this pathway directs cell alignment within tissues and is associated with the regulation of stem cell fate – whether a SC divides asymmetrically or not (van Amerongen 2012) - it could be speculated to be responsible for the single layer of p63 positive cells characteristically seen in organoids grown under high levels of R-Spondin1 (Figure 3.2).

In order to confirm that the effects observed on organoid culture under R-Spondin1 stimulation were indeed elicited via a canonical Wnt signalling pathway, a previously characterised tetracycline-inducible mouse model (Jardé et al. 2012), able to express a truncated, constitutively active version of the β-catenin protein (ΔN89β-Catenin) when treated with doxycycline, was used in an organoid growth assay. Here, organoids cultured under Nrg1 (100 ng/ml) and Noggin (100 ng/ml) supplemented conditions (N) were compared to those grown in the presence of R-Spondin1 (2.7 ng/ml) (NRL), Doxycycline (DOX) (2µg/ml)(DN), or both in combination (DNRL). It was observed, as previously seen with cells derived from FvB mice, that after 7 days, NRL treatment increased organoid formation and average diameter slightly, but not significantly (Figure 3.9A, B). DN or DNRL conditions however, had significant growth promoting effects on the organoids compared to those in N or NRL conditions ($p<0.05$, $n=3$). Importantly, DN and DNRL treated organoids exhibited the typical squamous morphology associated with high R-Spondin1 stimulation (Figure 3.9C), while DNRL media had no significant additional effect on organoid formation or diameter compared to DN, indicating β-catenin and R-Spondin1 to work via the same signalling pathway.

To further verify this finding, the experiment was conducted again, using the intestinal culture conditions (ERH) set out by Sato *et al.* (2009). In this case, organoid growth efficiency was similar between all of the treated conditions compared to the EGF only control, with each producing significantly more organoids (1.18, 1.25 and 1.20 fold,

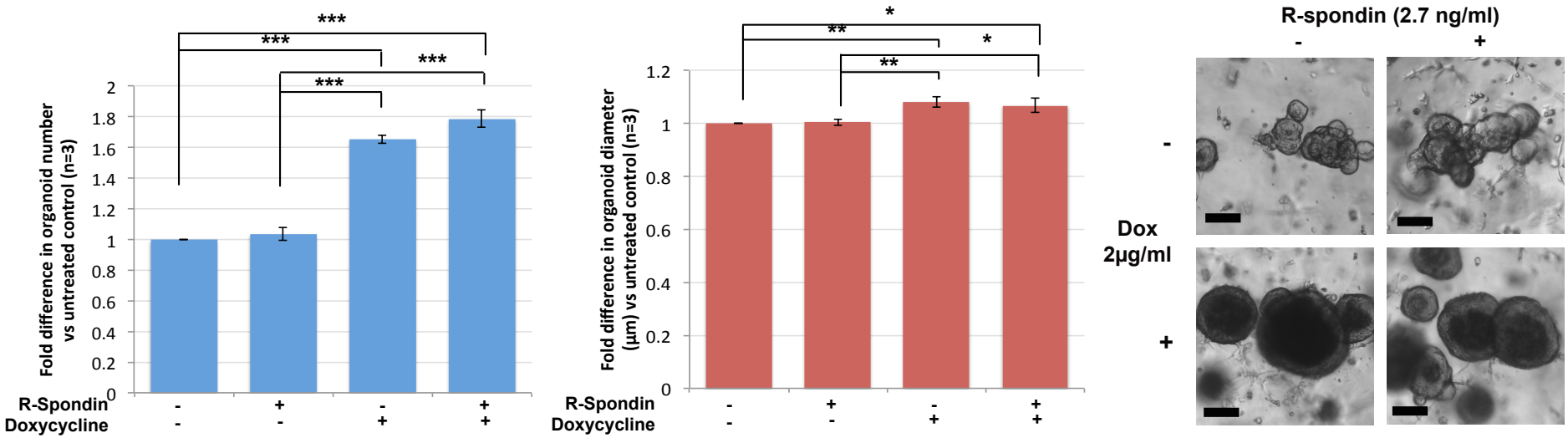

Figure 3.9. Constitutive Wnt pathway activation increases organoid formation and size in a similar fashion to R-Spondin1.

MECs were freshly isolated from a Tet-O-ΔN89β-Catenin mouse line and embedded in matrigel. (A) Cultures were treated with Nrg1 (100 ng/ml) and Noggin (100 ng/ml) supplemented media alone, or additionally given R-Spondin1 (2.656 ng/ml), Doxycycline (2 µg/ml), or both in combination. After 7 days, organoid number (A) and average diameter (B) were assessed using GelCountTM scanner and software from Oxford Optronix. Data are expressed as fold change (vs Neu, Nog only, n=3, means± standard deviation.). **, $p < 0.01$; ***, $p < 0.001$, ANOVA with Tukey's post-hoc comparison. (C) Representative pictures of mammary organoids cultured for 7 days under each condition. Scale bars 100 µm.

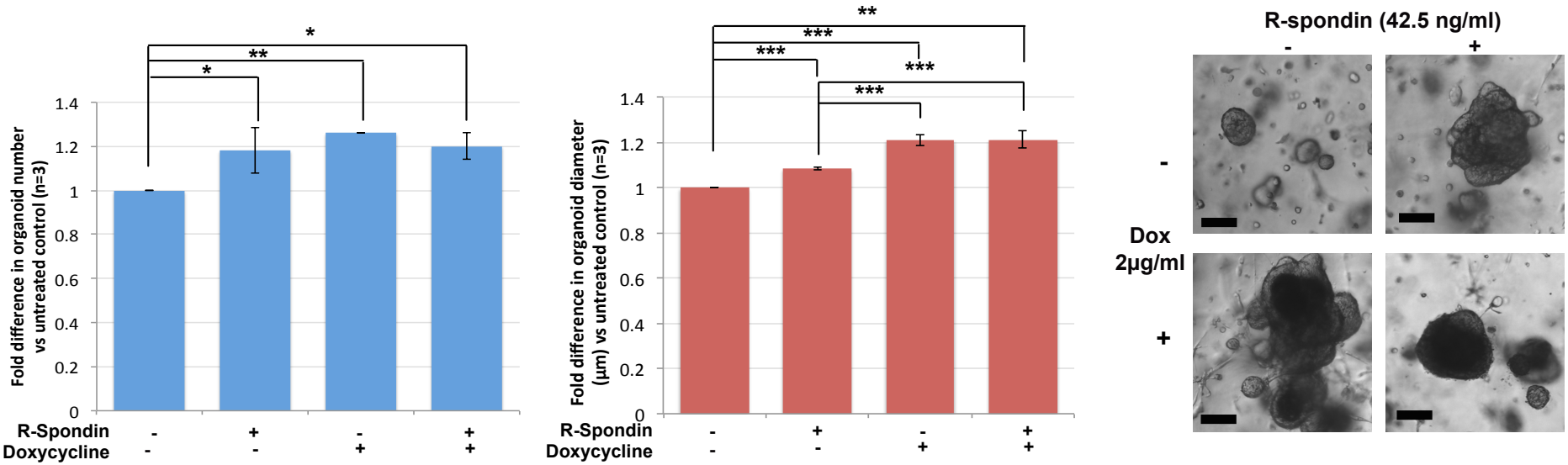

Figure 3.10 Constitutive Wnt pathway activation increases organoid formation and size in a similar fashion to high levels of R-Spondin1.

MECs were freshly isolated from a Tet-O-ΔN89β-Catenin mouse line and embedded in matrigel. Cultures were treated with EGF (50 ng/ml) and Noggin (100 ng/ml) supplemented media alone, or additionally given R-Spondin1 (42.5 ng/ml), Doxycycline (2 µg/ml), or both in combination. After 7 days, organoid number (A) and average diameter (B) were assessed using GelCountTM scanner and software from Oxford Optronix. Data are expressed as fold change (vs EGF, Nog only, n=3, means±standard deviation **, $p < 0.01$; ***, $p < 0.001$, ANOVA with Tukey's post-hoc comparison. (C) Representative pictures of mammary organoids cultured for 7 days under each condition. Scale bars 100 µm.

respectively, $p<0.05$ assessed by a one-way ANOVA, with Tukey's post-hoc analysis, n=3), while organoid diameter was also significantly increased in all treated conditions (Figure 3.10A, B).

Taken together, the data supports that effects observed under R-Spondin1 stimulation are indeed a result of canonical Wnt pathway activation.

3.2.1.2.1 In depth, extended analysis of organoids grown under optimised culture conditions.

Given all of the above evidence, culture conditions containing Nrg1 (100 ng/ml), Noggin (100 ng/ml) and R-Spondin1 (2.7 ng/ml), from here on termed "NRL", supported by the ROCK inhibitor Y-27632 (10µM) for the first 5 days in culture, were chosen as 'optimised conditions' for further detailed investigation.

The early growth, morphological and phenotypical status of organoids grown from freshly isolated epithelial fragments, unsorted trypsinised cells, and sorted, definitive single epithelial cells (see Material and Methods for further details of each preparation) under these conditions was assessed. As part of this investigation, it was important to determine the length of time required for fully heterogeneous (that is, comprising both luminal ER/PR- or ER/PR+ and basal K14, p63+ cell populations) and therefore 'useful' organoids to form in each case, and whether this differentiation status correlated with a particular morphology (e.g. definitive lobular).

Detailed analysis of later time points in culture was then performed to investigate key points previously described as crucial to any organoid system, such as the maintained phenotypic normality and functionality of structures and the cells of which they are comprised over time, and the capacity for the stable expansion of cell or organoid numbers.

3.2.1.3 Phenotypically 'normal' mammary organoids can be cultured from a variety of primary material preparations.

i. Organoids grown from epithelial fragments

Organoids were grown over a period of 14 days from epithelial fragments under the newly optimised levels of R-Spondin1, in the presence of Y-27632 (10µM) for the first 5 days of culture. As shown in Figure 3.11B, over a period of 11 days, organoids of around 150 to 300 µm in diameter formed, with characteristic lobular morphologies.

After just 3.5 days in culture (Figure 3.11D(i)), mammary structures of between 50 and 100 µm in diameter had begun to form in the 3D system. These structures were not yet closed balls of cells, instead possessing a visible luminal space. Importantly, a full complement of basal and luminal, hormone receptor positive and negative cell types was observed in these structures, even at such an early stage in development, indicative of 'normal' development.

After 7 days in culture, mammary organoids, while remaining at an average of around 50 to 100 µm in diameter, appeared more spherical, and had begun to lose their luminal space, with a larger quantity of cells in their centre. Structures retained distinct cell layers, possessing basal Keratin-14 and p63 expression around their outer edges, while the hormone receptors ER-α and PR, and Keratin-8 could be seen localised within the structures (Figure 3.11D(ii)).

At 14 days in culture, structures were no longer mainly spherical, having developed more convoluted structures, as seen in figures 3.8C and 3.8D(iii). Organoids again retained distinct layers of basal and luminal marker expression, seen clearly in Figure 3.11D(iv) where basal p63 and luminal PR did not co-localise. Co-expression of both steroid receptors was also identified to persist at this time point (Figure 3.11D(iv)), matching lengths of maintained receptor expression previously reported in culture (Obr et al. 2013).

At all time points, and both populations, β-catenin localisation was membranous, at cell junctions, and not nuclear. Larger structures exhibited a lack of β-catenin nearer their cores, where nuclear staining highlighted cells, but this appears to be an antibody penetration fault, that also can be seen upon E-cadherin staining. Overall, structures grown here possess a physiologically normal phenotype, thus justifying the use of these culture conditions.

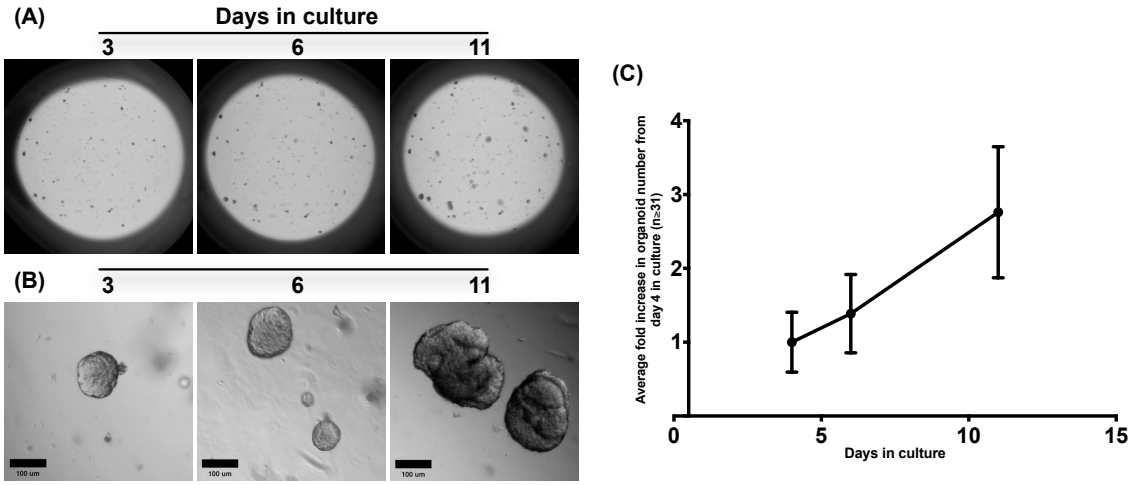

Figure 3.11 In depth analysis of organoids grown under Nrg1, R-Spondin1 low culture conditions from epithelial fragments.

Epithelial fragments were seeded at equal density on optical imaging plates in 9.5 µl growth factor reduced Matrigel, and cultured for 14 days in defined DMEM/F12 base media supplemented with Nrg1 (100 ng/ml), noggin (100 ng/ml) and R-Spondin1 (2.7 ng/ml). Y-27632 (10 µM) was added to media for the first 5 days as standard. **(A)** Representative whole well overview, taken at days 3, 6 and 11 in culture using Gelcount technology. **(B)** Representative image demonstrating morphological development of organoids from day 3 to day 13 in culture. **(C)** Average fold increase in organoid count per well (wells=31) compared to that at 4 days in culture. Data points are shown as mean ± standard deviation. **(D)** Confocal microscope images of immunofluorescence staining for luminal epithelial markers (Keratin 8, progesterone receptor), basal epithelial markers (Keratin 14, Keratin 5. p63), and β-catenin and E-Cadherin, in cultures at **(i)** 3.5 **(ii)** 7 **(iii)** 14 days in culture. **(iv)** Co-staining (PR/p63 or PR/ER) of organoids at day 14 in culture.

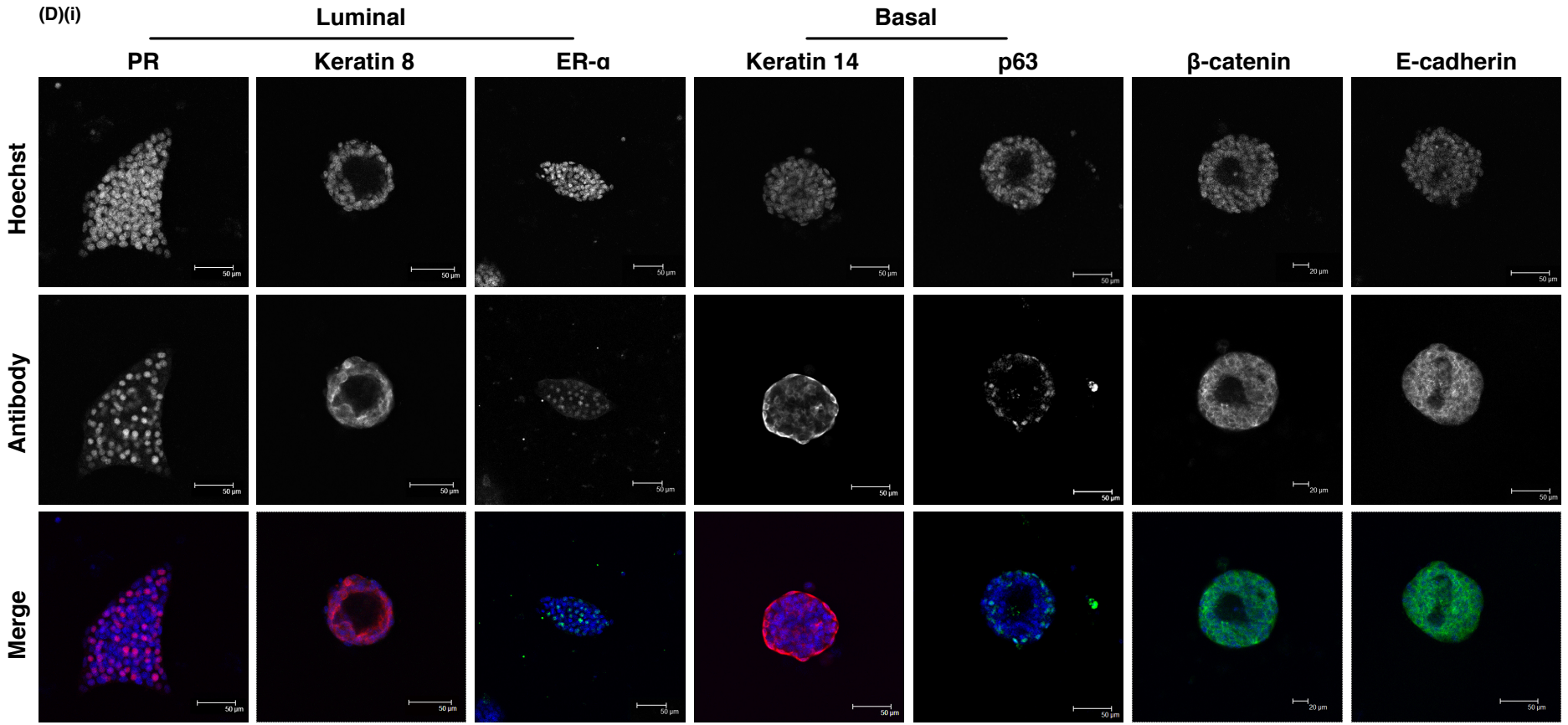
(D)(i)
Luminal
Basal
PR
Keratin 8
ER-α
Keratin 14
p63
β-catenin
E-cadherin
Hoechst
Antibody
Merge

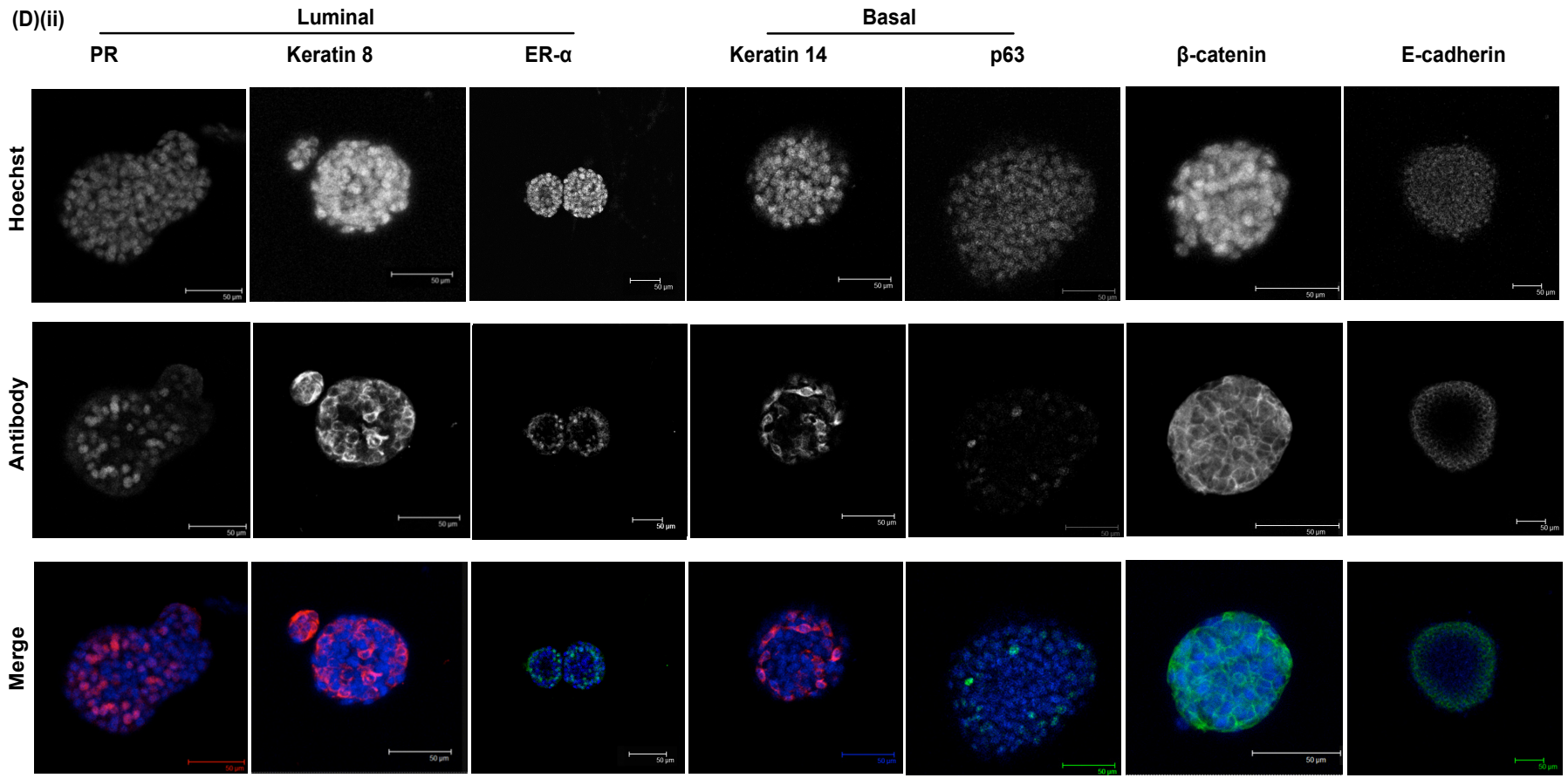
(D)(ii)
Luminal
Basal
PR
Keratin 8
ER-α
Keratin 14
p63
β-catenin
E-cadherin
Hoechst
Antibody
Merge

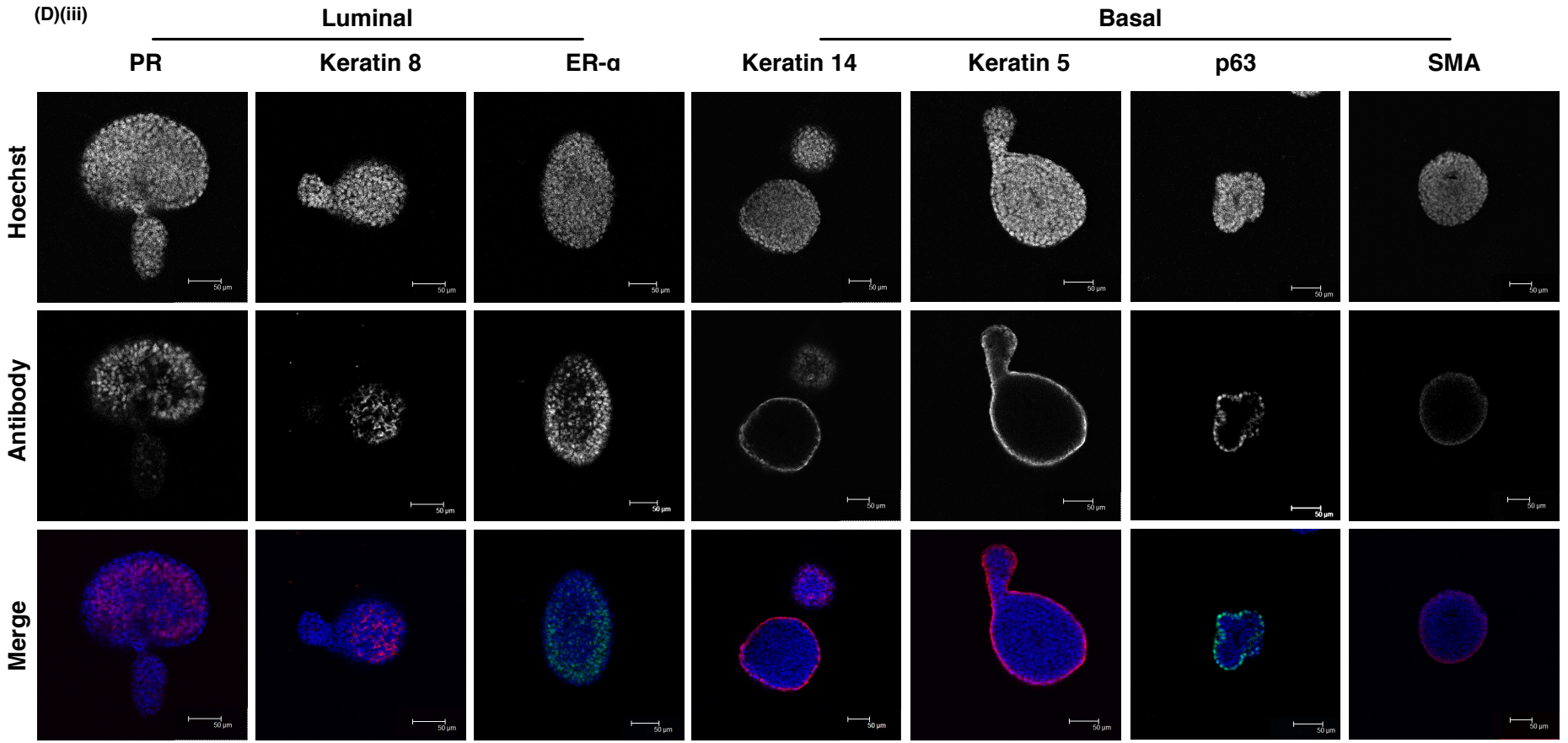
(D)(iii)
Luminal
Basal
PR
Keratin 8
ER-α
Keratin 14
Keratin 5
p63
SMA
Hoechst
Antibody
Merge

(D)(iii cont.)

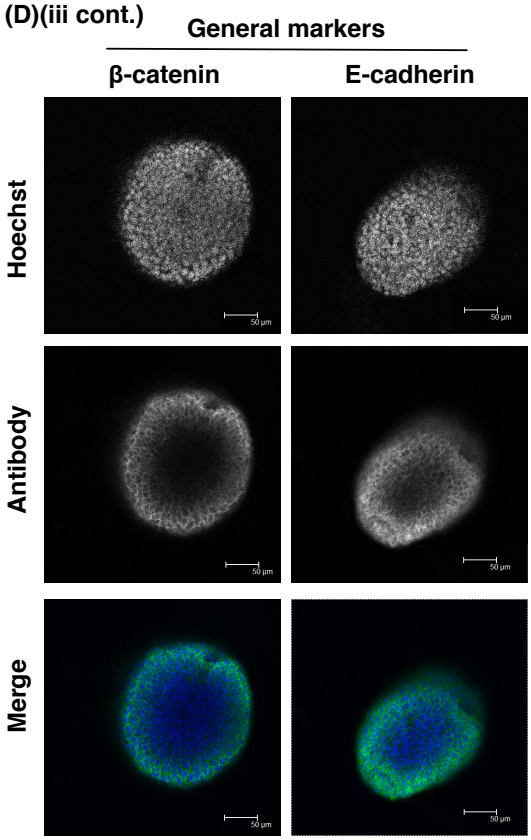

(D)(iv)

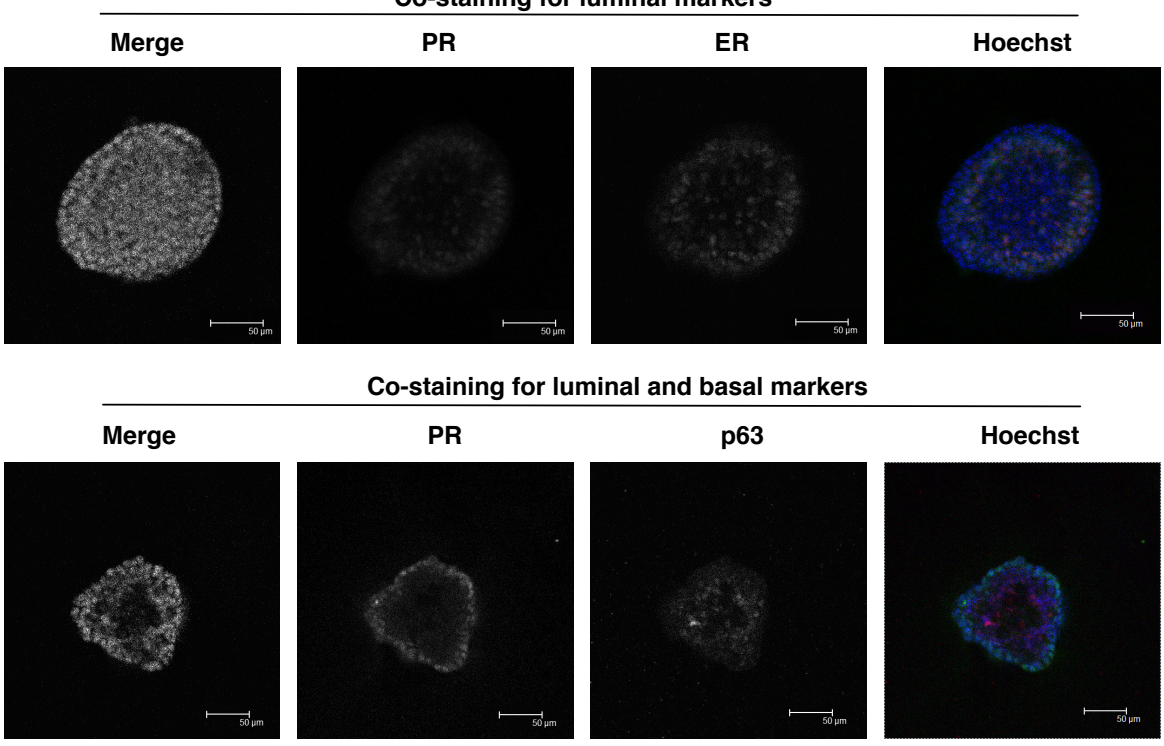

ii. Organoids grown from trypsinised epithelial cells

Organoids were next cultured from cells derived from trypsinisation of epithelial fragments, seeded at an approximate density of 1000 cells per microliter, under the newly optimised levels of R-Spondin, in the presence of Y-27632 (10μM) for the first 5 days in culture (Figure 3.12).

Morphologically, over 13 days organoids of around 100 μm developed from these cells. Interestingly, although these organoids were smaller than those found at a similar time point in cultures of epithelial fragments, the time taken for development of a distinct lobules remained the same.

The majority of structures seen in this experiment at 3.5 days were a maximum of 50 μm in diameter, composed of only a small number of cells (Figure 3.12D(i)). However, even at this early stage of culture, organoids were arranged into basal and luminal compartments, with full epithelial cellular differentiation heterogeneity as observed *in vivo*. In these smaller structures β-catenin localisation was observed at both the cell-cell junctions and within the nucleus, suggesting that Wnt signalling may be increased in these organoids compared to those grown from epithelial fragments. E-cadherin localisation also appeared more punctate, perhaps indicative of junctional remodelling. This could also however reflect the easier penetration of antibodies into the smaller structures.

By 7 days in culture, most organoids had reached 50 μm in diameter, and cell number per organoid, although not specifically quantified, was visibly increased from the earlier time point. Again, full, distinct patterns of differentiation were maintained, with basal cells found only at the outer edges of the structures (Figure 3.12D(ii)).

Interestingly, after 14 days in culture, although structures (around 100 μm) were smaller than their fragment derived equivalents, they too now showed a morphological change from rounded structures, to more lobular, developed shapes (Figure 3.12B, D(ii)). This repeated phenomenon may indicate that time taken to reach a physiologically relevant morphology may depend on cells adapting to their new *in vitro* environment, rather than on size of the organoids themselves.

After nearly 3 weeks in culture without passage, organoids still retained a morphology associated with a 'normal' phenotype, with overall organoid forming efficiency at 19 days in culture calculated to be 1.57% ± 0.25% per 1000 cells seeded.

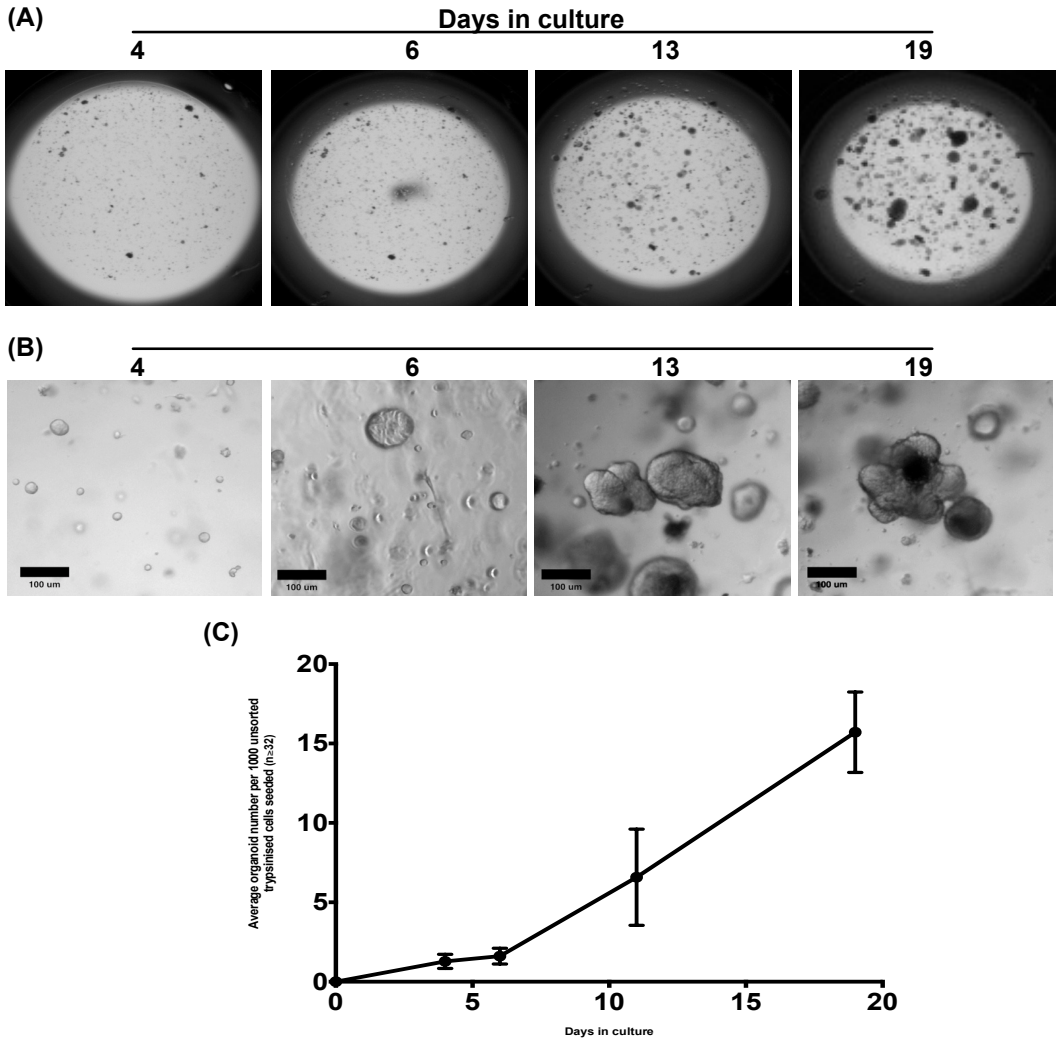

Figure 3.12 In depth analysis of organoids grown under Nrg1, R-Spondin1 low culture conditions from unsorted, single mammary epithelial cells.

Epithelial fragments were trypsinised to single cells, and seeded at 1000 per µl on optical imaging plated in 9.5 µl growth factor reduced Matrigel, and cultured for 19 days in defined DMEM/F12 base media supplemented with Nrg1 (100 ng/ml), noggin (100 ng/ml) and R-Spondin1 (2.7 ng/ml). Y-27632 (10 µM) was added to media for the first 5 days as standard. **(A)** Representative whole well overview, taken at days 4, 6, 11 and 19 in culture, using GelCount technology. **(B)** Representative image demonstrating morphological development of organoids from day 4 to day 19 in culture. **(C)** Average number of organoids formed per 1000 cells seeded (wells≥32). Data points are shown as mean per well ± standard deviation. **(D)** Confocal microscope images of immunofluorescence staining for luminal epithelial markers (Keratin 8, progesterone receptor), basal epithelial markers (Keratin 14, p63), β-catenin and E-Cadherin, in cultures at **(i) 3 (ii) 7** and **(iii) 14** days in culture. **(iv)** Co-staining (PR/p63 or PR/ER) of organoids at day 14 in culture.

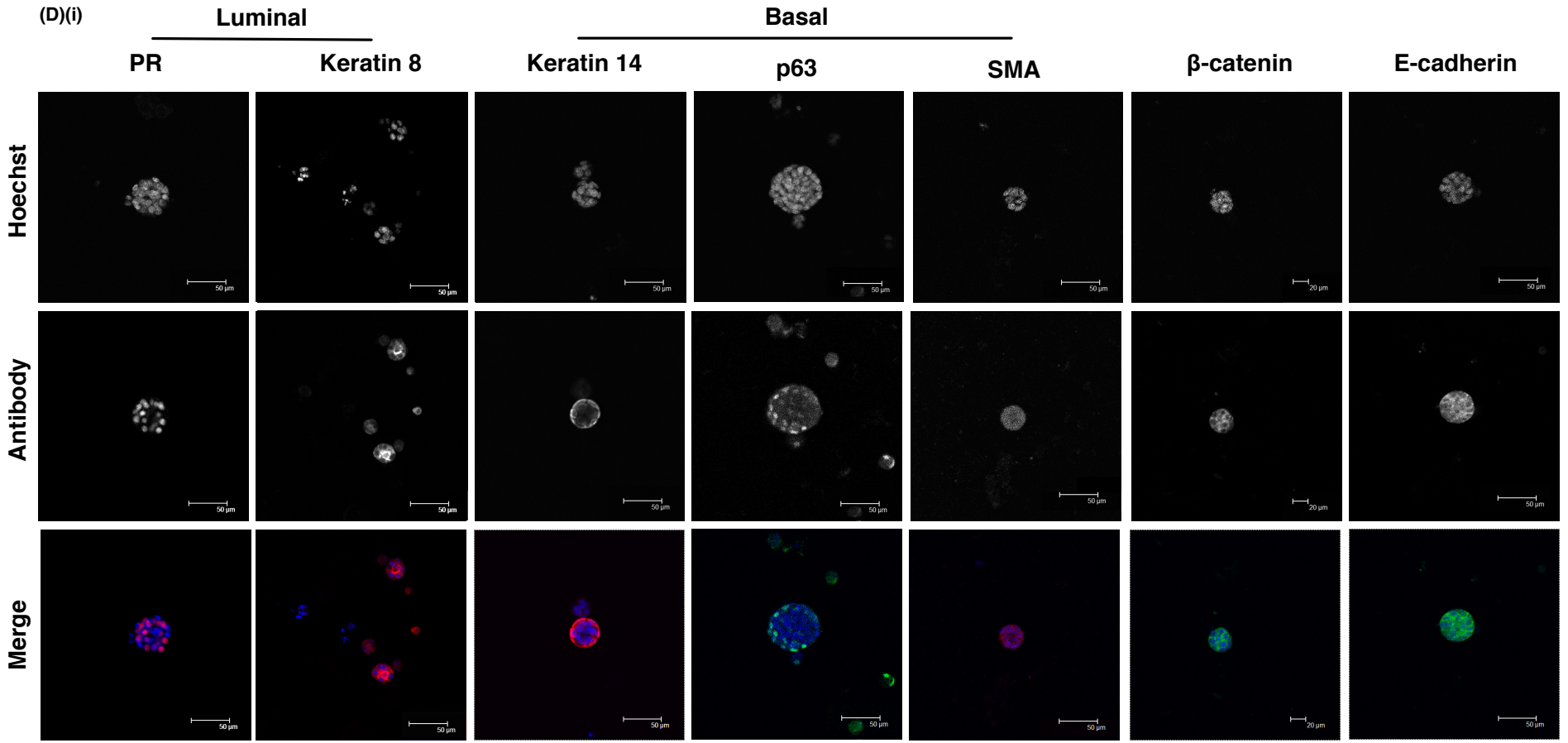
(D)(i)
Luminal
Basal
PR
Keratin 8
Keratin 14
p63
SMA
β-catenin
E-cadherin
Hoechst
Antibody
Merge

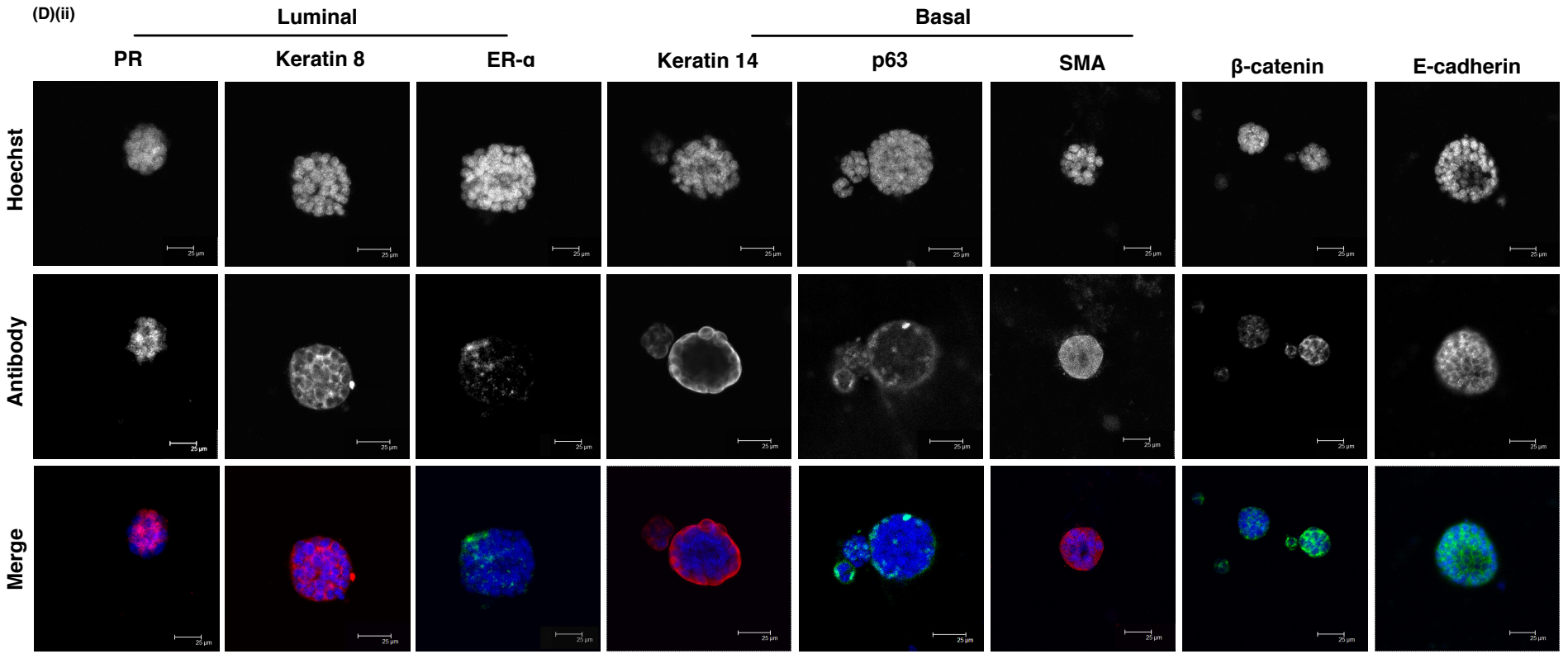
(D)(ii)
Luminal
Basal
PR
Keratin 8
ER-α
Keratin 14
p63
SMA
β-catenin
E-cadherin
Hoechst
Antibody
Merge

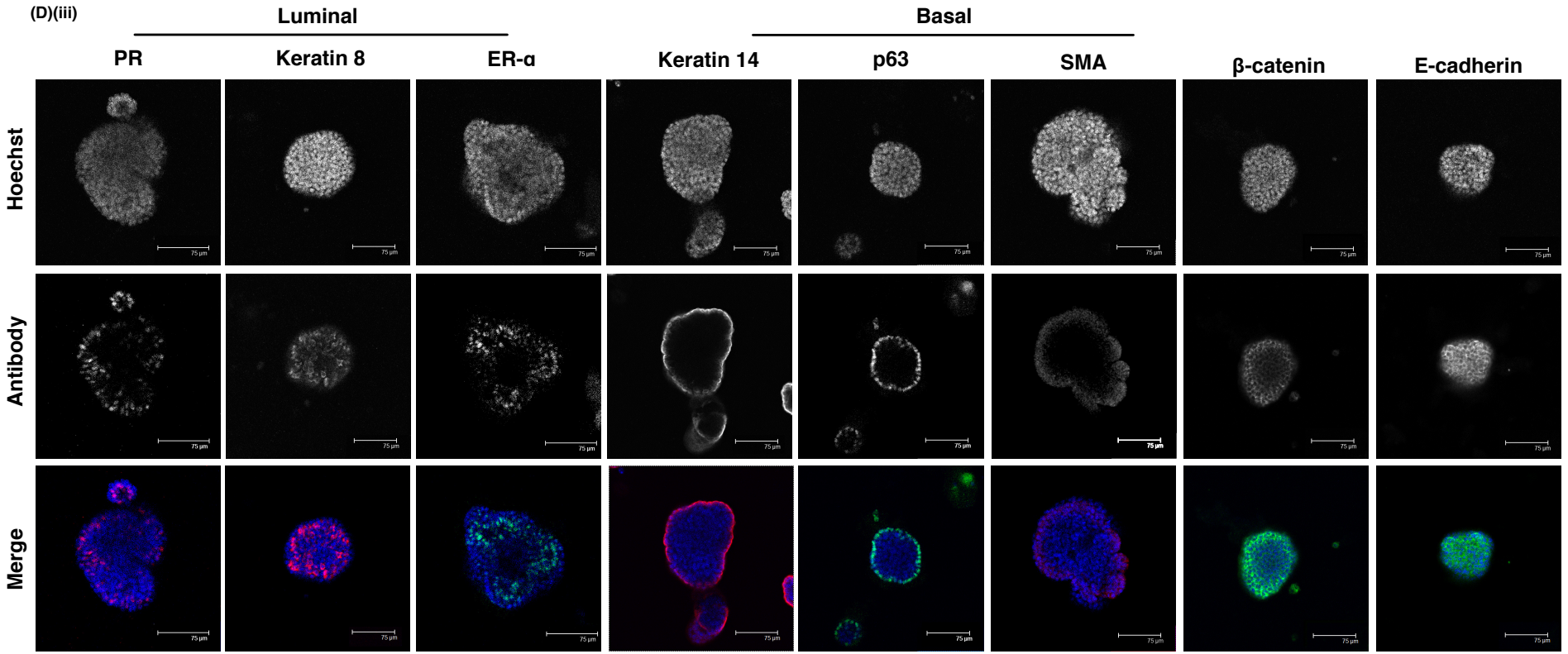
(D)(iii)
Luminal
Basal
PR
Keratin 8
ER-α
Keratin 14
p63
SMA
β-catenin
E-cadherin
Hoechst
Antibody
Merge

(D)(iv)

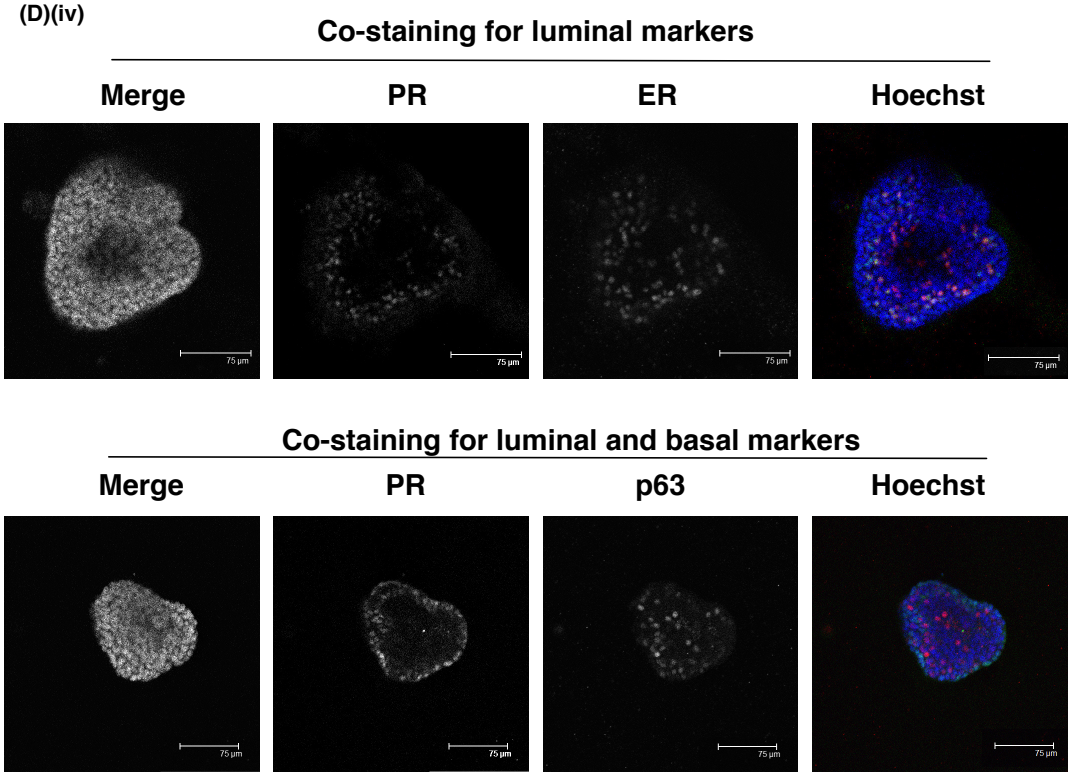
Co-staining for luminal markers
Merge
PR
ER
Hoechst
75 µm
Co-staining for luminal and basal markers
Merge
PR
p63
Hoechst
75 µm

iii. Organoids grown from definitive, sorted single cell populations

Definitively single (doublets excluded by FACS), live, sorted epithelial cell populations were next cultured at 1000 per µl of growth factor reduced Matrigel, over a period of 19 days, under optimised conditions, with additional support from Y-27632 (10 µM) for the first 5 days of culture.

After 7 days in culture, small, round organoids of around 25 µm (Figure 3.13B) were observed to possess the distinct basal keratin and p63 staining around the outer edges, while luminal markers were again solely present within the structures (Figure 3.13D(i)). These small organoids also exhibited β-catenin localisation at the cell-cell junctions and within the nucleus. E-cadherin localisation was also more punctate, thus suggesting junctional remodelling during organoid growth.

After 14 days in culture, average organoid diameter reached between 75-100 µm, and structures had evolved more lobular morphologies (Figure 3.13B). As previously observed with the fragments and unsorted cells, basal and luminal compartments remained distinct, with a single basal cell layer around the outer edges of the organoids, and ER+/PR+ luminal cells within the core of the structures (Figure 3.13D(ii)).

Moreover, by combining an EdU incorporation assay with immunostaining of mammary organoid cultures after 14 days, both with and without hormonal stimulation, it was observed that actively proliferating (EdU+) cells were a distinct population from hormone responsive (PR+) cells (Figure 3.14), in line with current knowledge of the *in vivo* mature mammary gland (Russo et al. 1999; Clarke et al. 1997). Here, hormone responses occur via a paracrine signalling mechanism, such that Estrogen or progesterone stimulation of ER or PR positive luminal cells leads to the release of amphiregulin or Wnt4, respectively (Ciarloni et al. 2007; Brisken et al. 2000) and these intermediate factors then stimulate basal mammary stem cell proliferation. Indeed, further study revealed EdU staining to co-localise with basally located p63 positive cells (Figure 3.15).

Quantification of the absolute proportions of proliferating cells following treatment with steroid hormones would have been expected to show increases compared to control conditions. Experiments to explore this, in collaboration with GE Healthcare (Joseph Williams) using InCell6000 based high content analysis were initiated, but software limitations abrogated full quantification within 3D structures.

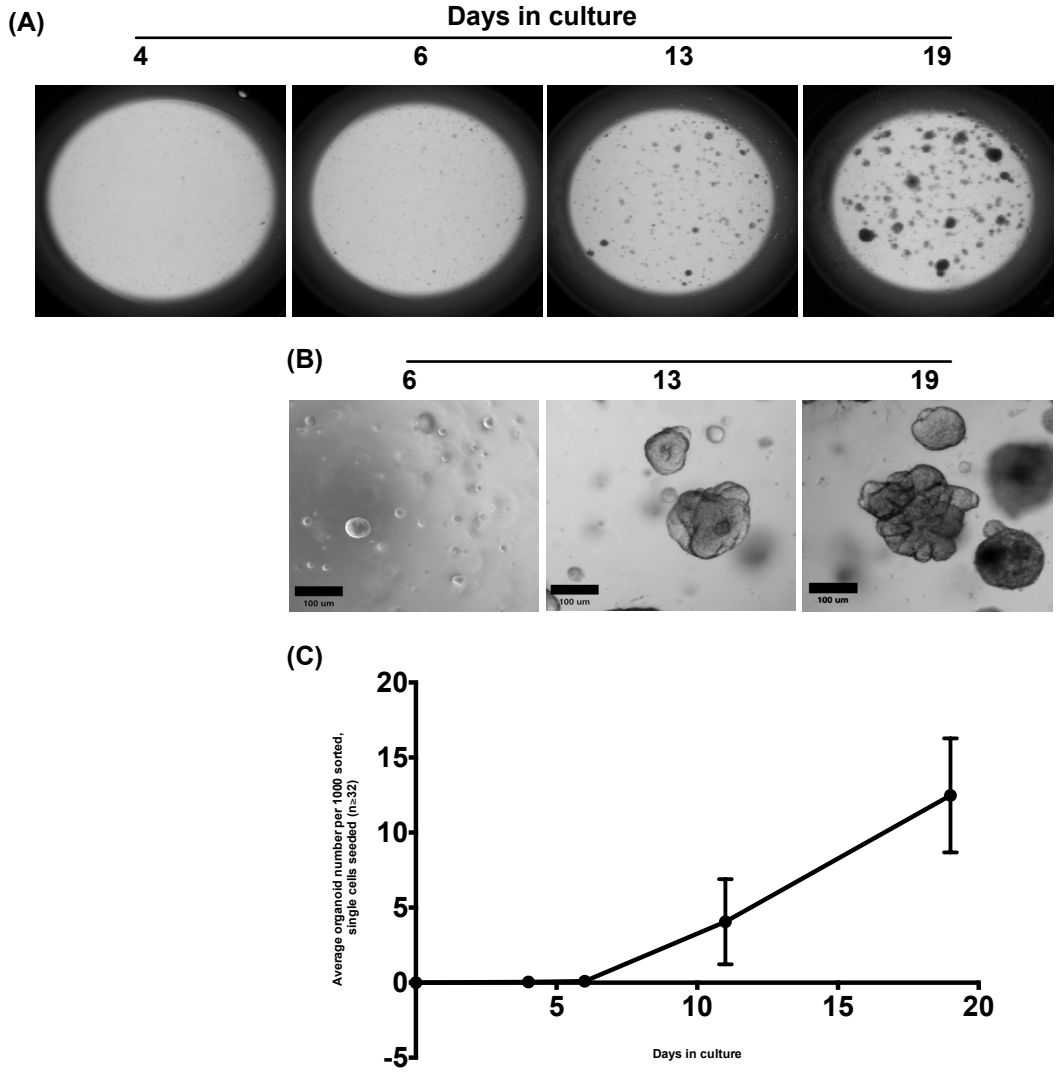

Figure 3.13. In depth analysis of organoids grown under Nrg1, R-Spondin1 low culture conditions from definitive, sorted single mammary epithelial cells.

Epithelial fragments were trypsinised to single cells, sorted to the single, live epithelial cell stage, and seeded at 1000 per µl on optical imaging plated in 9.5 µl growth factor reduced Matrigel. Cells were cultured for 21 days in defined DMEM/F12 base media supplemented with Nrg1 (100 ng/ml), noggin (100 ng/ml) and R-Spondin1 (2.7 ng/ml). Y-27632 (10 µM) was added to media for the first 5 days as standard. **(A)** Representative whole well overview, taken at days 4, 6, 11 and 19 in culture using GelCount technology. **(B)** Representative images demonstrating morphological development of organoids from day 6 to day 19 in culture. Scale 100 µm. **(C)** Average number of organoids formed per 1000 cells seeded (wells≥32). Data points are shown as mean per well ± standard deviation. **(D)** Confocal microscope images of immunofluorescence staining for luminal epithelial markers (Keratin 8, progesterone receptor), basal epithelial markers (Keratin 14, p63), β-catenin and E-Cadherin, in cultures at **(i) 7** and **(ii) 14** days in culture. **(iii)** Co-staining (PR/p63 or PR/ER) of organoids at day 14 in culture.

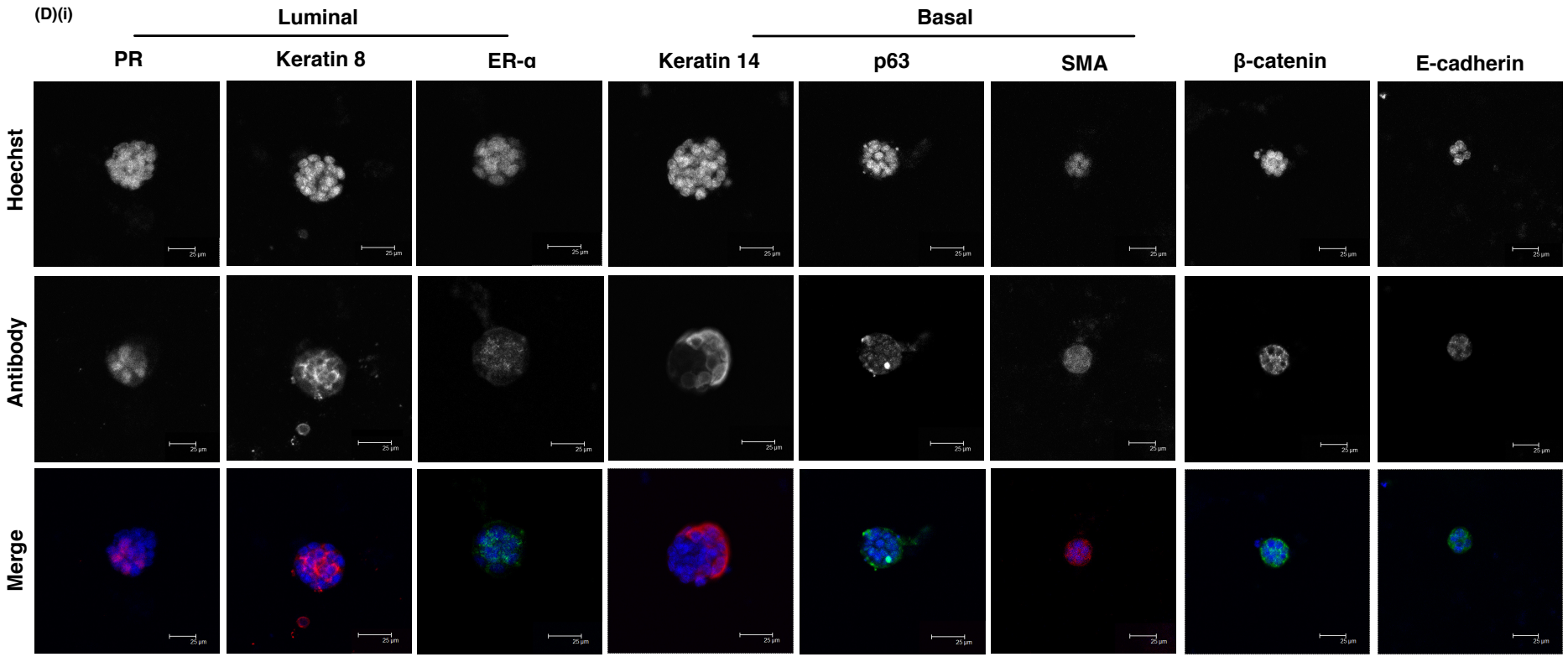
(D)(i)
Luminal
Basal
PR
Keratin 8
ER-α
Keratin 14
p63
SMA
β-catenin
E-cadherin
Hoechst
Antibody
Merge

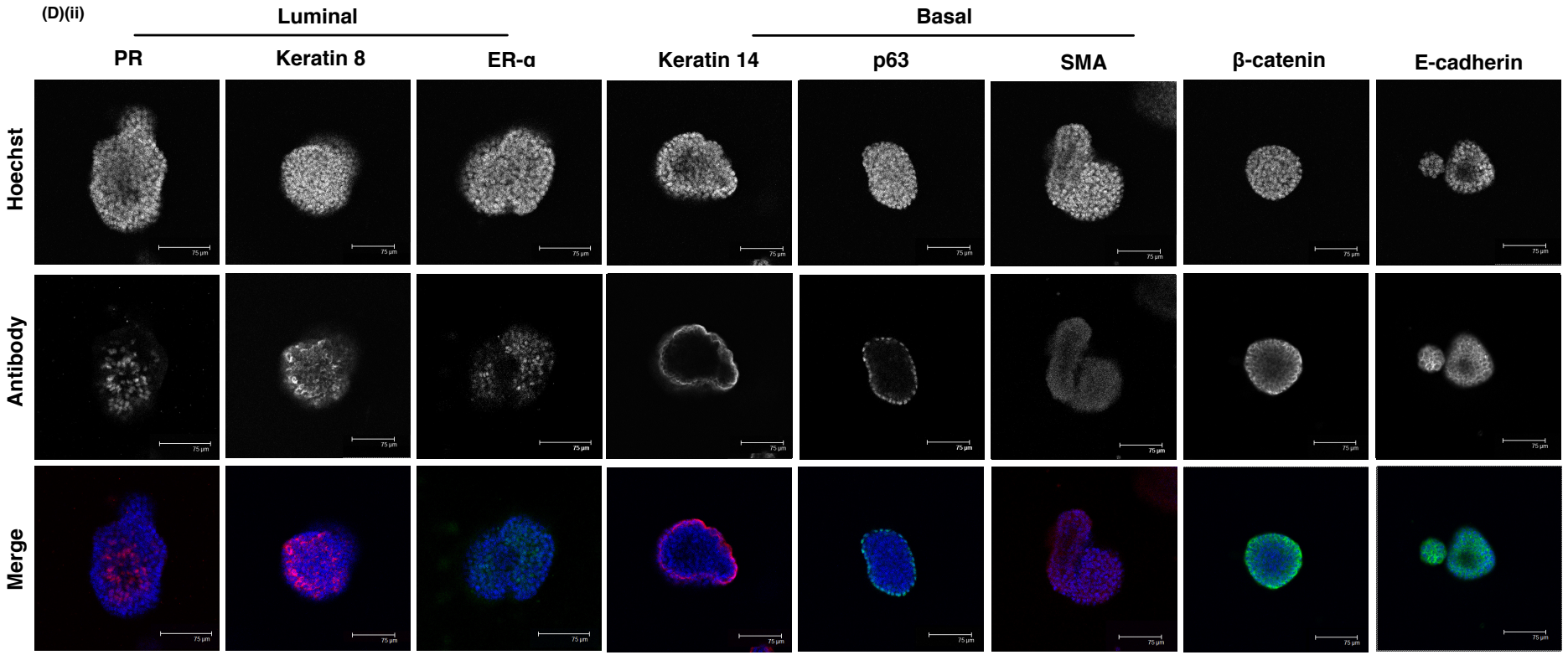
(D)(ii)
Luminal
Basal
PR
Keratin 8
ER-α
Keratin 14
p63
SMA
β-catenin
E-cadherin
Hoechst
Antibody
Merge

(D)(iii)

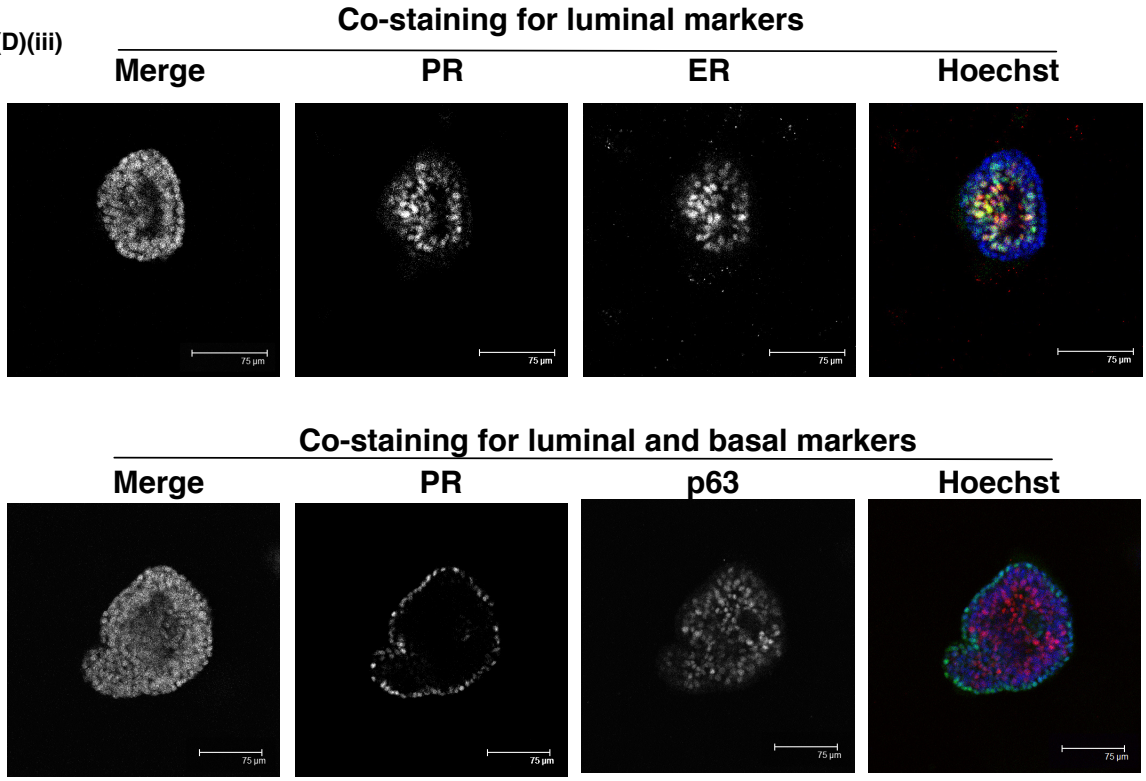
Co-staining for luminal markers
Merge
PR
ER
Hoechst
75 µm
Co-staining for luminal and basal markers
Merge
PR
p63
Hoechst
75 µm

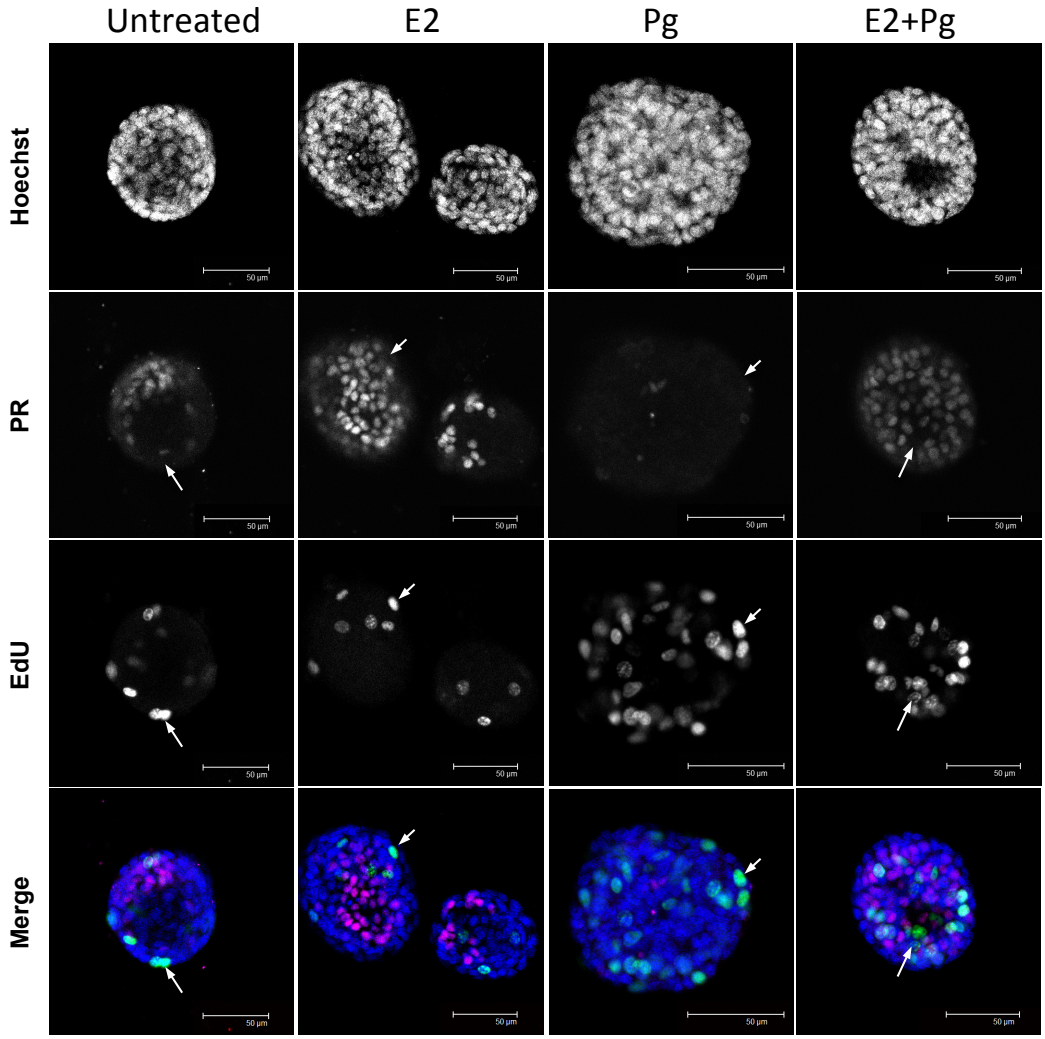

Figure 3.14 Analysis of proliferating populations following hormone treatment of organoids grown under defined media conditions.

Organoids grown for 14 days under defined media conditions were treated with steroid hormones Estrogen (2.5ng/ml), Progesterone (40 ng/ml), alone or in combination for 24 hours prior to fixation. EdU was added two hours prior to fixation and allowed to incorporate into the newly synthesised DNA of dividing cells. Confocal images depict immunofluorescence staining carried out against Progesterone receptor (PR), in red, and EdU, in green. White arrows indicate distinctly EdU positive, PR negative cells. Scale 50µm.

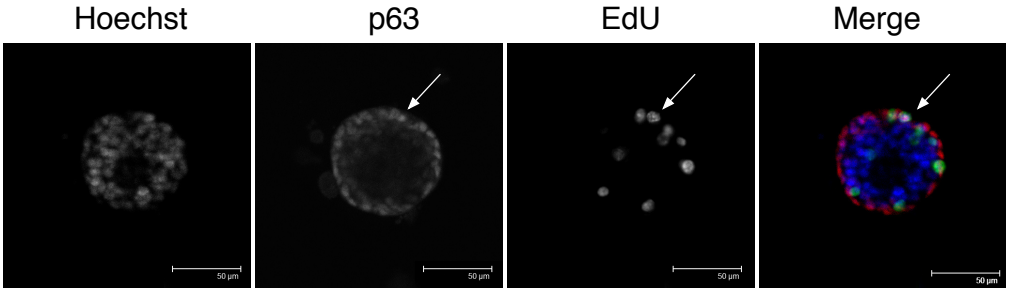

Figure 3.15 Analysis of EdU positive, dividing cell populations.

Organoids grown for 14 days under defined media conditions were treated with EdU two hours prior to fixation such that it incorporated into the newly synthesised DNA of dividing cells. Confocal images depict immunofluorescence staining carried out against basal cell marker p63, in red, and EdU, in green. White arrows indicate distinctly EdU positive, p63 positive cells. Scale 50µm.

Future work to assess this would be of use to the further understanding of organoid function and signalling.

After 19 days in culture (Figure 3.13B), highly lobular structures of greater than 100 µm were observed. Organoid formation efficiency was calculated at this stage to be on average 1.25% ± 0.39% per 1000 cells seeded (wells=32).

3.2.1.4 Mammary organoids can undergo considerable expansion, while maintaining phenotype, genomic stability and cell functionality for extended periods in culture under optimised conditions.

The culture system was next assessed over multiple time points, to define the period over which physiologically relevant structures can be maintained, and the utility of structures at various stages of culture. As previously detailed, attempts to grow mammary epithelial organoids possessing a full complement of functional differentiated cell types for extended periods *in vitro* have until now been limited. Although various groups have outlined suitable conditions for the short term culture of small, disorganised epithelial colonies, or the development of polarised epithelial structures with distinct hormone receptor positive luminal, and negative basal populations, no system has yet achieved maintained hormone receptor expression for longer than 14-21 days (Obr et al. 2013) Organoids grown for approximately 14 days in culture under NRL conditions were retrieved from Matrigel, trypsinised to single cells, replated at a density of 1000 per µl growth factor reduced Matrigel, and further cultured in a similar way for a total of 4 months, with investigations performed at early, (1 month, 1 passage), mid (2.5 month, 5 passage) and late (4 month, 10 passage) time points for comparison.

i. 1 month

Karyotype

After a month in culture, the first observation made was that of chromosomal stability. Structures were growth arrested in metaphase using colcemid, trypsinised, and karyotyped by DAPI staining and analysis of multiple chromosome spreads (Figure 3.16A). In this analysis, a range of 39 to 41 chromosomes was considered 'normal', as was an overall aneuploidy level of 5 to 20%, based on limitations of the method and precedents set by published organoid or mammary gland karyotyping data from several groups (Karthaus et al. 2014; Huch *et al.* 2013; GOEPFERT *et al.* 2000; Walen and

Stampfer 1989; Seewaldt *et al.* 2001). In total, 10 of 11 (91%) spreads were assessed to have a normal chromosome count at 1 month.

Contrastingly, chromosome counts from organoids grown for 30 days under the ERH condition previously described to produce abnormal organoids were considered to be only 71% normal, based on 7 samples counted (Figure 3.16B), suggesting this condition may be unsuited to normal development.

Hormonal response

Supplementary work performed by Jardé et al (in preparation) indicated that steroid hormone receptors retained physiologically relevant function at 30 days in culture (Appendix I-4). Results of qRT-PCR analysis of 1 month organoid cultures indicated that after 4 hours and 24 hours, estrogen and progesterone induced reductions in their respective receptor's gene expression. Furthermore, the two hormones were observed to have opposing effects on RankL gene expression; estrogen causing a significant reduction (5 fold lower than control) and progesterone a significant increase (6.4 fold higher than control)(both $p<0.05$, n=3, paired student T-test). *In vivo,* hormonal stimulation of ER or PR positive cells induces similar key changes in the expression of such genes within the gland, as will be discussed in Chapter 7 in more detail. This data however, indicated a crucial extension in the length of time mammary function can be retained in culture, and is advanced upon further in section 3.2.2.2.ii.

Regenerative capacity

Assessment of regenerative potential of structures was performed at 1 month in culture. The currently accepted "gold standard" stem cell assay for the mammary gland is that in which the developing mammary fat pads of 21 day old mice are cleared of primitive structures and injected with limiting dilution of cells, in order to evaluate their regenerative, and therefore stem, potential (Smalley and Ashworth, 2003; Dunphy et al. 2010). While this has been widely associated with caveats in recent years following extensive lineage tracing studies, including an argument for the induction of de-differentiation of cell populations under forced non-physiological conditions (Van Keymeulen et al. 2011; van Amerongen et al. 2012), it is still used as a general assessment of regenerative ability of cells to this day. Assays were performed using cells

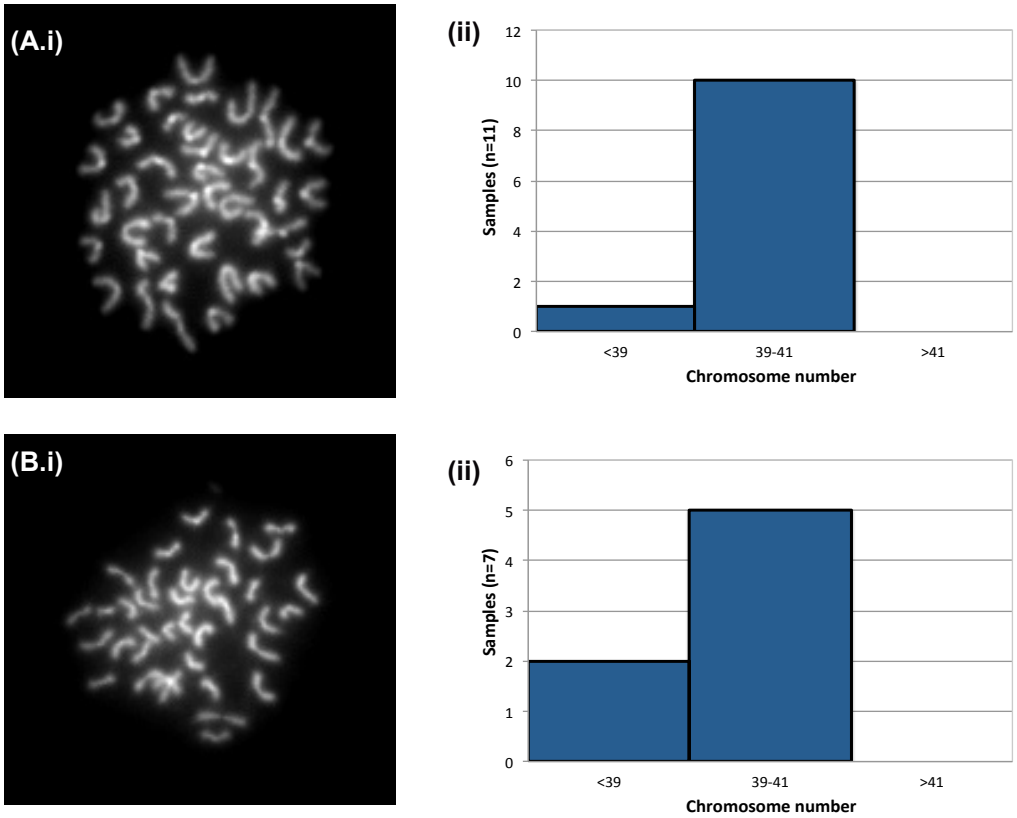

Figure 3.16 Karyotypic analysis of organoids cultured for 30 days under defined media conditions.

Organoids were grown from freshly isolated single cells under defined culture conditions, and karyotyped after 30 days. **(A)(i)** Representative image of a 'normal' DAPI stained 40 chromosome spread, from organoids grown under Nrg1, noggin, R-Spondin1 low conditions. **(ii)** Histogram of chromosome counts per spread, from a total of 11 spreads. **(B)(i)** Representative image of a DAPI stained 38 chromosome spread, from organoids grown under EGF, noggin, R-Spondin1 high conditions. **(ii)** Histogram of chromosome counts per spread, from a total of 7 spreads.

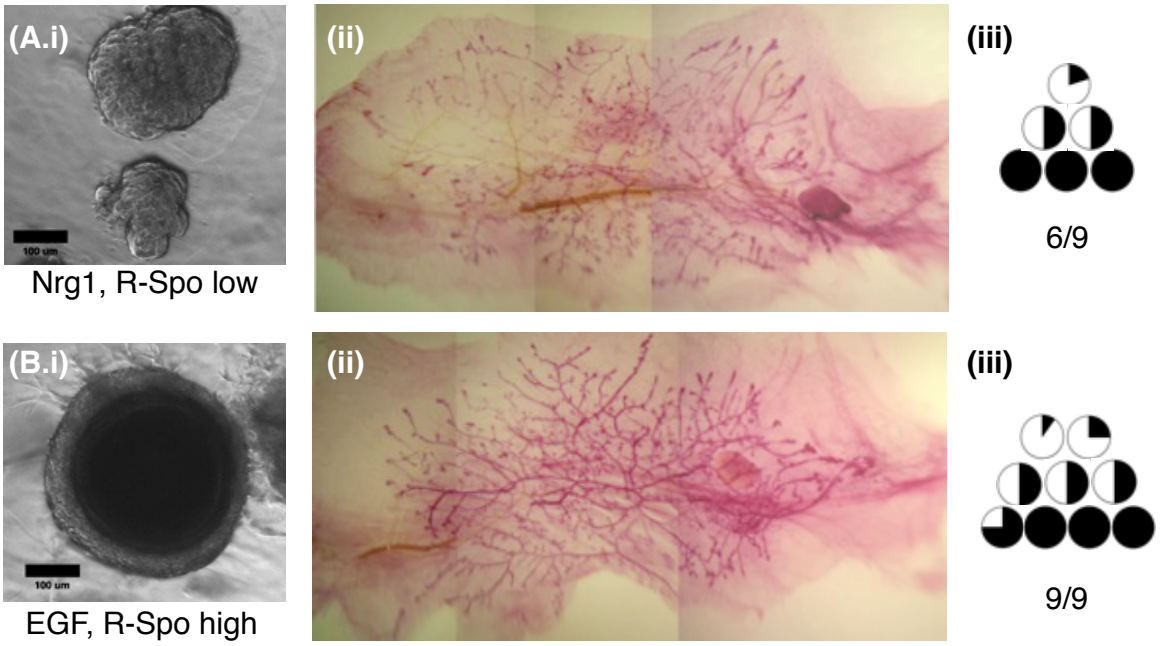

Figure 3.17 Cleared fat pad transplantation assays demonstrate regenerative ability of organoids grown under three key culture conditions.

Organoids were cultured for 30 days in matrigel, in media supplemented with either **(A)** Nrg1 and noggin (100 ng/ml each) and low R-Spondin1 (2.7 ng/ml), or **(B)** EGF (50 ng/ml), noggin (100 ng/ml) and high R-Spondin1 (42.5 ng/ml). Representative images of organoids grown under each condition are shown in **(i),** scale=100 µm. **(ii)** Examples of mammary outgrowths formed by organoids of each condition following transplantation **(iii)** Success rates of transplantation and percentage of the gland filled in each individual case (indicated in black).

derived from organoids grown for 30 days under NRL conditions. Allowing 8 weeks post-transplantation for repopulation of the mammary gland, transplantation success was evaluated by extraction of the entire fat pad, and whole mount staining for the presence of epithelial structures. 6 of 9 transplants were successful, with the percentage of the fat pad populated by the mammary gland ranging from 5 to 100 % (Figure 3.17.A), indicating a regenerative cell population maintained over passage.

In comparison, cells derived from organoids grown under ERH conditions (Figure 3.17.B) were found to repopulate with high success rates (5-100% repopulation of 9/9 fat pads). This result is perhaps unsurprising given that organoids grown under the ERH conditions were highly enriched in basal cells, the indicated stem cell compartment of the mammary gland.

ii. 2.5 months

Using the optimised Nrg1, R-Spondin1 low culture conditions, organoids were maintained in culture for 2.5 months with routine passaging every 14-18 days (5 passages total), by which point the total number of wells (comparable to number of cells, given a consistent plating density throughout passage) had expanded approximately 100 fold (n=2) since the start of culture, as indicated by the representative growth curve in Figure 3.18.

Phenotype

Crucially at this time point, organoids were characterised to be phenotypically normal, continuing to express luminal progesterone and estrogen receptors in addition to Keratin 8, basal keratin 14 and p63 (Figure 3.19), in a physiological architecture, while positive Ki67 staining confirmed a continued cycling of cells within these structures. β-catenin staining was found to be intercellular.

Karyotype

Furthermore, analysis indicated that organoids were able to maintain on the whole a ‘normal’ karyotype (87% of spreads in the 39-41 chromosome range), indicating genetic stability throughout this time culture (Figure 3.20).

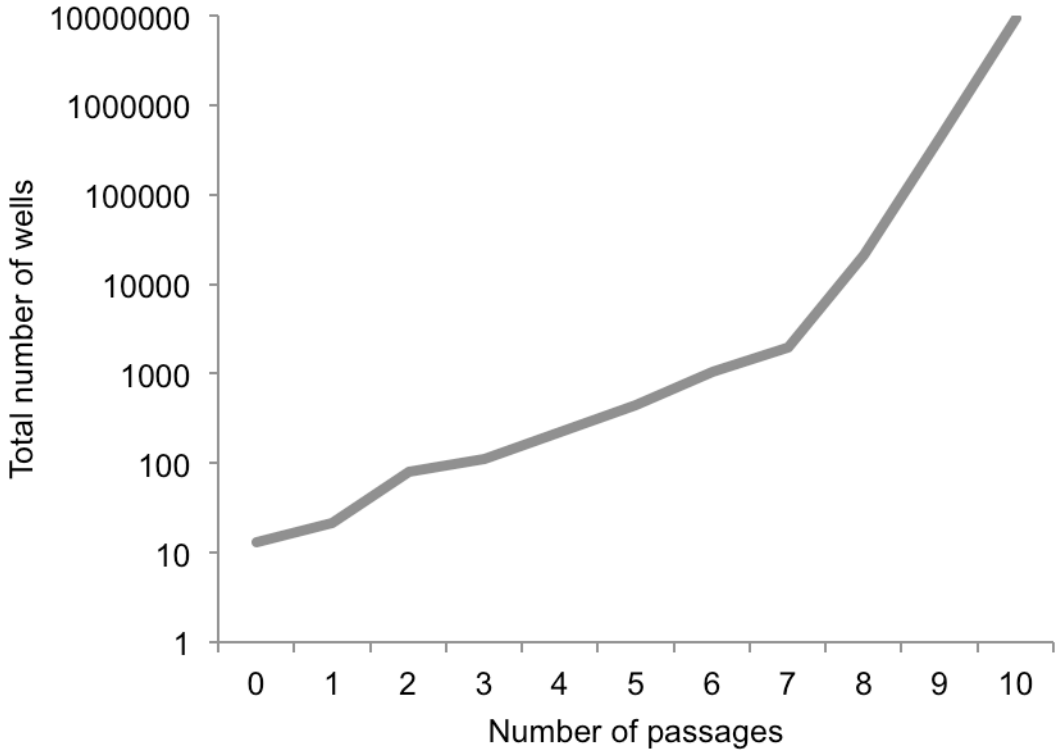

Figure 3.18 Organoid expansion increases rapidly upon extended culture.
Mammary organoids grown under Nrg1 (100 ng/ml), noggin (100 ng/ml) and R-Spondin1 low (2.7 ng/ml) culture conditions were consistently split in a 1:2 to 1:3 ratio for the first 5-6 passages, every 14-18 days. Organoids were trypsinised and replated as single cells, at a constant density of 1000 cells per µl growth factor reduced Matrigel, and total number of wells available recorded. After 7 passages, organoid well number expanded more rapidly and to a greater extent, such that passage frequency increased to every 7 days.

Hormonal response

The proportion of steroid hormone receptor positive cells per organoid was monitored, and found to be maintained or even increased between 14 days and 2.5 months in culture (54.7% ±17.7 vs 84.3 ±5.5, n=3), crucially indicating that PR/ER positive cells are not 'diluted' during culture and must be newly generated following each passage.

Furthermore, these cells were once again shown by qRT-PCR analysis to remain hormone responsive, exhibiting similar gene expression changes to those observed at the earlier time point (Figure 3.22). In all, this extended functionality in culture to 5 times that previously shown in the literature.

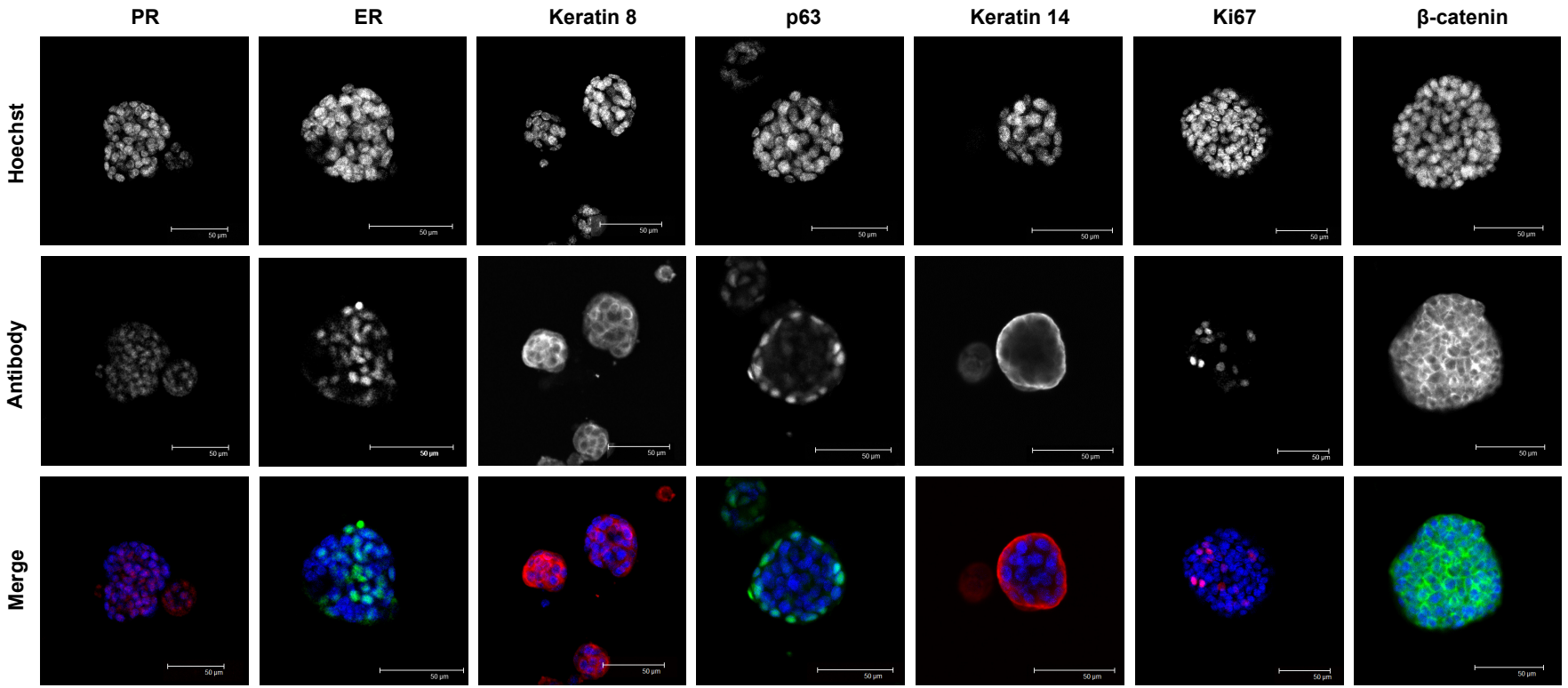

Figure 3.19 Mammary organoids grown under optimised conditions for 2.5 months days retain a normal phenotype.

Freshly isolated cells were seeded in growth factor reduced Matrigel, cultured in media supplemented with Nrg1 (100 ng/ml), Noggin (100 ng/ml) and R-Spondin1 (2.7 ng/ml) and passaged every 14-18 days. Organoids were then fixed after 70 days and immunostained for luminal (PR, ER, Keratin 8) and basal (p63, Keratin 14) markers, in addition to Ki67 and β-catenin. Scale 50 µm.

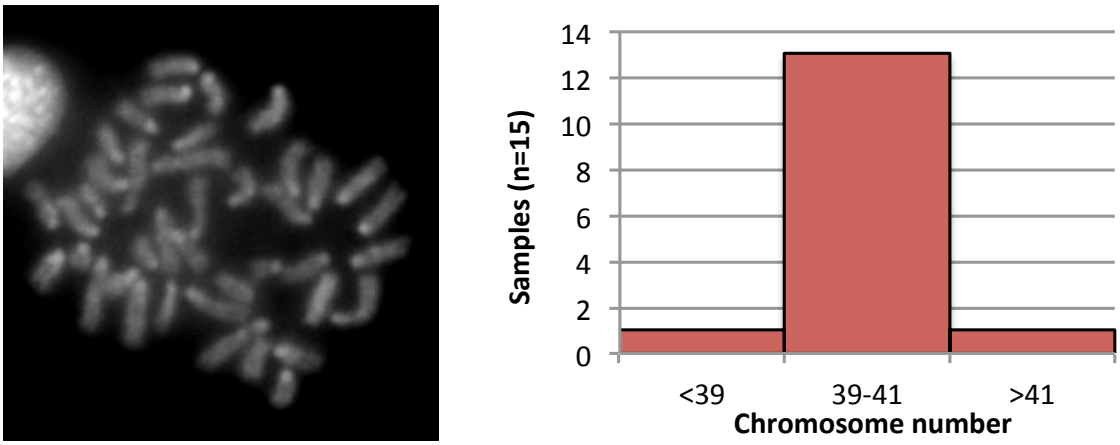

Figure 3.20 Mammary organoids grown under optimised condition for 2.5 months retain a normal karyotype.

Organoids were grown under Nrg1, noggin, R-Spondin1 low conditions for 2.5 months (5 passages) before karyotyping was performed. (A) Representative 'normal' DAPI stained chromosome spread. (B) Histogram of chromosome number per spread, from a total of 15 samples.

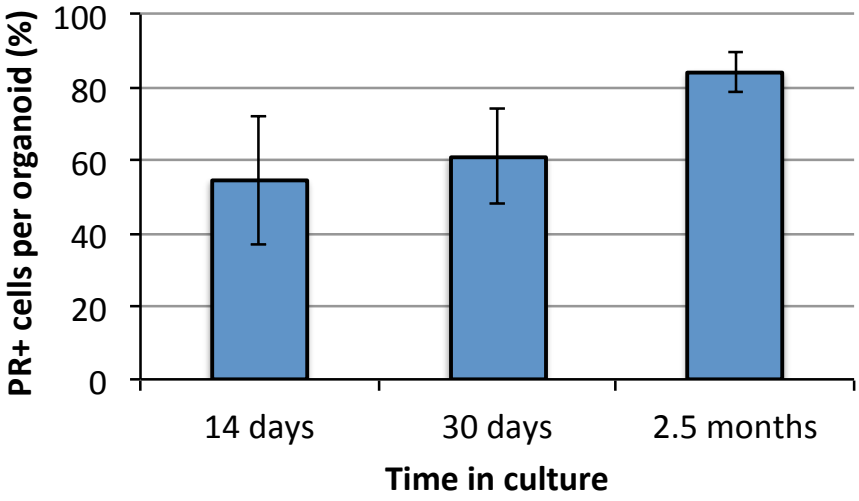

Figure 3.21 The proportion of PR+ cells per organoid increases over 2.5 months in culture.

The total number of cells (DAPI+) and number of PR+ cells per organoid were counted from confocal images taken at each time point indicated. Data shown as mean ± standard deviation, n=3.

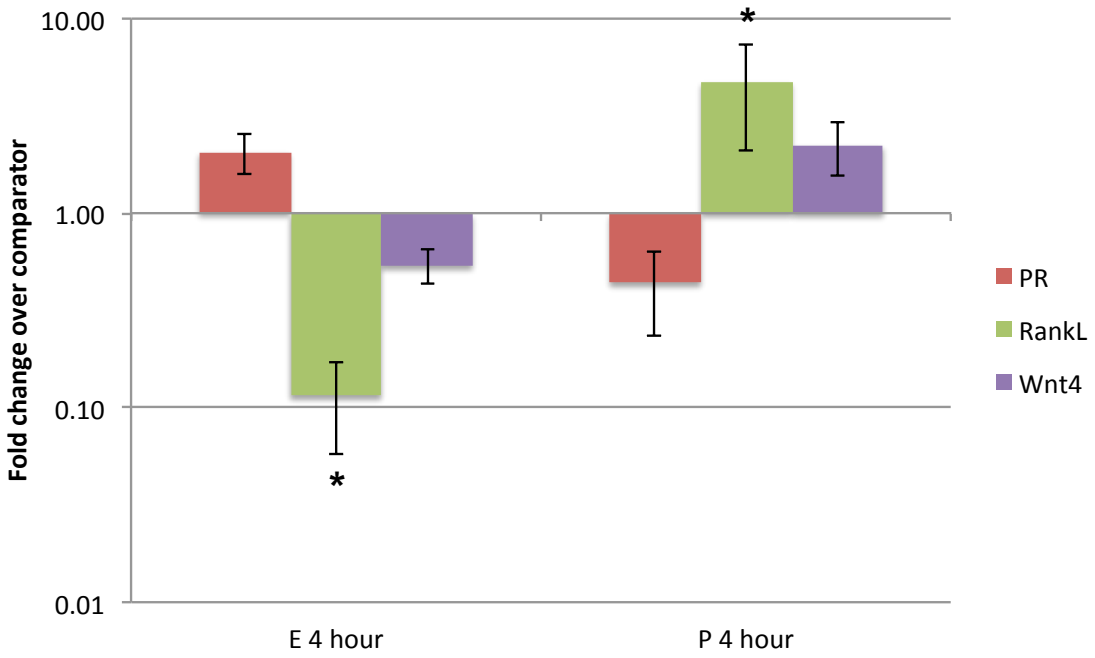

Figure 3.22. Mammary organoids exhibit physiologically relevant responses to steroid hormone treatment at 2.5 months in culture

Mammary organoids cultured for 5 passages were treated with steroid hormones estrogen (E, 4ng/ml) or progesterone (P, 40 ng/ml) for four hours, before RNA extraction and quantitative RT-PCR analysis to evaluate the expression of PR, RankL and Wnt4 genes. Data are expressed as fold change (vs untreated, n=3, means ± standard deviation), and statistical analysis performed using paired Student T test (*, $p<0.05$).

iii. 4 months

Organoids were cultured under Nrg1, R-Spondin1 low conditions for 4 months, during which time they were passaged a total of 10 times. Growth analysis over this time in culture indicated an increased expansion rate between the mid, 2.5 month time point and the end of culture and passages 7-10 actually took place weekly due to the rapid growth of structures.

Phenotype

Changes in growth rate were accompanied by the loss of expression of hormone receptors or keratin 8 and the strong expression of basal markers p63 and Keratin 14 (Figure 3.23). The localisation of β-catenin was significantly altered compared to that at earlier time points of analysis, such that intercellular, junctional β-catenin expression was markedly reduced in favour of strong nuclear expression (Figure 3.23).

Karyotype

Phenotypic changes were accompanied by frequent chromosomal abnormalities, with 25 of 29 samples (86%) exhibiting higher than normal counts (Figure 3.24).

Regenerative capacity

Furthermore, upon transplantation into the cleared fat pads of pre-pubertal mice, cells derived from these organoids produced tumours with 100% success (n=4).

Organoids grown under the ERH conditions set out by Sato et al (2009) and previously shown to produce squamous epithelial structures in mammary organoid culture, were also seen to be distinctly abnormal by passage 10, with high chromosome counts in 88% of samples (Figure 3.25B), and a profound lack of luminal marker expression (Figure 3.25C). Interestingly, although these organoids remained highly enriched in basal cells throughout culture, their morphology at later time points no longer resembled that of MMTV-Wnt1 squamous tumours, despite the presence of high levels of R-Spondin1. While Keratin 14 remained prominently expressed, cellular organisation appeared severely altered compared to earlier analysis points (Figure 3.25).

Taken together, data indicate that mammary organoids in NRL conditions do not have an indefinite lifespan, undergoing crisis at later timepoints of culture. As such, the utility of the NRL conditions is limited to 2.5 months or a 100-fold cellular expansion.

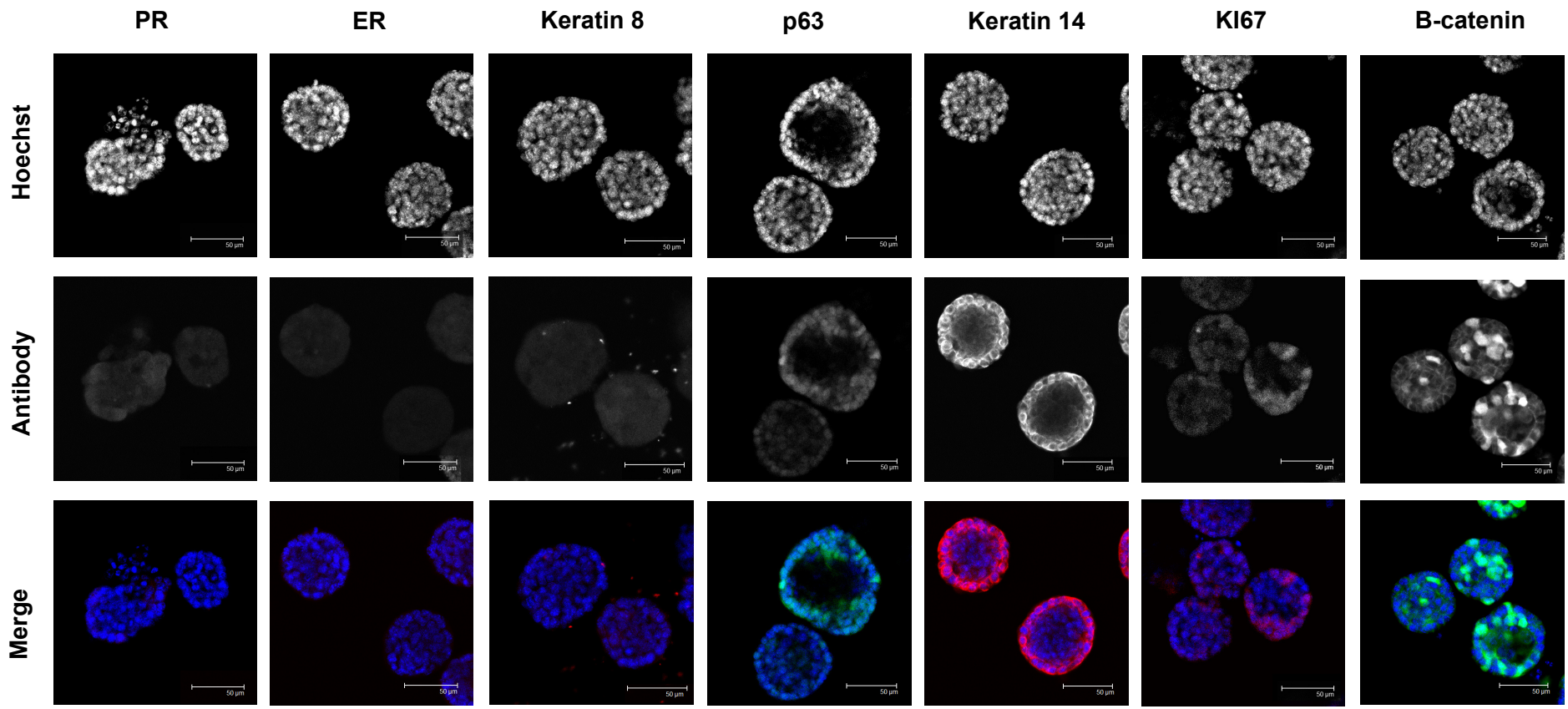

Figure 3.23 Mammary organoids grown under optimised conditions for 4 months exhibit abnormal phenotype and increased chromosome number.

Organoid were cultured in media supplemented with Nrg1 (100 ng/ml), Noggin (100 ng/ml) and R-Spondin1 (2.7 ng/ml). Organoids were then fixed after 4 months (10 passages) and immunostained for luminal (PR, ER, Keratin 8) and basal (p63, Keratin 14) markers, in addition to Ki67 and β-catenin. Scale 50 µm.

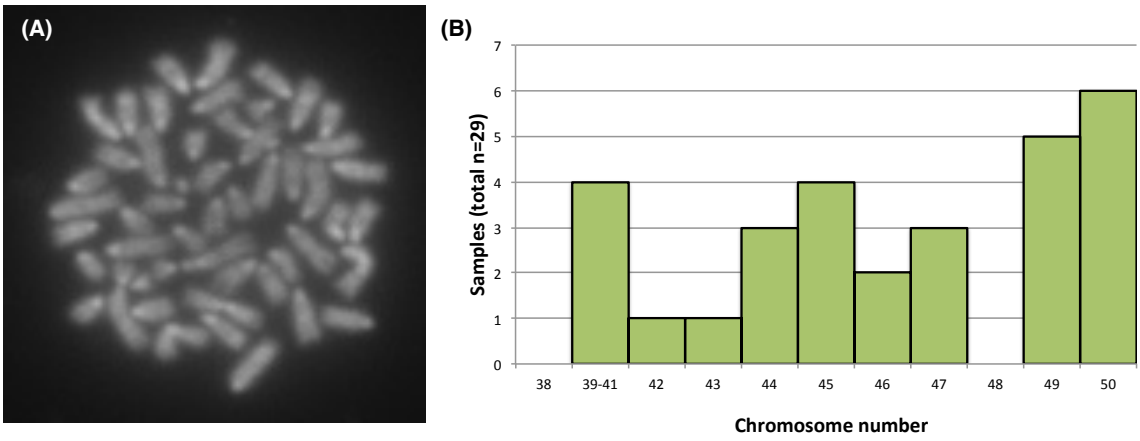

Figure 3.24 Mammary organoids grown for 4 months under optimised conditions acquire chromosomal abnormalities.

Organoids were grown under Nrg1, noggin, R-Spondin1 low conditions for 4 months (10 passages) before karyotyping was performed. (A) Representative abnormal DAPI stained chromosome spread. (B) Histogram of chromosome number per spread, from a total of 29 samples.

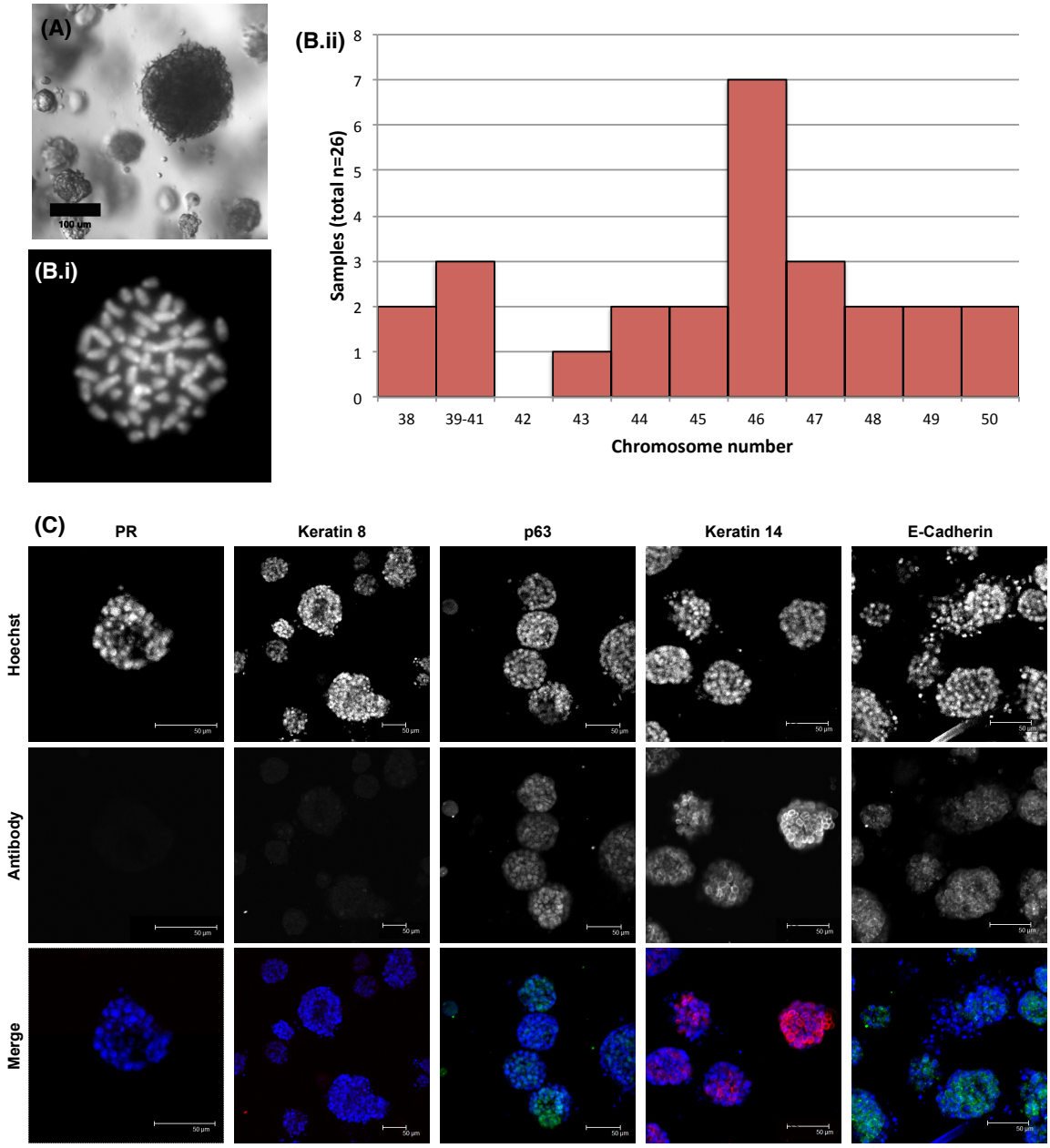

Figure 3.25 Mammary organoids grown under conditions promoting basal-like growth for 112 days exhibit abnormal phenotype and increased chromosome number.

Organoid were cultured in media supplemented with EGF (50 ng/ml), Noggin (100 ng/ml) and R-Spondin1 (42.5 ng/ml). **(A)** Representative image of organoid morphology at day 112. **(B)** Karyotyping was performed on organoids, indicating abnormal chromosomal numbers **(i)** Representative image of abnormal chromosome spread. **(ii)** Histogram of chromosome number per organoid. **(C)** Organoids were then fixed after 112 days and immunostained for luminal (PR, Keratin 8) and basal (p63, Keratin 14) markers, in addition to β-catenin. Scale 50 µm.

3.3 Summary

Here, culture conditions have been successfully optimised and studied in detail for the extended in-vitro, 3-dimensional development and expansion of functional, proliferative and differentiated mammary epithelial organoids recapitulating *in vivo* tissue architecture, from a variety of cell preparations. This 3D system is unlike any other currently available, retaining hormone responses for at least 5 times longer than present systems allow.

This work has highlighted the value of both the Wnt/R-Spondin1 and Nrg1 signalling pathways in normal mammary organoid development. The utility of the system for such investigations of growth factor signalling pathways could be extremely useful to the field of mammary biology, and is explored further in Chapter 4. Furthermore, the concurrent extended maintenance of mammary cells with regenerative ability and functional hormone responsive cells for the first time in accessible 3D culture may allow the individual properties of and interplay between mammary cell populations to be studied. This is explored further in Chapter 5.

Importantly, it has been demonstrated that structures grown under NRL conditions may have limited normal regenerative capacity when compared to those derived from other previously published tissues. This is of particular interest, and will be discussed later in this thesis.

Finally, highly Wnt driven conditions have been identified that promote a pro-tumorigenic environment, inducing the development of abnormal, undifferentiated basal-like structures from wild-type tissue. In addition to illustrating the importance of extracellular cues in regulating development, this suggests that the system may be amenable to the culture of cancer-derived organoids, under the correct conditions. This could, in turn, aid the identification of signalling pathways involved in tumour growth and development, and is studied further in Chapter 6.

4 Utilising the NRL mammary organoid culture system to study important signalling pathways in mammary development.

4.1 Introduction

In vivo, mammary gland development is known to be regulated and influenced by many factors, both pre and postnatally, as detailed in section 1.1.3. *In vitro* studies into such factors, their related signalling pathways and how their deregulation can lead to pathologies have thus far been primarily conducted either in cell lines, where lack of heterogeneity often means that important cell-subtype interactions cannot be truly assessed, or in animal models, in overexpression or knockout mutant mouse lines where dynamic changes in signalling are hard to study.

The mammary organoid culture system, conversely, in combination with the various forms of analysis described in Chapter 3, appears to be an appropriate system in which growth factor pathways effects on morphogenesis, proliferation and differentiation can be studied with ease. In light of this, the optimised NRL mammary organoid system was here utilised for the further investigation of several key signalling pathways known to regulate mammary gland development and maintenance *in vivo*. Work aimed to expand the biological understanding of such pathways within normal mammary development, but also to examine dysregulation of such pathways in disease and physiologically relevant regulators that may be able to further improve the potential of the organoid system to recapitulate normal development in the future.

In Chapter 3, the Wnt potentiator R-Spondin1, via the canonical Wnt signalling pathway, was required at a tightly controlled concentration that is consistent with a 'just-right' level of Wnt pathway activation (see Discussion). Given the suggestion (see Introduction) that the Wnt signalling pathway is critical for the maintenance of a subpopulation of basally located stem cells that are key for mammary development and regeneration (1.1.3.1), the first main focus of work in this chapter was the further detailed analysis of the role of and requirement for the canonical Wnt signalling pathway in 'normal' mammary organoid development.

Furthermore, signalling via various receptor tyrosine kinase ligand families, discussed at length in 1.1.3.2, has also been highly implicated in mammary gland development *in vivo*, at various stages, including the extensive FGF family, the known

mitogenic 'mammary growth factor' HGF, and one of the key components of our optimised media, Neuregulin1. Here, the biological effects of supplementing or ablating these signalling pathways were assessed using the mammary organoid culture system.

4.2 Results

4.2.1 Mammary organoids have little response to exogenous Wnt stimulation.

The observation that R-Spondin1 modulation can so drastically alter organoid morphology and phenotype supports the role of the Wnt signalling pathway as a crucial regulator of mammary development. Moreover, this data indicates that endogenous Wnt signalling must occur within our mammary organoid cultures, since R-spondin1 is only able to activate the pathway in the presence of Wnt ligands.

Here, the biological effect of increasing Wnt ligand availability was assessed in NRL conditions to determine whether exogenous sources of Wnt affected organoid formation efficiency or the ability of mammary organoids to differentiate correctly. Given the observed phenotype under high R-Spondin1 conditions, it was expected that improved organoid formation efficiency and a similar hyperkeratinisation and loss of luminal differentiation might be seen under higher Wnt stimulation. For this, purified Wnt3a ligand was used in culture in a similar way to that initially shown by Sato et al (2011,A).

For comparison, Wnt *conditioned* media (Wnt3A-CM) derived from the 2D culture of Wnt-3A expressing L-cells, was also analysed since 'poorly defined' conditioned medium was found to benefit human colonic epithelial culture; a function of colonic, but not small intestinal culture, in a way not replicated by purified Wnt-3A ligand alone (Sato et al., 2011,B; Luned Badder, Dale lab - personal communication).

4.2.1.1 Wnt3a

Cultures of primary epithelial fragments were treated with optimised NRL media supplemented with both Y-27632 (10 μM), and a set concentration of purified Wnt3a (R&D systems) (0, 25, 50 or 100 ng/ml). Importantly, this ligand had previously shown activity in 2D luciferase based Wnt reporter assays within the lab, using a cell line described by(Ewan *et al.* 2010). After 12 days, no substantial differences in organoid formation efficiency could be observed under any concentration of Wnt3a (Figure 4.1B, C).

Morphologically, organoids treated with Wnt3a remained rounded, with little to no lobular development at all, while the control condition did demonstrate early lobular development, as seen in Figure 4.1A, indicating some level of response to Wnt3a. However, against expectations, squamous, highly keratinous organoids were not observed in this experiment under any applied concentration of purified Wnt3a, although darker centres were noticeable at day 12 in Wnt3a treated organoids (Figure 4.1.A, white arrows), indicating that given more time in culture a more pronounced effect of Wnt3a may develop. Furthermore, phenotypical analysis demonstrated a maintained expression of both luminal hormone receptor and basal p63 markers under all concentrations of Wnt3a (Figure 4.2).

In all, results demonstrate that Wnt3a treatment does not reproduce effects on organoid growth and differentiation observed under high R-Spondin1 stimulation, possibly reflecting technical issues with the penetration of the ligand into organoids, or alternatively indicating biological phenomena that will be discussed further in Chapter 7.

4.2.1.2 Wnt3A-CM

Based on current work in other organoid systems in the Dale lab, where conditioned media is used as standard, epithelial cultures were set up such that media contained both the 'normal' concentrations of Nrg1, Nog, and R-Spondin1, with Y-27632 for the first 5 days of culture, and either 10, 20 or 40% Wnt3A-CM. A control, NRL condition was also created.

Compared to the control, average organoid number in cultures treated with 20% or 40% Wnt3a-CM increased (1.40 and 1.56 fold, respectively)(Figure 4.3), with slight increases in the average size of the organoids formed (1.17 and 1.28 fold, respectively), although these results (n=2) should be interpreted with caution and further repeats undertaken to establish any level of significance.

Morphologically, Wnt3a-CM treated organoids exhibited lobular development, in contrast to purified Wnt3a treated organoids, at as early as 3 days into culture. Organoids however also contained potentially keratinous patches, and were associated with contaminating fibroblast-like structures. Given that conditioned media produced by L- cells undoubtedly contains several unknown Wnt-induced secreted growth factors, it is highly likely that these induce such morphological changes.

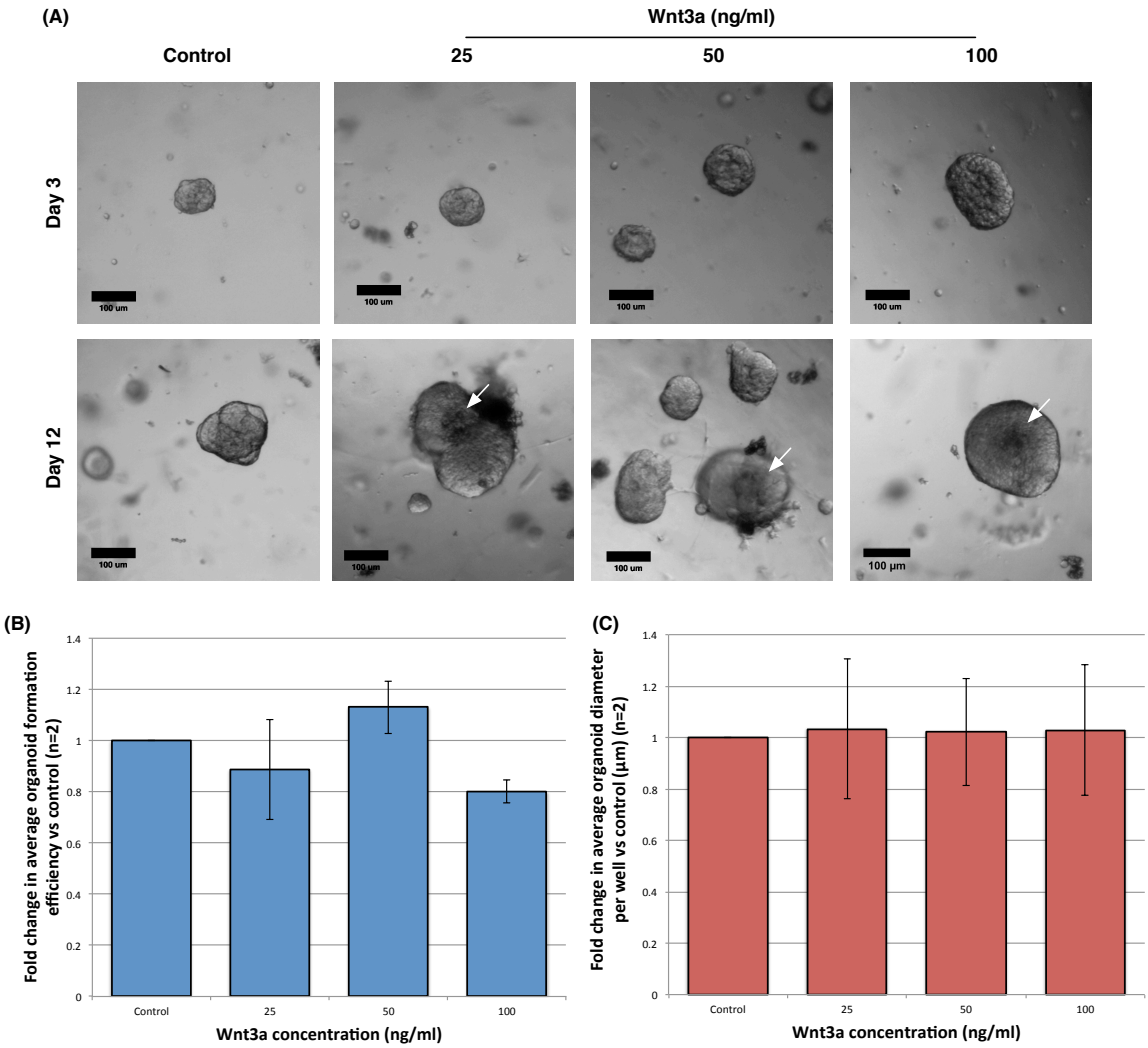

Figure 4.1 Analysis of effect of Wnt3a on mammary organoid morphology and growth over a period of 12 days from primary epithelial fragments.

Unsorted epithelial fragments were cultured for 12 days, in mammary organoid media containing Nrg1 (100 ng/ml), Noggin (100 ng/ml), R-Spondin1 (2.7 ng/ml), with Y-27632 (10µM) for the first 5 days. In addition to a control, cultures were then additionally treated with either purified Wnt3a (25, 50 or 100 ng/ml) **(A)** Representative images demonstrating morphological development of organoids from day 3 to day 12 of culture. Scale 100 µm. **(B)** Bar chart depicting fold change in average organoid number per well compared to the control condition after 12 days in culture (n=3). **(C)** Bar chart depicting fold change in average organoid diameter (µm) compared to the control condition after 12 days in culture. All data points shown as mean ± standard deviation (n=2).

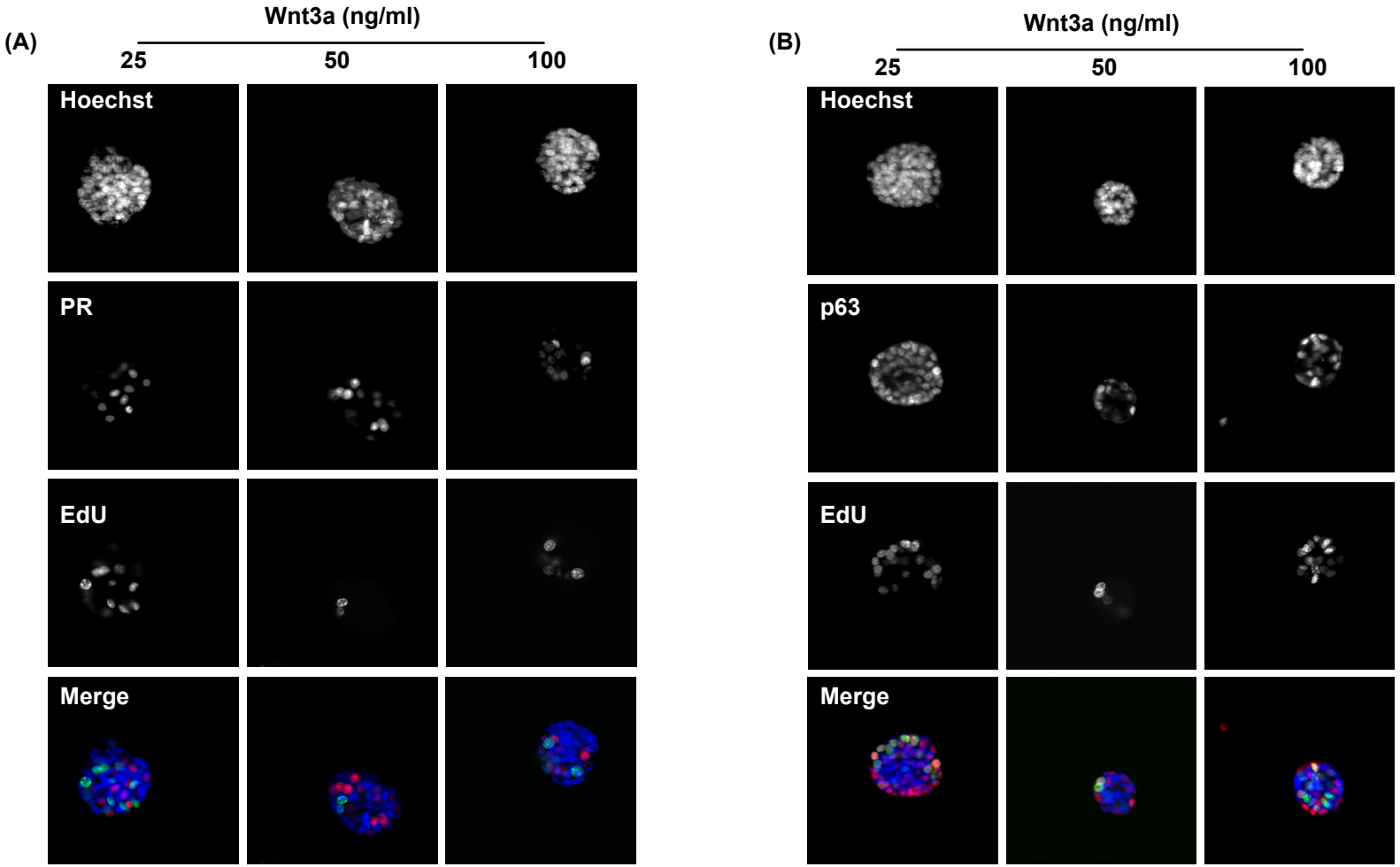

Figure 4.2 Mammary organoids grown under defined conditions supplemented with purified Wnt retain normal phenotypic marker expression.

Mammary organoids grown from freshly isolated material were grown in media containing Nrg1 (100 ng/ml), Noggin (100 ng/ml) and R-spondin1 (2.7 ng/ml), and either 25, 50 or 100 ng/ml purified Wnt3a, and fixed after 12 days in culture, with EdU treatment for 2 hours prior to fixing. Organoids were then co-immunostained for (A) luminal PR or (B) basal p63 expression, and EdU and counterstained with Hoechst. Images obtained by Bleddyn Williams during MSc project.

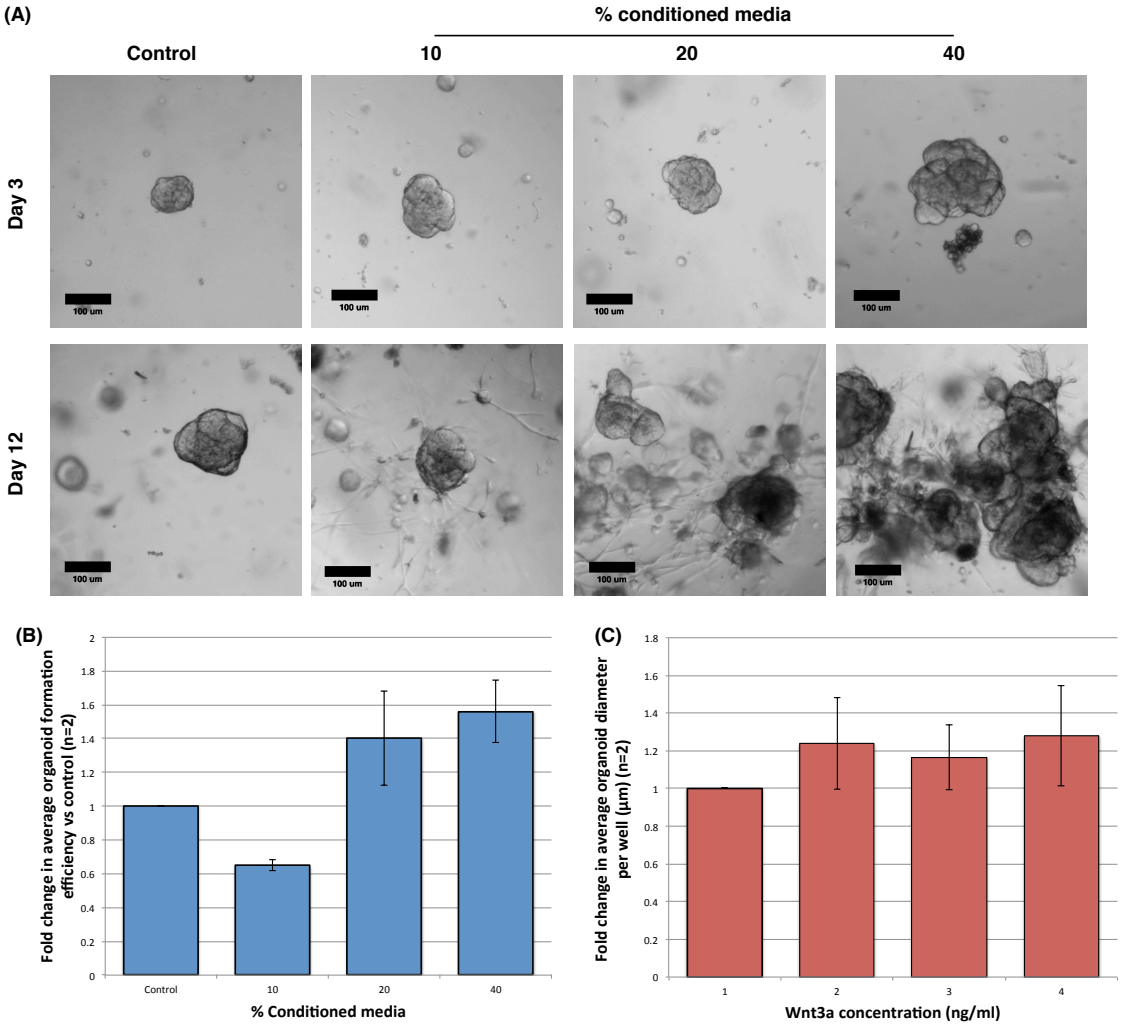

Figure 4.3 Analysis of effect of conditioned Wnt media on mammary organoid morphology and growth over a period of 12 days from primary epithelial fragments.

Unsorted epithelial fragments were cultured for 12 days, in mammary organoid media containing Nrg1 (100 ng/ml), Noggin (100 ng/ml), R-Spondin1 (2.7 ng/ml), with Y-27632 (10µM) for the first 5 days. In addition to a control, cultures were then additionally treated with 10%, 20% or 40% Wnt3a-CM **(A)** Representative images demonstrating morphological development of organoids from day 3 to day 12 of culture. Scale 100 µm. **(B)** Bar chart depicting fold change in average organoid number per well compared to the control condition after 12 days in culture (n=3). **(C)** Bar chart depicting fold change in average organoid diameter (µm) compared to the control condition after 12 days in culture. All data points shown as mean ± standard deviation (n=2).

4.2.1.3 Wnt4

Since Wnt3a is not an endogenously produced Wnt ligand in the mammary gland (although it is know to transform the mammary epithelium when expressed from the MMTV-promoter (Roelink *et al.* 1990), and has facilitated basal cell expansion *in vitro* (Zeng and Nusse 2010)), the known mammary specific ligand Wnt4 was instead applied in culture. However, similar to results previously observed under Wnt3a treatment, mammary epithelial cells grown under Wnt4 stimulation for 14 days exhibited no increase in organoid formation efficiency (Figure 4.4).

4.2.2 Wnt pathway activity is intrinsic to normal mammary organoid development

To further investigate the reliance of organoid culture on endogenous Wnt signalling, published small molecule Wnt inhibitors (Chen et al., 2009) were utilised: firstly, the Porcupine, and therefore Wnt production and release inhibitor, IWP-2 (cellular IC_{50}=50nM), and secondly, the Tankyrase inhibitor (TNKSi) IWR-1 (cellular IC_{50}=190nM). Organoids were grown from trypsinised cells, under the defined NRL conditions.

4.2.2.1 Inhibition of Wnt release by IWP-2 inhibits mammary epithelial organoid growth and normal differentiation

Inhibition of Wnt ligand production and release by addition of IWP-2 significantly reduced both the organoid formation efficiency of single mammary epithelial cells, under all concentrations applied, by approximately a third compared to control in all cases ($n=4$, $p<0.05$)(Figure 4.5 A(i)). Organoid diameter was also significantly affected by IWP-2 treatment, with a reduction of between 10 and 14% of the size control organoids observed ($n=4$, $p<0.05$ and $p<0.01$ respectively) (Figure 4.5A(ii)). Although not tested in this particular experiment, it might be expected that organoids grown under high R-Spondin1 conditions would exhibit a normal phenotype (including restored PR expression) when treated with IWP-2, instead of the usually observed 'abnormal' phenotype. Unexpectedly however, even in NRL culture conditions, phenotypical analysis showed inhibition with IWP-2 reduced PR expression within the organoids, while having little effect on p63 expression or localisation (Figure 4.5C), suggesting that there is an intrinsic need for endogenous Wnt signalling for the correct luminal differentiation of the organoids.

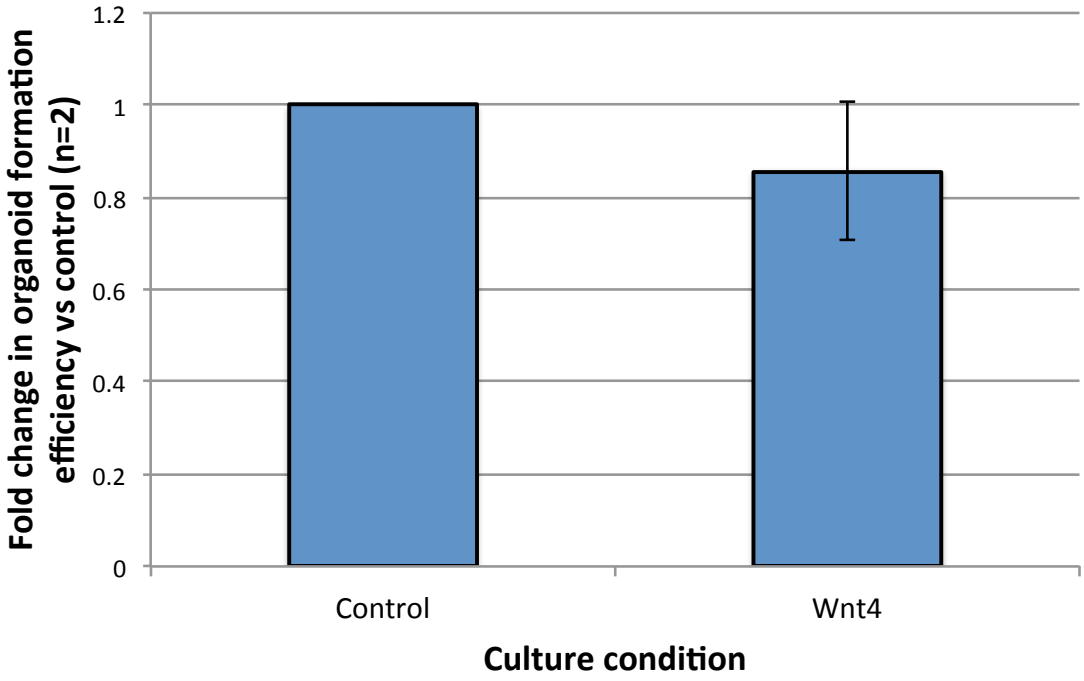

Figure 4.4 Effect of Wnt4 on mammary organoid formation efficiency.

Mammary epithelial cells were plated at a density of 1000 per µl growth factor reduced matrigel and overlaid with media containing Nrg1 (100 ng/ml), Noggin (100 ng/ml) and R-spondin1 (2.7 ng/ml) alone, or supplemented with Wnt4 (100 ng/ml), with Y-27632 (10µM) for the first 5 days in culture. Organoid formation efficiency was calculated after 14 days in culture. Data shown as mean±s.e.m, where n=2.

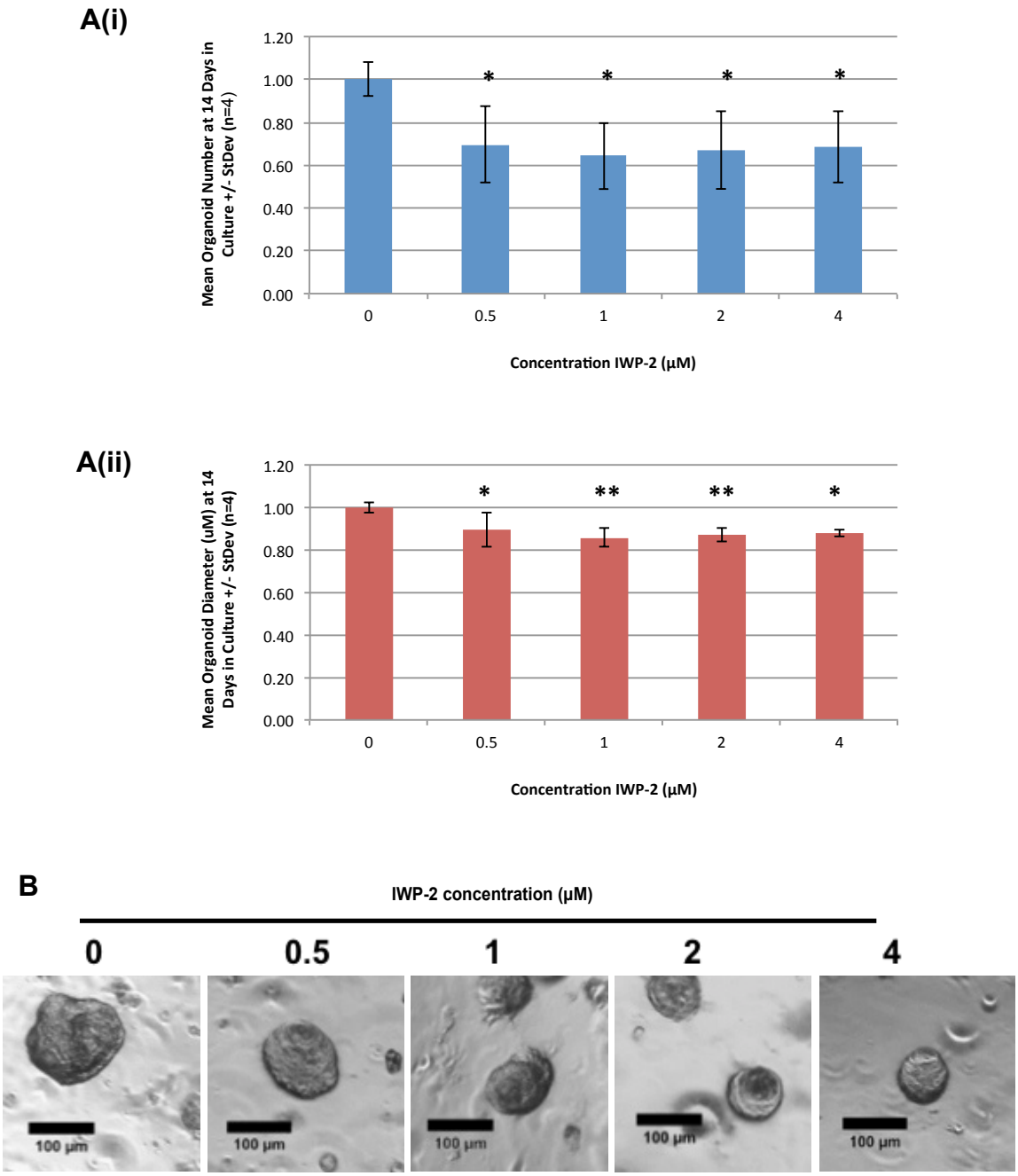

Figure 4.5 Effects of Wnt pathway inhibition by the porcupine inhibitor IWP-2, on normal mammary epithelial organoids.

Unsorted, trypsinised mammary epithelial cells were seeded at 1000 per µl growth factor reduced Matrigel, and overlaid with defined, R-Spondin1 low media, supplemented with Y-27632 (10µM) for the first 5 days in culture. Cultures were from seeding additionally treated with DMSO, as a control, or a range of IWP-2 concentrations. **(A)(i)** Bar chart depicting average organoid count per well (n=4). **(A)(ii)** Bar chart depicting average organoid diameter (µm) per well (n=4). Data are provided as mean ± standard deviation. Statistical significance as calculated by a one way ANOVA, followed by Dunnett's post-hoc testing, indicated by * ($p<0.05$) ** ($p<0.01$) **(B)** Representative images of morphology of organoids in each treatment condition, after 14 days in culture. Scale 100 µm. **(C)** Confocal images of immunofluorescence staining for **(i)** luminal progesterone receptor **(ii)** basal p63 expression. Scale 50 µm. Data obtained by Eleanor Cawthorne, under my supervision.

C(i)

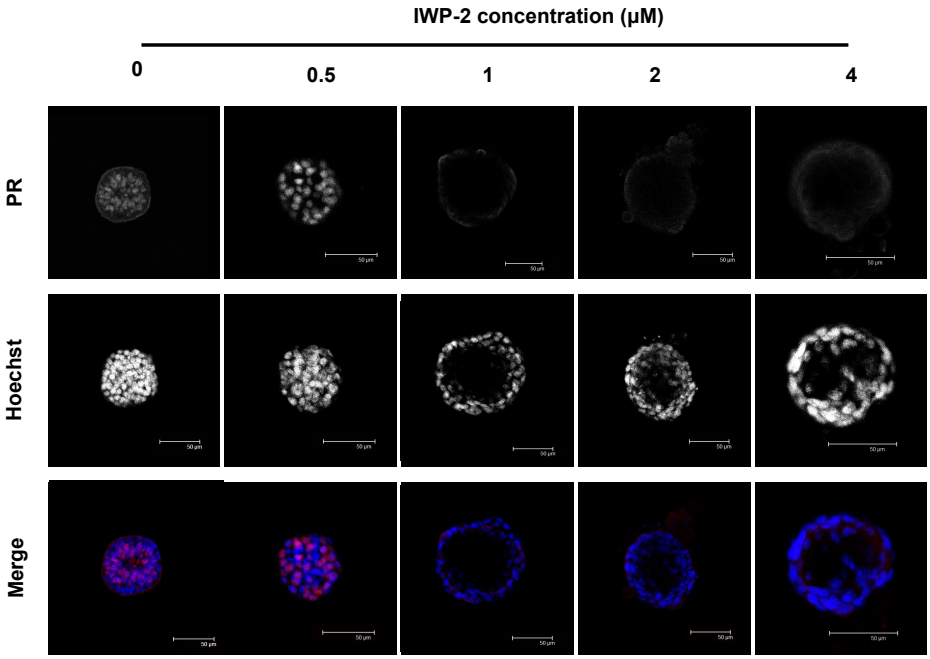
IWP-2 concentration (μM)
0
0.5
1
2
4
PR
Hoechst
Merge

C(ii)

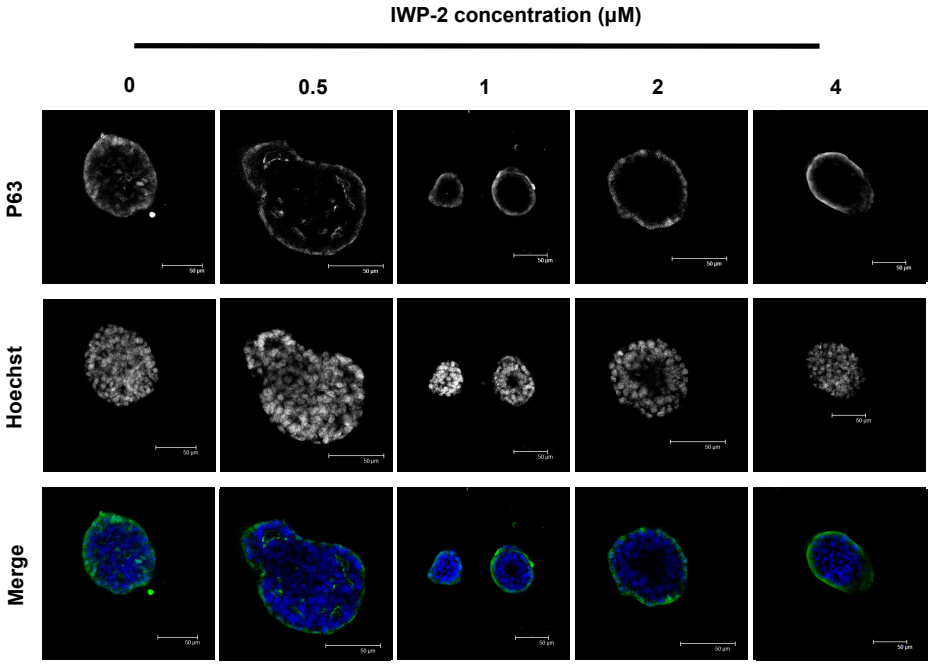
IWP-2 concentration (μM)
0
0.5
1
2
4
P63
Hoechst
Merge

4.2.2.2 *Inhibition of endogenous Wnt signalling by IWR-1 inhibits mammary epithelial organoid growth*

Organoid formation efficiency, compared to the untreated control, was noticeably reduced in organoids treated with the TNKS inhibitor IWR-1, with a statistically significant maximum effect of 40% reduction at 37.5nM ($n=4$, $p<0.01$), while organoid diameter was also reduced, by between 6 and 17% over the concentration range (Figure 4.6A). Morphologically, organoids appeared smaller, but not obviously altered (Figure 4.6B). As seen with responses to the Porcupine inhibitor (IWP-2), phenotypical analysis of the IWR-1 treated organoids indicated that at the higher inhibitor concentrations, PR expression was lost, while p63 expression remained fairly similar to the control condition (Figure 4.6C).

The identification of similar results whether inhibiting Wnt release from a producing cell or Wnt activity in a responding cell, implies a true biological effect rather than off-target side effects of the inhibitors, and taken together, results indicate that endogenous Wnt signalling activity is essential for normal mammary organoid growth, differentiation and organisation.

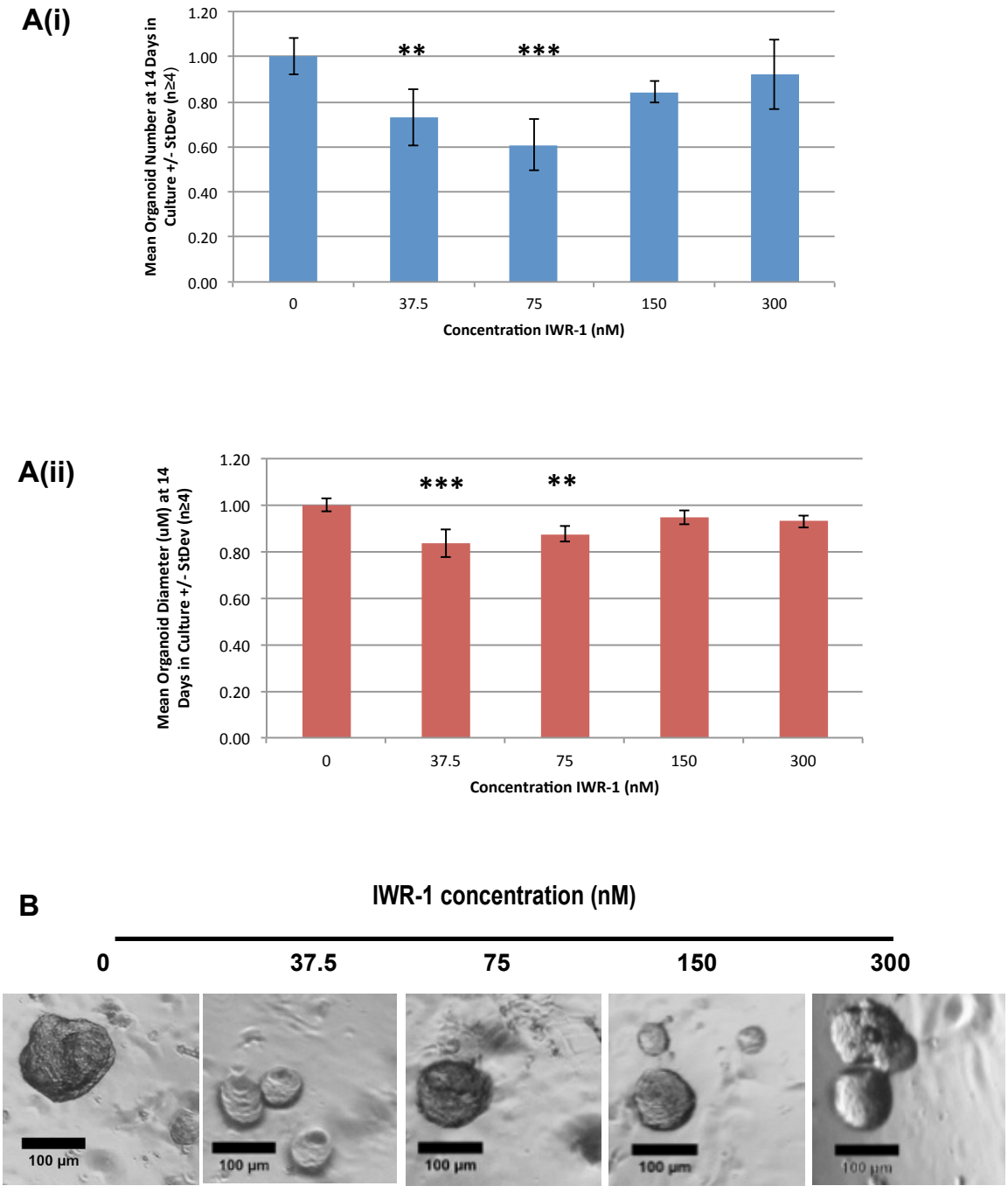

Figure 4.6 Effects of Wnt pathway inhibition by the tankyrase inhibitor IWR-1 on normal mammary epithelial organoids.

Unsorted, trypsinised mammary epithelial cells were seeded at 1000 per µl growth factor reduced Matrigel, and overlaid with defined, R-Spondin1 low media, supplemented with Y-27632 (10µM) for the first 5 days in culture. Cultures were from seeding additionally treated with DMSO, as a control, or a range of IWR-1 concentrations. **(A)(i)** Bar chart depicting average organoid count per well (n=4). **(ii)** Bar chart depicting average organoid diameter (µm) per well (n=4). Data are provided as mean ± standard deviation. Statistical significance as calculated by a one way ANOVA, followed by Dunnett's post hoc testing, indicated by ** ($p<0.01$) ***($p<0.001$) **(B)** Representative images of morphology of organoids in each treatment condition, after 14 days in culture. Scale 100 µm. **(C)** Confocal images of immunofluorescence staining for **(i)** luminal progesterone receptor **(ii)** basal p63 expression. Scale 50 µm. Data obtained by Eleanor Cawthorne, under my supervision.

C(i)

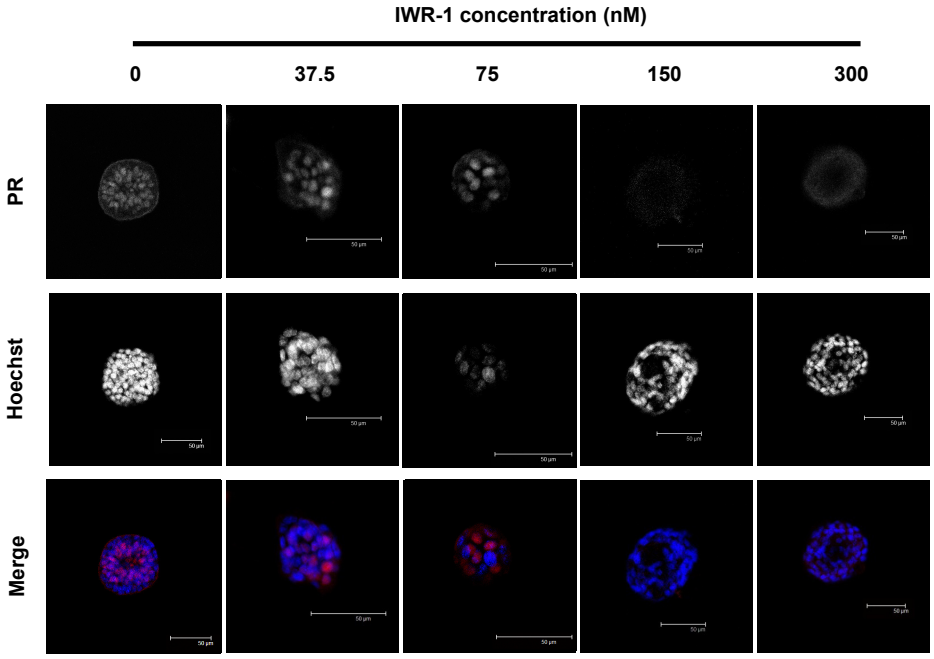
IWR-1 concentration (nM)
0
37.5
75
150
300
PR
Hoechst
Merge

C(ii)

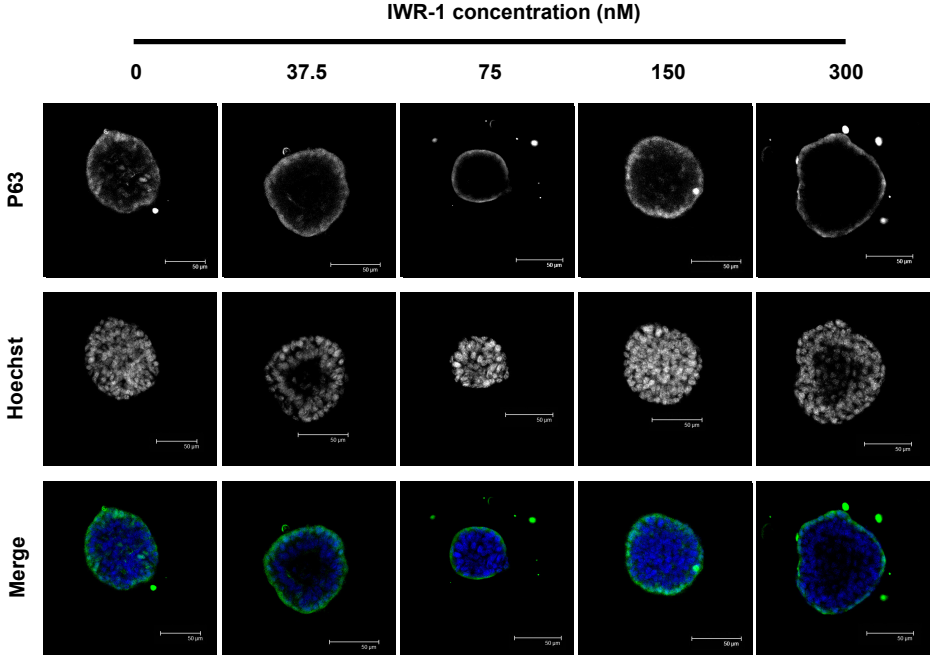
IWR-1 concentration (nM)
0
37.5
75
150
300
P63
Hoechst
Merge

4.2.3 The FGF family support normal mammary development

4.2.3.1 Fgf2

Although not widely discussed in literature detailing mammary gland development, FGF2 has previously been shown in 3D mammary gland morphological assays to promote growth and branching of structures *in vitro (*Sternlicht, 2005, Huebner et al., 2014), and as such was trialled in this organoid system as a comparison of this system with previously published evidence.

After 7 days in culture, FGF2 statistically significantly increased the number of organoids formed from unsorted material, regardless of concentration applied, in each case inducing approximately a 4.5 fold increase in organoid formation compared to the control condition (n=3, ANOVA with Dunnett's post-hoc analysis)(Figure 4.7Bi). These organoids were on average of significantly increased size compared to untreated counterparts, correlating positively with increasing FGF2 concentration (1.3 fold, p=0.0015; 1.4 fold, p=0.0006; 1.4 fold, p=0.0003 respectively, n=3, ANOVA with Dunnett's post-hoc analysis)(Figure 4.7Bii).

Morphologically, structures developed multiple noticeable lobules (Figure 4.7A). It was also noted that several fibroblast like structures appeared towards the end of culture.

In order to further investigate the fibroblastic structures, and whether they had derived from fibroblasts remaining in the unsorted material or were a result of an growth-factor induced epithelial-to-mesenchymal transition in culture, primary material was FAC sorted (Materials and Methods, Figure 2.1) to remove non-epithelial cells, before repeating the experiment with pure epithelial cell populations seeded at 1000 per µl growth factor reduced Matrigel (Figure 4.8). In this case, after 12 days in culture, FGF2 at every concentration induced a similar average fold increase in organoid number per well (5.6, 3.3, 4.6 fold vs control; n=2) and average fold increase in organoid diameter as in the previous experiment (1.1, 1.5, 1.7 fold vs control; n=2)(Figure 4.8B), while structures similarly exhibited an extremely lobular morphology (Figure 4.8A). Importantly, fibroblasts were not observed following FACS, indicating that previous observations were from contaminating cells.

Given the similarities between results from increasing concentrations of FGF2, the lowest concentration of 25 ng/ml was chosen as representative for more detailed analysis. Wholemount immunofluorescence staining of structures cultured under this condition for 14 days demonstrated a maintained co-expression of both steroid hormone receptors, in addition to internal Keratin-8 localisation, while the basal markers p63 and Keratin-14 were localised correctly at the outer edges of the organoids. β-catenin was found to be mainly located at cell-cell junctions throughout organoids (Figure 4.9). OcellO 3D morphometric analysis of organoids grown under 25ng/ml FGF2 for 14 days was performed, and overall heat map profiles of all parameters tested observed to be similar to control conditions (Figure 4.10.A). Data reconfirmed an increased organoid size compared to the control condition, as previously noted by GelCount analysis. The parameters with largest variations from the control condition were observed to be lumen roundness and complexity, indicating that in addition to the visible, external morphological effects of FGF2 on organoid development, internal alterations also occur. Finally, FGF2 appeared to have no effect upon cell survival in organoid culture, based on the fraction of apoptotic cells observed (Figure 4.10.B).

4.2.3.2 Fgf7

FGF7 is thought to have roles in mammary gland development both in the embryonic stage and postnatally, and is usually expressed by the stroma. Given that the mammary organoid is purely epithelial, the effect of stromally-derived signals on development was of interest.

Treatment with FGF7 significantly increased organoid outgrowth compared to the control condition, in a concentration dependent manner, with the largest increase at 100 ng/ml of approximately 4 fold ($p=0.0001$, $n=3$, ANOVA with Dunnett's post-hoc analysis)(Figure 4.7Bi). FGF7 at concentrations of 25, 50 and 100 ng/ml caused significant increases in average diameter of organoids (µm) compared to the control ($p= 0.0048$, 0.0018, 0.0011 respectively. $n=3$, ANOVA with Dunnett's post-hoc analysis)(Figure 4.7Bii). Organoids interestingly were larger, but did not exhibit any lobular development (Figure 4.7A). As in FGF2 supplemented cultures, many fibroblasts were observed, leading to a follow up experiment using FAC sorted definitive epithelial cells.

Following FAC sorting, results after 12 days were observed to differ greatly to those described without FACS. FGF7 concentrations of 25, 50, and 100 ng/ml induced 16, 30.2 and 18.1 fold increases in average organoid number per well (n=2) respectively, indicating a much larger effect of FGF7 on the organoid formation efficiency of single epithelial cells than unsorted fragments (Figure 4.8Bi). This might also imply indirect effects of the cultured fibroblasts in experiments with unsorted cells. Morphologically, the structures cultured from FAC sorted cells were primarily rounded, with very few lobular structures (Figure 4.8A). Although organoid number was increased compared to the control, analysis indicated that average organoid size was unaltered in all three FGF treatment groups (Figure 4.8Bii).

Phenotypical analysis of FGF7 (25 ng/ml) treated organoids performed at day 14 in culture highlighted the maintained co-expression and distinct localisation of hormone receptors, intra-organoid keratin 8, peripheral Keratin-14 and p63 and junctional B-catenin localisation (Figure 4.9). OcellO 3D morphometric analysis of multiple parameters indicated many differences in almost all organoid characteristics analysed under FGF7 (25 ng/ml) treatment when compared to the control condition (Figure 4.10.A). As in previous analyses of unsorted cells, organoid size was shown to increase with FGF7 treatment, while data revealed increased organoid lumen complexity and a reduction in apoptotic cell fraction (Figure 4.10.B), suggesting FGF7 may be a morphogenic and pro-survival factor for the mammary organoids.

4.2.3.3 Fgf10

FGF10 has been considered the key FGF for mammary gland embryonic and postnatal development, also supplied by stromal cells, much like FGF7. However, of the three FGF ligands applied to unsorted fragments in culture, FGF10 had the least effect. Nonetheless, all three concentrations (25, 50, 100 ng/ml) still significantly increased organoid formation compared to the control in a concentration dependent manner (2.1 ($p=0.0078$), 2.6 ($p=0.0012$) and 3.2 fold ($p=0.0001$), respectively (n=3, ANOVA with Dunnett's post-hoc analysis)(Figure 4.7Bi). Average organoid diameter was also increased slightly, but not significantly, under the influence of FGF10 (Figure 4.7Bii). Morphologically, structures lacked distinct lobules, and large fibroblasts could be observed on the base of the well (Figure 4.7A).

Trends were similar upon FAC purification and culture of single, epithelial cells. Increases in average organoid number per well compared to control was much greater than that seen in unsorted cultures for each of 25, 50 and 100 ng/ml FGF10 conditions (7.4, 11.5, 15 fold, respectively, n=2, Figure 4.8Bi). No difference in average organoid diameter was seen compared to the control condition, although by eye increases in size could be seen for a subpopulation of organoids within the cultures under each concentration, and morphologically, a subset of organoids developed more evolved shapes (Figure 4.8C, A).

Organoids grown 25ng/ml FGF-10 were also found to retain 'normal' phenotypic marker expression and localisation, including hormone receptors, Keratins and basal p63, as seen in Figure 4.9. Furthermore, OcellO 3D morphometric analysis of organoids grown for 14 days under FGF10 (25 ng/ml) treatment demonstrated that, of all three FGF ligands investigated, FGF10 generated a parameter heat-map most similar to that of control conditions (Figure 4.10.A). While the size of FGF10 treated organoids was determined to be slightly increased compared to the control conditions, several key changes from the control were noted, including an increase in lumen complexity and a reduction in apoptotic cell fraction of organoids, suggesting FGF10 as acted as a morphogenic and pro-survival factor in mammary organoid culture (Figure 4.10.B).

From this data, it can be seen that each FGF promoted mammary development. Moreover, these factors supported 'normal' development, whereby organoids retain distinct luminal and basal compartments consisting of all differentiated cell populations, albeit with a higher efficiency than previously defined conditions. As such, these three factors could in future be used to enhance the efficiency of expansion of normal mammary epithelial culture material, in preparation for large-scale assays.

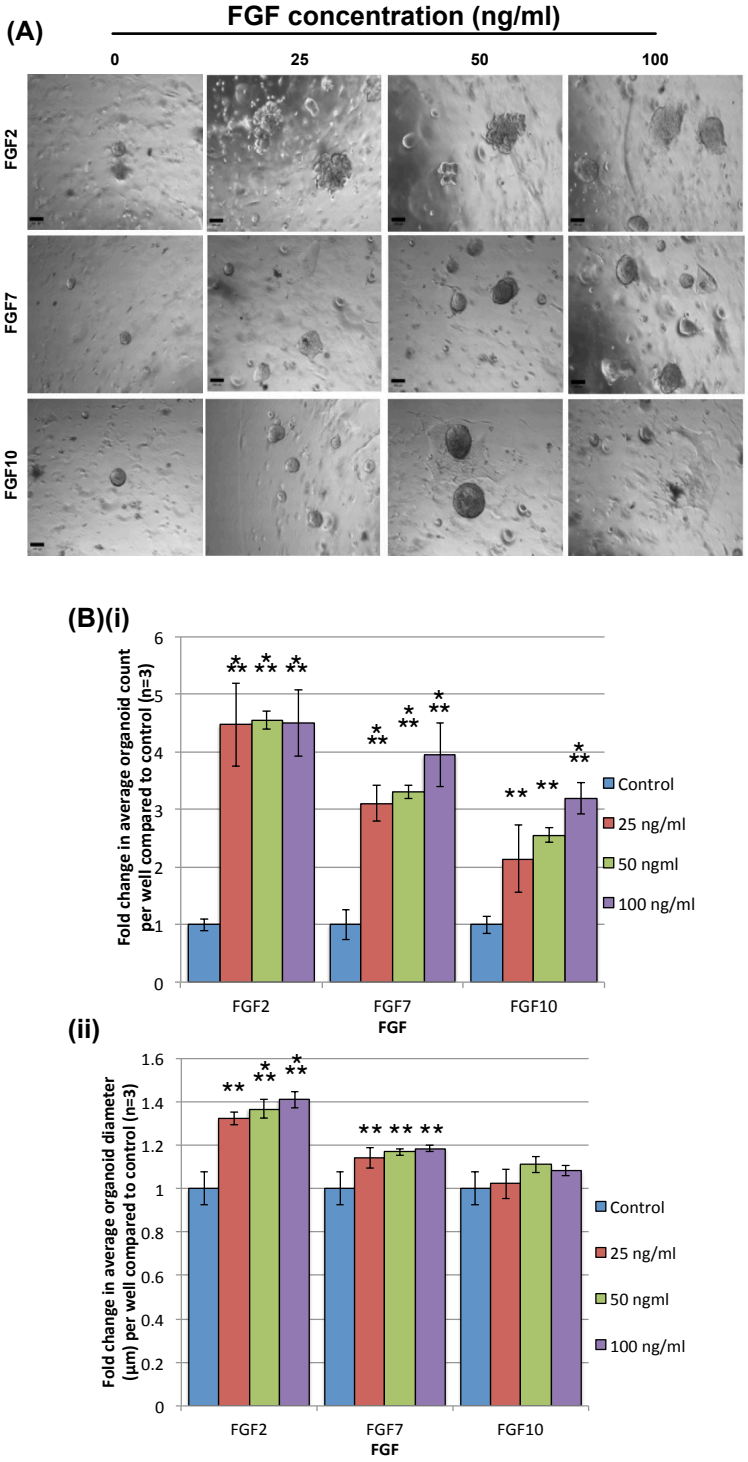

Figure 4.7 FGF treatment alters morphology and growth characteristics of mammary organoids from epithelial fragments.

Organoids were cultured for 10 days from epithelial fragments under NRL conditions supplemented with FGF2, FGF7 or FGF10 at 25, 50 or 100 ng/ml, and growth compared to a NRL only control. **(A)** Morphology of organoids at 5 days in culture. Scale 100 µm. **(B)(i)** Fold change in average organoid number per well vs control, at each concentration of each FGF family member, at 10 days in culture. **(ii)** Fold change in organoid diameter (µm) per well vs control, at each concentration of each FGF family member. N=3, means±s.e.m. Statistical analysis performed by one-way ANOVA with multiple comparisons, with Dunnett's post-hoc correction. **, $p < 0.01$; ***, $p < 0.001$.

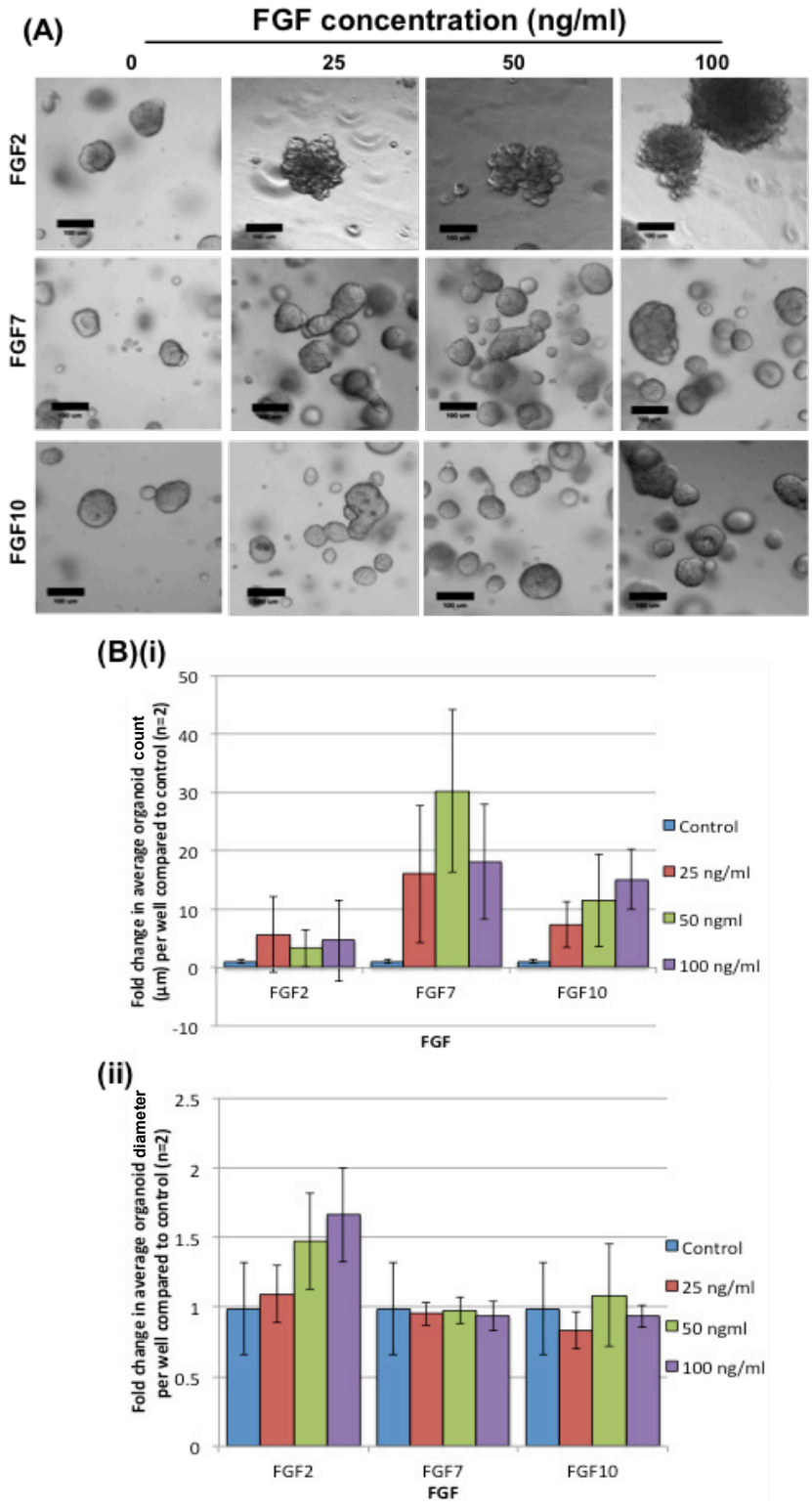

Figure 4.8 Effects of FGF treatment on mammary epithelial organoids derived from sorted single cells.

Organoids were cultured from unsorted mammary epithelial fragments under optimal conditions, supplemented with 0, 25, 50 or 100 ng/ml FGF2, FGF7 or FGF10. **(A)** Morphology of organoids at 12 days in culture. Scale 100µm. **(B) (i)** Bar chart depicting fold difference in average organoid number per well vs control, at each concentration of each FGF family member. **(ii)** Bar chart of fold change in average organoid diameter (µm) per well vs control, at each concentration of FGF 2,7 or 10. Data shown as mean ± s.e.m, n=2.

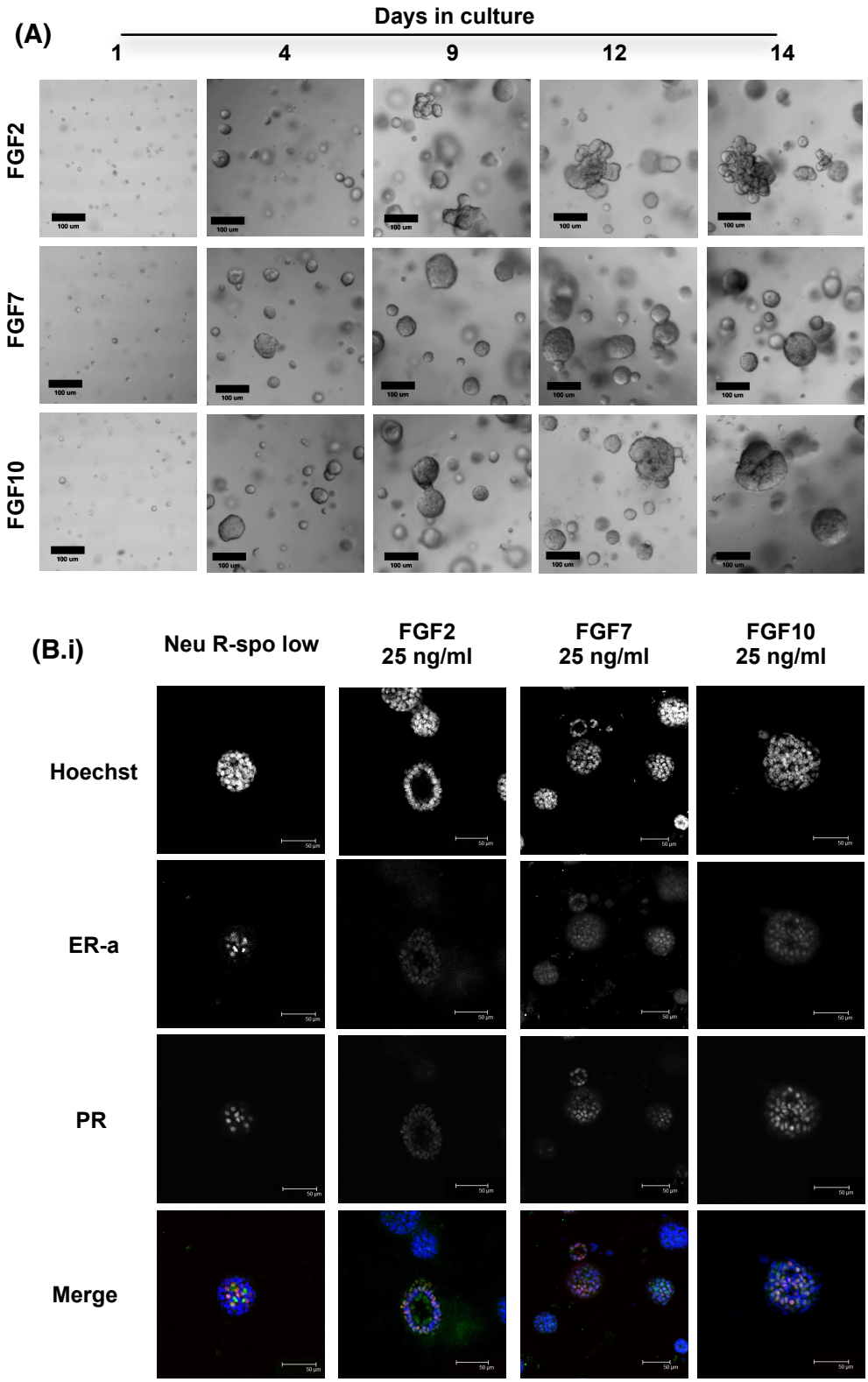

Figure 4.9 In depth analysis of the effect of FGF treatment on organoid morphology and phenotype.

Organoids were cultured from unsorted, trypsinised cells under optimal conditions supplemented with FGF2, 7 or 10 (25 ng/ml). **(A)** Morphology of organoids over 14 days in culture. Scale 100 µm. **(B)** Whole-cutlure immunofluorescence staining for: **(i)** Estrogen receptor-α, Progesterone receptor **(ii)** p63 and Keratin-8 **(iii)** Keratin-14 and β-catenin. Scale 50µm.

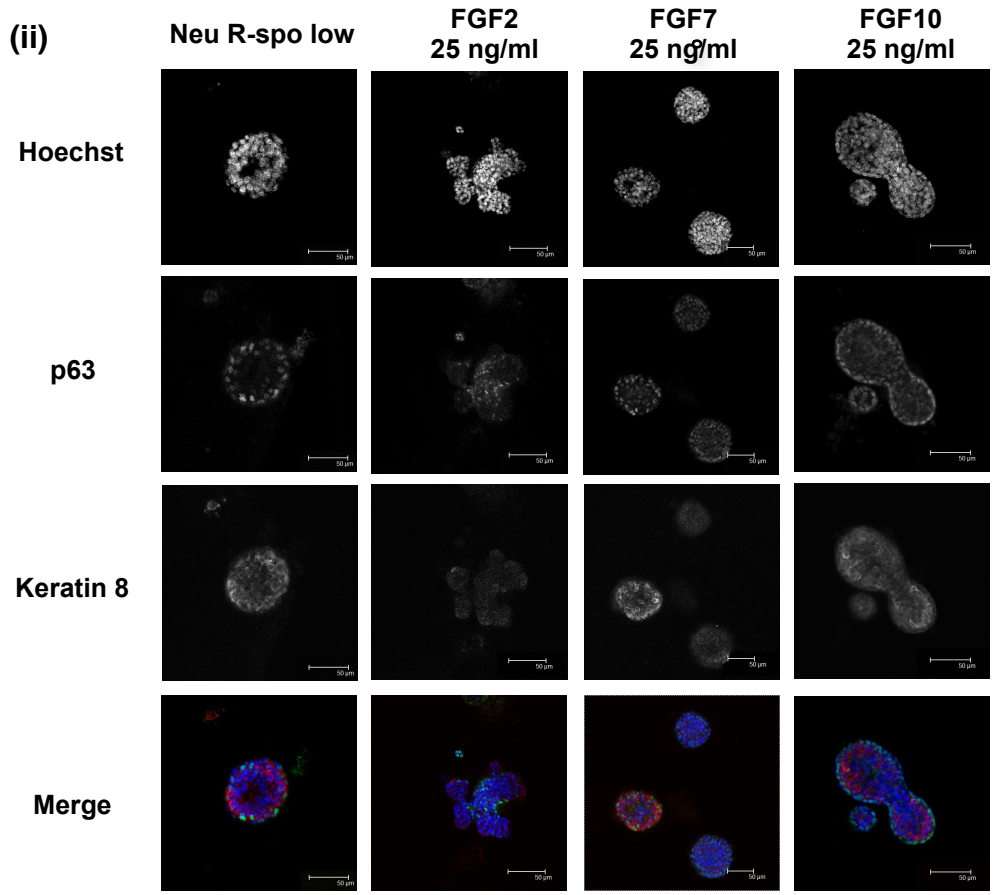
(ii)
Neu R-spo low
FGF2
25 ng/ml
FGF7
25 ng/ml
FGF10
25 ng/ml
Hoechst
p63
Keratin 8
Merge

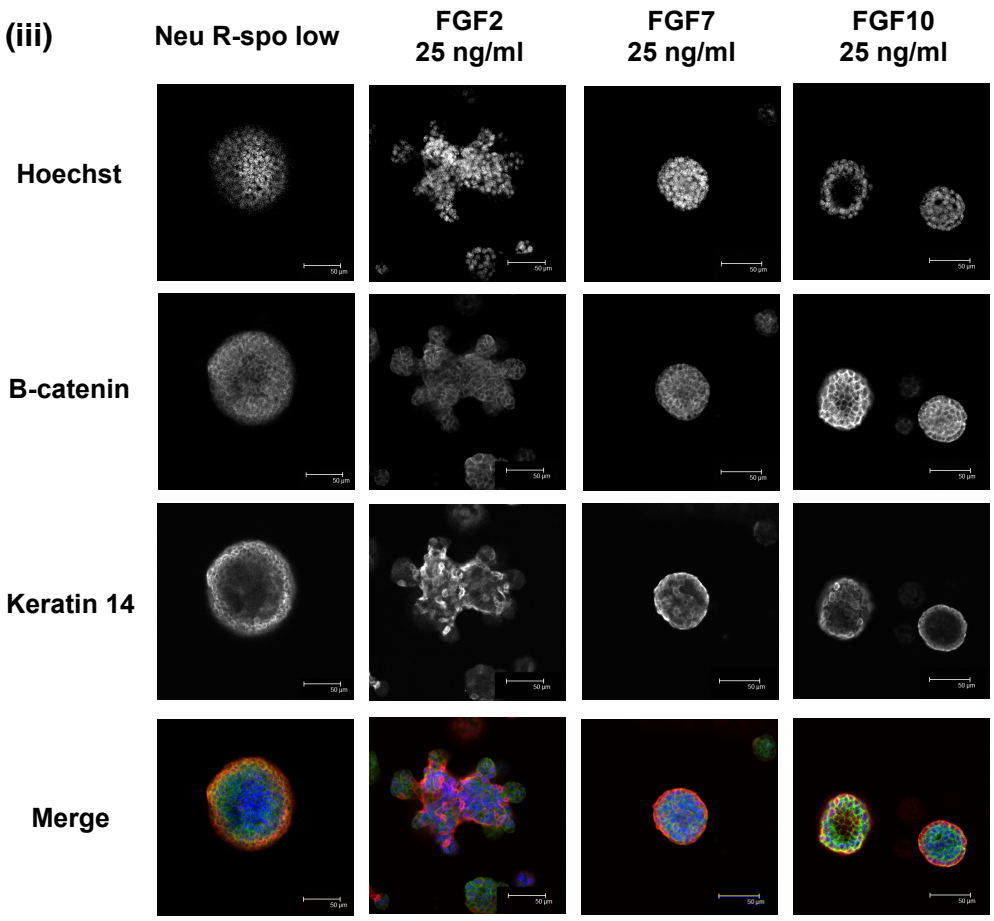
(iii)
Neu R-spo low
FGF2
25 ng/ml
FGF7
25 ng/ml
FGF10
25 ng/ml
Hoechst
B-catenin
Keratin 14
Merge

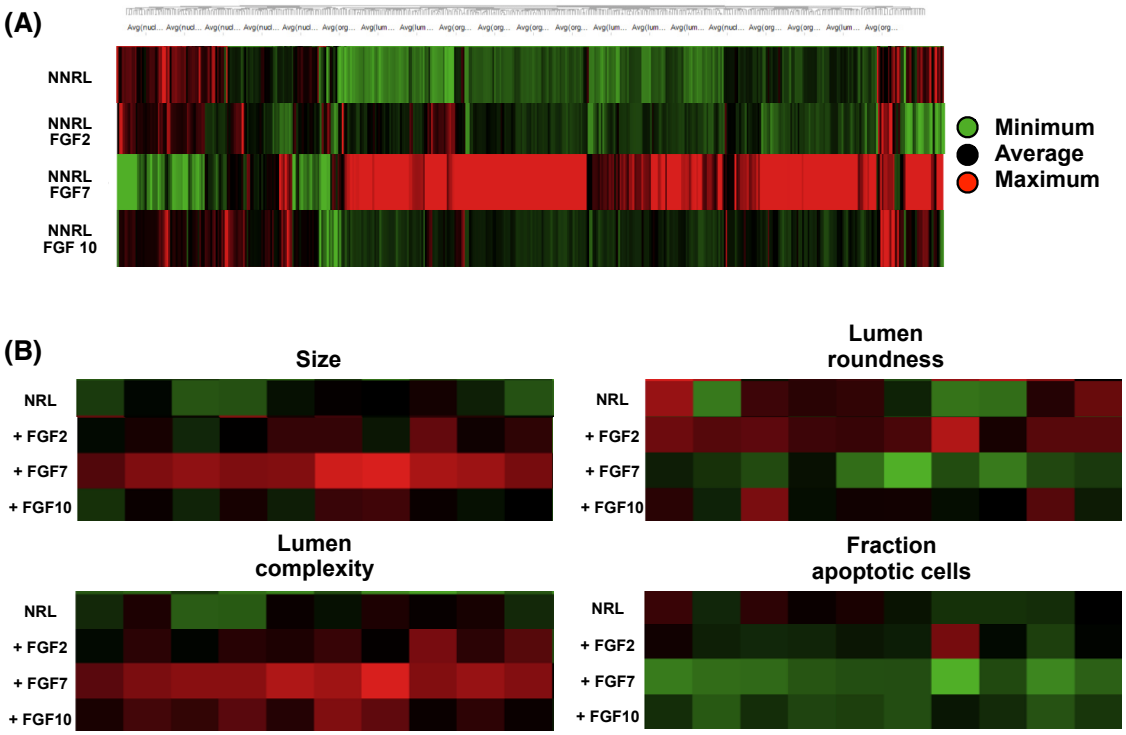

Figure 4.10 In depth OcellO analysis of organoids grown under FGF supplemented NRL media conditions.

Freshly isolated mammary epithelial cells were seeded in 384 well format in growth factor reduced Matrigel and grown for 14 days under conditions containing Nrg1 and Noggin in combination with R-Spondin1 (2.7 ng/ml) and FGF2, FGF7 or FGF10 at 25 ng/ml. Organoids were then fixed in OcellO proprietary stain and analysed by OcellO. **(A)** Feature cluster heat map indicating variation in multiple organoid properties between each culture condition. Over 400 parameters are summarized here. **(B)** Heat maps indicating variation in organoid size, lumen roundness, lumen complexity and fraction of apoptotic cells per organoid between culture conditions.

4.2.4 HGF signalling enhances mammary organoid development.

Hepatocyte growth factor has been widely discussed in the mammary gland culture field, as a factor expressed by the surrounding stroma to induce the migration and branching of mammary gland epithelial cells and was therefore deemed a relevant factor to investigate within our culture system.

Mammary epithelial cells were plated and cultured under NRL conditions supplemented with a range of HGF concentrations. In a preliminary experiment in which cultures were treated with 100 ng/ml HGF, extensive fibroblast growth was observed, to the detriment of organoid growth and Matrigel structure. Further investigations were therefore carried out using a lower range of HGF concentrations (3.125, 6.25, 12.5, 25, 50 ng/ml).

After 11 days in culture, HGF addition (3.125, 6.25, 12.5, 25, 50 ng/ml) significantly increased the number of organoids formed compared to the control condition, in a concentration dependent manner (1.86, 1.94, 2.09, 2.14 and 2.47 fold, respectively, ($n=4$, $p<0.001$, ANOVA with Dunnett's post-hoc analysis) (Figure 4.11A.i). Addition of the growth factor also significantly increased average organoid diameter (μm), to a maximum of 1.29 fold ($n=4$, $p<0.001$, ANOVA with Dunnett's post-hoc analysis), compared to the control (Figure 4.11A.ii). While organoids appeared larger, morphologically, HGF addition produced no obvious change, with structures remaining smooth and rounded (Figure 4.11B).

Organoids treated with HGF were observed by immunofluorescence analysis to retain normal, distinct areas of basal and luminal marker expression (Figure 4.11C). PR and Keratin 8 expression levels appeared to remain consistent across all treatment conditions, while p63 expression highlighted a continuous basal cell layer across both control and HGF treated organoids. Keratin 5 expression was also consistent across conditions. Interestingly, higher levels of HGF appeared to induce the formation of a pronounced lumen in the centre of the organoids, as seen by lack of Hoechst or antibody staining. OcellO analysis would greatly benefit the interpretation of this morphological assessment. In addition, unlike previous FGF experiments, HGF treatment following FACS was not performed here, but could benefit the understanding of fibroblast involvement in HGF effects in future studies.

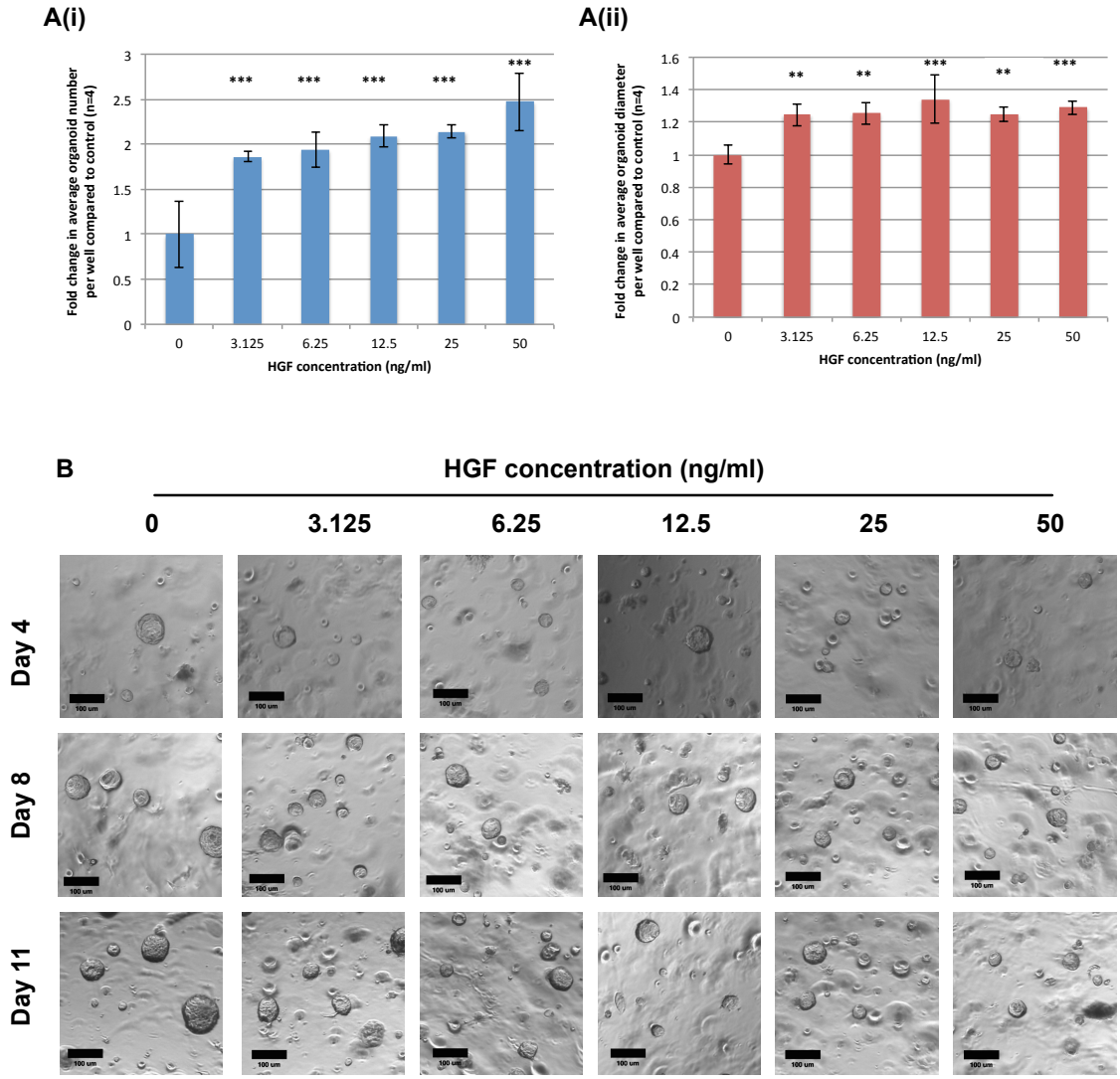

Figure 4.11 Effects of Hepatocyte growth factor (HGF) treatment on mammary epithelial organoids.

Organoids were cultured from unsorted, trypsinised epithelial cells under defined media conditions, supplemented with 3.125, 6.25, 12.5, 25 or 50 ng/ml HGF, for 11 days. **(A)(i)** Bar chart depicting fold change in average organoid number per well (n=4) at each concentration of HGF treatment, compared to the control condition, at day 11 in culture. **(ii)** Bar chart depicting fold change in average organoid diameter (µm) per well (n=4), compared to the control condition, at day 11 in culture. Data plotted as mean ± standard deviation. Statistical significance as compared to control indicated by ** ($p<0.01$) or ** ($p<0.001$), determined by one-way-ANOVA, with post-hoc Dunnett's testing. **(B)** Morphology of organoids at days 4, 8 and 11 in culture, under each HGF concentration. Scale bar 100µm. **(C)** Confocal microscope images of immunofluorescence staining for luminal markers **(i)** PR and **(ii)** Keratin 8, and basal markers **(iii)** p63 and **(iv)** Keratin 5, at 11 days in culture, under control and HGF treated growth conditions. Scale 50µm. Data obtained by Sarah Stanley, under my supervision.

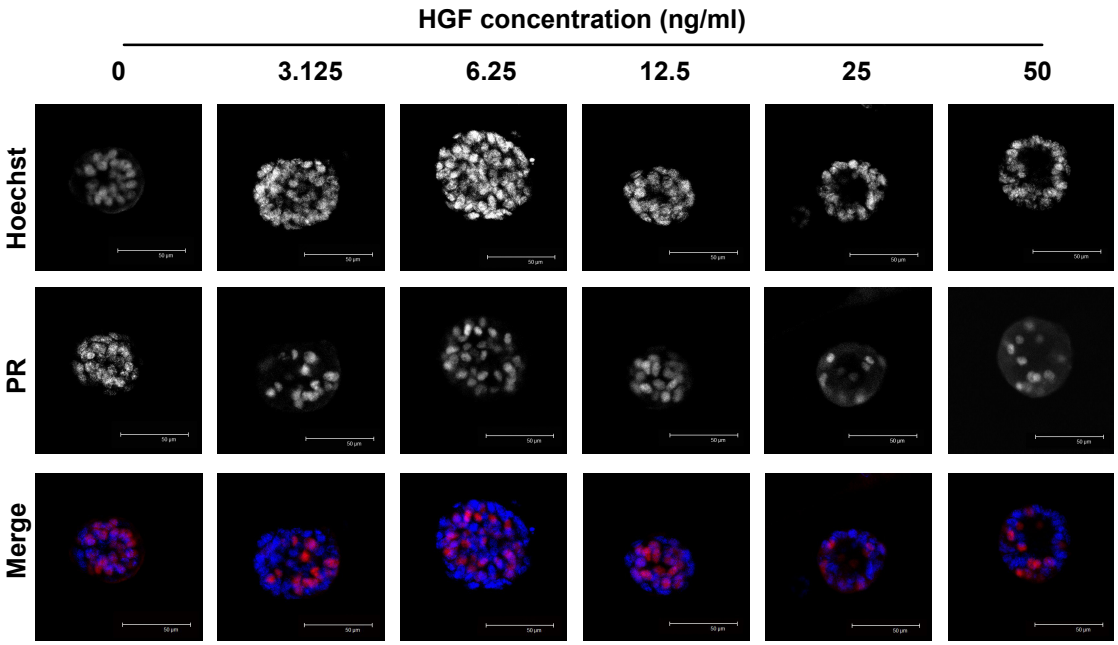
HGF concentration (ng/ml)
0
3.125
6.25
12.5
25
50
Hoechst
PR
Merge

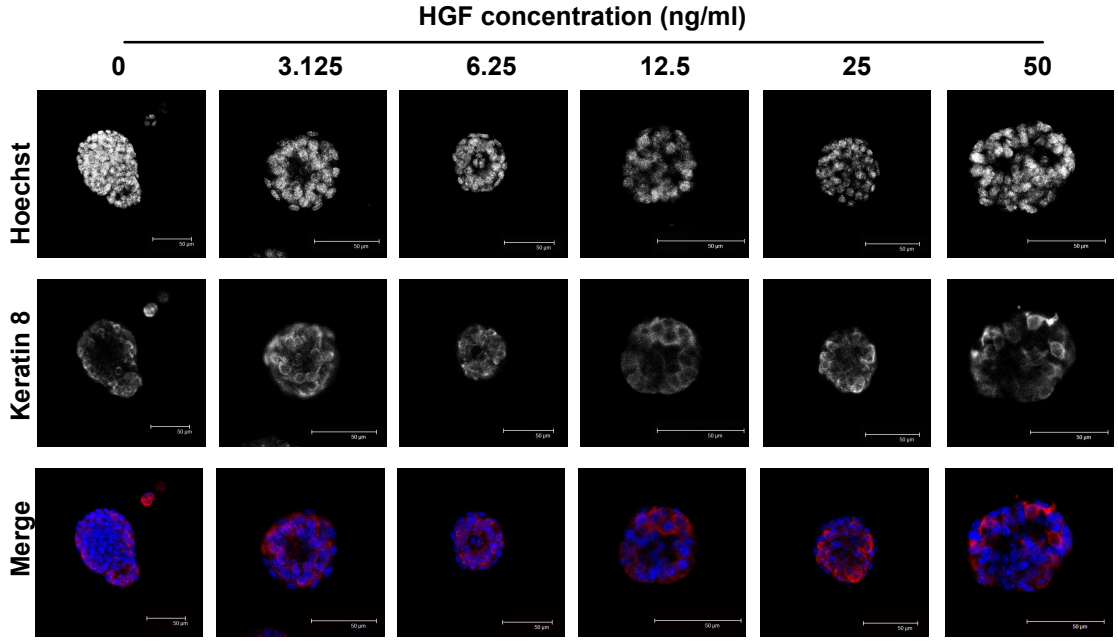
HGF concentration (ng/ml)
0
3.125
6.25
12.5
25
50
Hoechst
Keratin 8
Merge

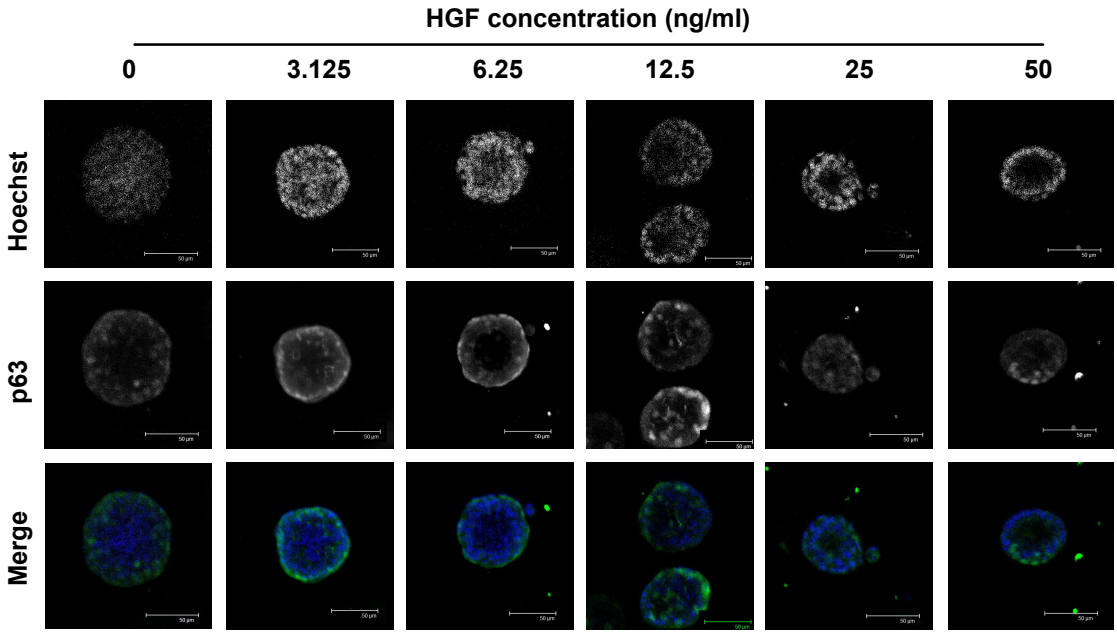
HGF concentration (ng/ml)
0
3.125
6.25
12.5
25
50
Hoechst
p63
Merge

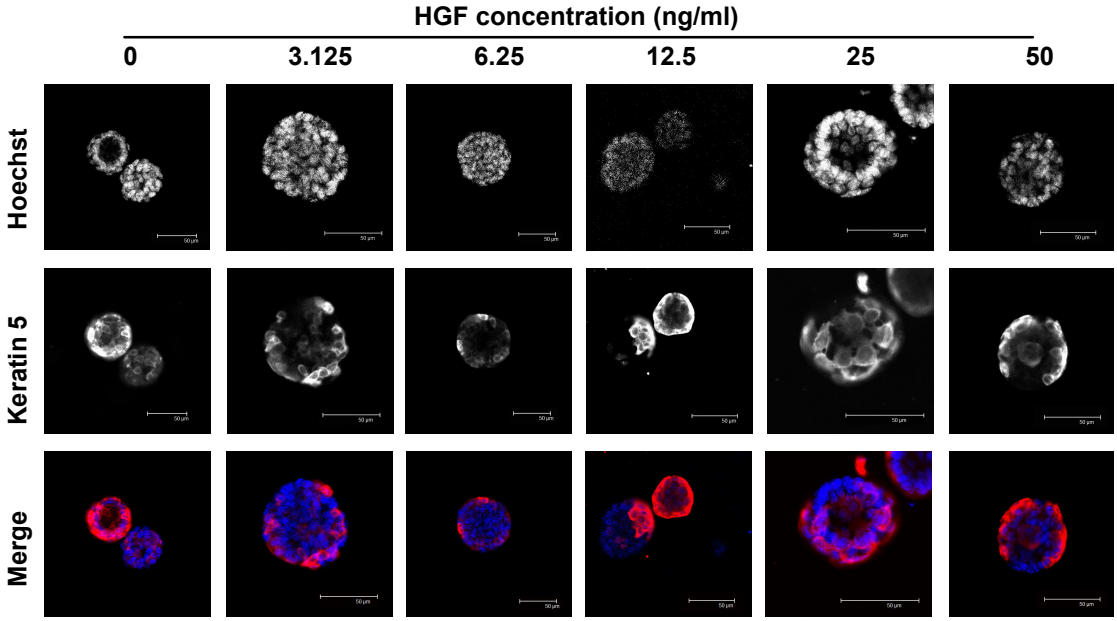
HGF concentration (ng/ml)
0
3.125
6.25
12.5
25
50
Hoechst
Keratin 5
Merge

4.2.5 Abrogation of the Neuregulin1 signalling pathway impairs organoid development.

The importance of the Nrg1 signalling pathway in mammary organoid development was next verified, simultaneously demonstrating an additional highly important utility of the mammary organoid system.

The key receptors for Nrg1 in the mammary gland are ErbB3 and ErbB4. Due to a lack of easily available inhibitor to the ErbB3 or ErbB4 Nrg1 receptors, lentiviral vectors were designed, expressing shRNAs against either receptor together with a GFP marker, and primary mammary epithelial cells infected upon seeding in Matrigel based organoid culture. Successful infection with virus was assessed by the presence of GFP, and calculated to be 64% (±17, n=3) and 45% (±8, n=3) for ErbB3 and ErbB4 knockdown, respectively (Figure 4.12B). This was comparable with the scrambled shRNA-expressing control virus infection rate (52% ±16.5, n=3), and was considered to be adequate for the purpose of the experiment since it verified the successful lentiviral infection protocol in the NRL organoid culture conditions.

Using fluorescent imaging techniques combined with image analysis software, the average area of GFP+ ErbB3 and ErbB4 knockdown organoids was calculated as a percentage of those infected with scrambled virus, indicating a reduction in organoid growth upon loss of either receptor subtype, (20% and 40%, respectively) (Figure 4.12C). Further analysis confirmed loss of ErbB4 to induce significant reductions in average organoid area ($p=0.049$, n=3, ANOVA with Dunnett's post-hoc analysis). Taken together with the profound effects of Nrg1 on organoid growth, the knock down data indicate that Nrg1 / ErbB signalling is important for the development of mammary organoids.

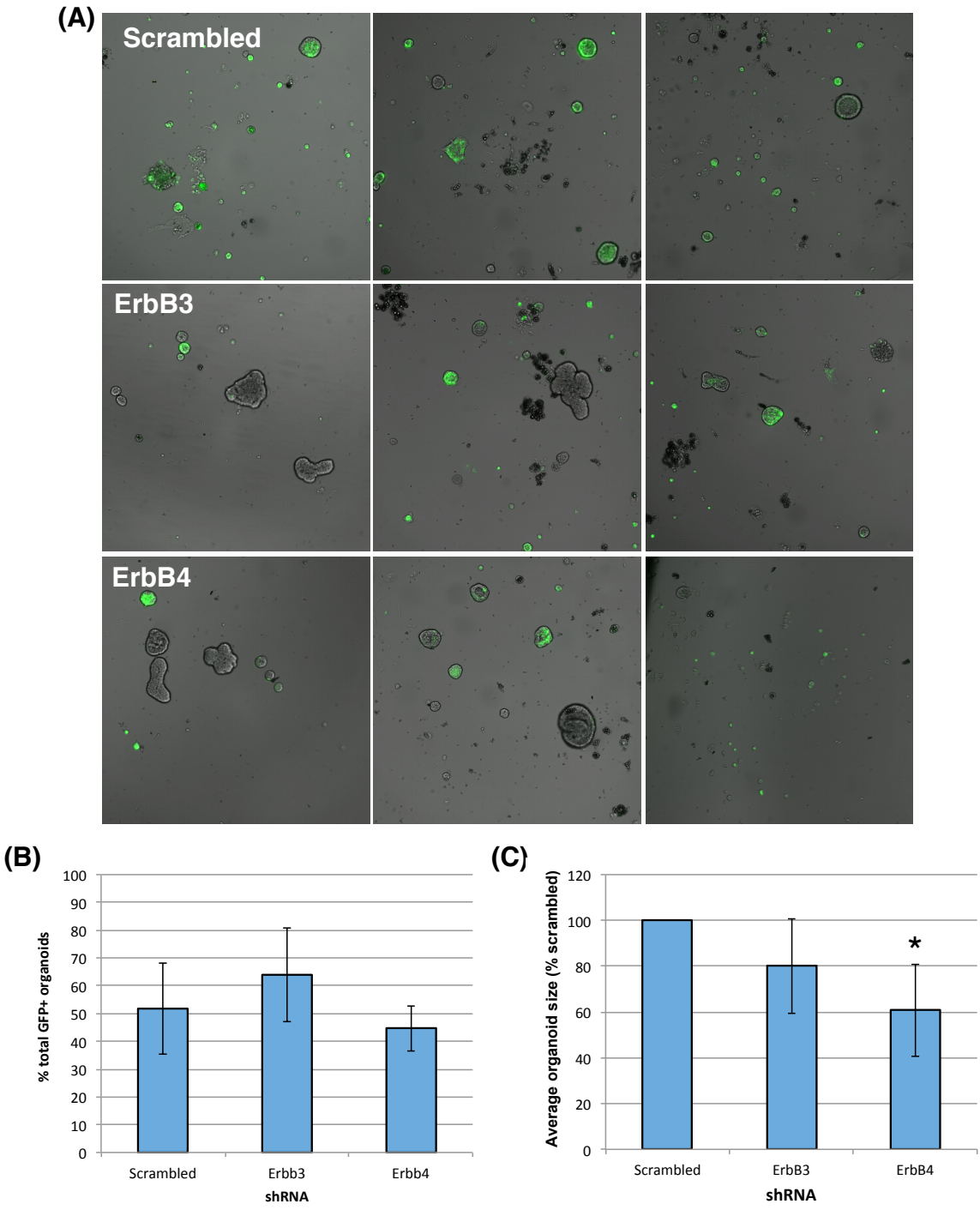

Figure 4.12 Nrg1 signaling loss through knockdown of ErbB3 or ErbB4 abrogates mammary organoid growth.

Mammary epithelial cells were freshly isolated and infected with a negative scrambled control lentivirus or lentivirus for knockdown of ither ErbB3 or ErbB4. Organoids were fixed at day 10 in culture. (a) Representative images of organoids infected with lentivirus, where successful infection was indicated by GFP positivity. Scale 100µm. (b) Organoid infection success was calculated as number GFP+ organoids/Total number organoids. Data shown as mean ± standard deviation (n=3). (c) Average GFP+ organoid area was analysed using ImageJ. Data are expressed as % of scrambled control (mean ± standard deviation, n=3) *=p value<0.05, ANOVA with Dunnett's post-hoc analysis.

4.3 Summary

Work detailed here has demonstrated a range of utilities of the organoid system. The growth and maintenance of multiple mammary cell types in culture has allowed the easy and comparatively rapid, repeatable investigation of mammary developmental signalling pathways that complement data from animal models and can help define responses and key intercellular interactions. Furthermore, the nature of the system has allowed the dose-dependent regulation of growth factor responses; a level of biological analysis that is difficult to assess in animal models.

Wnt signalling has been further confirmed as a crucial pathway in mammary organoid development, with important endogenous signalling apparent between cell populations. While it is interesting that exogenous application of the ligand has little effect on organoid development compared to previous observations of increased Wnt signalling under R-Spondin1, this could be simply a result of the differing potencies of the two factors in activating the pathway. A two-fold increase in R-Spondin1 concentration may in fact equate to a much higher level of Wnt than is presented in our experiments.

In addition, the FGF and HGF signalling pathways have been identified to increase organoid formation efficiency while retaining a normal mammary phenotype, and therefore are candidate factors for future enhancement of culture expansion in preparation for larger scale studies.

Lentiviral transfection within this system has not only allowed the importance of the Nrg1 signalling pathway in mammary development to be established, but also demonstrates the utility of the system for genetic manipulation.

5 Investigating the clonal origins and cell-cell interactions of the mammary organoid model.

5.1 Introduction

As detailed in section 1.1.4, well-documented *in vivo* evidence points strongly to the presence of a basally located, Wnt-responsive stem cell population in the mammary gland, responsible for its development (Shackleton et al. 2006; Sleeman et al; 2006, Stingl et al. 2006; Kendrick et al. 2008). More recently, studies have differed in opinion on the requirement for stem or progenitor cell populations in mammary gland development , and whether in fact long term mammary gland maintenance may actually predominantly rely on long lived progenitors (Van Keymeulen *et al.* 2011; van Amerongen *et al.* 2012; Wuidart *et al.* 2016; Rios *et al.* 2014).

Optimisation and analysis of the mammary organoid culture system thus far allowed the identification of multiple signalling pathways important for mammary development and expansion. Of these, the canonical Wnt/R-Spondin1 signalling pathway was identified as perhaps the most crucial in regulating organoid formation, as well as the physiologically relevant differentiation and organisation of heterogeneous cell populations. It was therefore hypothesised that mammary organoids, like the *in vivo* gland, may also be derived from a basal, Wnt responsive 'stem-cell' population. Earlier evidence for dividing cell populations located in the basal cell layer, often possessing p63 expression, would appear to support this theory (Figure 3.14), as would the demonstration of highly basal development under high Wnt conditions (Figures 3.1 & 3.2).

This chapter therefore details the investigation of the organoid forming cell population in this 3D system, and looks further into the potential cell-cell signalling networks required for mammary development.

5.2 Results

5.2.1 Luminal cell populations comprise the predominant organoid forming populations under optimised culture conditions

In an effort to establish the clonal origin of the organoids grown in the 3D culture system, fluorescence activated cell sorting (FACS) was utilised. Previous studies using FACS (Sleeman et al. 2005; 2006) have enabled the identification and characterisation of

up to four distinct populations of mouse mammary epithelial cells from primary tissue. Here, mammary cells isolated from the 3rd, 4th and 5th mammary fat pads of 8-12 week old virgin FvB mice were stained with fluorescently conjugated antibodies against: the cell adhesion molecule and luminal cell marker CD24; the mouse haematopoietic stem cell surface marker Sca-1; and the leukocyte marker protein CD45, in addition to 4',6-diamidino-2-phenylindole (DAPI), and sorted with doublet exclusion, using gating steps detailed in Figure 2.02.

The resulting three live, definitively single, CD45- cell populations obtained from this sorting process were: luminal estrogen receptor-α positive (ER+) ($CD24^{high}Sca1^{+}$), luminal estrogen receptor-α negative (ER-)($CD24^{high}Sca1^{-}$), and basal cells ($CD24^{low}Sca1^{-}$), as shown in Figure 2.02F.

Preliminary data first indicated that when individual cell populations were cultured under NRL conditions in growth factor reduced Matrigel following FACS, cell survival was extremely low, such that no measureable outgrowths were observed. Given previous evidence to support improved organoid formation efficiency upon treatment of cultures with ROCK inhibitor (10μM) for the first 5 days in culture, Y-27632 was added following sorting. Unexpectedly, this allowed organoid-forming efficiency to be seen by 14 days in culture from both the $CD24^{high}Sca1^{-}$ and $CD24^{high}Sca1^{+}$populations (at an average of 0.57% and 0.13%, respectively) with negligible growth from the $CD24^{low}Sca1^{-}$ population.

As organoid formation efficiency was still extremely low, trypsinised cells were next treated with 10μM ROCK inhibitor prior to cell sorting, in addition to the five days after seeding. Under these conditions, organoid formation, and perhaps therefore cell survival, was greatly increased from all cell populations by 14 days in culture. Again, organoids were predominantly formed by the $CD24^{high}Sca1^{-}$ and $CD24^{high}Sca1^{+}$ populations (at an average of 0.79% and 0.65%, respectively), while $CD24^{low}Sca1^{-}$ cell derived organoid formation efficiency remained the lowest, with 0.14% of cells seeded producing structures detectable as organoids compared to the control, sorted single epithelial cell organoid formation efficiency of 1.3% (Figure 5.2B). Of structures that were produced, little difference was observed in average organoid diameter (μm) between cell populations (Figure 5.2C).

Phenotypic analysis of organoids produced from sorted $CD24^{high}Sca1^{-}$ cells and fixed at day 14 in culture demonstrated a 'normal' mammary marker expression profile, such that both luminal hormone receptor (PR and ER) and Keratin 8 expression could be observed internally, while basal p63, keratin 5 and keratin 14 were located toward the external surfaces of the organoids, recapitulating in vivo tissue architecture. As previously observed in Chapter 3, hormone receptor and p63 localisation were distinct (Figure 5.3). Similarly, organoids derived from sorted $CD24^{high}Sca1^{+}$ cells fixed at day 14 in culture also expressed normal hormone receptors, and exhibited expected basal layer expression of both p63 and Keratin 14 (Figure 5.4).

Furthermore, as previously shown in Chapter 3 for organoids grown from unsorted populations, dividing (EdU+) cells within 14-day old organoids derived from either $CD24^{high}Sca1^{-}$ or $CD24^{high}Sca1^{+}$ cells were observed to be distinct from hormone receptor positive cells (depicted by white arrows, Figure 5.5). The same could be said following a 24-hour treatment period with steroid hormones Estrogen (2.5 ng/ml) or Progesterone (40ng/ml), both alone and in combination (Figure 5.5) indicating that the paracrine mechanism required for a hormone response is fully functional in these organoids. Again, as detailed in Chapter 3, absolute quantification of proliferation following hormone treatment was not possible in this experiment, but would greatly aid the understanding of luminal-derived organoid function.

Here, the presence of all functional differentiated cell types in organoid derived from luminal cell populations was surprising, and suggestive of luminal cell plasticity under NRL conditions, while the lack of significant colony formation from the basal cell population led to the belief that signals required for basal cell growth were lacking in single cell culture.

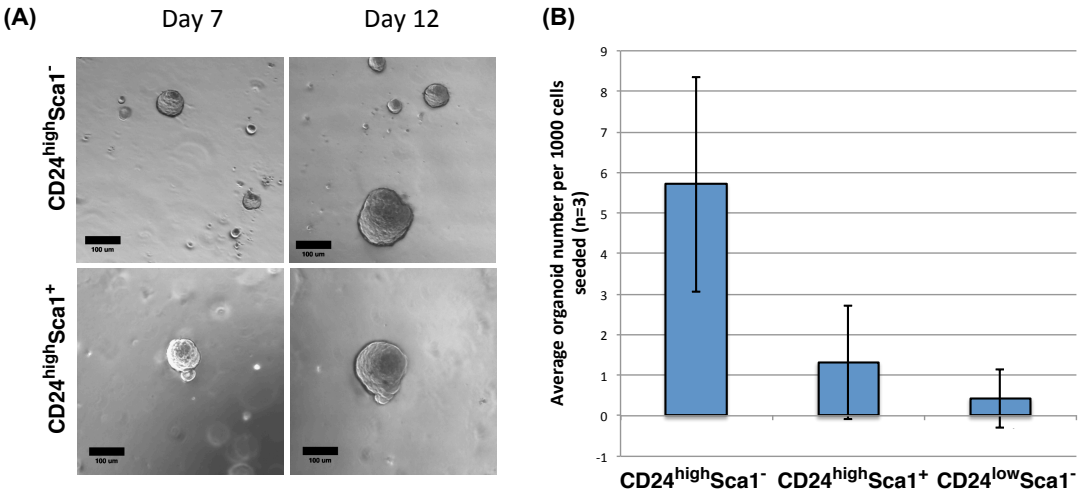

Figure 5.1 Growth of sorted mammary epithelial cell populations under low R-Spondin1 media conditions.

Each population was plated at 1000 cells per µl growth factor reduced Matrigel, and overlaid with mammary organoid media with noggin (100 ng/ml), Nrg1 (100 ng/ml), R-Spondin1 (2.7 ng/ml), with Y-27632 (10µM) for the first 5 days in culture. **(A)** Representative images of cultures 7 and 12 days after FACS. Scale 100 µm. **(B)** Bar chart of average organoid count per 1000 cells seeded, at 14 days in culture. (n=3, means ± standard deviation.).

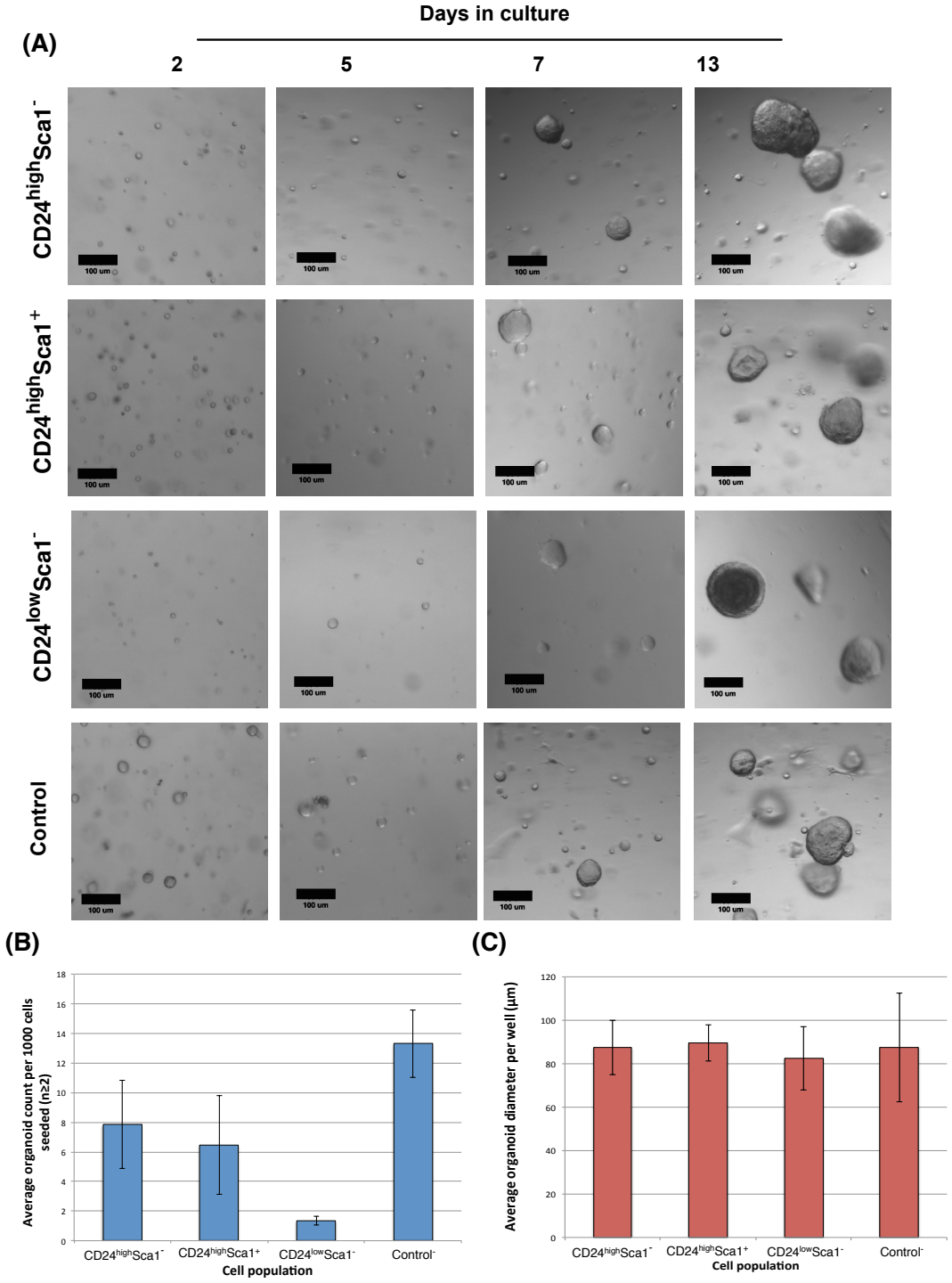

Figure 5.2 Growth of sorted mammary epithelial populations under optimised conditions.
Each defined cell population, along with an all-epithelial cell control population, was sorted in the presence of 10µM Y-27632, plated at 1000 cells per µl of growth factor reduced Matrigel, and overlaid with mammary organoid media containing Neuregulin (100 ng/ml), Nrg1 (100 ng/ml) and R-Spondin1 (2.7 ng/ml), with Y-27632 (10µM) for the first 5 days in culture. **(A)** representative images of organoid growth and morphology at regular time points throughout culture. Scale bars 100µm. **(B)** Bar chart depicting average organoid count per 1000 cells seeded, at 14 days in culture. **(C)** Bar chart depicting average organoid diameter (µm) per 1000 cells seeded. (n=3, means ± standard deviation.)

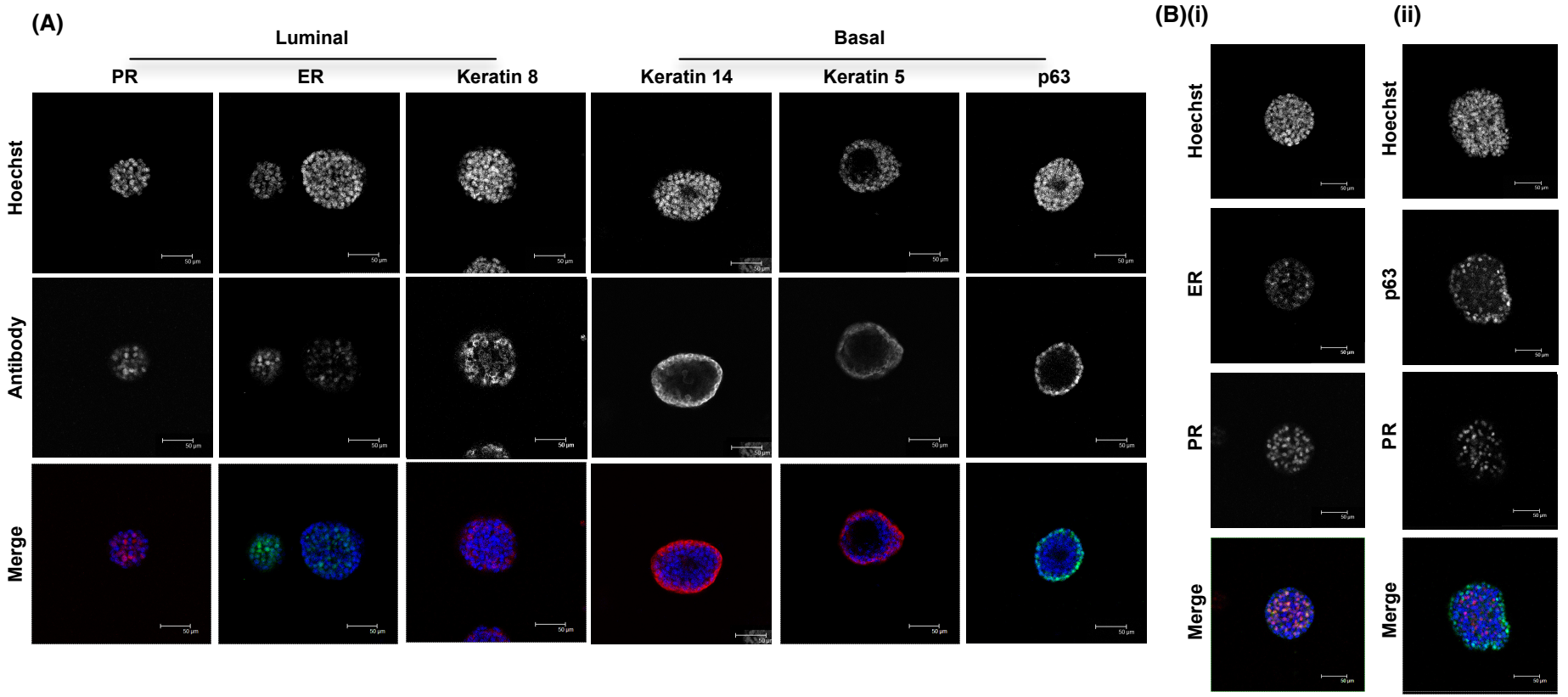

Figure 5.3 Immunofluorescence staining of organoids derived from CD24^{high}Sca1^{-} cell types.

FAC sorted CD24^{high}Sca1^{-} mammary epithelial cells were seeded in Matrigel at a density of 1000 per µl, and overlaid with mammary organoid media containing Nrg1 (100 ng/ml), Nrg1 (100 ng/ml) and R-Spondin1 (2.7 ng/ml), with Y-27632 (10µM) for the first 5 days in culture. Organoids were fixed at 14 days and **(A)** immunostained for luminal (PR, ER, Keratin 8) and basal (Keratin 14, Keratin 5, p63) marker expression **(B)** co-immunostained for **(i)** luminal steroid hormone receptors **(ii)** luminal PR and basal p63 expression. Scale bar 50µm.

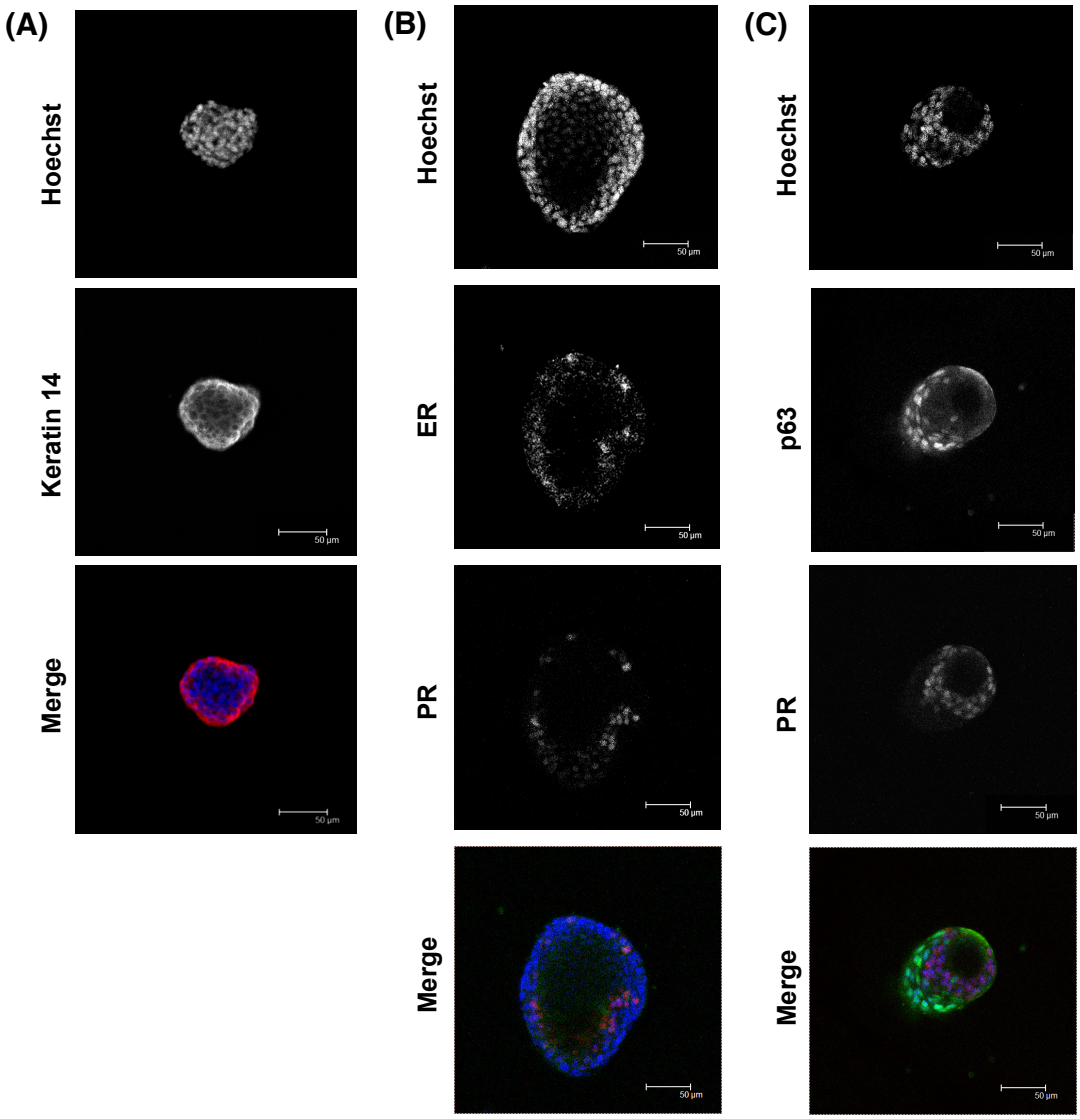

Figure 5.4 Immunofluorescence staining of organoids derived from FAC sorted CD24^{high}Sca1^{+} cells.

FAC sorted CD24^{high}Sca1^{+} mammary epithelial cells were seeded in Matrigel at a density of 1000 per µl, and overlaid with mammary organoid media containing Nrg1 (100 ng/ml), Nrg1 (100 ng/ml) and R-Spondin1 (2.7 ng/ml), with Y-27632 (10µM) for the first 5 days in culture. Organoids were fixed at 14 days and immunostained for **(A)** basal Keratin 14 **(B)** luminal hormone receptors ER and PR, or **(C)** co-expression of PR and p63.

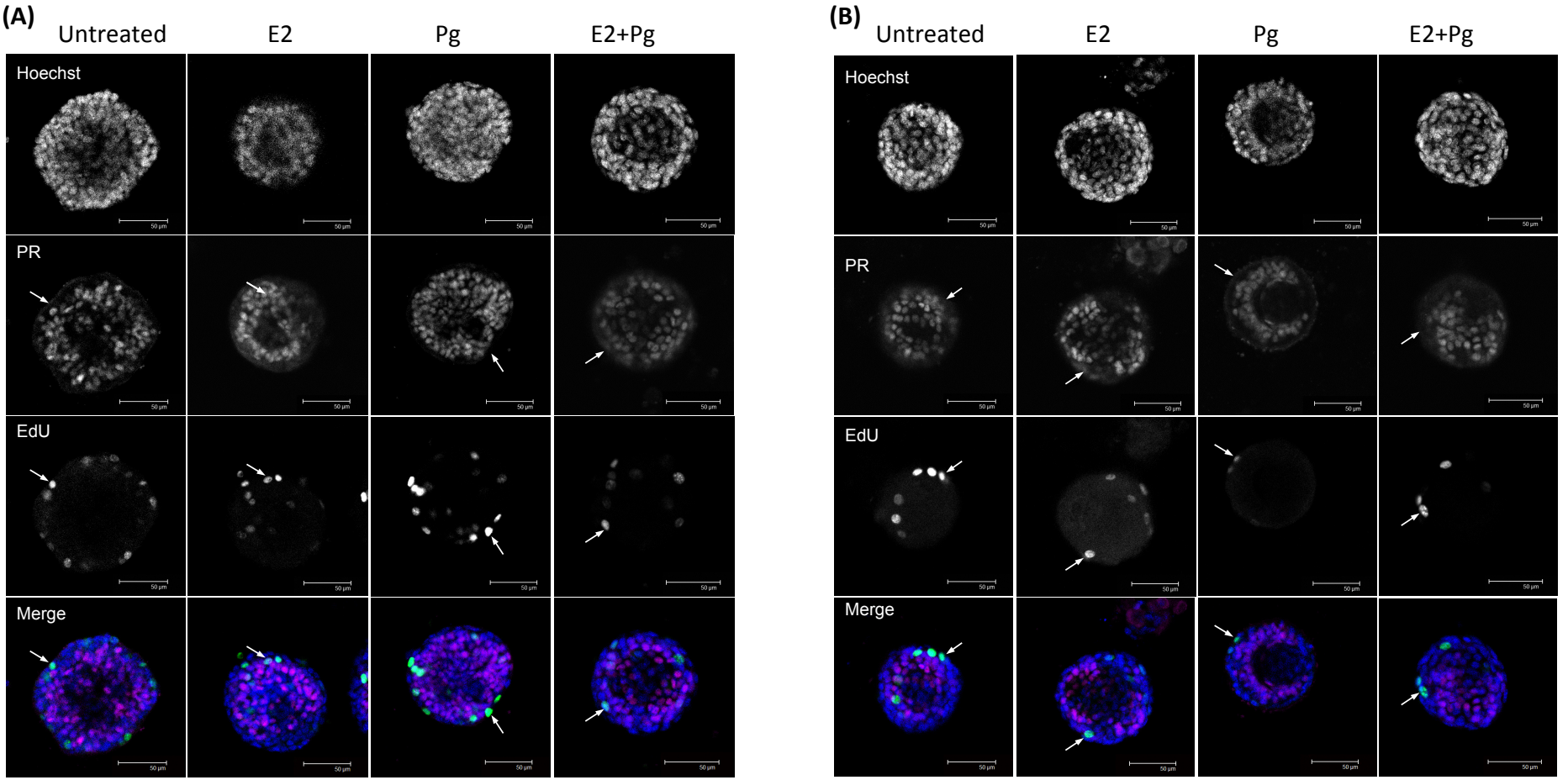

Figure 5.5 Analysis of the effect of steroid hormone treatment of organoids grown from FAC sorted luminal cell populations under defined media conditions.

Organoids grown for 14 days from **(A)** $CD24^{high}Sca1^{-}$ or **(B)** $CD24^{high}Sca1^{+}$ cell populations under defined media conditions were treated with steroid hormones Estrogen (2.5ng/ml), Progesterone (40 ng/ml), alone or in combination for 24 hours prior to fixation. EdU was added two hours prior to fixation and allowed to incorporate into the newly synthesised DNA of dividing cells. Confocal images depict immunofluoresecence staining carried out against Progesterone receptor (PR), in red, and EdU, in green. White arrows indicate distinctly EdU positive, PR negative cells. Scale 50µm.

5.2.2 Paracrine signals may have a role in forming the stem cell niche in the organoid system.

The finding that basal cells were not the predominant organoid forming population under NRL conditions was highly surprising, given the previously demonstrated Wnt/R-Spondin1 dependency of structures grown from mixed population cultures (Chapter 3). The observation of organoid formation from luminal cell populations could indicate that even in mixed cultures, it is only highly plastic luminal progenitors that comprise the organoid forming population. Alternatively, it could be the case that in addition to exogenously applied signalling factors, paracrine signalling from luminal populations is crucial in creating a niche for basal stem cells within the mammary organoid system. Such observations have been made in the intestinal organoid culture system, where Paneth cell-stem cell doublets show a significantly increased plating efficiency compared to stem cells alone, an effect reproduced by the application of niche factor Wnt3a to single stem cells (Snippert *et al.* 2010; Sato *et al.* 2011). Indeed, evidence in the mammary system had already proven that the removal of cell doublets or clusters from cultures, and therefore spatial separation of cells, reduced organoid formation efficiency (3.2.1.1).

In vivo, luminal progenitors are reportedly stimulated to proliferate during pregnancy by basally secreted Nrg1 (Forster *et al.* 2014). Therefore under a paracrine signalling hypothesis, despite their isolation in culture, the presence of Nrg1 in NRL media likely compensates for a lack of such basal stimulation, allowing organoid formation (although the mechanism allowing the generation of basal cells from committed luminal populations is unclear). Conversely, basal cells *in vivo* have been shown to rely on luminally derived R-Spondin1 and Wnt (at least) for their proliferation (Cai *et al.* 2014; Brisken et al., 2000). While R-Spondin1 is provided exogenously by NRL media, Wnt is not, suggesting that the basal niche may not be entirely fulfilled in this system. In order to investigate such a hypothesis, and identify any potential signalling factors involved in the basal cell niche, both recombination experiments and single cell growth factor assays were used.

5.2.2.1 *Recombination of single cell populations supports the presence of paracrine signalling between basal and luminal populations*

Highly effective, but straightforward experiments performed by Sato et al., (2011), whereby sorted cell populations were recombined *in vitro*, demonstrated that in intestinal organoid culture as observed *in vivo*, Paneth cells secrete soluble signals such as EGF and Wnt3 that are absolutely required for the maintenance and survival of intestinal stem cells. To first further verify the presence of a supporting paracrine signal between cell populations in the mammary organoid system, experiments mirroring those in the intestinal system were performed. Sorted cell populations were seeded in paired combinations, and cultured in 'normal' mammary organoid media containing Nrg1 (100 ng/ml), Nog (100 ng/ml) and R-Spondin1 (2.7 ng/ml) with Y-27632 (10 μM) for the first five days in culture. In this case, for every 1000 cells seeded in a recombination, 500 were of each distinct population. Therefore it would be expected that in the event of no paracrine signalling between cell population A and B in culture, the organoid formation efficiency in an 'AB' recombination would be no greater than half of the efficiency of cell type A, plus half of the efficiency of cell type B, while the presence of a signalling network may increase organoid formation in recombinations.

Investigations implied that based on this assumption, predicted and calculated additive organoid formation efficiencies did indeed differ greatly in combinations between basal and luminal cell populations, supporting the hypothesis for a paracrine signalling mechanism in mammary organoid culture. While luminal ER-/ER+ pairings demonstrated an almost identical organoid formation efficiency to that based on the sum of those seen for their single counterparts, indicating little to no signalling between these populations, a synergistic effect was strongly seen between luminal cell populations and basal cells. This was seen particularly strongly between $CD24^{low}Sca1^{-}$ and $CD24^{high}Sca1^{+}$ cells, where organoid formation efficiency was 1.5 fold the expected additive value (Figure 5.6). The clear promotion of organoid formation in this experiment further corroborated our belief that the NRL conditions, while optimal in mixed culture, may not contain all of the required factors for stem cell renewal and proliferation, and that in fact paracrine signalling between cell types is indeed highly important in forming the stem cell niche. The search for the potential identity of these signals will now be discussed.

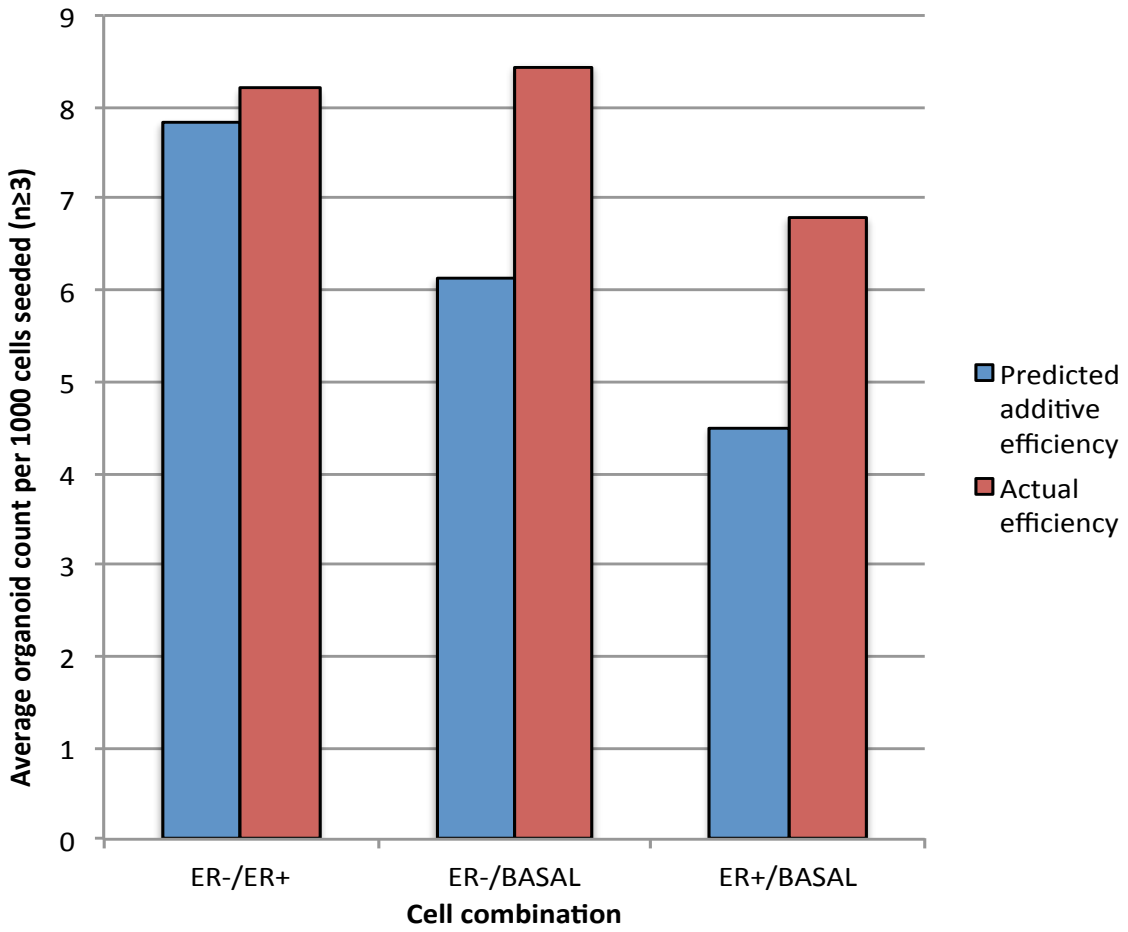

Figure 5.6 Organoid formation efficiency of cell recombinations compared to predicted values from single cell growth efficiencies.

Single, sorted live $CD45^-$ mammary cells were seeded as individual populations at a density of 1000 per µl growth factor reduced Matrigel, under NRL conditions, and the organoids formed by each population counted. From this, an predicted additive organoid count was calculated for pairwise combinations of cells, depicted here as "predicted additive efficiency". Within the same experiment, individual populations were also sorted into pairwise combinations, to a final density of 1000 total cells per µl growth factor reduced Matrigel, such that 500 cells were of an individual population. Organoid outgrowth was assessed from recombinations, depicted here as "Actual efficiency". Results were averaged from at least three wells of each condition.

5.2.2.2 *Stimulation of the canonical Wnt signalling pathway alone cannot support organoid formation from the basal cell population.*

Having identified paracrine signalling between basal and luminal populations, the identity of the signal(s) was next investigated. Based on both the *in vivo* evidence for a paracrine Wnt signal in the mammary gland (Brisken *et al.* 2000), and the demonstrated importance of Wnt/R-Spondin1 signalling activity in mammary organoid development from mixed cell populations in previous work, the canonical Wnt pathway was the first considered as a potential niche factor.

It has previously been established that isolated, basally located, Wnt-responsive mammary stem cells can be expanded vastly in colony formation assays using exogenous Wnt3a supplementation (Zeng and Nusse 2010), while the aforementioned study by Sato et al., (2011) efficiently highlighted that exogenous Wnt3a supplementation (100ng/ml) for the first 3 days in culture could act as a substitute for Paneth cells, supporting crypt formation from single, sorted Lgr5+ stem cells. As such, exogenous modulators of the Wnt pathway, namely Wnt3a, R-Spondin1, or Wnt4, were applied alone or in combination to single, sorted, live $CD45^-$ mammary cell populations in culture.

Isolated populations were first seeded under Nrg1, Noggin, R-Spondin1 high (42.5 ng/ml) culture conditions, with short term ROCK inhibition at the start of culture. Measurements taken at day 15 in culture demonstrated that under high R-Spondin1 conditions, average mammary epithelial organoid growth from the $CD24^{high}Sca1^-$ or $CD24^{high}Sca1^+$ cell populations occurred at 0.61% and 0.6%, respectively, and was therefore not significantly different to that observed at lower R-spondin1 concentrations, while $CD24^{low}Sca1^-$ cell outgrowths were once again virtually undetectable (Figure 5.7B). Structures formed from luminal cell populations differed in morphology and phenotype to those seen under lower R-Spondin1 concentrations, demonstrating a lack of cell heterogeneity, such that keratinous cores and basal markers were prevalent (Figure 5.7C).

A further experiment in which a high 'burst' of R-Spondin1 (42.5 ng/ml) was given for the first five days in culture alongside the ROCK inhibitor, before being replaced with the optimal lower concentration of 2.7 ng.ml failed to produce any

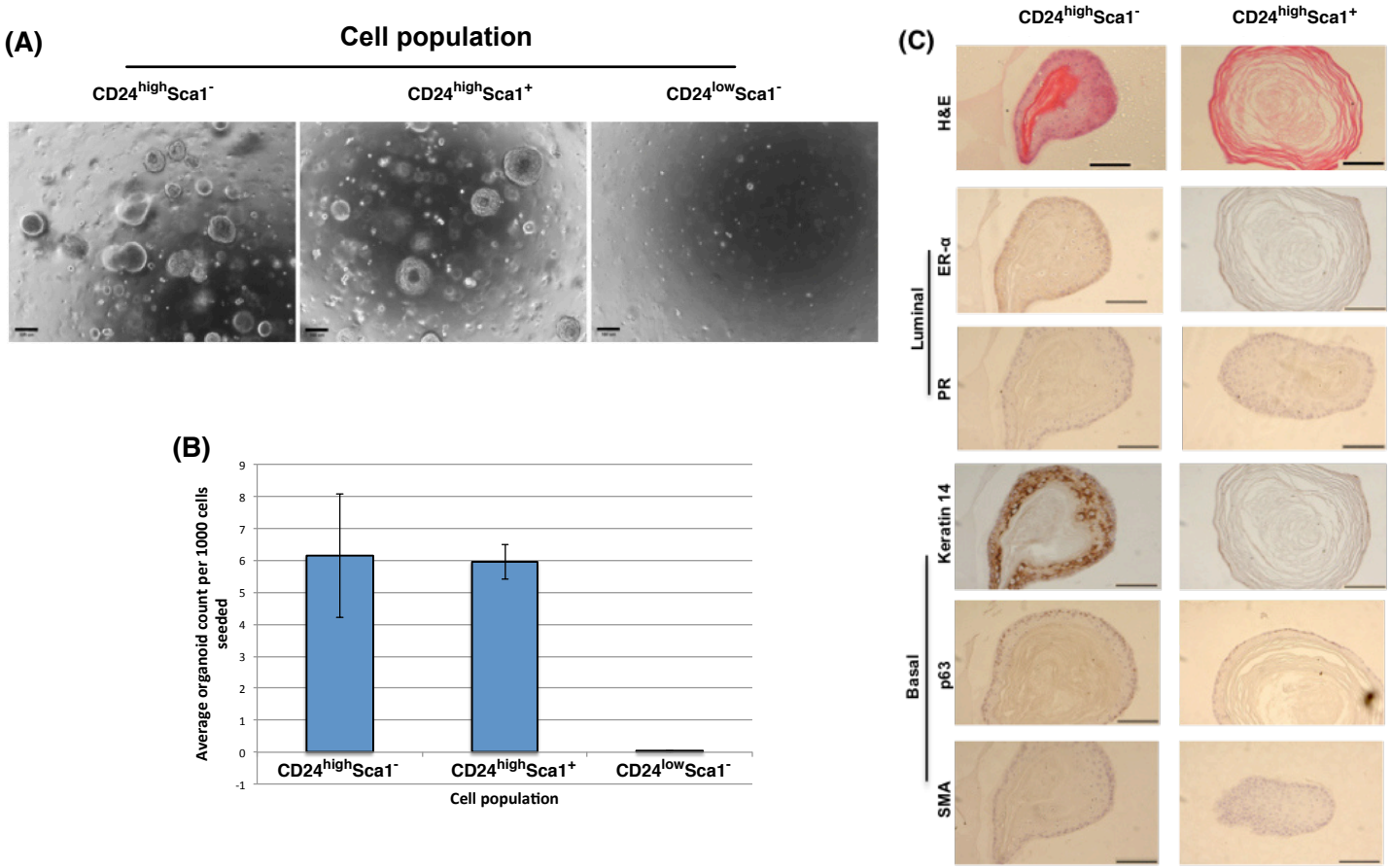

Figure 5.7 Growth of sorted mammary epithelial cell populations under high R-Spondin1 supplemented media conditions.

Each population was plated at 1000 cells per µl growth factor reduced Matrigel, and overlaid with defined organoid media (Noggin (100 ng/ml), Nrg1 (100 ng/ml), R-Spondin1 (42.5 ng/ml), with or without 10uM Y-27632 for the first 5 days in culture. (A) Representative images of cultures 7 days after FACS, with and without Y-27632 treatment. Scale 100 µm. (B) Bar chart of average organoid count per 1000 cells seeded, at 15 days in culture, with Y-27632 for the first 5 days in cutlure. n=1, mean± standard deviation from ≥4 wells. (C) Histological analysis of organoids grown from single $CD24^{high}Sca1^{-}$ or $CD24^{high}Sca1^{+}$ mammary epithelial cell population using Y-27632 (10µM). Slides were stained with Haemaoxylin and eosin (H&E), and antibodies against luminal markers ER-α, and PR, and basal markers keratin 14, p63 and smooth muscle actin, Scale 100µm.

$CD24^{low}Sca1^{-}$ cell derived organoids, and did little to promote 'normal' formation from the luminal populations, resulting again in only squamous, basal-like structures.

Single cell populations plated in growth factor reduced Matrigel and overlaid with NRL culture medium were next supplemented with Y-27632 (10µM) and Wnt3a (100ng/ml). Surprisingly, as previously observed for mixed populations (section 4.2.1), Wnt3a supplementation for 14 days had no effect on organoid formation from any particular cell population. Moreover, using a combination of Wnt3a (100 ng/ml) and a high concentration of R-Spondin1 (42.5 ng/ml) to increase Wnt pathway stimulation, it was found that after 14 days in culture no effect on the efficiency of organoid formation from the $CD24^{high}Sca1^{-}$ or $CD24^{low}Sca1^{-}$ cell populations was observed. However, Wnt3a actually showed preferential enhancement of formation of organoids from the $CD24^{high}Sca1^{+}$ cell population (Figure 5.8), increasing it two-fold (n=3, p=0.04, paired student t-test) (Figure 5.8).

Since Wnt3a is not a naturally occurring Wnt ligand in the mammary gland, a more relevant ligand, Wnt4, was also implemented as an exogenous factor in culture media. Again, no significant increases in organoid formation were observed from any of the three single cell populations under Wnt4 treatment, with results highly variable in the case of $CD24^{high}Sca1^{+}$ cells in particular.(Figure 5.9). Further work would be needed to assess the true nature of response to Wnt4 by this cell population. Similarly, at high R-Spondin1 concentrations, no clear response to Wnt4 was detected after 14 days in culture from any cell population.

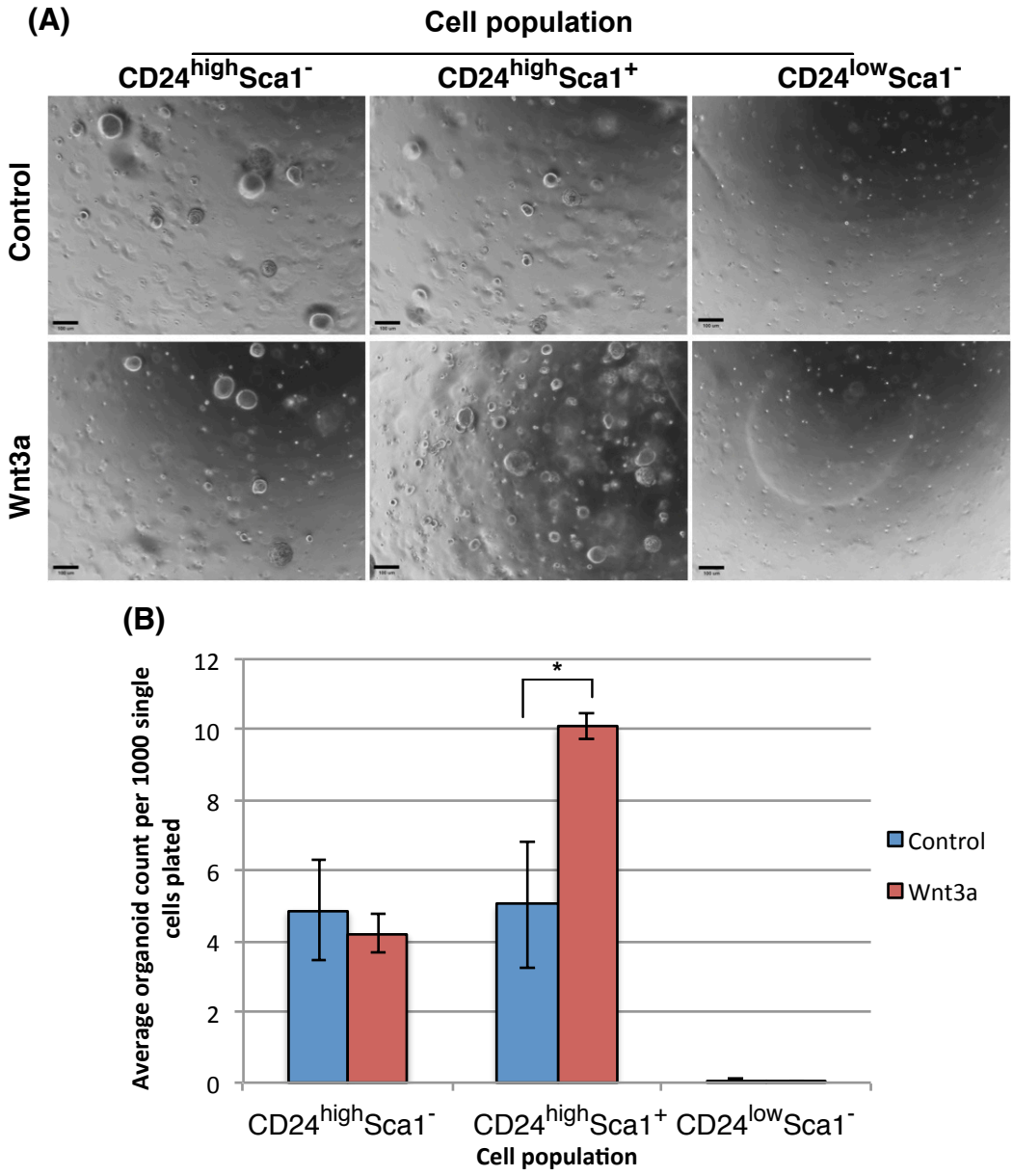

Figure 5.8 Growth of sorted mammary epithelial cell populations under high R-Spondin1 and Wnt3a treatment.

Each population was plated at 1000 cells per µl growth factor reduced Matrigel, and overlaid with media containing Nrg1 (100 ng/ml), Noggin (100 ng/ml), R-Spondin1 (42.5 ng/ml) and Y-27632 (10µM, 5 days), with or without Wnt3A supplementation (100ng/ml) for the first 3 days in culture. **(A)** Representative images of cultures 7 days after FACS. Scale 100 µm. **(B)** Bar chart of average organoid count per well at 14 days in culture. n=3, data shown as mean ± standard deviation. *$p < 0.05$ using a paired student's t-test.

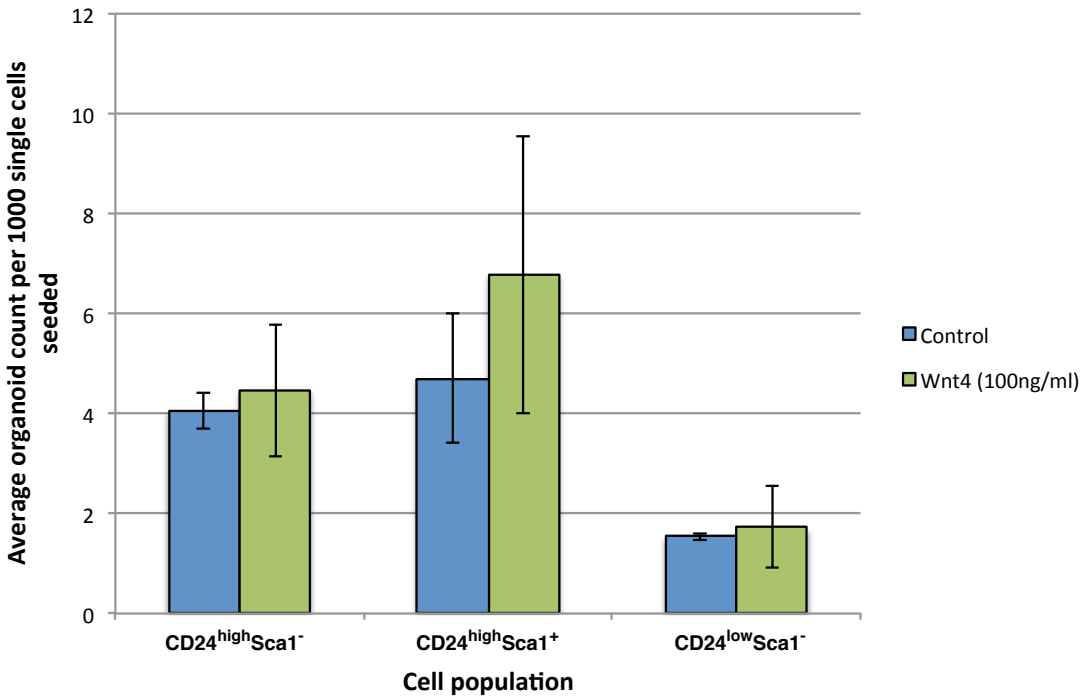

Figure 5.9 Growth of sorted mammary epithelial populations under NRL conditions and Wnt4 treatment.

Each population was plated at 1000 cells per µl growth factor reduced Matrigel, and overlaid with media containing Nrg1 (100 ng/ml), Noggin (100 ng/ml), R-Spondin1 (2.7 ng/ml) and Y-27632 (10µM, 5 days), with or without Wnt4 supplementation (100ng/ml). Average organoid count per well was assessed at 14 days in culture. Data shown as mean ± standard deviation (n=2).

5.2.2.3 *Basal cells require combined EGF and high Wnt signalling activity for optimal organoid formation efficiency.*

Since Wnt pathway stimulation alone was not enough to support organoid formation from the basal cell population, alternative factors that could constitute the basal stem cell niche were considered. As discussed in Chapter 3, evidence from a qRT-PCR study previously conducted on mammary epithelial populations by Jardé et al., (in preparation), indicated that while Nrg1 and it's receptors are expressed by almost all cell types to an extent, the ligand is expressed most prevalently by the basal population, as also recently described by Forster et al., (2014), while ErbB3/4 receptor expression is highest in the luminal subtype. Importantly, the stem cell enriched fraction was in fact found to entirely lack ErbB4 expression. It was therefore hypothesised that while in NRL conditions luminal progenitor cells can expand under stimulation by Nrg1, the basal cell population may require an alternative RTK ligand for survival, which it receives in mixed culture through paracrine signalling.

The basal epithelium is known to express ErbB1/EGFR (DiAugustine *et al.* 1997). In support of this, previous attempts to culture mammary organoids in our system under EGF and high R-Spondin1 conditions resulted in outgrowths enriched solely in basal cells, while reports from Zeng and Nusse (2010), and Wang et al., (2014) indicate that EGF, in combination with Wnt3a, enables MaSC expansion in colony forming assays. The ligand was therefore considered as a factor in the stem cell niche.

Basal ($CD24^{low}Sca1^{-}$) cells were sorted by FACS and seeded at 1000 cells per µl growth factor reduced Matrigel, under a range of media compositions (see Table 5.1 for full details of conditions), and organoid outgrowth measured after 14 days. As previously observed, organoid growth from basal cells under standard NRL conditions was very low, at 0.13% (n=1). In fact, no substantial outgrowth was observed from any Nrg1 containing media conditions, further promoting the conclusion that basal cells do not rely heavily this RTK ligand for their growth (Figure 5.10A).

Overall, it was evident that organoid formation from the basal cell population could be vastly improved by EGF ligand stimulation, such that the ligand alone (50 ng/ml), induced a 6 fold increase in organoid formation efficiency compared to the standard NRL culture conditions defined in Chapter 3 (from 0.1% to 0.6%) (Figure 5.10A).

Interestingly, and perhaps unsurprisingly, in light of previous results under similar conditions (Chapter 3), the highest organoid formation efficiencies were observed in those conditions incorporating both EGF stimulation and high concentrations of Wnt ligand, in combination with R-Spondin1, regardless of noggin presence or absence (8.9 and 8.6 fold increase compared to control NRL conditions, respectively).

In standard mixed culture, previously described work illustrated a lack of physiologically normal differentiation under the highly Wnt driven, EGF supplemented conditions shown to promote basal expansion here. As such, a further experiment was performed to question the possibility of using two different media compositions in succession: one to drive the activation and expansion of basal stem cells, and a second to drive the correct differentiation of the cells produced by this to form organoids recapitulating *in vivo* architecture and biology.

Organoids were grown for the first 7 days in culture under the full range of conditions used in the previous experiment, before treatment for a further 7 days with the defined Nrg1, Noggin, R-Spondin1 low media (Figure 5.10B). Unfortunately phenotypical analysis of these organoids was not possible due to technical error, so it is as yet unknown whether organoids grown under these conditions represented physiologically normal mammary tissue. Nevertheless, basic morphological assessment indicated a lack of the keratinous development characteristically associated with abnormal phenotype, under any condition trialled (Figure 5.10C). Moreover, trends in growth factor responses were highly similar to those seen in the previous experiment. Interestingly, while conditions using Nrg1 consistently showed similar organoid forming efficiencies to the initial study, conditions where EGF was replaced with Nrg1 at day 7 demonstrated a reduction in overall organoid formation efficiency by day 14 as compared to the first experiment, again highlighting the preference of basal cells for EGF.

Condition	Components
NRL	Nrg1 (100 ng/ml), Noggin (100 ng/ml), R-Spondin1 (2.7 ng/ml)
NN	Nrg1 (100 ng/ml), Noggin (100 ng/ml)
NNW	Nrg1 (100 ng/ml), Noggin (100 ng/ml), Wnt3a (200 ng/ml)
NNrW	Nrg1 (100 ng/ml), Noggin (100 ng/ml), 1 (2.7 ng/ml), Wnt3a (200 ng/ml)
E	EGF (50 ng/ml)
EW	EGF (50 ng/ml), Wnt3a (200 ng/ml)
ERW	EGF (50 ng/ml), R-Spondin1 (42.5 ng/ml), Wnt3a (200 ng/ml)
EN	EGF (50 ng/ml), Noggin (100 ng/ml)
ENR	EGF (50 ng/ml), Noggin (100 ng/ml), R-Spondin1 (42.5 ng/ml)
ENW	EGF (50 ng/ml), Noggin (100 ng/ml), Wnt3a (200 ng/ml)
ENRW	EGF (50 ng/ml), Noggin (100 ng/ml), R-Spondin1 (42.5 ng/ml), Wnt3a (200 ng/ml)

Table 5.1 Culture conditions used in organoid culture from sorted basal cell populations

n.b. All conditions were additionally supplemented with Y-27632 (10μM) for the first 5 days of culture.

.

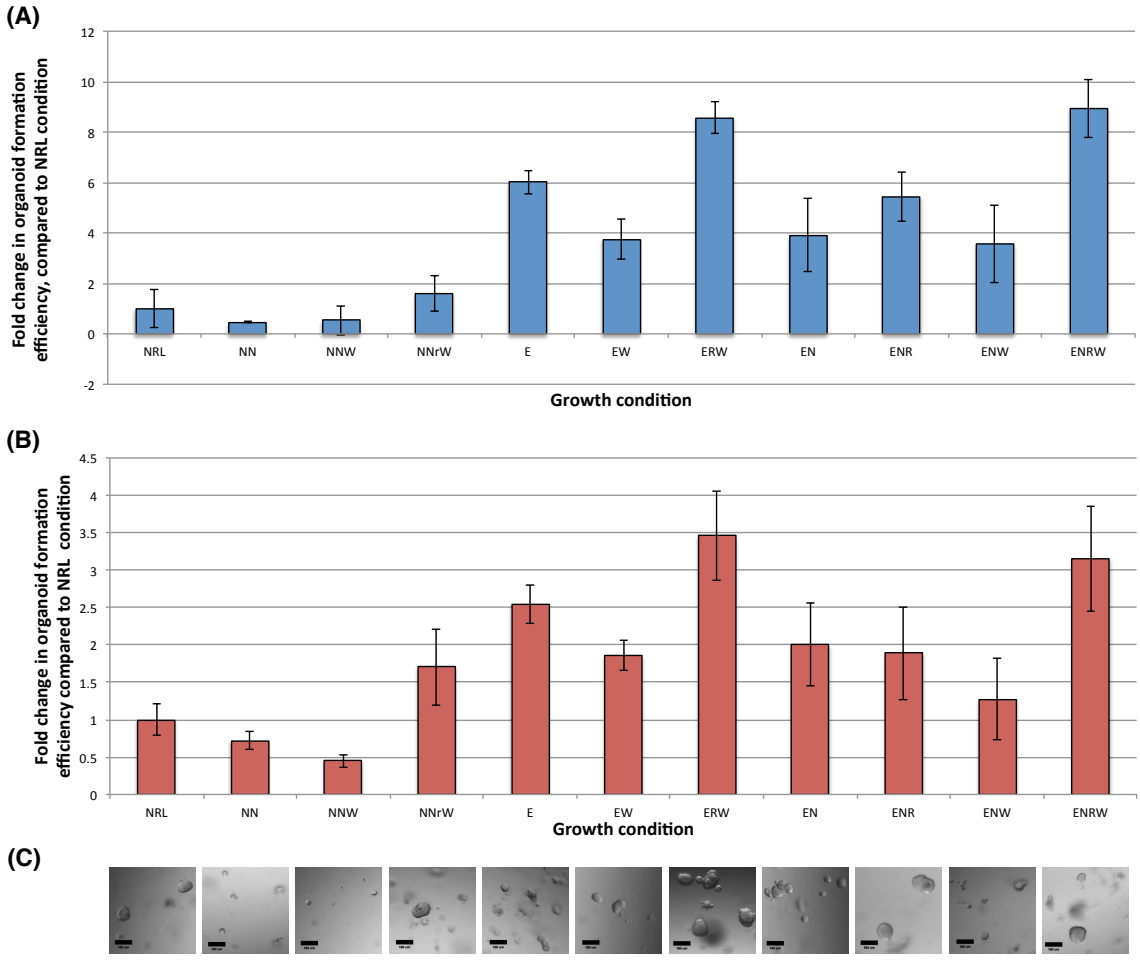

Figure 5.10 Organoid formation from basal cells varies with culture condition.

Single, sorted basal ($CD24^{-}$ Sca^{1-}) cells were seeded at 1000 cells per µl growth factor reduced Matrigel, and overlaid with media containing combinations of growth factors: **Nrg1, Noggin, EGF, Wnt3a, R-Spondin1** (full details in Table 5.1). **(A)** Organoids were grown for 14 days and formation efficiency compared to control NRL conditions calculated. Data are shown as mean ± standard deviation (n=2)**(B)** Organoids were grown for 7 days under the indicated conditions, before media replacement with control NRL media for 7 days in all cases. Data are shown as mean ± standard deviation from ≥3 wells (n=1). **(C)** Representative images of organoids at day 14 in culture following initial treatment with indicated culture conditions and subsequent control media replacement. Scale bar 100 µm.

5.2.3 Summary

The 3D mammary culture system provides a platform like no other currently available; easily accessible, modifiable and quantifiable. It has here enabled the study of the properties and growth requirements of individual mammary cell types; first uncovering a potential for high plasticity in luminal cell populations, before enabling the interrogation of possible signalling networks between populations and identification of factors required to fulfil the stem cell niche.

This work has raised several interesting questions about the cellular dynamics within the mammary gland, including the importance of luminal progenitors in mixed populations, and whether in heterogeneous cultures the limited lifespan observed could be a result of purely luminal cell expansion or if the basal cell niche is fulfilled by EGF (or a similar ligand) given via a paracrine signal. These questions will be discussed in detail in chapter 7.

6 Utilising the organoid model to investigate the potential for Wnt inhibition in the treatment of basal-like breast cancers.

6.1 Introduction

In vitro studies of breast cancer currently depend on many of the previously mentioned, somewhat limited, 2D and 3D culture systems (Chapter 1.4), while the pre-clinical rationalisation and development of drugs for breast cancer treatment relies heavily on high throughput 2D screening assays and use of mouse tumour models. Such methods of drug discovery often have high rates of compound failure - partly due to disparities between cell responses in 2D and 3D culture - cost huge amounts of money, and require large animal cohorts to achieve statistically relevant results before clinical Phase I trials can begin.

The study of mammary cancers - their cells of origin, growth requirements, step-wise progression, and response to pharmacological agents amongst other aspects - could therefore be greatly aided by the use of a model such as the 3D mammary organoid culture system that better represents physiological responses of tumour cells within more *'in vivo'* like contexts. If implemented at a point between 2D and animal assays, better 3D tumour models could not only improve the range and number of compounds able to be tested (by comparison with *in vivo* studies), but could also allow studies of the combinatorial effects of drugs. The ease of expansion of organoids *in vitro* means that material from just one animal could be cultured and used for multiple drug screening assays.

The current standard of care treatment for basal breast cancers is Taxol, a microtubule stabilising cytotoxic compound, targeting all rapidly proliferating cell populations. As described in Chapter 1, despite showing strong initial efficacy in treating highly proliferative basal breast cancers, Taxol is commonly associated with high relapse rates in this cancer subtype, contributing to low 5-year survival rates in patients. This phenomenon is thought to be a result of the maintained presence of a small slowly dividing, and thus Taxol resistant, tumour initiating / cancer stem cell population, that can lie dormant until inhibition is removed and subsequently reinitiate tumour growth and even metastasis. As a consequence, the removal of this population is considered key

to preventing the recurrence of basal breast tumours, and the search for a suitable targeted therapy for this purpose is on-going.

As detailed extensively in Chapter 1, Wnt signalling has been strongly linked to both stem cells **and** basal breast cancers. Basal tumours enriched in stem/progenitor cells concurrently exhibit increased observed levels of active β-catenin, relating to poorer prognosis (Khramtsov *et al.* 2010). The Wnt signalling pathway has therefore been proposed to have potential as a targeted cancer stem cell inhibitor in basal breast tumours.

Given that the mammary organoid system is able to successfully demonstrate Wnt dependency in normal culture, the work detailed in this chapter utilised 'normal' NRL and 'abnormal' ERH culture conditions to support the growth of basal-like Wnt-dependent mammary tumour-derived organoids, which were then used as a easily quanitifable model in which to determine the benefit of Wnt inhibition in treating such tumours. In addition to single inhibitor assays, the advantages of combination therapy (with Taxol) were assessed in this model, and efforts made to determine the true degree to which cancer stem cells were affected, using novel replating assays.

6.2 Results

6.2.1 Establishing organoid cultures from basal like mouse tumours

6.2.1.1 T1/TP53$^{-/-}$ tumour model

The Rosen laboratory (Baylor College of Medicine, Houston, Texas) previously generated a bank of over 50 p53 null tumours, from the transplantation of p53-/- mammary epithelial tissue from transgenic mice into the cleared mammary fat pads of syngeneic wild-type mice (Herschkowitz et al. 2012). The array of tumours obtained in this way was shown to be highly heterogeneous, ranging from those retaining hormone receptor expression and luminal markers to those that were wholly undifferentiated; although all exhibited aneuploidy. Of this bank, one tumour (T1) was characterised as a heavily keratinous, squamous adenocarcinoma, lacking hormone receptor expression. Importantly, the T1 tumour showed evidence of being driven by a Wnt responsive population; 6.1% of total cells were shown by FACS analysis to exhibit TOP-eGFP expression, indicative of Wnt activity; this population overlapping considerably (90%) with a CD29^{+}CD24^{+} tumour initiating cell population (Zhang *et al.* 2010). Most recently,

these TIC populations have been demonstrated to express high levels of Wnt targets Axin2, Tcf7 and Fzd7 (Zhang *et al.* 2015).

Tumours derived in this way have previously been successfully grown and used in orthotopic transplants as a substitute for genetically engineered mouse models in the study of small compounds, aiming to generate a tool for predicting therapeutic response in human cancers (Usary et al. 2013). In the experiments described below, fragments of the T1 tumour were obtained from the Rosen Lab and were orthotopically expanded in the cleared mammary fat pads of 3-week-old female BALB/c mice, before *in vitro* culture.

6.2.1.2 Establishing media requirements for T1 tumour derived organoid growth.

Basic growth requirements of organoids from primary T1 tumour tissue were ascertained by plating a trypsinised tumour cell suspension at a density of 1000 per ul growth factor reduced Matrigel and treating for 7 days with a variety of culture media compositions. In an initial experiment, basic serum-free DMEM/F12 culture medium was applied to cultures for 7 days and an extremely small number of low diameter organoids were produced, at a plating efficiency of less than 1% (Figure 6.1); this efficiency was much lower than the known Wnt dependent proportion of the T1 tumour, (6.1%).

The defined media conditions required for 'normal' phenotypic mammary organoid growth (NRL), and the high Wnt condition (ERH) demonstrated to induce an abnormal phenotype in wild-type mammary organoid cultures were trialled. Organoid formation efficiency was found to be markedly higher under both NRL and ERH growth conditions compared to that of basic media conditions, at approximately 5% in both cases (Figure 6.1). Organoid diameter was also increased compared to that under basal media conditions (1.63 and 1.67 fold, respectively). Additional factors such as FGF2, FGF7 and FGF10 (results not shown) were found to have little additional benefit to growth efficiency of the T1 organoids.

After 7 days in culture, phenotypic analysis of organoids under each culture condition was carried out. Regardless of culture condition, luminal cell markers were not observed, while p63 expression could be distinctly seen in organoids, indicating a basal phenotype (Figure 6.2). Karyotyping of the T1 organoids was also performed,

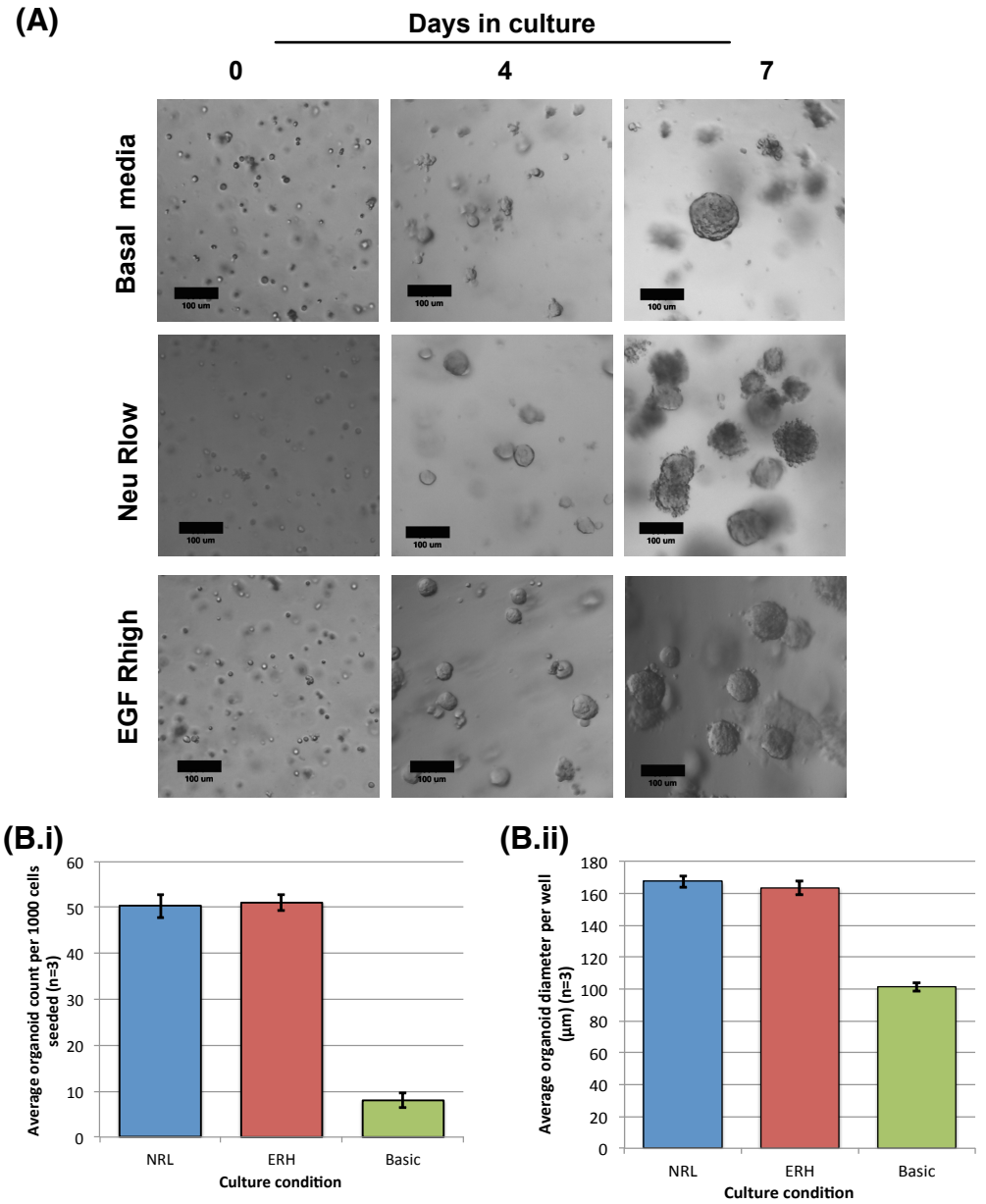

Figure 6.1 Analysis of growth of T1 tumour organoids under various growth media conditions.

T1 tumour fragments were processed to trypsinised single cells, plated at 1000 cells per µl of growth factor reduced Matrigel, and overlaid with either stock basal media, or basal media supplemented with either: Nrg1 (100 ng/ml), Noggin (100 ng/ml) and R-Spondin1 (2.7 ng/ml), or EGF (50 ng/ml), Noggin (100 ng/ml) and R-Spondin1 (42.5 ng.ml) **(A)** Representative images demonstrating the morphological development of organoids under each growth condition, over 7 days in culture. Scale 100 µm. **(B) (i)** Graph depicting average organoid count 1000 cells originally seeded, after 7 days in culture, under each growth condition. **(ii)** Graph depicting average organoid diameter (µm) after 7 days in culture, under each growth condition. Data shown as mean ± standard deviation, (n=3).

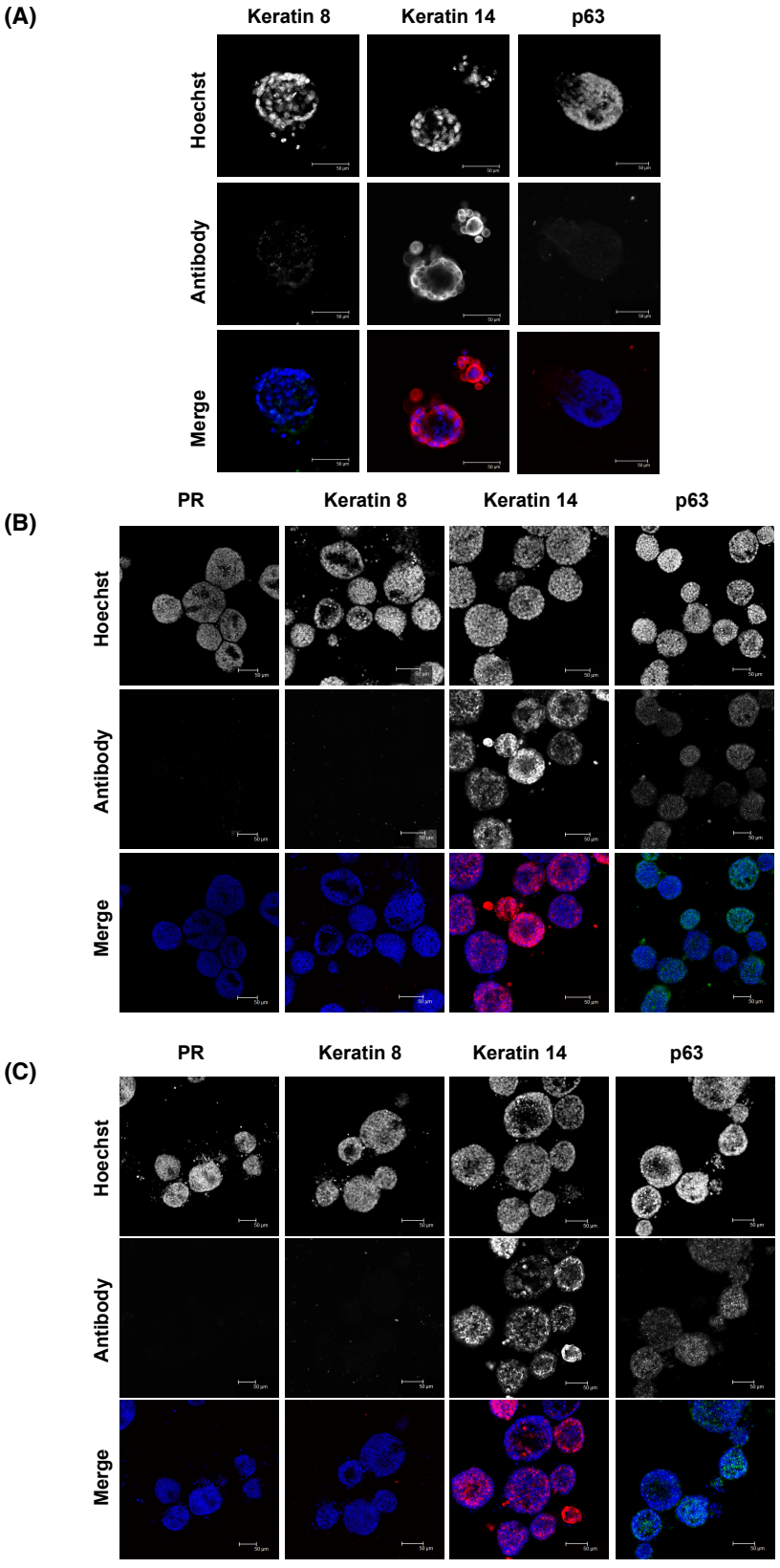

Figure 6.2 Phentotypic analysis of T1 tumour organoids grown under various media conditions.

Organoids were fixed at day 7 in culture and immunostained for luminal (Progesterone receptor (PR) and Keratin 8) and basal (p63 and Keratin 14) markers. T1 tumour organoids grown under **(A)** basic **(B)** Nrg1 (100 ng/ml), Noggin (100 ng/ml), R-Spondin1 low (2.7 ng/ml) **(C)** EGF (50 ng/ml), Noggin (100 ng/ml), R-Spondin1 high (42.5 ng/ml) media conditions. Scale 50 µm.

highlighting distinct aneuploidy in almost all spreads assessed (n=16), with the most prevalent chromosome counts between 49 and 52 chromosomes (Figure 6.3).

Importantly, organoids were shown to exhibit similar growth characteristics over passage. Although small fluctuations in organoid formation efficiency were observed this was likely due to a variety of reasons, including the recovery of cells put into 3D culture, their adjustment to culture conditions, and minor variations in seeding density accuracy. Overall, organoid behaviour remained stable over several passages and organoids could therefore be confidently expanded for use in assays (Figure 6.4).

In order to support repeat inhibitor experiments, tumour organoid freezing protocols were established. Small organoids grown from single cells for 3-4 days were frozen at -80°C in a serum-rich, DMEM-F12 based freezing medium. Organoids were thawed and replated in growth factor reduced Matrigel, and given culture media (NRL or ERH, corresponding to growth conditions prior to freezing) supplemented with Y-27632 for the first 3 days in culture. It was observed that although organoids took approximately 7 days to recover and grow to a size suitable for passage, organoid formation efficiencies, over several successive passages, were comparative to those seen from non-frozen material (Figure 6.5).

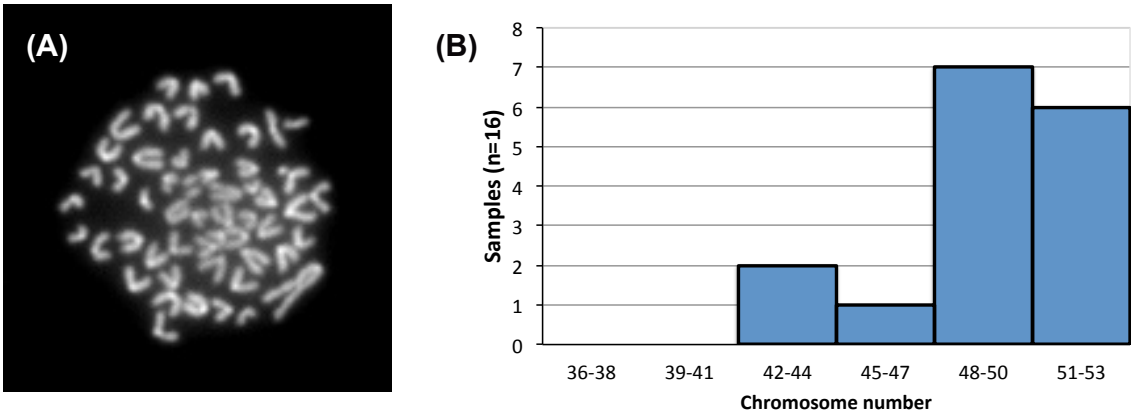

Figure 6.3 Karyotypic analysis of T1 tumour organoids.

(A) Representative DAPI stained chromosome spread, depicting 52 chromosomes. **(B)** Histogram of chromosome counts per spread, from a total of 16 spreads. All images were taken at 40X and chromosomes counted manually using ImageJ ROI manager.

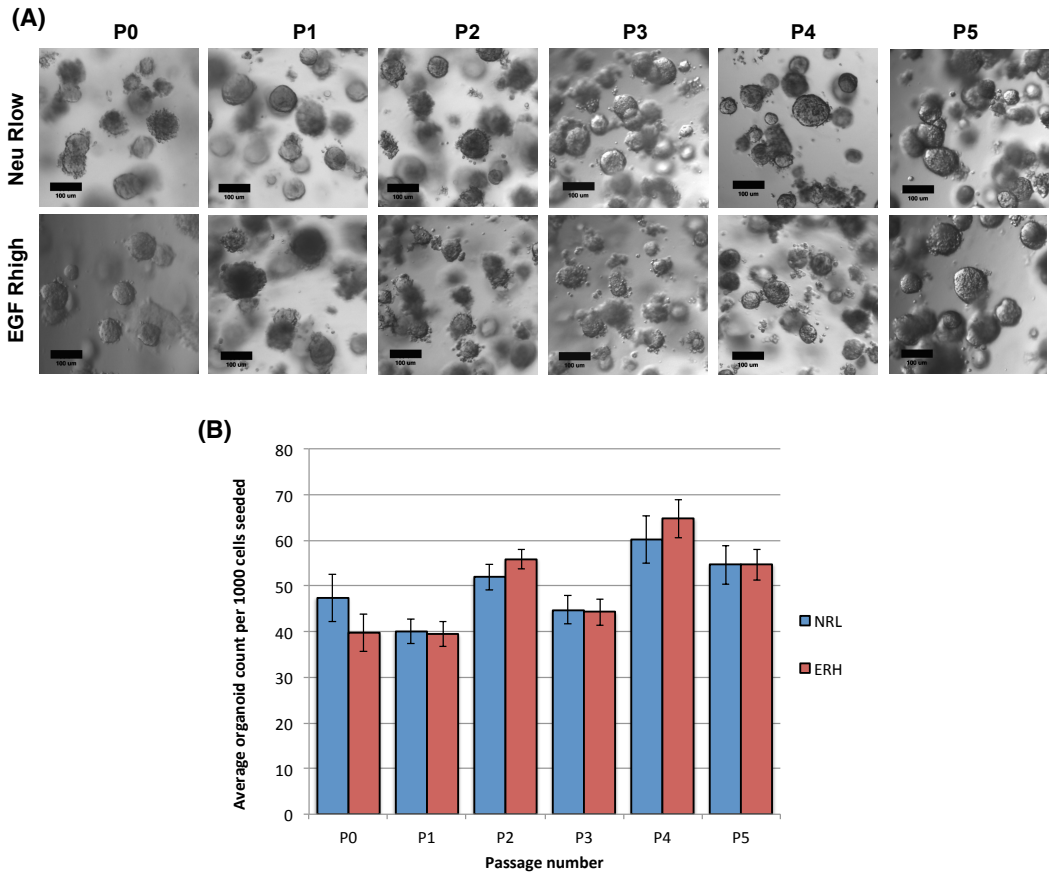

Figure 6.4 Analysis of T1 tumour organoid growth over long-term passage.

Trypsinised tumour cells were plated at 1000 cells per µl growth factor reduced Matrigel and overlaid with either Nrg1 (100 ng/ml), Noggin (100 ng/ml), R-Spondin1 (2.7 ng/ml) media, or EGF (50 ng/ml), Noggin (100 ng/ml), R-Spondin1 (42.5 ng/ml) media, and passaged using a trypsin based approach, every 7 days. **(A)** Representative images of T1 tumour organoids at day 7 in culture at various stages of passage. Scale 100 µm. **(B)** Bar chart depicting average organoid formation efficiency per 1000 cells plated, over five passages, under both growth conditions. Data are shown as mean ± standard deviation of ≥4 wells in one plate (n=1).

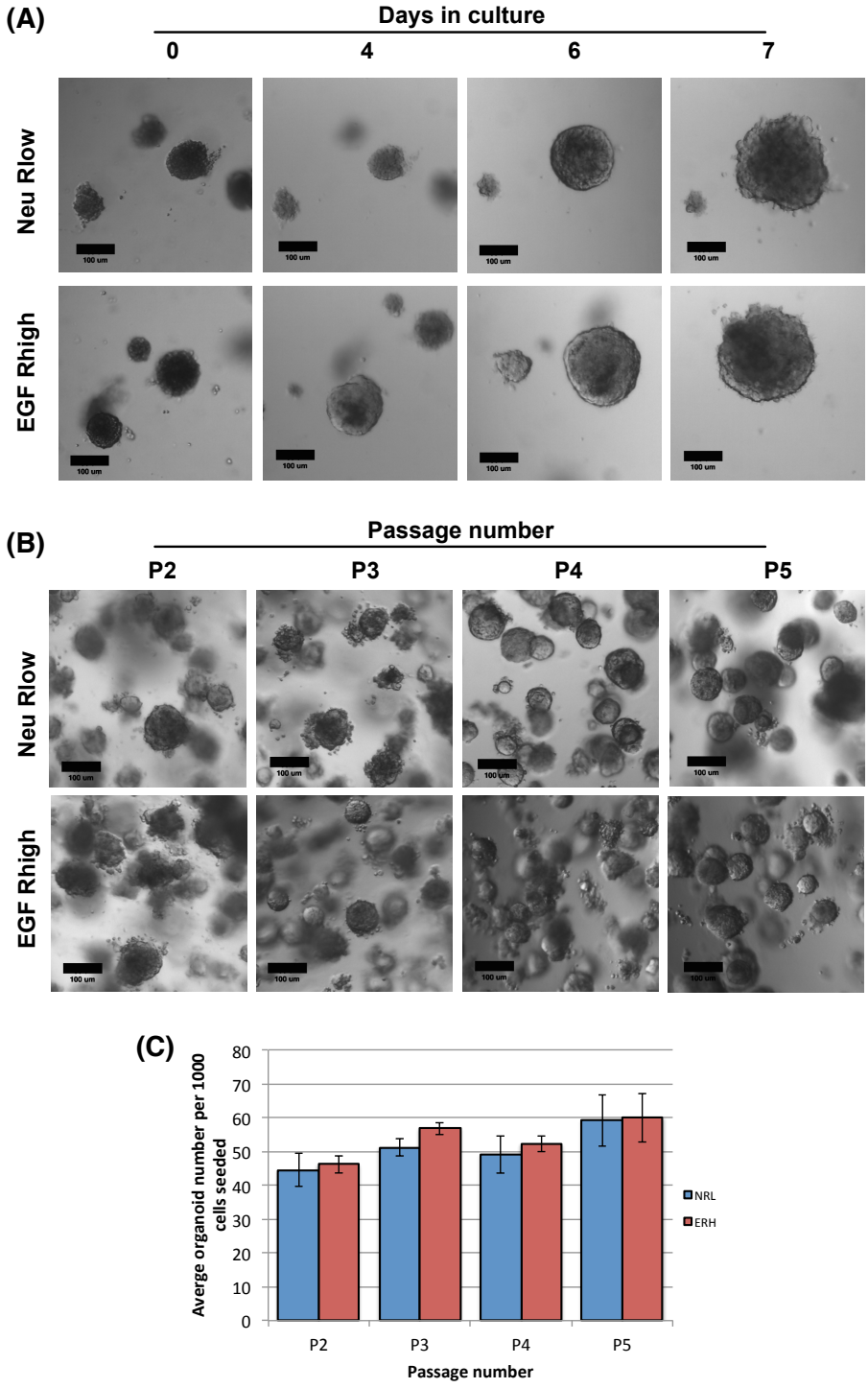

Figure 6.5 Analysis of T1 tumour organoid growth from previously frozen organoids.

Organoids grown for 7 days were frozen in freezing media and stored at -80°C, before thawing at 37°C and plating in growth factor reduced Matrigel. Organoids were then overlaid with their original growth media, and monitored over multiple passages. **(A)** Representative images of morphological development of organoids freshly thawed and plated, over 7 days in culture. **(B)** Representative images of T1 organoids at day 7 in culture, from passage number 2 to 5. Scale 100 µm. **(C)** Bar chart depicted organoid growth efficiency per 1000 cells seeded, from passage 2 to 5. Data are shown as mean ± standard deviation of ≥4 wells in one plate (n=1).

6.2.1.3 MMTV-Wnt1 tumour model

The MMTV-Wnt1 mouse model has contributed widely to the investigation of the Wnt dependency of the mammary gland *in vivo,* particularly with respect to the stem cell compartment. In contrast to the T1 model, the MMTV-Wnt1 model has shown possession of both luminal and basal tumour initiating cell populations (Kim et al. 2011). As a Wnt dependent tumour model with a known mechanism, this system was considered as another ideal candidate for growth in organoid culture for the investigation of inhibitors of the Wnt pathway.

Moreover, *in vivo* experiments have already been performed in the Dale group in which orthotopic transplants of MMTV-Wnt1 tumour into athymic mice were shown to respond robustly to Wnt inhibition, indicating the model as suitable for the purpose of corresponding in vitro (Dale *et al.* 2015).

6.2.1.4 Establishing media requirements for growth of MMTV-Wnt1 derived organoids.

Preliminary investigations confirmed that due to their inherent Wnt activity, MMTV-Wnt1 tumour organoids were able to grow in R-Spondin1 deficient media and that developing structures exhibited slight keratinisation; tumour organoids lacked hormone receptor expression when grown under Nrg1, Noggin only conditions (Figure 6.6).

Interestingly, plating efficiency under NRL conditions occurred at a similar efficiency to Nrg1, Noggin only conditions (Lacking Rspo; 1.06 fold ±0.15, n=3). However, each organoid was larger (1.18 fold ±0.08, n=3) and of a higher optical density (1.27 fold ±0.16, n=3) - the latter indicating increased keratinisation, as confirmed by immunofluorescence analysis (Figure 6.6C). MMTV-Wnt1 cells under ERH (EGF, Noggin, R-Spondin1 high) conditions showed increased organoid formation (1.73 fold ±0.23, n=3, p=0.002, One Way ANOVA with Dunnett's post-hoc analysis), again with each organoid also larger in diameter (1.41 fold ±0.23, n=3, p=0.02, One Way ANOVA with Dunnett's post-hoc analysis) and of a higher optical density (1.39 fold ±0.16, n=3, p=0.02, One Way ANOVA with Dunnett's post-hoc analysis) than under the Nrg1 only condition (Figure 6.6). As keratinisation of structures makes trypsinisation of structures for passage technically challenging, the R-Spondin1 deficient, Nrg1, Noggin only condition was chosen for routine culture and passage. Conversely, for inhibitor experiments, R-

Spondin1 driven conditions were used as a fair parallel to the T1 culture conditions, representing a ‘normal’ and ‘abnormal’ environment for growth.

Further experiments were performed prior to titration assays to determine optimal seeding density of MMTV-Wnt1 organoids. Interestingly, organoid formation efficiency in the MMTV-Wnt1 model, as assessed by the average organoid number counted per 1000 cells seeded, was inversely correlated with seeding density. As such, the highest organoid formation efficiency, and that closest to that given by the T1 organoids, was established at 750 cells per µl Matrigel, at approximately 4.2% (Figure 6.7). In all future assays the MMTV-Wnt1 organoids were seeded at this density.

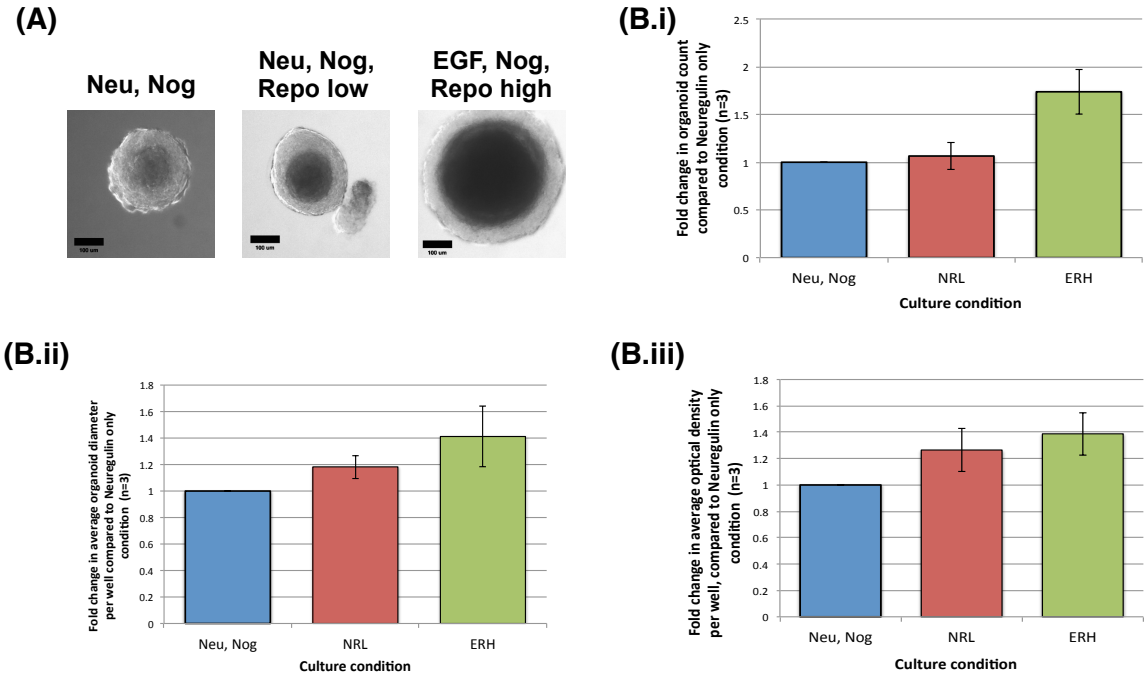

Figure 6.6 Analysis of growth of MMTV-Wnt1 tumour organoids under various media conditions.

MMTV-Wnt1 tumour fragments were processed to trypsinised single cells, plated at 1000 cells per µl of growth factor reduced Matrigel, and overlaid with basal media supplemented with either: Nrg1 (100 ng/ml) and Noggin (100 ng/ml); Nrg1 (100 ng/ml), Noggin (100 ng/ml) and R-Spondin1 (2.7 ng/ml); or EGF (50 ng/ml), Noggin (100 ng/ml) and R-Spondin1 (42.5 ng.ml) **(A)** Representative images demonstrating the morphological development of organoids under each growth condition, over 7 days in culture. Scale bar 100 µm. **(B) (i)** Graph depicting organoid count at day 7 in culture under each growth condition. **(ii)** Graph depicting average organoid diameter (µm) at day 7 in culture under each growth condition. **(iii)** Graph depicting average organoid optical density (OD) at day 7 in culture under each growth condition. Data shown as fold change (vs Neu Nog only, mean ± standard deviation, n=3). Nrg1 (100 ng/ml), Noggin (100 ng/ml) **(C)** Immunostaining of MMTV-Wnt1 organoids grown under **(i)** Nrg1, Noggin only **(ii)** Nrg1, Noggin, R-Spondin1 low **(iii)** EGF, Noggin, R-Spondin1 high conditions, fixed at 7 days. Organoids were stained for luminal (PR, Keratin 8) and basal (p63, Keratin 14) and B-catenin expression. Scale bar 50 µm.

(C.i)

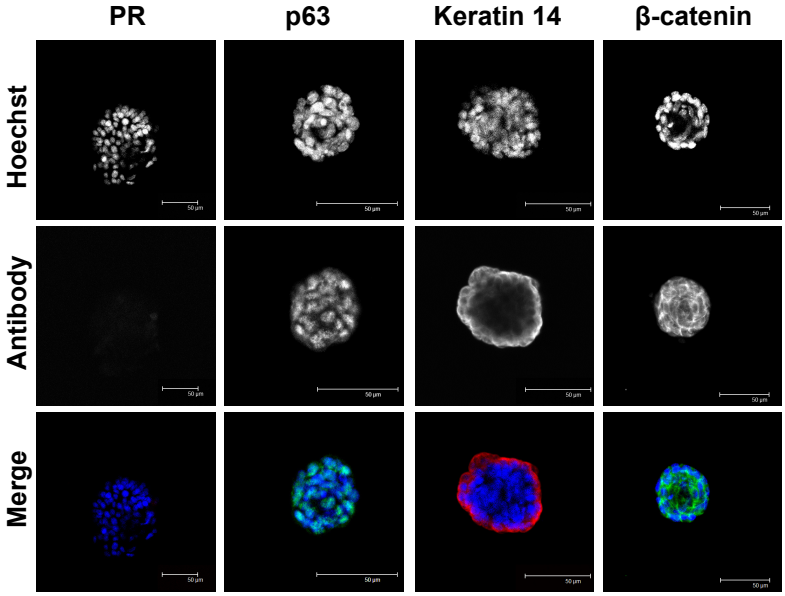
PR
p63
Keratin 14
β-catenin
Hoechst
Antibody
Merge

(C.ii)

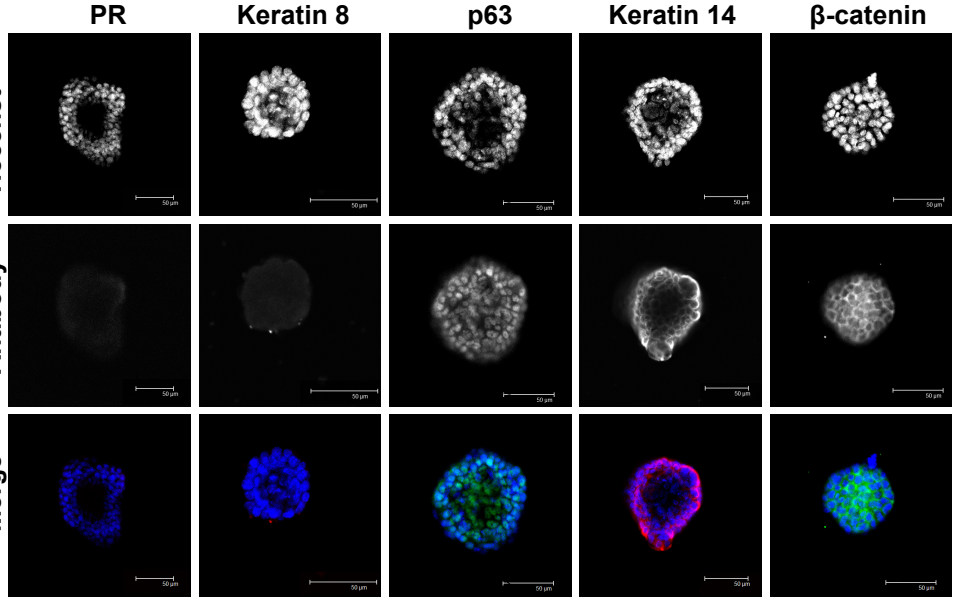
PR
Keratin 8
p63
Keratin 14
β-catenin
Hoechst
Antibody
Merge

(C.iii)

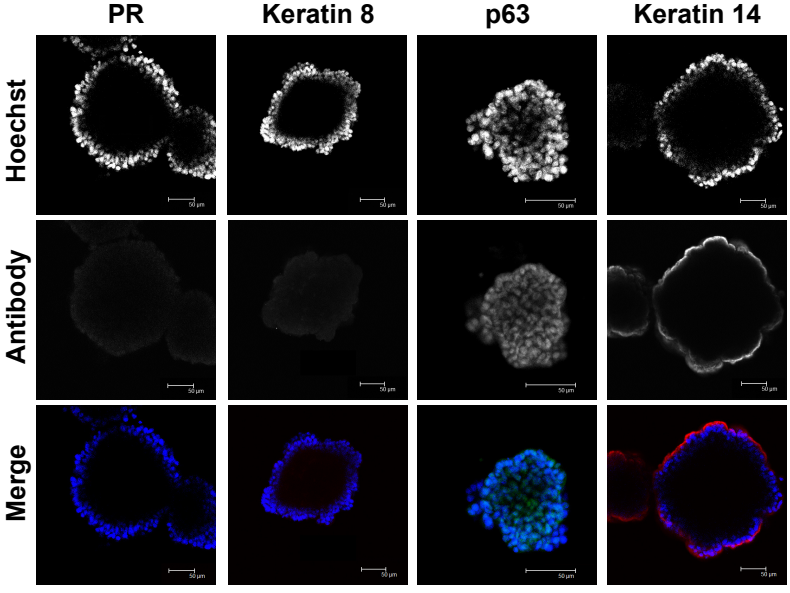
PR
Keratin 8
p63
Keratin 14
Hoechst
Antibody
Merge

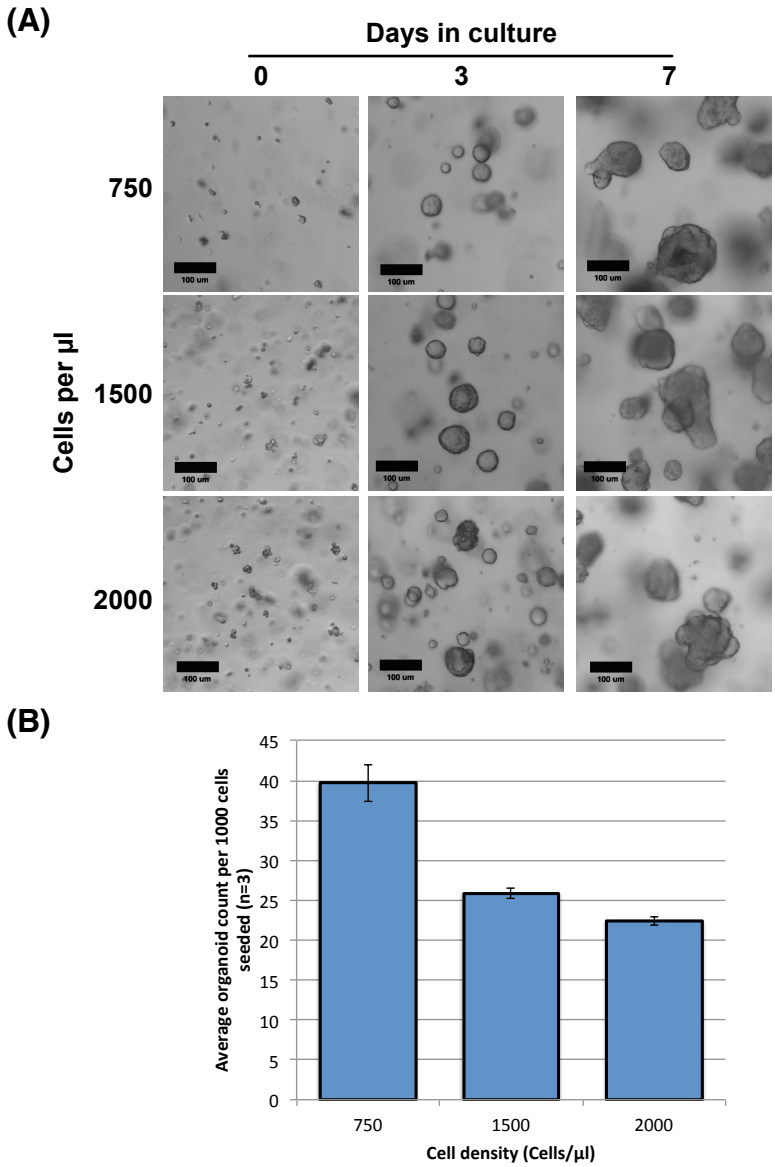

Figure 6.7 Analysis of optimal MMTV-Wnt1 tumour cell seeding density for organoid growth.

MMTV-Wnt1 tumour fragments were digested and trypsinised to a single cell suspension, before seeding at densities of 750, 1500 and 2000 per µl growth factor reduced Matrigel. Cultures were overlaid with Nrg1 (100 ng/ml), Noggin (100 ng/ml) only media. **(B)** Bar chart depicting average organoid formation efficiency per 1000 cells seeded, per well. Data are presented as mean ± standard deviation, where n=3.

6.2.2 Wnt-dependent mammary tumour organoids respond robustly to inhibition by the standard of care therapy, Taxol

As an initial positive control confirming the ability to robustly detect a response of the tumour organoid models to treatment in the chosen 96 well assay format, and to later Wnt inhibitor treatments, the current standard of care (SOC) treatment for basal/triple negative, or metastatic breast cancer, Taxol, was utilised.

Cultures were initiated from freshly trypsinised cells, with treatments applied immediately upon cell plating. *In vivo,* the local tumour environment can be highly varied depending on the type of tumour and its stage, amongst other factors. Therefore to encompass a wider range of potential *in vivo* scenarios, responses of both of the tumour organoids to inhibition were investigated and compared under both 'normal' (Nrg1, noggin, R-Spondin1 low; 'NRL') and abnormal (EGF, noggin, R-Spondin1 high; 'ERH') growth conditions.

Analysis over a 7-day period was aided by GelCount^{TM} technology, whereby total organoid volume was calculated per well as an overall measurement of organoid growth, encompassing both formation efficiency and size. IC_{50} (that is, the concentration at which a 50% reduction in total organoid volume was observed) calculations were generally performed at day 4, during exponential growth phase, unless otherwise indicated. Maximum efficacy was also calculated for each compound, defined as the maximum reduction in organoid volume possible under inhibitor treatment at any concentration. Where stated, an endpoint CellTiterGlo 3D cell viability assay was implemented, in which the quantitation of ATP, and therefore quantity of metabolically active cells per well was compared to that of a non-treated control. In each experiment, at least three technical replicates were present within each condition.

Alongside a control DMSO only condition, a range of Taxol concentrations from 0.625 nM to 160 nM were applied to freshly seeded cells of each tumour organoid type, and multiple parameters measured to determine response. As expected for a SOC breast cancer therapeutic, Taxol showed high efficacy in both the T1 and the MMTV-Wnt1 organoid model systems, regardless of the culture condition provided.

Based on GelCount^{TM} measurements of total organoid volume per well, the T1 model demonstrated an IC_{50} of 1.8 nM (±1.8nM, n=3) at day 4 in culture under NRL conditions, and a similar value of 1nM (±0.9nM, n=2) under ERH conditions (Figure 6.8,

Table 6.1). Growth curves based on organoid volume indicated that Taxol effects were immediate, with separation of curves already clear from the earliest time point of measurement, day 3 (Figure 6.8A.i, B.i), while GelCount^{TM} and endpoint Cell Titer Glo 3D measurements on the final day of culture indicated that effects were persistent over 7 days in culture (Figure 6.8A.iii, iv, B.iii, iv).

The MMTV-Wnt1 model also responded well to growth inhibition by Taxol. Under low R-Spondin1 stimulation (NRL), the Taxol IC_{50} at day 4 in culture was 9.4nM (n=1), while under high R-Spondin1 stimulation (ERH), it approximately doubled, to 18.3 nM (n=1), suggesting a possible increased resistance to inhibition under higher Wnt driven conditions (Table 6.1, Figure 6.8A.ii, B.ii). Cell Titer Glo-3D readouts corroborated GelCount measurements, such that reduction in ATP based fluorescence was slightly greater at 10nM under NRL conditions compared to ERH conditions (Figure 6.9A.iv, B.iv). As in the T1 model, inhibition of growth was sustained to day 7 in both cases.

Overall, these results indicated that the organoids responded to SOC treatment, with only a minimal proportion of organoids remaining at the highest doses compared to the control. Furthermore, this work indicated that growth inhibition could be successfully quantified using the T1 and MMTV-Wnt1 models in the described assay format and the various readout methods described, validating the system for the following work.

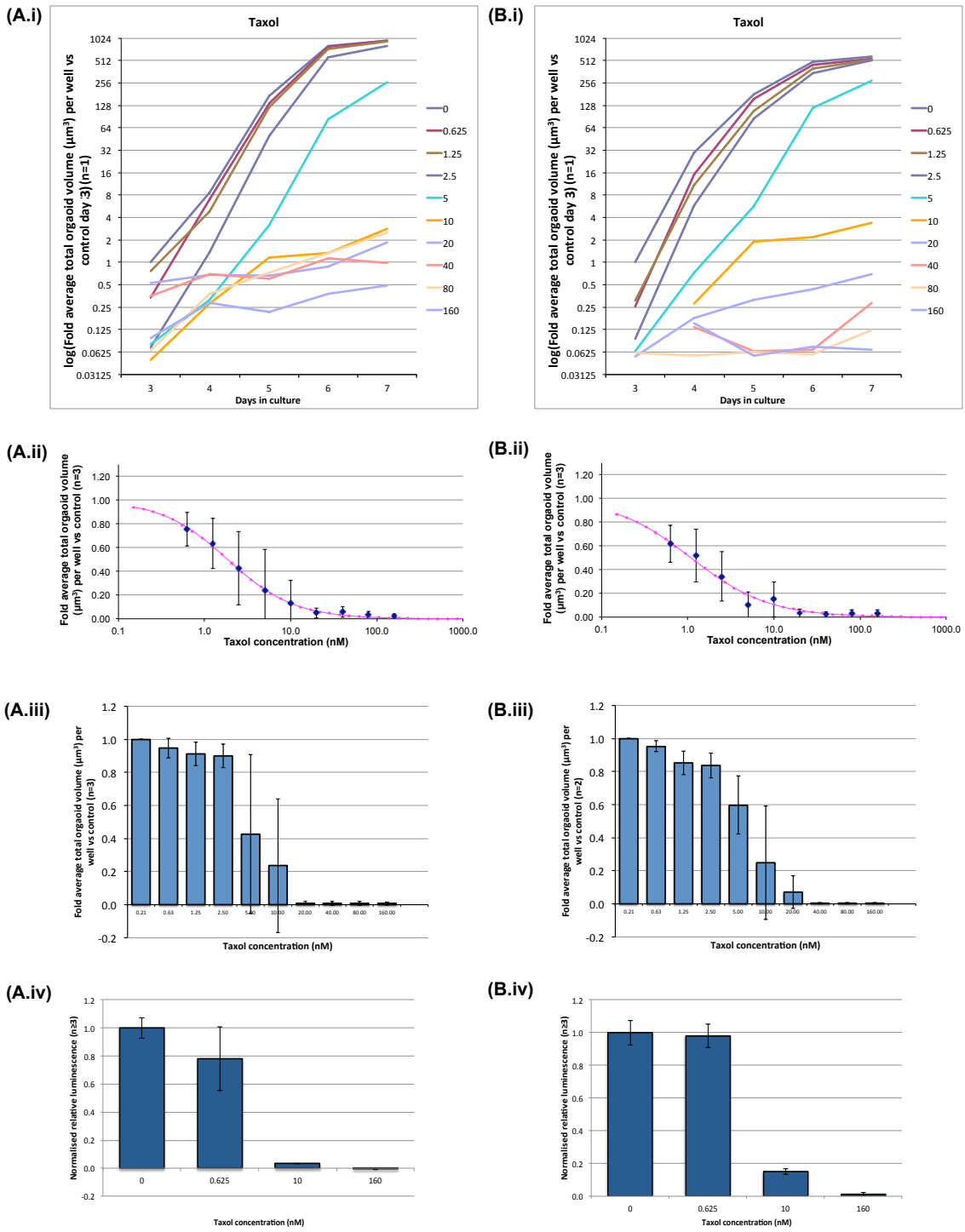

Figure 6.8 Analysis of the effects of Taxol on T1 tumour organoid growth.

Freshly trypsinised T1 tumour cells were seeded at 1000 per µl Matrigel and overlaid with media containing **(A)** Nrg1 (100 ng/ml), Noggin (100 ng/ml) and R-Spondin1 (2.7 ng/ml); or **(B)** EGF (50 ng/ml), Noggin (100 ng/ml) and R-Spondin1 (42.5 ng.ml), supplemented with either a set concentration of Taxol from a two fold titration range (0.625 nM – 160 nM), or a matched DMSO control.

(i) Growth curves from days 3 to 7 in culture. Organoid volume was measured daily using GelCountTM analysis software under the Taxol titration range, expressed here as log values (n=1).

(ii) IC_{50} best fit curves were generated at culture day 4, and **(iii)** Fold total organoid volume (vs control) graphs at day 7 (mean ± standard deviation, NRL n=3, ERH n=2).

(iv) Endpoint Cell Titer Glo 3D viability (mean ± standard deviation, n=1) measurements.

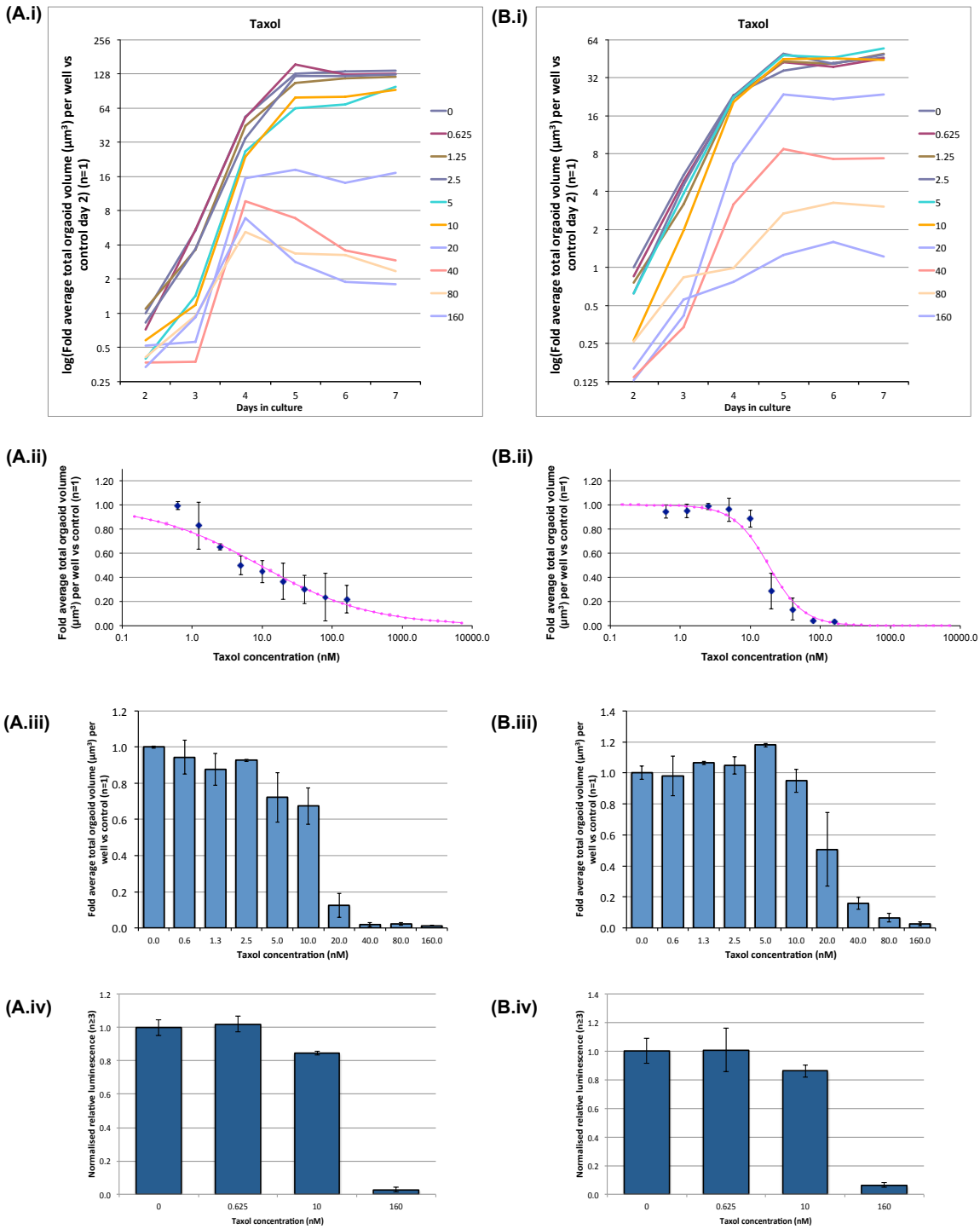

Figure 6.9 Analysis of Taxol effects on MMTV-Wnt1 tumour organoid growth.

Freshly trypsinised MMTV-Wnt1 tumour cells were seeded at 750 per µl Matrigel and overlaid with media containing **(A)** Nrg1 (100 ng/ml), Noggin (100 ng/ml) and R-Spondin1 (2.7 ng/ml); or **(B)** EGF (50 ng/ml), Noggin (100 ng/ml) and R-Spondin1 (42.5 ng.ml), supplemented with either a set concentration of Taxol from a two fold titration range (0.625 nM – 160 nM), or a volume matched DMSO control.
(i) Growth curves from days 2 to 7 in culture. Organoid volume was measured daily using GelCountTM analysis software under the Taxol titration range, expressed here as log fold vs control at day 2 values (n=1). **(ii)**IC_{50} best fit curves were generated at culture day 4 and **(iii)** Fold total organoid volume (vs control) graphs at day 7 (mean ± standard deviation, n=1, *≥3 wells*). **(iv)** Endpoint Cell Titer Glo 3D viability (mean ± standard deviation, n=1) measurements.

Inhibitor		IC_{50} (nM) T1 organoids NRL	IC_{50} (nM) T1 organoids ERH	IC_{50} (nM) MMTV-Wnt1 organoids NRL	IC_{50} (nM) MMTV-Wnt1 organoids ERH	Maximum efficacy (%) T1 organoids NRL	Maximum efficacy (%) T1 organoids ERH	Maximum efficacy (%) MMTV-Wnt1 organoids NRL	Maximum efficacy (%) MMTV-Wnt1 organoids ERH
Standard of care	Taxol	1.8 (±1.8)	1 (±0.9) †	9.4*	18.3*	98 (±1)	98 (±3)†	88*	97*
Wnt release	IWP-2	148*	193*	106 (±68)	2753 (±339)	86*	88*	78 (±3)	71 (±30)
Wnt Receptor	Anti-Frizzled	2.1 (±2.9) †	14.5 (±1.5) †	226(±279)†	No curve†	70 (±15)†	63 (±8)†	75†	26†
Tankyrase inhibitor	IWR-1	127*	95*	235 (±62)	No curve	78*	83*	71	27
	MSC2526550A	No curve†	No curve†	No curve	No curve	31 (±30) †	35 (±47) †	71 (±15)	67 (±12)
	MSC2501490A-5	45 (±17) †	521(±160)†	392(±45)	1420(± 224)	87 (±11) †	77 (±4) †	89 (±8)	88 (±16)
	MSC2504877-A	No curve†	1833(±226)†	No curve	No curve	80 (±25) †	67 (±11) †	83 (±8)	82 (±20)
	MSC2504070	No curve*	268*	No curve	No curve	85 (±14) *	77 (±20) *	69 (±19)	62 (±6)
CDK8/CDK19 inhibitor	CCT251545	349(±128)	538 (±78)†	N/A	N/A	87 (±19)	77 (±10)†	N/A	N/A

Table 6.1 IC_{50}s and maximum efficacies (%) of inhibitors tested in tumour organoid assays.

Data collected from GelCount™ "Total volume" analysis of tumour organoids treated with the indicated inhibitors for 4 days was used to generate IC_{50} curves and calculate maximum inhibitor efficacy. Data shown as mean± standard deviation, where n=3, unless indicated by symbols: *, n=1; †, n=2. Cases where IC_{50} curves could not be generated are indicated as such. *See Appendix 2 for detailed analysis of each condition*.

6.2.3 Mammary tumour organoids are susceptible to inhibition at several points within the Wnt pathway.

As discussed in detail in Chapter 1, the canonical Wnt pathway is regulated at many levels; alteration of any one of the stages in the signalling pathway has the potential to initiate or promote abnormal development. As such, there are several targets that may be amenable to manipulation by drug candidates (Figure 6.10), the effects of which are described here in the context of both the T1 and MMTV-Wnt1 tumour organoid models. While several of the inhibitors used in this study are published with known efficacy and 2-D cell or *in vivo* responses, development compounds from Merck Serono were also investigated for their potential to inhibit growth of Wnt dependent tumour organoids.

6.2.3.1 Inhibition of endogenous Wnt release

Wnt ligand release from the cell in which it is produced is tightly regulated by a requirement for it to be post-translationally modified in the endoplasmic reticulum, through the addition of a palmitoyl group by the action of the membrane bound O-acyltransferase enzyme Porcupine (Porcn). Multiple inhibitors to this process have been established and published previously, including the Inhibitor of Wnt Production-2 (IWP-2) (Chen et al. 2009) used here.

6.2.3.1.1 IWP-2

After 4 days in culture, total organoid volume measurements of T1 organoids under a two-fold dilution range of the Porcn inhibitor between 7.8nM and 2000nM demonstrated a dose response effect on growth inhibition under both NRL and ERH media conditions, with similar IC_{50} values of 148nM and 193nM, respectively (n=1) (Table 5.01, Appendix II-1). Despite this, by day 7 in culture, treated organoid volumes had begun to 'catch up' to that of control organoids; furthermore end-point relative ATP values compared to control, as assessed by Cell Titer Glo 3D, were not greatly different (Appendix II-1.iv).

This phenomenon could be explained in several ways. Acquired resistance may be a factor; cells could upregulate other components of the Wnt pathway to subvert inhibition. Stem cell outgrowth may still occur, but at a slower rate, such that sufficient TA numbers to promote organoid formation are not available until later time points.

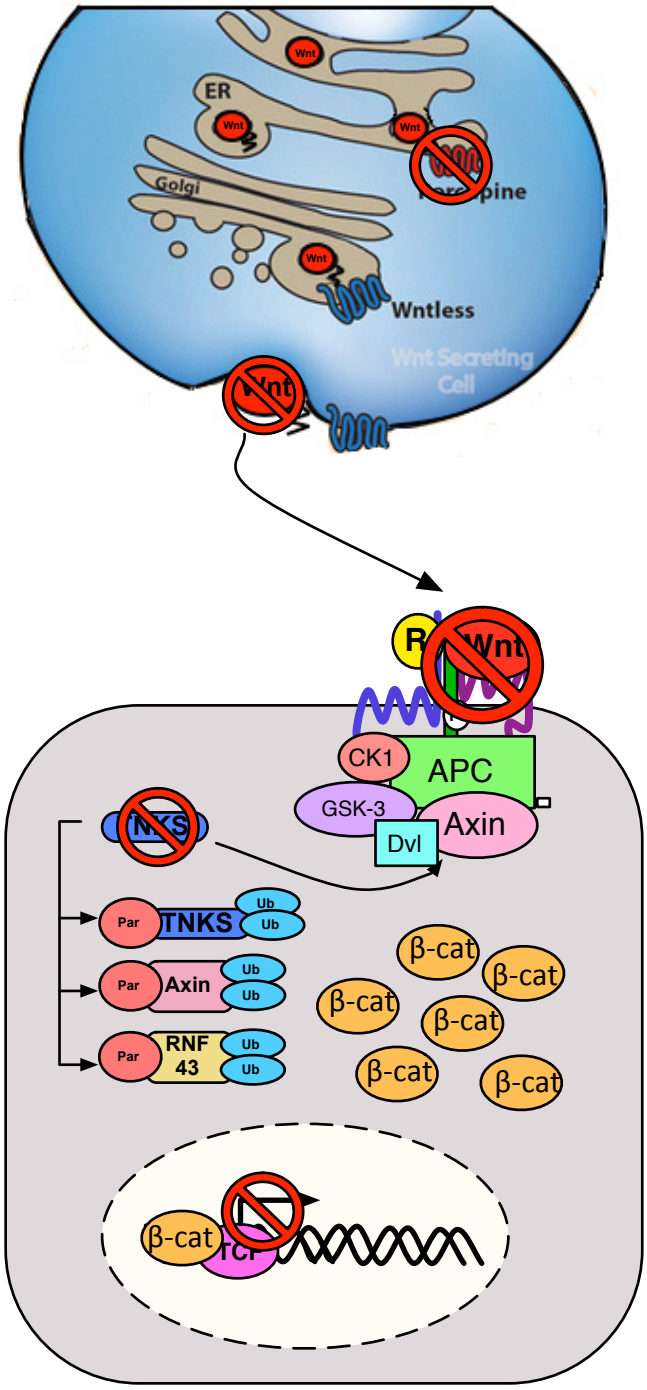

Figure 6.10 Targeting the Wnt signalling pathway in tumour organoids.

The Wnt signalling pathway has several possible points or levels of inhibition, indicated by red ⃠ symbol: the interruption of Wnt release, blocking of Wnt ligand binding to either the Frizzled or Lrp6 co-receptor, the interference with Tankyrase activity required to control Axin levels and therefore destruction complex assembly, and finally the abrogation of Wnt target gene transcription.

However, most simply, and arguably most likely, in a technical artefact of the system, control samples by day 7 likely become growth restricted (termed the growth restriction effect from here on). Growth curves from the above assays (Appendix II-1) indicate that between day 6 and 7, growth of control organoids slowed relative to the initial days in culture. Increasing organoid number and size can cause nutrients and even physical space for further growth to become limiting factors, with hypoxia also possible at the core of larger structures. Therefore, during this slower growth stage, smaller organoids under partial Wnt inhibition have the opportunity to 'catch up'. In this case, the delay in reaching the same volume as control organoids can be seen as related to the potency of Wnt inhibition, adding another level of quantification to the IC_{50} during the exponential growth phase.

MMTV-Wnt1 organoid sensitivity to inhibition by IWP-2 was assessed to be much more dependent on culture condition, the compound having an IC_{50} of 106nM (±68 nM, n=3) under low R-Spondin1 stimulation, and 2753nM (±339, n=3) under high R-Spondin1 stimulation (Table 5.01, Appendix II-2). In contrast to the T1 model, a dose-response effect persisted under NRL conditions until day 7, while under ERH conditions lessened over culture time (Appendix II-2.Aiii, Biii). End-point Cell Titer Glo 3D measurements (0.61 of control vs 07.8 of control) also demonstrated a greater effect of IWP-2 under low R-Spondin1 stimulation than ERH conditions (Appendix II-2.Aiv,Biv). This result might be expected of partial, and not complete Wnt inhibition by IWP-2; a proportion of growth is inhibited, such that the higher Wnt level at the outset under ERH conditions is reflected in a higher remaining Wnt activity after inhibition.

6.2.3.2 Inhibition of Wnt-Receptor Binding

Wnt ligand generates an intracellular response through binding to the Wnt receptor Frizzled, and it's co-receptor Lrp6, the point of R-Spondin1 co-stimulation. In theory, the blocking of these receptor sites with specific antibodies should reduce their availability to bind Wnt ligand and thus reduce canonical Wnt signalling and Wnt driven tumour growth, particularly if an excess of the ligand itself causes the tumour. Studies involving shRNA knockdown of Fzd7 in TNBC *in vitro* and *in vivo* have already demonstrated a concurrent reduction in tumour growth (Yang et al. 2011), giving valid

reason to believe that similar antibodies may do the same in the described organoid models.

6.2.3.2.1 Anti-Frizzled antibody

As the main receptor for Wnt ligand, the Frizzled (Fzd) seven transmembrane domain cell surface receptor is responsible for enabling canonical Wnt signalling in the breast. Anti-Fzd antibody was shown to be extremely potent in the T1 model at day 4 in culture, under both low and high R-Spondin1 growth conditions (IC_{50}s of 2.1 nM (±2.9, n=2) and 14.5 nM (±1.5 nM, n=2), respectively, Table 5.01, Appendix II-3). However, like results under IWP-2 treatment, this inhibition appeared to be overcome by day 7, as indicated by both GelCount™ and Cell Titer Glo 3D measurements (Appendix II-3). Growth curves indicated that although strong inhibition occurred rapidly, a growth restriction effect was once again observed.

In the MMTV-Wnt1 model under low R-Spondin1 stimulation the antibody had an IC_{50} of 226nM (±279nM, n=2)′ and maximum efficacy at 1µM of 75%, while under the higher R-Spondin1 condition a maximum of only 26% growth inhibition could be attained compared to the control. The effect of the inhibitor could be sustained until day 7 in culture, strongly under low R-Spondin1 stimulation (Appendix II-4.A.iii). Again, this effect can be attributed to a partial inhibition of Wnt signalling, with a much higher initial level under ERH conditions presenting a larger obstacle to overcome. Similarly, the differences in response between the two tumour models likely reflect the inherently higher Wnt production level in the MMTV-Wnt1 organoids.

6.2.3.2.2 Anti-Lrp6 antibodies

Two forms of Lrp6 antibody were supplied for testing by Merck Serono. However, little to no significant response was seen to either antibody at any concentration in preliminary experiments in the tumour models. Given that these were trial compounds however, and as such of unknown efficacy, it cannot be excluded that an Lrp6 antibody would be highly useful in the treatment particular Wnt dependent tumours.

6.2.3.3 Reducing intracellular Wnt effector activity by tankyrase inhibition.

Responses to canonical Wnt ligand-receptor stimulation occur through a complex intracellular pathway of proteins (previously discussed, Chapter 1), many of which have the potential to be susceptible to inhibition.

One key protein regulating the canonical Wnt pathway is Axin; a member of the β-catenin destruction complex, regulated itself by a poly-ADP-ribosylase family of tankyrase proteins. Increased tankyrase activity promotes ubiquitination and degradation of Axin, leaving the destruction complex incomplete. The subsequent accumulation of β-catenin protein causes increased Wnt pathway activity (Figure 6.10). As such, tankyrase inhibitors (TNKSi) have in other studies been demonstrated to reduce overall Wnt pathway activity (Lau et al. 2013; Bao et al. 2012), and were considered as suitable compounds of interest in this study. Again, work here was partly carried out in collaboration with Merck Serono, such that several compounds trialled were novel and unpublished. The tool compound, MSC2524070, will be available in the future for study.

6.2.3.3.1 Commercially available IWR-1

IWR-1 is a previously published TNKSi (Huang et al. 2009). A range of concentrations from 4.7nM to 1200 nM were tested on the tumour organoids, based around cellular IC_{50} (~190nM) previously published by (Chen et al. 2009) in 2D assays.

T1 organoid responses to IWR-1 at day 4 were similar under both low and high R-Spondin1 stimulation, with IC_{50} values at 127nM (n=1) and 95nM (n=1), and maximum efficacies of 78 and 83%, respectively (Table 5.1, Appendix II-5.Aii, Bii). Responses were not sustained in the longer term however, with growth again exhibiting a catch up to control organoids. Furthermore, growth curves indicate this catch up to occur faster in ERH conditions (Appendix II-5).

MMTV-Wnt1 organoids were found to be highly dependent on their culture conditions for a response to IWR-1, such that at day 4 under low R-Spondin1 concentration, an IC_{50} of 235 nM (±62 nM, n=3) was calculated, while under ERH conditions an IC_{50} could not be calculated (Table 5.01, Appendix II-6). In this case, a maximum efficacy of just 27% was seen at the highest inhibitor concentration (n=3) (Appendix II-6.Bii). Cell Titer Glo 3D measurements at day 7 confirmed that responses to

IWR-1 were sustained under the low R-Spondin1 concentration, but not at the higher level (Appendix II-6.Aiv, Biv). Again, this reflects a higher initial level of Wnt signalling to inhibit under ERH conditions, and a lack of full Wnt inhibition by the compound.

Under NRL conditions, IWR-1 IC_{50} values were in the range of those given by cellular assays ((Chen *et al.* 2009)

6.2.3.3.2 Merck Serono Tankyrase inhibitors (MS-TNKSi)

Four development compounds (MSC2526550A, MSC2501490A-5, MSC2504877-A, MSC2524070) were tested in the tumour organoid models, in comparison to the published IWR-1 compound. Further information provided by a 2D TNKS luminex assay performed by Merck Serono indicated the cellular IC_{50}s of the compounds to be 35nM, 300nM, 30nM and 3nM respectively. Of these, MSC2524070 has been chosen as a tool compound, and will be made available in future for testing by the research community. All TNKSi were tested across a range of 31.25 nM to 8000nM, in a similar two fold titration to those used in previous assays.

After 4 days in the T1 model treatment with MSC2501490A-5, determined least potent in 2D assays, elicited an IC_{50} of 45 nm (±17, n=2)(Table 5.1, Appendix II-9) under NRL conditions, while MSC2504877-A (Appendix II-11) and MSC2524070 (Appendix II-13) were too effective to calculate IC_{50} under the concentration ranges used, requiring further titration in future studies. Under ERH conditions, higher IC_{50}s of 521 nM (±160, n=2), 1833 nM(±226, n=2) and 268 nM (n=1)(Table 5.1) were calculated for all three compounds, reflecting the higher starting Wnt level under these conditions.

Although IC_{50} values of individual compounds differed, overall trends of response to MS-TNKSi in the T1 model were similar to those under IWR-1 inhibition; initial efficacy was observed at 4 days, but a growth restriction effect occurred by day 7 (with the exception of *MSC2526550A,* which showed little to no efficacy in the T1 model (35% maximum inhibition under NRL conditions). Notably, in comparison to IWR-1 treatment, the time taken to 'catch up' to control volumes under each of MSC2501490A-5, MSC2504877-A and MSC2524070 was substantially longer (Appendix II-9, 11, 13), seemingly indicating more effective Wnt inhibition by these compounds.

The MS-TNKSis showed a similar high potency in the MMTV-Wnt1 model after 4 days; IC_{50} could again only be calculated for MSC2501490A-5 (NRL=392nM (±45, n=3); EGF=142nM (±224, n=3) (Appendix II-10), while MSC2526550A, MSC2504877-A and MSC2524070 exceeded 50% growth inhibition even at the lowest concentration tested, showing 71, 83 and 69% maximum efficacy under NRL conditions, and 67, 82 and 62% maximum efficacy under ERH conditions (Table 5.1).

Under MSC2501490A-5 treatment, organoids showed similar trends of response to MS-TNKSi treatment as to IWR-1; a distinct correlation of IC_{50} with culture condition (Appendix II-10). Moreover, each MS-TNKSi could sustain reductions in organoid volume compared to the control until day 7 in culture (Appendix II-8, 10, 12, 14), even under the higher Wnt conditions, indicating an increased strength of inhibition of Wnt signaling using these compounds than that of IWR-1. In fact of all Wnt inhibitors trialled in this thesis, the MS-TNKSi collection elicited the most pronounced departures from control organoid volume across the duration of growth curve analysis.

Taken together, data supports the use of tankyrase inhibition for the reduction of Wnt-dependent tumour growth. Moreover, several novel compounds have been trialled for this purpose, showing similar trends in response as commercially available IWR-1 compound and indicated to have substantially lower IC_{50}s (and therefore increased potencies) than IWR-1. This could be beneficial in terms of reducing off-target effects of compounds.

6.2.3.4 Inhibition of Wnt target gene expression

A novel inhibitor of the Wnt pathway has recently been developed and investigated by Merck Serono in collaboration with the Dale laboratory (Dale *et al.* 2015). The compound, CCT251545 (CCT), inhibits Cyclin dependent kinases 8 and 19 (CDK8/19), reportedly reducing Wnt related gene transcription (See Introduction).

In vivo experiments performed on an animal model of β-catenin dependent intestinal hyperplasia showed the compound successfully reducing crypt proliferation, while in MMTV-Wnt1 induced mouse breast cancer allografts, CCT slowed tumour growth rate, and reduced Wnt target gene signature (Axin2, Lbh) (Dale *et al.* 2015). Similarly, *in vitro* experiments on MMTV-Wnt1 tumour organoids showed successful response to the compound (Ewan; unpublished).

Given the existing evidence for the compound as a successful Wnt inhibitor in the MMTV-Wnt1 model, we next endeavoured to explore effects on organoids from the T1 tumour model. Application of a two-fold titration range of the compound (8000 nM to 31.25 nM) to freshly seeded cells from the T1 tumour organoid model enabled the identification of a response and calculation of an IC_{50} by day 7 in culture. Interestingly, in comparison to previous inhibitors, the dose response observed was stronger after 7 days in culture compared to 4 days. Much like responses seen to previous Wnt inhibitors, growth condition affected response; under 'normal' R-Spondin1 low conditions the IC_{50} calculated for the compound was 349nM (±128 nM, n=3), while under 'abnormal' R-Spondin1 high conditions, the IC_{50} was higher at 538 nM (±78, n=2)(Table 6.1, Figure 6.11), reflecting a partial Wnt inhibition and higher initial level of Wnt signalling under ERH conditions. Moreover, this response would appear to fit with the partial reduction in TCF-dependent transcription seen under CCT treatment by Dale et al., (2015) and (Mallinger *et al.* 2015).

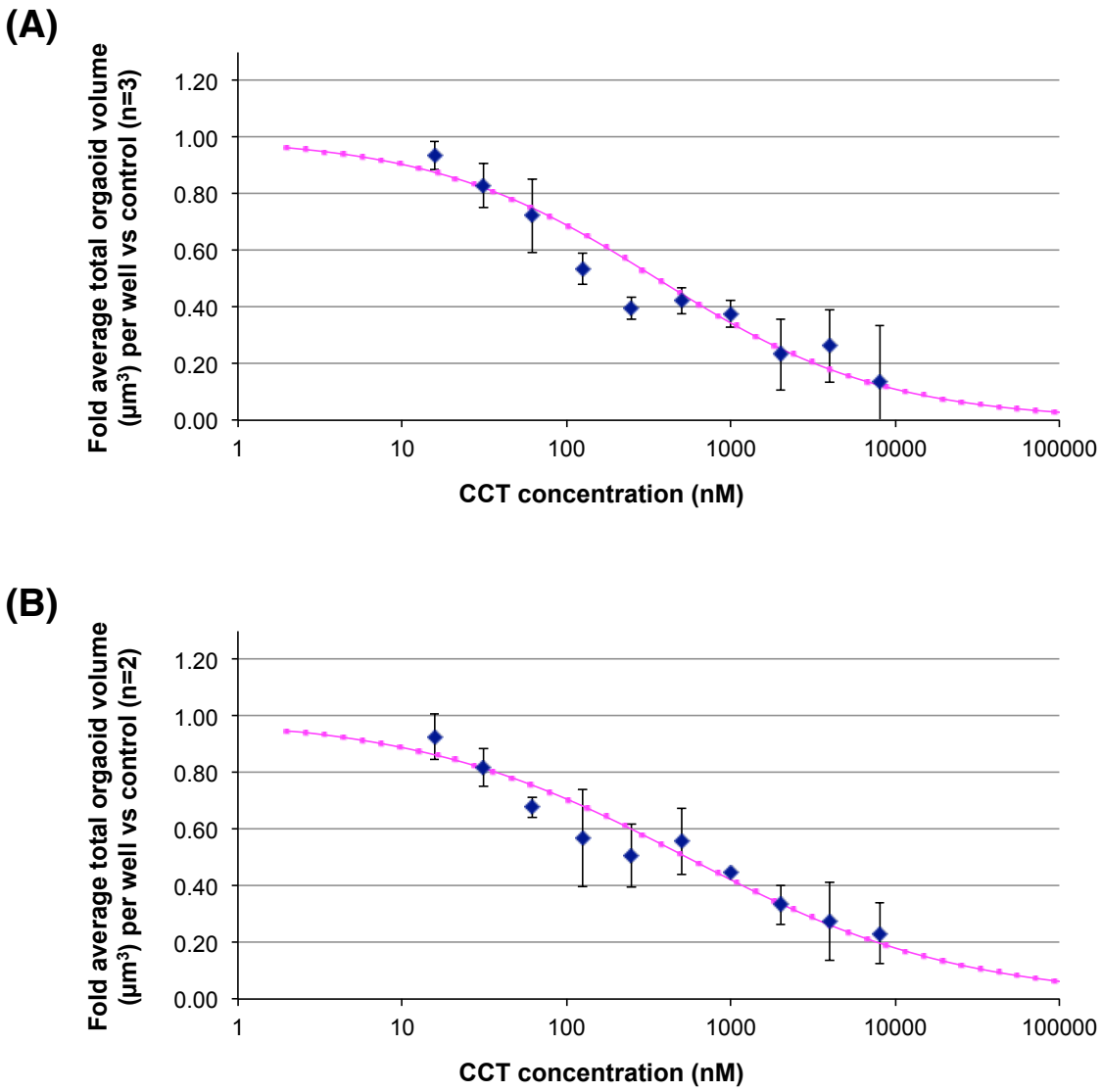

Figure 6.11 T1 tumour organoids respond to a novel inhibitor of the Wnt pathway.

Freshly passaged T1 tumour cells were seeded in growth factor reduced Matrigel at a density of 1000 per µl and overlaid with **(A)** Nrg1 (100 ng/ml), noggin (100 ng/ml) and R-Spondin1 (2.7 ng/ml) or **(B)** EGF (50 ng/ml), noggin (100 ng/ml) and R-Spondin1 (42.5 ng/ml), supplemented with a range of CCT251545 from 15.625 nM to 8000 nM, or DMSO alone as a control. GelCount™ analysis was then performed at day 7 and IC_{50} curves generated. Data shown as mean±s.e.m (NRL, n=3; ERH, n=2).

6.2.4 Inhibition of CDK8/CDK19 can sensitise Wnt dependent tumour organoids to Taxol treatment.

It is now common practice in the clinic to treat patients with more than one chemotherapeutic drug at a time, primarily in an attempt to reduce the doses of individual drugs required for the same effect, by targeting two separate aspects of the tumour at once. This can also reduce the likelihood of a small resistant cell population becoming dominant, and enable the ablation of a heterogeneous cell population. Combination therapy also has additional benefits, in that patient tolerance to the drugs is often improved, and adverse treatment side effects reduced.

As previously discussed, basal breast cancers in particular are thought to have high rates of recurrence after conventional SOC therapy due to a small sub-population of slowly dividing Wnt-responsive stem cells that evade the cytotoxic effects of treatment. As such, this class of breast cancer is an ideal candidate for combination therapy – specifically, using the SOC compound Taxol to kill the rapidly dividing cells that comprise the bulk of the tumour, and a stem cell specific inhibitor to prevent recurrence.

Having successfully utilised the mammary organoid system for the identification of multiple Wnt inhibitory compounds with the potential to abrogate Wnt dependent tumour organoid growth, the potential for such combination therapy in this tumour type was next investigated.

The Wnt inhibitor used in these experiments was CCT, given that it had shown efficacy in previous experiments. Moreover, the Dale group had extensive knowledge of the characterisation and use of this compound in other systems, and had previously demonstrated a combinatorial effect of the compound in organoid studies with Taxol in the MMTV-Wnt1 model (Ewan; unpublished). In this study, the T1 tumour model was chosen, and for simplicity, only the NRL conditions were investigated.

6.2.4.1 Chou-Talalay combination analysis

For assessment of combination experiments, experiments that would allow a Chou-Talalay analysis to be implemented were set up as detailed in section 2.12.4 (Chou and Talalay 1984). This method is commonly used in the analysis of chemotherapeutic combinations, and has previously successfully shown synergistic activity of targeted breast cancer therapeutics with standard of care compounds in breast cancer cell lines

(Pegram et al. 2004). Key to the assay is the analysis of drug combinations where each drug is utilised over a range of concentrations based on its system-specific IC_{50} and where drug A and drug B are represented in a constant ratio throughout the titration range.

Individual IC_{50} values of CCT and Taxol after 7 days of culture were calculated in single inhibitor assays (303 and 5.33nM, respectively) prior to combination, thus setting the IC_{50} ratio in combination to approximately 60. In theory, an additive effect of the compounds in which each failed to affect the efficacy of the other would have been expected to be in the range of 310nM. However, application of the two inhibitors in such a ratio to freshly passaged T1 tumour cells (Figure 6.12.A, B, C) and further linear regression analysis (Figure 6.12.D) indicated that while alone in this particular experiment, the IC_{50}s of Taxol and CCT were 1.4nM and 345nM respectively, the combined IC_{50} of the two compounds was 39.6nM, nearly 8 fold lower than that expected for an additive effect. Synergistic action of the two compounds was then confirmed both by isobologram generation (Figure 6.12.E) and combination index calculation of 0.4, using equation 2.

Specifically, the concentration of CCT required to reduce organoid growth by 50% (the IC_{50}) when given in combination with Taxol, proved to be nearly 11.7 fold lower than CCT alone, while Taxol was made 3.4 times more effective in combination than alone (Figure 6.12.C).

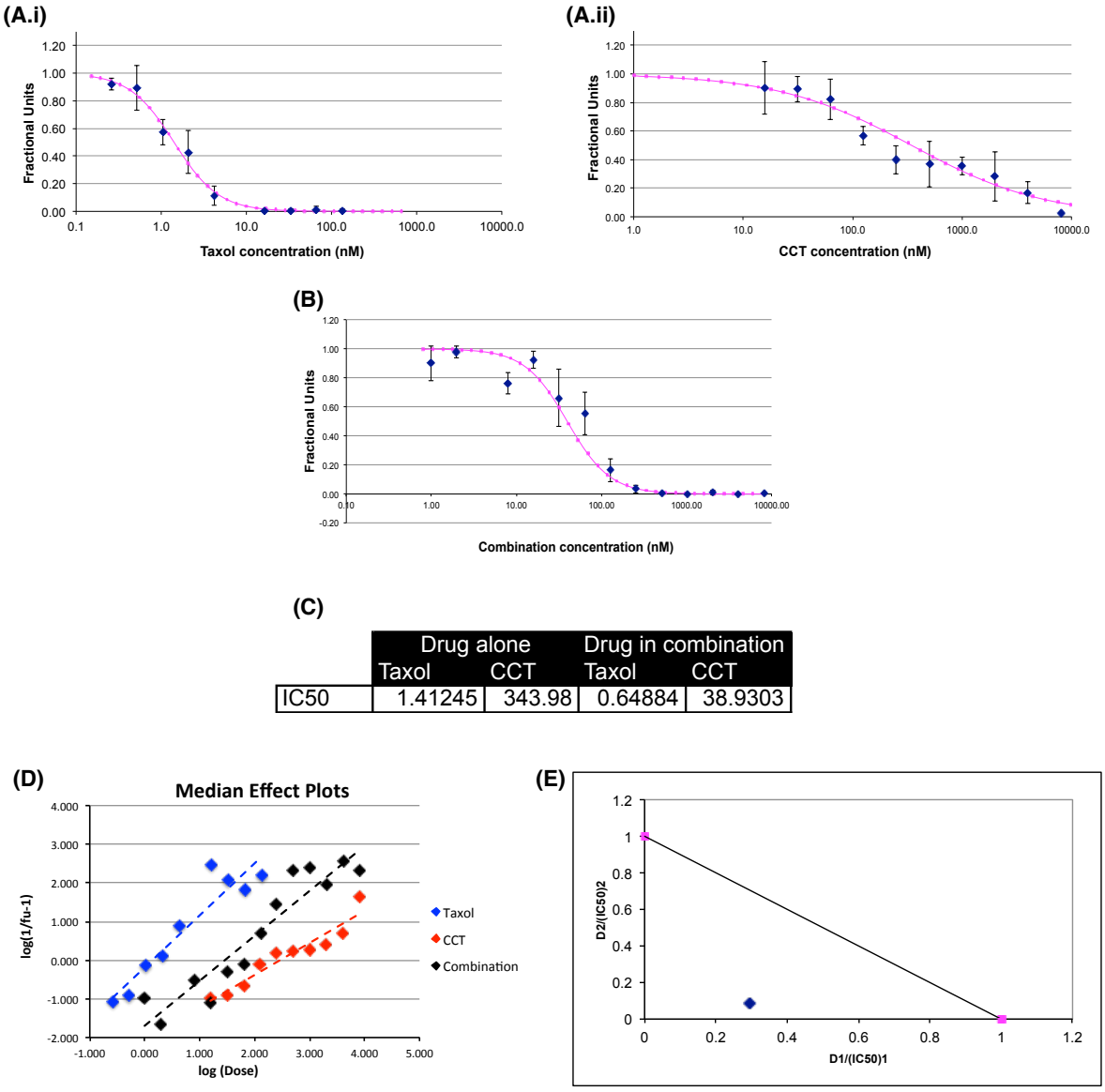

(C)

	Drug alone		Drug in combination	
	Taxol	CCT	Taxol	CCT
IC50	1.41245	343.98	0.64884	38.9303

Figure 6.12 CCT251545 and Taxol exhibit synergistic effects in inhibiting T1 tumour organoid growth.

Freshly trypsinised T1 tumour cells were seeded at 1000 per µl Matrigel and overlaid with media containing Nrg1 (100 ng/ml), Noggin (100 ng/ml) and R-Spondin1 (2.7 ng/ml supplemented with either: **(A.i)** a two fold titration of CCT251545 (1.0 nM – 8000 nM) **(ii)** a two fold titration of Taxol (0.02 nM – 133.33 nM), or **(B)** a combination of both CCT251545 and Taxol in 60:1 ratio (1.0 – 8133.33 nM), for 7 days in culture and IC_{50} calculations performed. Data are mean ± standard deviation from ≥3 wells, n=1 **(C)**. Chou-Talalay analysis was carried out using a pre-developed spreadsheet using to enable **(D)** median effect plot and **(E)** Isobologram generation.

6.2.4.2 *Short term CDK8/19 inhibition unexpectedly increases organoid-forming efficiency of T1 tumour cells.*

Given the clear efficacy of CCT in single and combination therapy in the T1 model, the 3D culture system was next used to study the degree to which the inhibitors might work in hypothetical stem and proliferative transit amplifying cell (TA) subpopulations within organoids. Here the hypothesis was that each organoid could contain both stem and TA cells. To examine the potential of treated and untreated cell 'subpopulations' within organoids, an organoid 'replating assay' was initially designed to try to identify stem cell function.

The basic assumption was made that the organoid formation and growth efficiencies of a cell population are related to the proportion of stem cells present upon seeding. Based on this interpretation of previous experiments, the use of CCT alone would have reduced total organoid volume by lowering Wnt activity within stem cells. As a consequence, transit amplifying cell production from stem cell progenitors would have been reduced, leading to an overall reduced organoid outgrowth compared to control conditions. It was therefore hypothesised that if the inhibitor truly worked by reducing stem cell activity, cells treated with CCT for a period of time and replated as single cell suspensions should have lower potential for organoid formation than an untreated control population. NB: It was unclear whether untreated single stem cells would be able to respond rapidly enough to the Wnt pathway inhibitor to reveal the effects of the inhibitor without the use of a pre-treatment step.

Freshly trypsinised T1 tumour cells were plated and allowed to form small structures for 72 hours under control NRL conditions, before a 12 or 24-hour treatment with 500 nM CCT (slightly above the IC_{50} previously established at day 7 in assay, given the shorter treatment time, and treatment of small structures and not single cells). Organoids were then rescued from Matrigel, trypsinised to single cells and replated at their original density under either control conditions or a second inhibitor treatment for 7 days. Organoid replating efficiency was calculated using GelCount™ analysis software.

In contrast to the original hypothesis, treatment with CCT for 12 or 24 hours followed by replating under control conditions actually induced an increased organoid replating efficiency compared to control alone (1.29 fold (±0.12, n=3, p=0.05, ANOVA with Dunnett's post-hoc analysis) and 1.68 fold (±0.10, n=3, p<0.001, ANOVA with

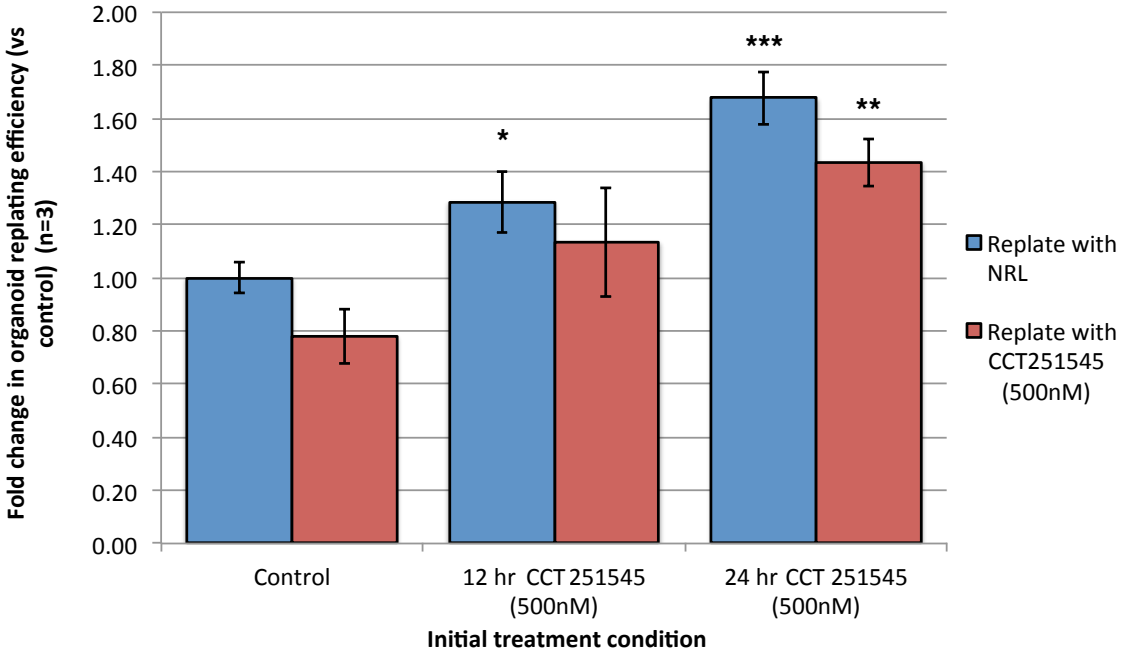

Figure 6.13 Replating efficiency of cells initially treated CCT251545 for 12 or 24 hours.

Freshly trypsinised T1 tumour cells were seeded at a density of 1000 per µl growth factor reduced Matrigel and cultured under Nrg1 (100 ng/ml) Noggin (100 ng/ml), R-Spondin1 low (2.7 ng/ml) conditions for 72 hours. Media was then replaced with either fresh NRL media, or NRL media supplemented with CC251545 (500 nM) for 12 or 24 hours. Following treatment, organoids were trypsinised to single cells and replated at 1000 per µl in growth factor reduced Matrigel, under NRL or NRL+CCT251545 conditions, for 7 days, and organoid number per well counted. Data shown as fold change vs Control (NRL only) condition, mean±standard deviation, n=3. *, $p<0.05$; ** $p<0.01$; ***, $p<0.001$, as determined by ANOVA with Dunnett's post-hoc analysis.

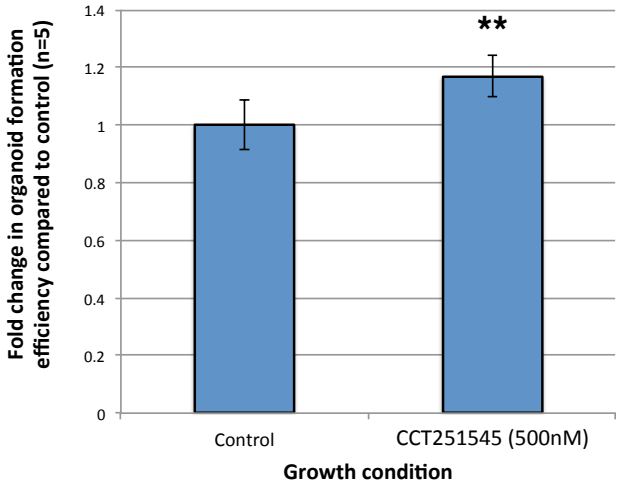

Figure 6.14 Replating efficiency of cells initially treated with CCT251545 for 72 hours.

Freshly trypsinised T1 tumour cells were seeded at a density of 1000 per µl growth factor reduced Matrigel and cultured under Nrg1 (100 ng/ml) Noggin (100 ng/ml), R-Spondin1 low (2.7 ng/ml) conditions for 72 hours. Media was then replaced with either fresh NRL media, or NRL media supplemented with CCT251545 (500 nM) for 72 hours. Following treatment, organoids were trypsinised to single cells and replated at 1000 per µl in growth factor reduced Matrigel, under NRL only conditions for 7 days, and organoid number per well counted. Data shown as fold change vs Control (NRL only) condition. Data shown as mean ±standard deviation, n=3. (**, $p<0.01$, Mann-Whitney U test).

Dunnett's post-hoc analysis), respectively) (Figure 6.13). In each case, while retreatment of previously treated cells with CCT reduced organoid replating efficiency compared to its untreated counterpart, overall replating efficiency still exceeded that of control alone or control cells replated in inhibitor, regardless of the initial treatment duration.

Similarly, organoids grown for 72 hours were treated for a longer time period of 72 hours with 500nM CCT, and subsequently replated with only control media. Counts of trypsinised material before replating indicated reduced total live cell numbers in CCT-treated wells (~60%), indicating that initial treatment had either inhibited cell growth, or killed already established cells. Again, organoid formation efficiency upon replating was increased compared to the entirely untreated control (1.17 fold ± 0.02, n=5, p=0.008, Mann Whitney U test)(Figure 6.14). This further indicated that although CDK8/19 inhibition had a clear initial effect on organoid growth or survival, remaining cells were equally as capable, if not more, of forming new structures upon replating. It was noted however that the fold increase in organoid formation, while significant, was reduced compared to the previously observed results after 12 or 24-hour inhibitor treatments.

6.2.4.3 Cells may undergo a population shift from stem cell to TA under CDK8/19 inhibition

From this evidence, the hypothesis was formed that CDK8/19 inhibition may not kill stem cells, but simply drive them into a lower Wnt activated state. Given that a strong Wnt signal may be necessary for continued self-renewal of stem cells by asymmetric division (Piccin and Morshead 2011), it was proposed that in treating the organoids for a short time with inhibitor and thus lowering their Wnt stimulation, symmetric division of stem cells to instead form two TA cells is favoured (Figure 6.15.B). A similar cell shift from stem to TA cell signature has in fact been recently observed in the intestine of Tet-O-ΔN89β-Catenin mice treated with CCT in the Dale lab, based on gene expression profiles of sorted cell populations (manuscript under review).

Under this hypothesis, consequent removal of the Wnt inhibitor would allow the TA cells to expand considerably, forming a large number of organoids, while retreatment with CCT would likely both further increase TA numbers and yet inhibit their further expansion somewhat, favouring differentiation (Figure 6.15.C).

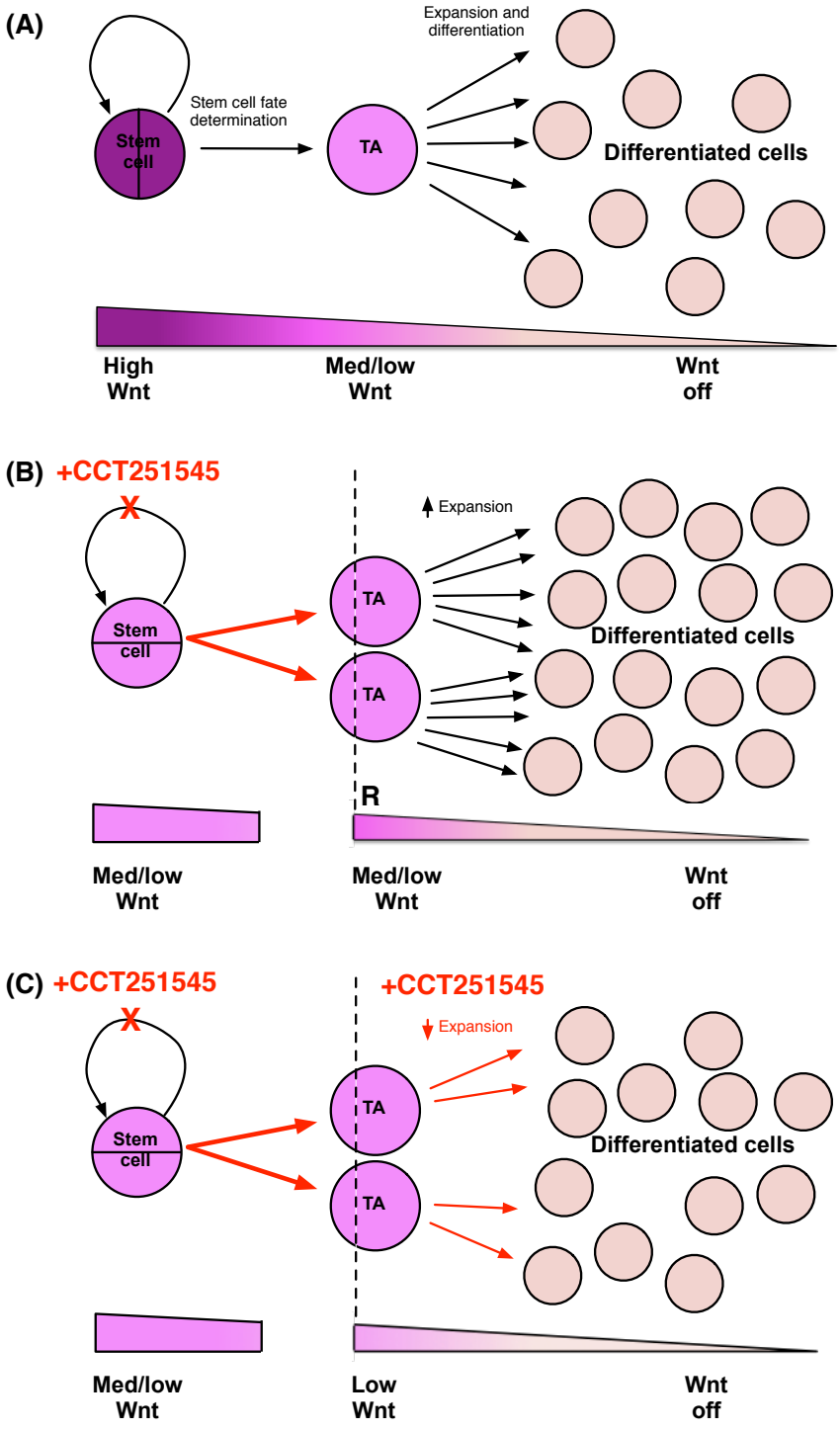

Figure 6.15 Model for possible mechanism of action of CDK8/19 inhibition on Stem and TA cell populations.

(A) Under normal conditions, a stem cell under high Wnt stimulus divides asymmetrically to regenerate itself and form a new TA cell. The TA cell, under a medium-low Wnt stimulation, then proliferates several times to before differentiation occurs, at which point very little to no Wnt is required. **(B)** CDK8/CDK19 inhibition reduces Wnt activity in stem cells, forcing a fate switch enabling two TA cells to be formed, depleting the stem cell compartment. Upon replating (indicated by dashed line) in control conditions, and return to normal Wnt containing conditions, these TA cells can expand considerably, allowing increased organoid formation. **(C)** Upon replating under further CDK8/CDK19 inhibition, TA cells are subjected to a low Wnt stimulus, and their expansion limited, with differentiation favoured, reducing organoid formation.

It is difficult however, in absence of a definite stem/TA marker in the mammary gland, to distinguish a stem cell from a TA cell. In cultures of wild-type cells, the question of whether outgrowths following CDK8/19 inhibition are derived from stem cell or TA cell expansion could be addressed through serial replating of the treated population, given that TA cells due to their limited proliferation capacity would eventually exhaust in the absence of stem cells. However, this characteristic cannot be confidently assumed in a tumour cell population. In the tumour model, the most obvious difference between the two cell populations is their rate of division. As such, the easiest method for determining the effects of the CCT compound on the tumour stem cell population was actually to remove the other population entirely – ie. If organoids are first treated with a compound (eg. Taxol) that will surely kill the fast cycling, transit amplifying cells, is CCT still consequently able to increase organoid outgrowth from the stem cells left behind?

In line with the hypothesis, it might also be expected that initial CDK8/19 inhibition would evoke from stem cells a large number of TA cells able to initiate further organoid outgrowths, and that these fast cycling populations would consequently be sensitised to Taxol treatment. Indeed, it has already been shown that the compound does in fact sensitise to Taxol when in combination. However, this new possibility could mean that the order in which treatment is given is essential in influencing outcome – a crucial point that should be noted in the clinic. Full predictions of sequential treatment outcomes are detailed in Table 6.2.

Single cells were plated and allowed to grow to small organoids for 72 hours, before 72 hr treatment with control media, CCT (125, 500 or 1000 nM), or Taxol (5nM). Organoids from each treatment condition were then trypsinised to single cells, replated, and given either control media, CCT, or Taxol and grown for 7 days in culture.

Results confirmed that pre-treatment with CCT does indeed appear to sensitise T1 tumour cells to Taxol treatment, as under each concentration of CCT applied, organoid formation in CCT>Taxol treated wells was consistently reduced compared to Control>Taxol treated wells (4.3 fold, $n \geq 2$; 5.6 fold, $n=1$; 1.9 fold, $n \geq 2$, respectively) (Figure 6.16). Contrary to expectations, Taxol pre-treatment did not reduce CCT efficacy, instead actually reducing organoid formation efficiency compared to cells pre-treated only with control media, regardless of CCT concentration applied, implying that each

Primary treatment	Predicted effect	Secondary treatment	Predicted effect
Control (NRL)	'Normal' growth: SC + TA + differentiated cells	**Control (NRL)**	'Normal' growth
		CCT	↓SC; ↓ TA and differentiation cell = Increased organoid formation
		Taxol	↓ TA expansion = Reduced organoid formation
CCT	↓SC; ↑TA	**Control (NRL)**	Large number of TA allowed to expand = Increased number of organoids
		CCT	Reduced Wnt level, ↓ TA expansion = Reduced organoid formation
		Taxol	Faster cycling TA killed = Very few organoids*
Taxol	SC unaffected; ↓TA	**Control (NRL)**	Stem cell rich population = normal or increased organoid formaton.
		CCT	Stem cell rich population driven to TA = increased organoid formation†
		Taxol	Prolferation of any cell type reduced = reduced organoid formation

Table 6.2 Predicted outcomes of sequential treatments on T1 mammary tumour organois growth and development.

*, Indicates lowest predicted organoid formation efficiency. †, Indicates highest predicted organoid formation efficiency.

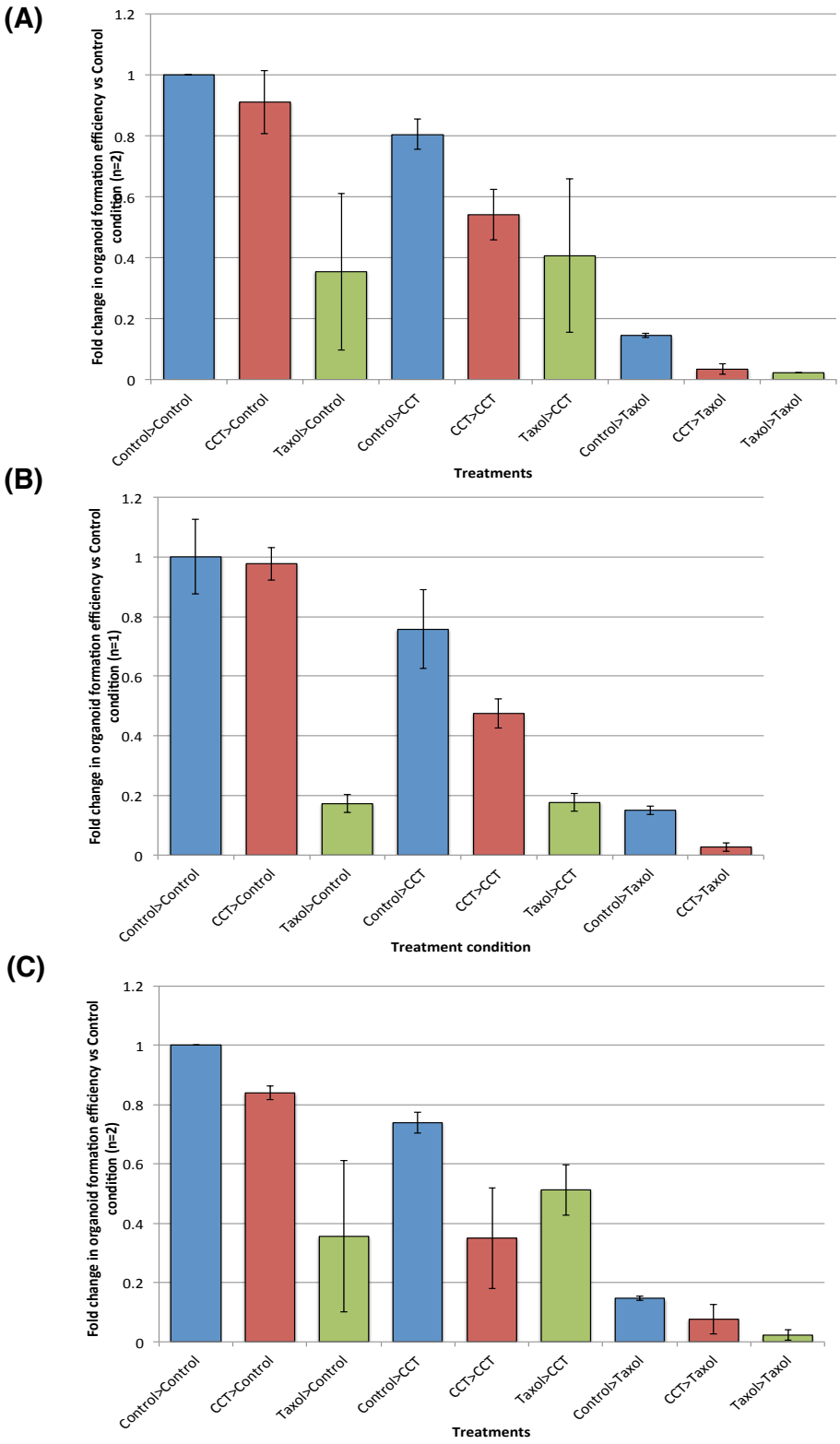

Figure 6.16 Effects of sequential treatments on organoid replating efficiency.

T1 tumour cells were seeded at 1000 per µl in growth factor reduced matrigel and cultured for 72 hours in Nrg1 (100 ng/ml) Noggin (100 ng/ml), R-Spondin1 low (2.7 ng/ml) containing media, before a 72 hour treatment with either control media, CCT (**(A)** 125nM **(B)** 500nM **(C)** 1000nM)150
or Taxol (5 nM). Organoids were then trypsinised to single cell and replated under each one of the three conditions and organoid replating efficiency measured after 7 days. Data shown as mean ±standard deviation (A, C, n=2) (B, n=1).

compound sensitises to the other (2 fold, n≥2; 2 fold, n=1; 1.4 fold, ≥2, respectively). Nevertheless, the order in which the two inhibitors were applied was in fact still seen to be important, with CCT pre-treatment having a much larger effect on Taxol efficacy.

Interestingly, it was clear that the condition reducing tumour organoid outgrowth the most efficiently was in fact that in which Taxol was used constantly. However, it was notable that not even this condition could entirely abrogate tumour organoid development, indicating the presence of a resistant cell population in this assay.

While this is useful data, it is based on multiple assumptions about differential cell types within organoid populations and as such a definite conclusion cannot yet be made on the role of Wnt inhibition in affecting stem cell compartments. A more accurate evaluation of the effects of the Wnt pathway inhibitor on stem and TA populations would require further detailed investigations, as described further in Chapter 7.

6.3 Summary

Work described here has shown a further key utility of the mammary organoid system, such that mammary tumours from various mouse models, in combination with the culture conditions previously discovered, can be cultured successfully to enable the investigation of the Wnt pathway in their development. Although this study has been narrowed down to this particular signalling pathway, alternative inhibitor groups (and tumour models) could be easily tested in the same way given the highly adaptable nature of the assay format.

Through this system, the importance of Wnt signalling in two basal-like tumour types has been demonstrated, and several novel compounds identified for the inhibition of tumour growth in these cases. Furthermore, the assay system has strongly indicated the significance of the tumour microenvironment in determining the degree of response to certain therapeutic interventions, which could prove beneficial in the targeting of drugs for particular stages of cancer in later points of the drug discovery pipeline.

Using the organoid model as a proxy for *in vivo* situations has also enabled the initial interrogation of a presumed relationship between Wnt dependent stem cells and tumour development and the discovery of a potential mechanism by which depleting a tumour of its stem cells may increase sensitivity to cytotoxic compounds. The implications and value of this work will be discussed further in chapter 7.

7 Discussion

The main outcome of this thesis was the development of a novel 3D mammary organoid culture system unlike any other currently available, concomitantly recapitulating *in vivo* mammary gland epithelial composition, architecture and functions. Using this system, several areas were investigated, from the optimisation of culture conditions, to signalling pathways, single cell growth analysis and even tumour biology. From this work, many interesting discussion points were raised, including; the importance of the Wnt signalling pathway in mammary development, the potential for cell plasticity in culture, the requirement for a basal niche for mammary development, the limited lifespan of mammary organoids and the role of the Wnt pathway in tumour growth. Each will be discussed in turn in this chapter.

7.1 Mammary development relies on a 'just-right' level of Wnt signalling.

The most notable observation from this work was the varied developmental responses of mammary epithelial cells to R-Spondin1 levels in organoid culture. High levels of R-Spondin1, mirroring those applied to intestinal organoid cultures by Sato et al (2009), caused a high number of large, dense structures to form (Figure 3.3). However, these conditions also inhibited luminal differentiation, favouring strong hyperkeratinisation and basal p63 expression in mammary organoid culture (Figure 3.2). Interestingly, this phenotype of normal mammary epithelial cells was similar to that of basal-like tumours – in particular those from the MMTV-Wnt1 mouse model, in which Wnt1 is constitutively expressed (Appendix I-1). R-Spondin1, released from luminal ER- populations *in vivo*, is known to promote the maintained surface expression of the Wnt receptors Fzd and Lrp to potentiate Wnt signalling, and as such its levels can be linked to the absolute level of Wnt pathway activity in cultures, as confirmed by the resemblance of high R-Spondin1 treated organoids to those possessing constitutive Wnt activation (Figure 3.10). Although Wnt signalling is considered one of the key pathways regulating mammary ductal and lobuloalveolar growth (Dale 2011), it appeared that a lower level of R-Spondin1/Wnt may be required for normal development to take place in the organoid system.

Conversely, the complete removal of R-Spondin1 from mammary organoid culture enabled only very few small organoids to form (Figure 3.3). Although these

possessed differentiated luminal cell populations (Figure 3.4), they were shown by Jardé et al (2016) to lack a complete basal myoepithelial layer. While Wnt/R-Spondin1 signalling has previously proven important to the success of many other organoid systems (Sato *et al.* 2011), the degree to which Wnt/R-Spondin1 pathway activity was able to shift the balance of proliferation and differentiation in the mammary system was unprecedented. Basal cells clearly depended on Wnt signalling for their expansion and development - perhaps unsurprisingly, since *in vivo*, the basal population is widely shown to possess a Wnt responsive stem cell population (Zeng and Nusse, 2010; Wang, *et al.,* 2015). By contrast, luminal development was inversely regulated by Wnt activity in the presence of levels of R-Spondin1 that have previously been shown to support differentiation of all intestinal epithelial cell lineages. The hypothesis was formed that for concurrent, balanced differentiation of both mammary lineages, a 'just-right' level of R-Spondin1 and as such, Wnt activity might be required. Analogous 'just right' Wnt signalling requirements for tissue development have been widely discussed in historical literature; in the intestine, high levels of Wnt signalling in the crypts promote the proliferation of stem cells, while reduced Wnt signalling further away from the crypt encourages differentiation of the various intestinal epithelial cell types. Similarly, the development of colorectal tumours has been shown to require a precise level of Wnt signalling (Albuquerque *et al.* 2002). Following APC loss in the tissue, downstream target genes are only switched on once the transcriptional regulator β-catenin reaches a minimum threshold, while conversely, the over-accumulation of β-catenin in the nucleus promotes cell death, inhibiting tumour development (Albuquerque *et al.* 2002).

Titration experiments showed that normal mammary biology could indeed be recapitulated in organoid culture using a determined 'low' level of R-Spondin1, in combination with Neuregulin1 (Nrg1; discussed in a later section). Structures, formed from cells characterised as Wnt responsive (based on nuclear β-catenin localisation, (Figure 3.12)), contained distinct luminal and basal compartments, comprising all differentiated cell populations (Figure 3.13). Interestingly, the low levels of R-Spondin1 were able to support the formation of a complete myoepithelial cell layer as shown by a-SMA staining (Figure 3.12), whilst still allowing luminal differentiation. Organoids grown under these conditions showed physiologically relevant function and self-renewal; hormone responses were maintained (Figure 3.22) and a 100 fold expansion in organoid

number observed (Figure 3.18) over the 2.5 months that structures remained karyotypically normal in culture (Figure 3.20). This presented a significant advance on any culture system currently published (Obr *et al.* 2013). It was therefore concluded that carefully orchestrated 'just-right' Wnt signalling is absolutely essential for normal mammary organoid development.

Interestingly, despite Wnt signalling's role in promoting stem and basal cell function, small molecule inhibition of endogenous Wnt signalling in mammary organoid culture abrogated luminal PR+ cell development (Figure 4.5, 4.6), suggesting that some Wnt signalling may be necessary for luminal differentiation. This result could point to a Wnt responsive luminal progenitor, similar to Axin2 positive luminal cells demonstrated to have roles in alveolar development during pregnancy (van Amerongen et al., 2014), or TCF1 rich luminal progenitors expandable under hormone induced Wnt stimulation (Joshi et al., 2015). Alternatively, it may highlight the complexity of sequential interactions between basal and luminal cells. These could act as a network of reciprocal interactions regulating mammary development, in which luminal cells indirectly respond to a Wnt-dependent 'just-right' signal from basal cells to support their expansion (discussed in a later section).

7.1.1 Wnt signalling in the mammary gland; ligands, their regulation and potential sources.

The possibility that a 'just-right' level of Wnt signalling may be generated *in vivo* poses many more questions than can currently be answered. For example, which Wnt ligand(s) are involved in mammary development? Which cells produce them? How is the overall Wnt activity in the system controlled? At least 19 Wnt ligands are known and several are differentially expressed by distinct cell populations within the mammary gland and at distinct phases of mammary gland development (Jardé and Dale, 2011). Furthermore, 8 Fzd receptors and 2 LRP co-receptors (LRP5/6) bind Wnt ligands and a range of other Wnt binding proteins are expressed during development (van Amerongen, 2012). The complexity of the known expression patterns together with their differing ligand-binding capacities preclude any a priori predictions of Wnt pathway activity based exclusively on Wnt ligand expression profiles. However, several inferences may be made based on data obtained in this thesis.

The ligand Wnt3a, when exogenously applied in mammary organoid culture initiated wholly different developmental responses to R-Spondin1 in culture despite working via a common pathway - causing a slight reduction in lobular morphology while R-Spondin1 caused more pronounced, tumour-like development (Figure 4.1). While such results may merely indicate that Wnt3a is not the ligand important for mammary organoid development, the result might instead be linked to the role of *multiple* Wnt ligands and/or receptors. Alternatively, the differing outcomes of Wnt3a and R-Spondin1 treatment might also be a consequence of spatio-temporal differences in Wnt signalling. As short-range signalling molecules, it is often the gradient or location of Wnt in a local environment that instructs development - asymmetric cell division in embryonic development is known to depend upon a morphogenic gradient, while cell polarisation relies on the distribution of Wnt receptors toward a local stimulus (Habib *et al.* 2013) - therefore, a global increase in Wnt concentration by exogenous addition to cultures may not be sensed in the same way as a defined, localised signal. Receptor expression and localisation likely also play a part in this coordination of 'just-right' signalling; the intricate combination of parameters involved further complicate the understanding of Wnt signalling in the gland.

Wnt3a itself is not a naturally occurring mammary Wnt ligand; in fact, the only Wnt ligand that has been definitively shown to exist within this mammary organoid system to date is Wnt4 (Brisken, *et al*., 2000). Expressed *in vivo* by luminal PR+ cell populations in response to progesterone stimulation during pregnancy, Wnt4 usually acts in a paracrine fashion alongside RankL to promote the expansion of mammary stem cell populations, preparing the gland for lactation (Joshi et al., 2010). In line with this known biology, progesterone treatment of mammary populations in organoid culture in this study showed similarly upregulated Wnt4 expression (Figure 3.22), While the organoid culture system is in general, definitively progesterone free, a basal level of Wnt4 likely exists; however, this Wnt may not comprise the main Wnt ligand in the observed R-Spondin1 dependent organoid development. In fact, that luminal cells do not exist in 'high R-Spondin1' treated mammary organoids (Figure 3.2) not only contradicts the existence of a paracrine Wnt4 involvement in this development, but also actually implies any Wnt signal involved would be definitively autocrine (Figure 7.1). Wnt-6 and Wnt-10a are currently the only identified basally produced Wnt ligands, with as yet unknown

functions, and as such may warrant further study in this system (Dale 2011). When considering the developmental potential of a luminal Wnt responsive progenitor (as discussed above), an entirely different Wnt ligand would likely be involved. Wnt-2, and Wnt-7b, for example, are alternate mammary Wnts that could also be involved, but without further study the complete combination of Wnt ligands involved in R-Spondin1 mediated development are still a subject for speculation. For a summary of known Wnt ligand signalling that incorporates data from this report and existing data see Figure 7.1.

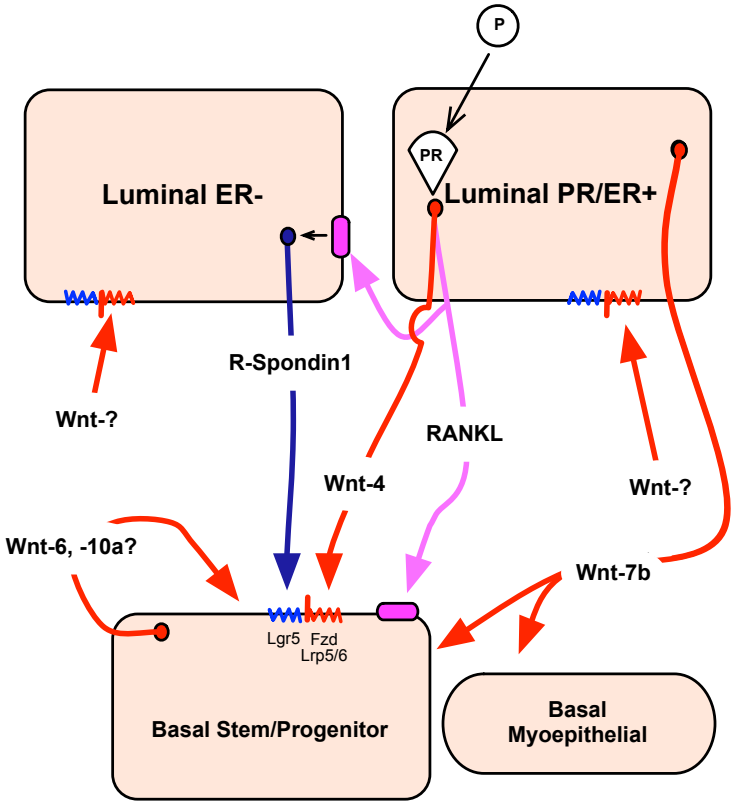

Figure 7.1 Suggested Wnt pathways in the mammary organoid system.
Multiple Wnt ligands are likely involved in the orchestration of mammary development. In the presence of progesterone, luminal PR+ cell populations up-regulate Wnt4 expression, acting on the basal stem cell population. Wnt6 and Wnt10a have been indicated to be released from basal populations, and could, based on evidence described in 7.1.1, act in an autocrine manner. Luminal ER+ cells release Wnt7b, with unknown function, but could act on any one of the cell populations, in theory. A subpopulation of Wnt responsive luminal cells may also exist, with unknown stimulating Wnts.

7.2 Wnt signalling is just one of several signalling pathways required for normal mammary organoid development

7.2.1 Neuregulin1 signalling supports luminal populations

The second key pathway identified for mammary organoid development in this thesis was that of Nrg1. Jardé et al (2016) previously demonstrated that Nrg1 more efficiently promoted organoid formation than the related RTK ligand, EGF – as used in intestinal organoid culture. In this thesis, the Nrg1 signalling pathway was proven through lentiviral knockdown of Nrg1 receptors (ErbB3 or ErbB4) to be crucial to organoid formation and growth (Figure 4.12). Luminal cell populations in particular showed a strong proliferative response to Nrg1 in the system (Figure 5.1). *In vivo*, Nrg1 stimulates ErbB3/4 rich luminal progenitor expansion and lobular-alveolar development during pregnancy (Forster *et al.,* 2014). Moreover, Nrg1 is shown to be released in a paracrine manner from p63 positive basal cell populations, with the knockout of p63 abrogating luminal progenitor proliferation and differentiation. Paracrine signalling from basal to luminal cells, in combination with the known requirement for Wnt in basal development, may explain how and why the balance of luminal and basal differentiation shifts so dramatically with Wnt activity; under an insufficient Wnt stimulus, basal cells may not produce paracrine signals that are able to support luminal cell development (figure 7.2).'

7.2.2 EGF may be a factor in the basal cell niche

Given such clear effects of Nrg1 on organoid outgrowth, along with evidence in this thesis and indeed mammary literature for a basal Wnt responsive, stem cell population, it was highly surprising to find that basal cells isolated by FACS were unable to form organoids under NRL conditions (Figure 4.1), while luminal cells could do so readily. Moreover, the data also showed an unexpected plasticity of luminal populations; this is considered as a separate point in a later section.

Stem cells are known to require a particular supporting niche, commonly involving Wnt ligand. Since the addition of R-Spondin1 or Wnt to NRL media was not sufficient to promote organoid formation the hypothesis was formed that alternative signalling pathways may also be involved. Indeed, the Nrg1-related RTK ligand EGF was found to markedly increase organoid formation in culture from basal cell populations following FACS (Figure 5.10), with the combination of EGF, Wnt3a and R-Spondin1 promoting the

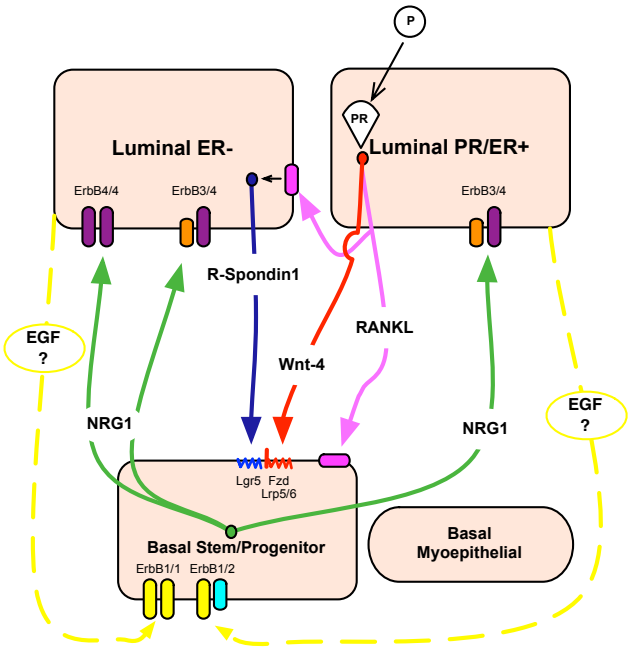

Figure 7.2 Proposed model of paracrine signalling networks in mammary organoid development

Progesterone signalling to PR+ luminal cells induces upregulated expression of Wnt4 and RANKL. RANKL induces R-Spondin1 release from luminal ER- cells, which co-operates with Wnt4 and RANKL to induce expansion of the basal stem/progenitor population. Activation of the p63+ basal subset induces Nrg1 release, which feeds back to luminal populations and induces their lobulo-alveolar like differentiation. RTK stimulation of basal stem cells is required in conjunction with activation of the Wnt/R-Spondin1 axis, the ligand for which (EGF) may be produced by luminal ER populations.

highest level of organoid formation. A similar role for EGF in the basal niche has been shown in many previous studies; attempts to culture basal cells in mammosphere culture or in Matrigel have included EGF since it was suggested to encourage proliferation (Dontu *et al.* 2003; Zeng and Nusse 2010), while Wnt3a in combination with EGF, has been shown to significantly promote stem cell self-renewal *in vitro* (Zeng and Nusse 2010).

Given such a demonstrable requirement for EGF for basal cell development in isolation, it was intriguing that under apparently EGF deficient NRL conditions, basal cells were clearly identified to be actively dividing in mixed cell cultures (Figure 3.15). Therefore, it was proposed that other cell types fulfil the basal cell niche. Indeed, the enhanced organoid plating efficiency of cell recombinations (Figure 5.6) support the existence of such a paracrine signal. There is currently little literature to suggest the release of EGF from anything other than stromal cell types, of which there are none in the mammary organoid system. As EGF was the only alternative RTK ligand trialled in single population cultures however, it has not been disproved that other factors might in

fact be similarly (or alternatively) involved in basal cell stimulation. FGF ligands in mixed culture, forexample, showed increased potency when applied to definitively single (and thus spatially separated) epithelial cell populations compared to epithelial fragments (Figures 4.7 and 4.8) potentially supporting a naturally occurring, close-range paracrine signalling FGF network. Interestingly, FGFs and EGF have similar stimulating effects on basal stem cells in mammosphere culture (Dontu *et al.* 2003), perhaps implicating a level of factor redundancy and potential pathway crosstalk in the mammary gland. Further work would be required to address this possibility; one of the advantages of the mammary organoid system is that larger scale investigation of growth factor effects could be carried out with ease.

7.3 Luminal cell populations exhibit unusual plasticity in certain contexts

As briefly described above, under NRL culture conditions, luminal ER- or ER+ mammary epithelial cells were unexpectedly observed to successfully generate mammary organoids consisting of both luminal (ER- and ER+) and basal cell populations, arranged in a tissue specific architecture (Figure 5.1). Although luminal progenitors are known to rely on Nrg1 for their expansion in pregnancy (Forster *et al.* 2014), given that various mammary hierarchy models dictate that stem or progenitor populations maintain each adult lineage in a solely unidirectional manner (Figure 1.5), organoids formed by progenitor expansions would not be expected to possess basal populations. Results therefore imply a degree of plasticity of luminal populations following FACS.

Such plasticity of luminal mammary epithelial cells is not entirely unparalleled in the literature. Historical transplantation studies have shown luminal to basal transdifferentiation in altered physiological settings, such that an otherwise lineage restricted single luminal cell can reconstitute an entire, functional mammary epithelial tree upon transplantation (Sleeman *et al.* 2007; Rodilla *et al.* 2015) (van Amerongen *et al.* 2012), while both ER- and ER+ luminal progenitor populations have multilineage differentiation potential in short term 3D culture (Shehata *et al.* 2012). Since in mixed population organoid cultures, luminal cells have been definitively shown as distinct from dividing cell populations (Figure 3.14), it would appear that it is the artificial isolation by FACS or the subsequent single cell culture conditions that induce the unusual differentiation potentials of luminal cells. Interestingly, luminal ER+ cell populations,

described as non-dividing populations (Clarke, *et al.,* 1997) showed a significantly enhanced organoid formation potential under highly Wnt stimulated conditions in this work (Figure 5.8). While a small population of dividing ER+ cells (around 0.05% in absence of estrogen) are seen to exist in the mammary gland (Mastroianni et al. 2009), the division of which can be supressed by TGF- β mediated signalling (i.e. indicating a level of Wnt responsiveness)(Ewan et al., 2005), this cannot account for the level of organoid outgrowth observed, instead implicating the altered microenvironment as another crucial determinant in the acquisition of stem-like properties.

Taken together, evidence here supports the idea that mammary lineage may not have a steadfast, predetermined pathway of development (Chaffer et al. 2011); that is, while under physiological conditions a traditional hierarchy may be observed, a potential for bidirectionality of such a hierarchy can be uncovered in unusual contexts (eg. cell isolation, altered microenvironment such as the tumour context; see later). An alternative 'high plasticity' cellular hierarchy map to that originally described in Figure 1.5 is therefore proposed in Figure 7.3.

Such plasticity may not be unique to luminal populations; perhaps much like luminal cells in isolation develop highly plastic differentiation abilities, basal cells following FACS assume a more primitive state, requiring supportive signals that are redundant in physiological settings. As such, the above-described requirement for EGF (or FGF, etc) may merely be an artefact of the assay, in an alternative explanation to the paracrine signalling hypothesis.

7.3.1.1 Cell plasticity and cancer stem cells

The ability to observe plasticity of non-stem cells under 'stress' conditions indicates the organoid system as an important tool in breast cancer research, providing insight into mechanisms by which cancers can develop. The 'cancer stem cell' (CSC) hypothesis suggests that a tumour is derived from a population with stem cell-like properties; not necessarily the 'normal' stem cell of the tissue in question, but any cell that has acquired characteristics such as multilineage potential, long term regeneration and expansion – much like the luminal cells described above. *In vivo*, despite numerous associations of basal breast cancers with faults in and expansion of a Wnt- responsive basal stem cell population, strong evidence now suggests that this subset of cancer may

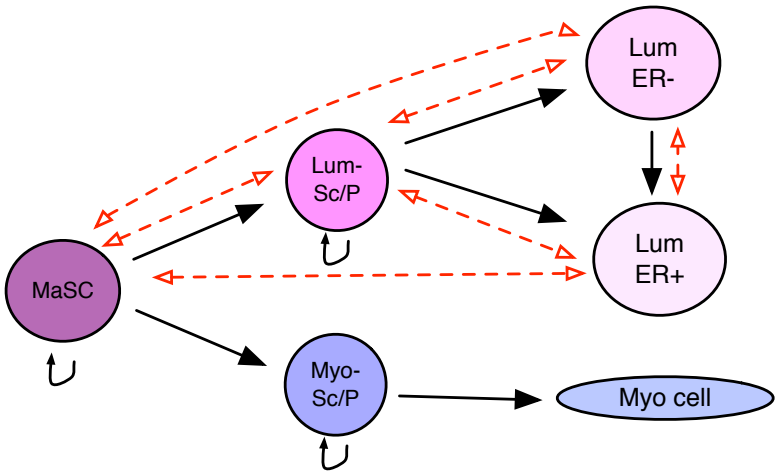

Figure 7.3 Cellular hierarchy under 'high plasticity' conditions.

A consensus hierarchy in which an initial basal MaSC population forms either luminally (Lum) or myopithelially resitricted stem cells (Sc), or progenitors (P), which each serve to repopulate their individual lineage, is shown, based on findings from (Van Keymeulen *et al.* 2011) and (van Amerongen *et al.* 2012). In this hierarchy, luminal ER+ cells are terminally differentiated, either through direct luminal Sc/P differentiation or transition from an intermediary luminal ER- cell. Red dotted arrows indicate the newly proposed "high plasticity" transdifferentiation capabilities of the luminal population, including the terminally differentiated luminal ER+ population.

actually derive from a luminal population (Lim *et al.* 2009). Molyneux *et al.* (2010) reported that BRCA1 deficient luminal progenitors initiate tumours more closely resembling basal-like tumours than BRCA1 deficient basal cells do, while tumour invasion also has been shown to rely on a similar acquisition of basal identity by luminal populations (Cheung *et al.* 2013). Moreover, oncogenic insult *in vitro* also promotes luminal transdifferentiation; retrovirally mediated oncogenic transformation of luminal populations (Hein *et al.* 2016), the transient expression of MaSC transcription factors Sox9 and Slug (Guo *et al.* 2012), and overexpression of the usually basal ΔNp63 isoform in luminal cells (Chakrabarti *et al.* 2014) each promote basal properties and confer multilineage differentiation capacity. The genetic manipulation of cells in the organoid system could be of particular benefit in studies of tumour development; allowing the stepwise progression of tumour initiation in individual cell populations to be monitored.

7.4 A finite lifespan of mammary organoids may reflect inherent biology.

Under NRL conditions, a normal organoid phenotype and karyotype could be maintained for around 2.5 months in culture. Although a significantly longer period than currently published culture conditions allow, such a limited life span notably contrasted

with long term organoid growth from other tissues; expansion in the liver and pancreatic organoid systems can exceed 8 and 9 months, respectively, while the small intestine and prostate can grow in culture for more than 1.5 years (Huch, *et al.* 2013; (Huch *et al.* 2013; Sato *et al.* 2009; Karthaus *et al.* 2014).

The most likely explanation for this phenomenon is that the organoid culture system accurately reflects the inherent biology of the mammary gland. Historical *in vivo* evidence strongly supports a natural senescence of mammary epithelial cells after a relatively small number (5 to 8) of sequential transplants or divisions, (Daniel and Young 1971; Smith and Boulanger 2003), while *in vitro* assays have identified similar traits of MaSCs in culture (Dey *et al.* 2009). Since the tissue is required to undergo relatively little tissue remodelling compared to, for example, the small intestine, which replenishes its entire epithelia every 3 to 5 days as part of normal homeostasis, it is perhaps unsurprising that the respective long term renewal capacities of the respective tissues differ so dramatically.

An alternate explanation could of course be inferred by the combination of evidence from luminal and basal population cultures, as discussed above. If, contrary to assumptions, a required niche forming EGF signal were *not* provided in a paracrine manner, short-lived luminal progenitors might be forced to de-differentiate to form the main organoid forming population. Since progenitors have a finite expansion capacity, a corresponding limited regenerative ability of organoid cultures might be expected. However, confirmed activity in mixed culture of basal cells by EdU staining (Figure 3.15) significantly reduces the likelihood of this explanation. This question could be definitively resolved by the extended culture and characterisation of mammary organoids under conditions comprising both Nrg1 and EGF in combination. If culture limitations truly reflect an inherent biological property of the gland then the addition of EGF to cultures would be expected to have no benefit to the duration of phenotypically normal culture.

The observation of a ‘crisis’ at 2.5 months, in which mammary cells with clear chromosomal abnormalities and loss of normal phenotypic marker expression are generated after a brief period of slowed growth, is also not an unprecedented biological phenomenon. The Hayflick limit, discovered in 1961 (Hayflick and Moorhead 1961), states that two-dimensional cultures of fibroblasts will stop dividing after 50 cumulative population doublings, in a process now also known as replicative senescence. This limit is

controlled by the length of telomeric DNA at the end of each chromosome; at a critically minimal length, mitosis is prevented to inhibit potential damage to the coding region of DNA that could lead to pro-tumourigenic mutations. However, HMECs in particular have shown the unique ability to spontaneously emerge from such senescence and enter a telomere-based crisis, generating chromosomal abnormalities resembling those seen in early breast cancers (Romanov *et al.* 2001), and therefore its is possible that the system presented here accurately reflects this previously observed biology, modelling early steps in carcinogenesis.

7.5 Features of a 'just-right' Wnt signalling requirement are apparent in basal-like tumour organoids.

Culture conditions developed and characterised in earlier sections of this thesis also allowed the culture of tumour derived organoids in the system, thus widening the scope of understanding of 'just-right' Wnt signalling in mammary development. As described above, high R-Spondin1, and as such, highly Wnt activated conditions could induce a tumour-like development of mammary organoids in culture, mimicking the MMTV-Wnt1 phenotype (Figure 1.1, Appendix I-1). Basal-like breast cancers in particular often exhibit similar strong 'Wnt-on' profiles, and so the investigation of the Wnt pathway in this cancer subtype was of interest; namely, the effect of Wnt inhibition on their growth, and the effect to which inhibition affected CSC compartments, discussed in turn here.

MMTV-Wnt1 organoids showed differential growth characteristics under NRL and ERH conditions (Figure 5.1); a somewhat unexpected result given the inherently high level of Wnt signalling already present in the tumour. In contrast, the T1 model showed no difference in routine organoid growth under either condition. Given that the T1 model has been characterised to overexpress the Fzd7 receptor (Zhang *et al.* 2015), the main target of R-Spondin1 upregulation, results further indicate the importance of not just the level of Wnt ligand, but also the level of receptor expression, in controlling 'just-right' Wnt activity. Moreover, tumours are not simply defined by a 'Wnt on' profile – a sliding scale of tumourigenic phenotypes may be observed depending on the degree to which 'just-right' Wnt activity has been altered.

Multiple inhibitors of the Wnt pathway, including novel compounds from drug discovery programs, showed efficacy in reducing tumour organoid growth (Table 6.1).

Importantly, responses appeared to accurately reflect the inherent biology of the tumour type; T1 tumour organoids known to overexpress Fzd7 responded extremely well to Anti-Frizzled antibody administration (Appendix II-3), while MMTV-Wnt1 organoids showed less sensitivity to the treatment (Appendix II-4), indicating the organoid system as a reliable model of biological response.

Crucially, response to inhibition relied upon the initial level of Wnt activity present; higher IC_{50}s were often observed under EGF, R-Spondin1 high conditions compared to NRL conditions. This effect was particularly obvious in the MMTV-Wnt1 model, where the IC_{50} of porcupine inhibitor IWP-2, for example, increased 23.5 fold over that observed under 'normal' conditions (Table 6.1). Such a phenomenon supports that analogous to the sliding scale of tumour development described above, Wnt dependent tumour growth cannot be simply switched off in response to inhibitors in a binary manner; instead, reductions in organoid volume are representative of the starting level of Wnt activity, and the degree to which 'just-right' Wnt signalling levels can be restored.

7.5.1 'Just-right' Wnt signalling likely controls CSC populations

In the above studies of Wnt inhibition, while a reduction in tumour volume was considered a positive outcome, the true degree of effects on prospective CSC populations was not clear from direct growth assays alone. In an ideal situation, Wnt inhibition would prevent CSC activity and thus reduce the likelihood of tumour recurrence.

The inhibitor CCT251545, while showing efficient inhibition of organoid growth alone and in synergy with Taxol in conventional inhibitor assays, unexpectedly caused an increased replating efficiency of mammary epithelial cells (Figure 6.13), perversely indicating increased CSC or TA number, through an as yet unconfirmed mechanism. It is known that SCs generally renew by asymmetric division, forming one TA cell and one SC to maintain SCs at a steady state. Such a mechanism relies on a 'just-right' Wnt stimulus, whereby too low an activity prevents stem cell self-renewal, while too high an activity inhibits TA formation and differentiation, favouring SC formation. It is therefore possible that CCT reduces Wnt activity to alter SC dynamics, promoting a SC to TA population shift that results in increased outgrowth of secondary mammary organoids (ie. organoid formation may be a property of both stem cells and TA cells). The specific biological

function of CCT may also control such dynamics. CCT is a CDK8/19 inhibitor, designed to abrogate the function of Wnt-related Mediator transcriptional machinery (Dale *et al.* 2015); in C. elegans, components of the Mediator complex homologous to the MED12 and MED13 subunits in mammals are key regulators of asymmetric cell division, their mutation favouring symmetric division (Yoda *et al.* 2005). While the role of CDK8 in this regulation has not been confirmed, it is possible that as part of the same transcriptional complex, its abrogation could cause similarly altered SC dynamics. Whether such a mechanism is entirely Wnt dependent or unique to CDK8 inhibition would require similar assays using a different inhibitor.

CCT treatment prior to replating, presumably by virtue of an increase in TA proportions, paradoxically aided the secondary treatment of T1 tumour organoids with SoC, Taxol (Figure 6.16), potentially indicating a benefit of such sequential therapy. Indeed, similar approaches are currently used in treating patients with metastatic breast cancers; sequential doxorubicin and taxol administration increases disease free survival compared to concurrent therapy (Henderson *et al.* 2003), while tamoxifen shows improved results when given after SoC therapy, compared to simultaneous treatment (Albain *et al.* 2009).

Given that sequential treatment did not entirely ablate tumour organoid outgrowth (Figure 6.16), further detailed investigation of its potential is required, with indications that different assay formats are needed. On one hand, results may suggest a dual-treatment resistant population, or even only a partial inhibition of Wnt activity by CCT, such that a subpopulation of SCs remains able to undergo asymmetric division, producing CSCs able to evade SoC therapy, thus contraindicating the use of sequential therapy in the clinic. Alternatively, since it has already been demonstrated in 'normal' culture that cell plasticity may occur under altered conditions, results may simply be an artefact of a similar induced plasticity upon replating. That is, treated cells may not possess SC like qualities prior to replating, but upon replating and removal or change of inhibition, acquire CSC potential to enhance replating efficiency. Such plasticity has been shown to occur in basal breast cancers; non CSCs undergo a epithelial-to-mesenchymal-like transition to form cells with a CSC profile under the regulation of the EMT transcription factor ZEB1 (Chaffer *et al.* 2013). If this latter explanation is indeed true, the current replating assay format may actually provide more useful data in the context of

metastasis, where primary tumour cells adapt to form a tumour in a new environment. An alternative assay system illustrating the effects of sequential therapy in a non-replating format would be required to pinpoint which of the above mechanisms, if any, causes such persistent tumour organoid outgrowth. For this, a tumour model in which CSC populations could be easily distinguished from more differentiated cell types would be of great benefit.

7.6 Further work in the mouse mammary organoid model

7.6.1 Defining basal cell involvement and 'long-term' capabilities

Despite showing expansion in culture, maintained functionality, phenotype and karyotype over extended periods, it is evident that for definitive characterisation as 'recapitulative' of the *in vivo* gland, the question of whether long-term mammary organoid culture can be performed needs resolving. As described above, the extended culture of organoids in Nrg1, EGF and R-Spondin1 low containing media would achieve this.

The role of EGF in supporting basal cells in mixed culture is as yet unconfirmed. qRT-PCR analysis of mammary expression of EGF and its receptor in sorted cell populations could be performed to better understand this potential network. Moreover, the extended investigation of other growth factors (eg. FGFs) that may be involved in a basal cell niche could be performed. For example, *in vivo*, an as yet unstudied (in this system) paracrine network is known to exist in the mammary gland; the amphiregulin signalling pathway. Estrogen stimulation of luminal ER+ populations induces AREG release, the ligand then acting upon stromal cells to initiate release of factors promoting basal cell activity – reportedly including FGFs, amongst other factors (Ciarloni *et al.* 2007). Currently, mammary organoid cultures lack stromal cells, such that this exact pathway cannot occur. Thus, inclusion of stromal components into the system in future experiments could enable physiological function of the ligand may also be a key consideration. Recent work in the intestinal organoid field supports the role of intestinal stromal cells in providing niche forming factors such as Wnt3 and R-Spondin when co-cultured in Matrigel (Kabiri *et al.* 2014). Indeed, this method may also be beneficial in the context of tumour organoid growth, for further assessment of the role of the tumour microenvironment in response to therapeutic regimes.

7.6.2 Optimisation of the CSC assay format.

Despite best efforts to generate a CSC assay, the complicated hierarchies of mammary epithelial and tumour cells mean that true dynamics within the system cannot really be confidently determined in the above assays without a unique marker of SC or TA identity. A T1 tumour lentivirally infected with a dual fluorescent (7xTcf-eGFP/SV40-mCherry) reporter of Wnt activity has been obtained from the Rosen laboratory, with the intention to repeat the above assays and quantitatively analyse Wnt responsive and more differentiated population proportions by FACS, before and after Wnt inhibition. Future studies into inhibitor effect on stem populations would greatly benefit from this work, and would be easily performed with the aid of the 3D system.

7.6.3 Modelling the initiation and progression of cancer

Genetic predisposition to cancer is a major factor that could be assessed with organoid culture. The culture conditions detailed in this thesis support the growth of mammary tissue from several genetic backgrounds, and could in turn aid the culture of tissue derived from countless existing mouse models with known genetic predisposition to breast cancer, i.e. BRCA1-/+, BRCA1-/-, MMTV-Her2, MMTV-Met, MMTV-Neu. In depth analysis of the propensity of individual cell populations to form tumours, their response to signalling pathways or even exhibit growth factor independence in culture, would be possible in the context of this system. NRL conditions should allow a range of differentiation to be observed from different backgrounds.

Separately, organoids in this culture system are demonstrably amenable to genetic manipulation by lentiviral transfection, allowing the targeted gene knockdown or overexpression and the assessment of consequence to mammary development. The study of breast tumour initiation and progression could benefit from such targeted alterations in organoid culture. In other organoid systems, complex gene editing has also been performed using increasingly popular ‘clustered regularly interspersed palindromic repeat’-associated protein 9 (CRISPR-Cas9) based techniques. In brief, this method uses a guide RNA template and the Cas9 endonuclease to selectively introduce breaks in the genome for gene removal or addition. CRISPR-Cas9 has been successfully implemented in cultures of normal human colon organoids, enabling the stepwise progression of a tumour and the associated growth factor dependencies to be monitored in an accessible

system (Matano *et al.* 2015). Targeting gene mutation or even gene correction in individual cell populations using this approach in the mammary organoid system may aid the resolution of CSC identity in various breast tumour subtypes.

Non-genetic factors, including age and parity, shown to predispose to cancer, could also be studied in the organoid system. For the purposes of this thesis, tissue has been obtained from young virgin mice to study the effect of signalling pathways on, and the cell of origin in, mammary organoid culture. However, since human breast cancer risk is raised in women of post-menopausal age, and can be linked to lifetime estrogen and progesterone exposure (Brisken and O'Malley 2010) - early menarche increasing risk, while increased parity reduces risk (Dall *et al.* 2016) - the study of cells obtained from older mice, and those having produced offspring, could greatly benefit the study of tumour predisposition. How does cell plasticity change with age? Can pregnancy-induced maturation of progenitors reduce plasticity, conferring protection against tumour development? Mammary organoid culture shows potential to answer questions such as these, and many more.

7.7 Future directions for mammary organoid technology

7.7.1.1 Human mammary organoid culture

Despite the clear benefits of mouse derived organoid systems over current 2D or *in vivo* experimental models, some disparities still exist between mouse and human tissues. This can contribute to the identification of toxicities that may not be relevant in a patient, or false negative responses to targeted therapies - both of which can cause compound failure - or conversely, the failed detection of toxicity due to a unique effect in human tissues, only detected in Phase I clinical trials. A human organoid system therefore is the ideal representative *in vitro* model.

Many organoid culture systems originally optimised using mouse-derived tissues are now adapted for the culture of human tissue. Notably, the original intestinal crypt culture system allows the growth of not only human small intestine, but also oesophageal and colonic epithelium (Sato *et al.* 2011). A rapidly growing list of human organoid systems now includes the liver (Huch *et al.* 2015), prostate (Anon 2014), pancreas (Boj *et al.* 2015; Huang *et al.* 2015) and stomach (Bartfeld *et al.* 2014), to name a few. In the liver organoid system, species-specific hepatotoxicity has been shown

between rat and human organoids, confirming the need for species relevant models (Kostadinova *et al.* 2013). Importantly, many of these systems now allow the growth of matched normal and disease-affected tissues, allowing non-specific toxicities to be studied.

Although breast carcinoma cultures have reportedly been established by Hubrecht Organoid Technology (the HUB) under a non-disclosed protocol, a system enabling extended normal human breast organoid culture has not yet been described in the literature. Recently, attempts to culture patient derived wild type material have described a simple growth of primary tissue, but show no expansion capabilities (Linnemann *et al.* 2015; Sokol *et al.* 2016) As such, the adaptation of the 3D system described in this thesis for the culture of human breast tissue would be of considerable value to the mammary field.

7.7.1.2 Organoids as commercially available drug screening tools

Although the inhibitor studies performed in this thesis were on a relatively small scale, in the drug discovery pipeline the demand exists for such assays on a much larger scale. Significant correlations of drug sensitivity and tumour phenotype require high throughput screening of compounds across a large range of tumours, and are not reliably made in 2D, while *in vivo* work is costly and time-consuming.

A recent study demonstrated that a 'living bio-bank' of around 20 paired colorectal cultures could accurately represent the spread of mutations found in colorectal cancers, and was amenable to high throughput drug screening for the identification of mutation-linked sensitivities (van de Wetering *et al.* 2015). Similarly, unwanted drug-related toxicity to wild-type tissue, and drug delivery mechanisms can be modelled in such *in vitro* systems, refining the likelihood of compound success in later animal and clinical based stages of the process (Astashkina and Grainger 2014; Astashkina *et al.* 2014). Indeed the HUB, as mentioned briefly above, have begun to build such bio-banks from a range of tissues. Using the knowledge of mammary organoid development gained in this thesis, similar advances could reasonably be made in the mammary system, with huge benefit to the drug discovery process.

Taken together, work in this thesis has demonstrated the utility and advantages of the mammary organoid system as a physiologically relevant tool for investigating various aspects of mammary biology. Conclusions have not only been drawn about normal mammary development requirements as a whole, but also about individual mammary epithelial cell functions, cellular interactions and dependencies, and about mechanisms that may control tumour initiation and development. In the case of novel compounds, the organoid culture system has proven useful in the rapid identification of efficacious inhibitors and their suitable treatment ranges, and work has also begun to illustrate the benefits of such a system in understanding CSCs.

Organoid culture is now a rapidly expanding field, with no doubt countless benefits left to be discovered. Work detailed in this thesis has by no means exhausted the utilities offered by a mammary organoid system, instead offering up many points of further enquiry that could be easily addressed using such cultures.

8 References

Al-Hajj, M., Wicha, M.S., Benito-Hernandez, A., Morrison, S.J. and Clarke, M.F. (2003). Prospective identification of tumorigenic breast cancer cells. *Proceedings of the National Academy of Sciences* **100**:3988.

Albain, K.S., Barlow, W.E., Ravdin, P.M., Farrar, W.B., Burton, G.V., Ketchel, S.J., Cobau, C.D., *et al.* (2009). Adjuvant chemotherapy and timing of tamoxifen in postmenopausal patients with endocrine-responsive, node-positive breast cancer: a phase 3, open-label, randomised controlled trial. *Lancet (London, England)* **374**:2055–2063.

Albuquerque, C., Breukel, C., van der Luijt, R., Fidalgo, P., Lage, P., Slors, F.J.M., Leitão, C.N., *et al.* (2002). The 'just-right' signaling model: APC somatic mutations are selected based on a specific level of activation of the beta-catenin signaling cascade. *Human molecular genetics* **11**:1549–1560.

Alexander CM, Goel S, Fakhraldeen SA, Kim S. Wnt signaling in mammary glands: plastic cell fates and combinatorial signaling. Cold Spring Harb Perspect Biol. 2012 Oct 1;4(10)PubMed PMID: 22661590.

Alvi AJ, Clayton H, Joshi C, Enver T, Ashworth A, Vivanco Md, Dale TC, Smalley MJ. Functional and molecular characterisation of mammary side population cells. Breast Cancer Res. 2003;5(1):R1-8. PubMed PMID: 12559051; PubMed Central PMCID: PMC154129.

Ashworth, A. and Smalley, M.J. (2006). CD24 staining of mouse mammary gland cells defines luminal epithelial, myoepithelial/basal and non-epithelial cells. *Breast Cancer Research* **8**:R7

Astashkina, A. and Grainger, D.W. (2014). Critical analysis of 3-D organoid in vitro cell culture models for high-throughput drug candidate toxicity assessments. Advanced Drug Delivery Reviews 69-70:1–18.

Astashkina, A.I., Jones, C.F., Thiagarajan, G., Kurtzeborn, K., Ghandehari, H., Brooks, B.D. and Grainger, D.W. (2014). Nanoparticle toxicity assessment using an in vitro 3-D kidney organoid culture model. Biomaterials 35:6323–6331.

Badve, S., Dabbs, D.J., Schnitt, S.J., Baehner, F.L., Decker, T., Eusebi, V., Fox, S.B., *et al.* (2011). Basal-like and triple-negative breast cancers: a critical review with an emphasis on the implications for pathologists and oncologists. *Modern pathology : an official journal of the United States and Canadian Academy of Pathology, Inc* **24**:157–167.

Bao, R., Christova, T., Song, S., Angers, S., Yan, X. and Attisano, L. (2012). Inhibition of tankyrases induces Axin stabilization and blocks Wnt signalling in breast cancer cells. PLoS ONE 7:e48670.

Bartfeld, S., Bayram, T., van de Wetering, M., Huch, M., Begthel, H., Kujala, P., Vries, R., et al. (2014). In Vitro Expansion of Human Gastric Epithelial Stem Cells and Their Responses to Bacterial Infection. Gastroenterology.

Bhatia, S.N. and Ingber, D.E. (2014). Microfluidic organs-on-chips. Nature biotechnology 32:760–772.

Bocchinfuso, W.P. and Korach, K.S. (1997). Mammary gland development and tumorigenesis in estrogen receptor knockout mice. Journal of Mammary Gland Biology and Neoplasia 2:323–334.

Boj, S.F., Hwang, C.-I., Baker, L.A., Chio, I.I.C., Engle, D.D., Corbo, V., Jager, M., et al. (2015). Organoid Models of Human and Mouse Ductal Pancreatic Cancer. Cell 160:324–338.

Breast Cancer Now, 2015. *Breast Cancer Statistics* [Online] London, Breast Cancer Now. Available at http://breastcancernow.org/about-breast-cancer/what-is-breast-cancer/breast-cancer-statistics. [Accessed: 10 May 2016].

Brewer GJ, Torricelli JR, Evege EK, Price PJ. Optimized survival of hippocampal neurons in B27-supplemented Neurobasal, a new serum-free medium combination. J Neurosci Res. 1993 Aug 1;35(5):567-76. PubMed PMID: 8377226.

Brisken, C. and O'Malley, B. (2010). Hormone action in the mammary gland. Cold Spring Harbor Perspectives in Biology 2:a003178–a003178.

Brisken, C., Heineman, A., Chavarria, T., Elenbaas, B., Tan, J., Dey, S.K., McMahon, J.A., et al. (2000). Essential function of Wnt-4 in mammary gland development downstream of progesterone signaling. Genes & Development 14:650–654.

Brisken, C., Kaur, S., Chavarria, T.E., Binart, N., Sutherland, R.L., Weinberg, R.A., Kelly, P.A., et al. (1999). Prolactin controls mammary gland development via direct and indirect mechanisms. Developmental Biology 210:96–106.

Brisken, C., Park, S., Vass, T., Lydon, J.P., O'Malley, B.W. and Weinberg, R.A. (1998). A paracrine role for the epithelial progesterone receptor in mammary gland development. Proceedings of the National Academy of Sciences 95:5076–5081.

Cai, C., Yu, Q.C., Jiang, W., Liu, W., Song, W., Yu, H., Zhang, L., et al. (2014). R-spondin1 is a novel hormone mediator for mammary stem cell self-renewal. Genes & Development 28:2218.

Campbell, J.J. and Watson, C.J. (2009). Three-dimensional culture models of mammary gland. Organogenesis 5:43–49.

Chadi, S., Buscara, L., Pechoux, C., Costa, J., Laubier, J., Chaboissier, M.-C., Pailhoux, E., et al. (2009). R-spondin1 is required for normal epithelial morphogenesis during mammary gland development. Biochemical and Biophysical Research Communications 390:1040–1043.

Chaffer, C.L., Brueckmann, I., Scheel, C., Kaestli, A.J., Wiggins, P.A., Rodrigues, L.O., Brooks, M., et al. (2011). Normal and neoplastic nonstem cells can spontaneously convert to a stem-like state. Proceedings of the National Academy of Sciences of the United States of America 108:7950–7955.

Chaffer, C.L., Marjanovic, N.D., Lee, T., Bell, G., Kleer, C.G., Reinhardt, F., D'Alessio, A.C., *et al.* (2013). Poised chromatin at the ZEB1 promoter enables breast cancer cell plasticity and enhances tumorigenicity. *Cell* **154**:61–74.

Chakrabarti, R., Wei, Y., Hwang, J., Hang, X., Andres Blanco, M., Choudhury, A., Tiede, B., et al. (2014). ΔNp63 promotes stem cell activity in mammary gland development and basal-like breast cancer by enhancing Fzd7 expression and Wnt signalling. Nature Cell Biology 16:1004–15–1–13.

Chen Y, Stevens B, Chang J, Milbrandt J, Barres BA, Hell JW. NS21: re-defined and modified supplement B27 for neuronal cultures. J Neurosci Methods. 2008 Jun 30;171(2):239-47. PubMed PMID: 18471889; PubMed Central PMCID: PMC2678682.

Chen, B., Dodge, M.E., Tang, W., Lu, J., Ma, Z., Fan, C.-W., Wei, S., et al. (2009). Small molecule-mediated disruption of Wnt-dependent signaling in tissue regeneration and cancer. Nature Chemical Biology 5:100–107.

Chen, M., Wang, J., Lu, J., Bond, M.C., Ren, X.-R., Lyerly, H.K., Barak, L.S., et al. (2009). The anti-helminthic niclosamide inhibits Wnt/Frizzled1 signaling. Biochemistry 48:10267–10274.

Cheung, K.J., Gabrielson, E., Werb, Z. and Ewald, A.J. (2013). Collective invasion in breast cancer requires a conserved basal epithelial program. Cell 155:1639–1651.

Chou, T.C. and Talalay, P. (1984). Quantitative analysis of dose-effect relationships: the combined effects of multiple drugs or enzyme inhibitors. Advances in enzyme regulation 22:27–55.

Ciarloni, L., Mallepell, S. and Brisken, C. (2007). Amphiregulin is an essential mediator of estrogen receptor alpha function in mammary gland development. Proceedings of the National Academy of Sciences 104:5455–5460.

Clarke RB, Howell A, Potten CS, Anderson E. Dissociation between steroid receptor expression and cell proliferation in the human breast. Cancer Res. 1997 Nov 15;57(22):4987-91. PubMed PMID: 9371488.

Clinicaltrials.gov. (2016). *A Study of LGK974 in Patients With Malignancies Dependent on Wnt Ligands - Full Text View - ClinicalTrials.gov*. [online] Available at: https://clinicaltrials.gov/ct2/show/NCT01351103 [Accessed 2 Dec. 2016].

Coleman, S., Silberstein, G.B. and Daniel, C.W. (1988). Ductal morphogenesis in the mouse mammary gland: evidence supporting a role for epidermal growth factor. 127:304–315.

Curtis, C., Shah, S.P., Chin, S.-F., Turashvili, G., Rueda, O.M., Dunning, M.J., Speed, D., et al. (2012). The genomic and transcriptomic architecture of 2,000 breast tumours reveals novel subgroups. Nature 486:346–352.

Dale, T., Clarke, P.A., Esdar, C., Waalboer, D., Adeniji-Popoola, O., Ortiz-Ruiz, M.-J., Mallinger, A., et al. (2015). A selective chemical probe for exploring the role of CDK8 and CDK19 in human disease. Nature Chemical Biology 11:973–980.

Dall, G., Risbridger, G. and Britt, K. (2016). Mammary stem cells and parity-induced breast cancer protection- new insights. The Journal of steroid biochemistry and molecular biology.

Daniel, C.W. and Young, L.J. (1971). Influence of cell division on an aging process. Life span of mouse mammary epithelium during serial propagation in vivo. Experimental cell research 65:27–32.

Daniel, C.W., De Ome, K.B., Young, J.T., BLAIR, P.B. and FAULKIN, L.J. (1968). The in vivo life span of normal and preneoplastic mouse mammary glands: a serial transplantation study. Proceedings of the National Academy of Sciences of the United States of America 61:53–60.

de Lau, W., Barker, N., Low, T.Y., Koo, B.-K., Li, V.S.W., Teunissen, H., Kujala, P., et al. (2011). Lgr5 homologues associate with Wnt receptors and mediate R-spondin signalling. Nature 476:293–297.

De Moerlooze, L., Spencer-Dene, B., Revest, J.M., Hajihosseini, M., Rosewell, I. and Dickson, C. (2000). An important role for the IIIb isoform of fibroblast growth factor receptor 2 (FGFR2) in mesenchymal-epithelial signalling during mouse organogenesis. Development 127:483–492.

Debnath J, Muthuswamy SK, Brugge JS. Morphogenesis and oncogenesis of MCF-10A mammary epithelial acini grown in three-dimensional basement membrane cultures. Methods. 2003 Jul;30(3):256-68. PubMed PMID: 12798140.

DEOME, K.B., FAULKIN, L.J., BERN, H.A. and BLAIR, P.B. (1959). Development of mammary tumors from hyperplastic alveolar nodules transplanted into gland-free mammary fat pads of female C3H mice. Cancer Research 19:515–520.

Dey, D., Saxena, M., Paranjape, A.N., Krishnan, V., Giraddi, R., Kumar, M.V., Mukherjee, G., et al. (2009). Phenotypic and functional characterization of human mammary stem/progenitor cells in long term culture. PLoS ONE 4:e5329.

Di, Z., Klop, M.J.D., Rogkoti, V.-M., Le Dévédec, S.E., van de Water, B., Verbeek, F.J., Price, L.S., et al. (2014). Ultra high content image analysis and phenotype profiling of 3D cultured micro-tissues. Oshima, R. (ed.). PLoS ONE 9:e109688.

DiAugustine, R.P., Richards, R.G. and Sebastian, J. (1997). EGF-related peptides and their receptors in mammary gland development. Journal of Mammary Gland Biology and Neoplasia 2:109–117.

Dong Q, Wang D, Bandyopadhyay A, Gao H, Gorena KM, Hildreth K, Rebel VI, Walter CA, Huang C, Sun LZ. Mammospheres from murine mammary stem cell-enriched basal cells: clonal characteristics and repopulating potential. Stem Cell Res. 2013 May;10(3):396-404. PubMed PMID: 23466563; PubMed Central PMCID: PMC3622180.

Dontu, G., Abdallah, W.M., Foley, J.M., Jackson, K.W., Clarke, M.F., Kawamura, M.J. and Wicha, M.S. (2003). In vitro propagation and transcriptional profiling of human mammary stem/progenitor cells. Genes & Development 17:1253–1270.

Early Breast Cancer Trialists' Collaborative Group (EBCTCG), Davies, C., Godwin, J., Gray, R., Clarke, M., Cutter, D., Darby, S., et al. (2011). Relevance of breast cancer hormone receptors and other factors to the efficacy of adjuvant tamoxifen: patient-level meta-analysis of randomised trials. Lancet (London, England) 378:771–784.

Emerman, J.T., Enami, J., Pitelka, D.R. and Nandi, S. (1977). Hormonal effects on intracellular and secreted casein in cultures of mouse mammary epithelial cells on floating collagen membranes. Proceedings of the National Academy of Sciences 74:4466–4470.

Emre N, Vidal JG, Elia J, O'Connor ED, Paramban RI, Hefferan MP, Navarro R, Goldberg DS, Varki NM, Marsala M, Carson CT. The ROCK inhibitor Y-27632 improves recovery of human embryonic stem cells after fluorescence-activated cell sorting with multiple cell surface markers. PLoS One. 2010 Aug 13;5(8):e12148. PubMed PMID: 20730054; PubMed Central PMCID: PMC2921395.

Ewald, A.J., Brenot, A., Duong, M., Chan, B.S. and Werb, Z. (2008). Collective epithelial migration and cell rearrangements drive mammary branching morphogenesis. Developmental Cell 14:570–581.

Ewan KB, Oketch-Rabah HA, Ravani SA, Shyamala G, Moses HL, Barcellos-Hoff MH. Proliferation of estrogen receptor-alpha-positive mammary epithelial cells is restrained by transforming growth factor-beta1 in adult mice. Am J Pathol. 2005 Aug;167(2):409-17. PubMed PMID: 16049327; PubMed Central PMCID: PMC1603552.

Ewan, K., Pajak, B., Stubbs, M., Todd, H., Barbeau, O., Quevedo, C., Botfield, H., et al. (2010). A useful approach to identify novel small-molecule inhibitors of Wnt-dependent transcription. Cancer Research 70:5963–5973.

Forget, M.-A., Turcotte, S., Beauseigle, D., Godin-Ethier, J., Pelletier, S., Martin, J., Tanguay, S., et al. (2007). The Wnt pathway regulator DKK1 is preferentially expressed in hormone-resistant breast tumours and in some common cancer types. British journal of cancer 96:646–653.

Förster, C., Mäkela, S., Wärri, A., Kietz, S., Becker, D., Hultenby, K., Warner, M., et al. (2002). Involvement of estrogen receptor beta in terminal differentiation of mammary gland epithelium. Proceedings of the National Academy of Sciences 99:15578–15583.

Forster, N., Saladi, S.V., van Bragt, M., Sfondouris, M.E., Jones, F.E., Li, Z. and Ellisen, L.W. (2014). Basal Cell Signaling by p63 Controls Luminal Progenitor Function and Lactation via NRG1. Developmental Cell 28:147–160.

Foucquier, J. & Guedj, M., 2015. Analysis of drug combinations: current methodological landscape. Pharmacology research & perspectives, 3(3), pp.e00149–n/a.

Gauger, K.J., Shimono, A., Crisi, G.M. and Schneider, S.S. (2012). Loss of SFRP1 promotes ductal branching in the murine mammary gland. BMC developmental biology 12.

Gelmini, S., Poggesi, M., Distante, V., Bianchi, S., Simi, L., Luconi, M., Raggi, C.C., et al. (2004). Tankyrase, a positive regulator of telomere elongation, is over expressed in human breast cancer. CANCER LETTERS 216:81–87.

GOEPFERT, T.M., McCarthy, M., Stephens, C., Ullrich, R.L., Brinkley, B.R. and Medina, D. (2000). Progesterone facilitates chromosome instability (aneuploidy) in p53 null normal mammary epithelial cells. FASEB journal : official publication of the Federation of American Societies for Experimental Biology 14:2221–2229.

Guo, W., Keckesova, Z., Donaher, J.L., Shibue, T., Tischler, V., Reinhardt, F., Itzkovitz, S., et al. (2012). Slug and Sox9 Cooperatively Determine the Mammary Stem Cell State. Cell 148:1015–1028.

Gupta, P.B., Onder, T.T., Jiang, G., Tao, K., Kuperwasser, C., Weinberg, R.A. and Lander, E.S. (2009). Identification of selective inhibitors of cancer stem cells by high-throughput screening. Cell 138:645–659.

Gurney, A., Axelrod, F., Bond, C.J., Cain, J., Chartier, C., Donigan, L., Fischer, M., *et al.* (2012). Wnt pathway inhibition via the targeting of Frizzled receptors results in decreased growth and tumorigenicity of human tumors. *Proceedings of the National Academy of Sciences of the United States of America* **109**:11717–11722.

Habib, S.J., Chen, B.-C., Tsai, F.-C., Anastassiadis, K., Meyer, T., Betzig, E. and Nusse, R. (2013). A localized Wnt signal orients asymmetric stem cell division in vitro. Science 339:1445–1448.

Hao, H.-X., Xie, Y., Zhang, Y., Charlat, O., Oster, E., Avello, M., Lei, H., et al. (2012). ZNRF3 promotes Wnt receptor turnover in an R-spondin-sensitive manner. Nature 485:195–200.

Hayflick, L. and Moorhead, P.S. (1961). The serial cultivation of human diploid cell strains. *Experimental cell research* **25**:585–621.

Hein, S.M., Haricharan, S., Johnston, A.N., Toneff, M.J., Reddy, J.P., Dong, J., Bu, W., et al. (2016). Luminal epithelial cells within the mammary gland can produce basal cells upon oncogenic stress. Oncogene 35:1461–1467.

Henderson, I.C., Berry, D.A., Demetri, G.D., Cirrincione, C.T., Goldstein, L.J., Martino, S., Ingle, J.N., *et al.* (2003). Improved outcomes from adding sequential Paclitaxel but not from escalating Doxorubicin dose in an adjuvant chemotherapy regimen for patients with node-positive primary breast cancer. *Journal of clinical oncology : official journal of the American Society of Clinical Oncology* **21**:976–983.

Hennighausen L, Robinson GW. Information networks in the mammary gland. Nat Rev Mol Cell Biol. 2005 Sep;6(9):715-25. PubMed PMID: 16231422.

Herschkowitz JI, Zhao W, Zhang M, Usary J, Murrow G, Edwards D, Knezevic J, Greene SB, Darr D, Troester MA, Hilsenbeck SG, Medina D, Perou CM, Rosen JM. Comparative oncogenomics identifies breast tumors enriched in functional tumor-initiating cells. Proc Natl Acad Sci U S A. 2012 Feb 21;109(8):2778-83. PubMed PMID: 21633010; PubMed Central PMCID: PMC3286979.

Holland, J.D., Klaus, A., Garratt, A.N. and Birchmeier, W. (2013). Wnt signaling in stem and cancer stem cells. Current Opinion in Cell Biology 25:254–264.

Howard, B., Panchal, H., McCarthy, A. and Ashworth, A. (2005). Identification of the scaramanga gene implicates Neuregulin3 in mammary gland specification. Genes & Development 19:2078–2090.

Howard, B.A. and Lu, P. (2014). Stromal regulation of embryonic and postnatal mammary epithelial development and differentiation. Seminars in Cell and Developmental Biology 25-26:43–51.

Huang, L., Holtzinger, A., Jagan, I., BeGora, M., Lohse, I., Ngai, N., Nostro, C., et al. (2015). Ductal pancreatic cancer modeling and drug screening using human pluripotent stem cell- and patient-derived tumor organoids. Nature Medicine 21:1364–1371.

Huang, S.-M.A., Mishina, Y.M., Liu, S., Cheung, A., Stegmeier, F., Michaud, G.A., Charlat, O., et al. (2009). Tankyrase inhibition stabilizes axin and antagonizes Wnt signalling. Nature 461:614–620.

Huch, M., Bonfanti, P., Boj, S.F., Sato, T., Loomans, C.J.M., van de Wetering, M., Sojoodi, M., et al. (2013). Unlimited in vitro expansion of adult bi-potent pancreas progenitors through the Lgr5/R-spondin axis. The EMBO Journal 32:2708–2721.

Huch, M., Bonfanti, P., Boj, S.F., Sato, T., Loomans, C.J.M., van de Wetering, M., Sojoodi, M., Li, V.S.W., Schuijers, J., Gracanin, A., Ringnalda, F., Begthel, H., Hamer, K., Mulder, J., van Es, J.H., de Koning, E., Vries, R.G.J., Heimberg, H. and Clevers, H. (2013a). Unlimited in vitro expansion of adult bi-potent pancreas progenitors through the Lgr5/R-spondin axis. The EMBO Journal 32:2708–2721.

Huch, M., Dorrell, C., Boj, S.F., van Es, J.H., Li, V.S.W., van de Wetering, M., Sato, T., et al. (2013). In vitro expansion of single Lgr5+ liver stem cells induced by Wnt-driven regeneration. Nature 494:247–250.

Huch, M., Gehart, H., van Boxtel, R., Hamer, K., Blokzijl, F., Verstegen, M.M.A., Ellis, E., et al. (2015). Long-term culture of genome-stable bipotent stem cells from adult human liver. Cell 160:299–312.

Hynes, N.E. and Watson, C.J. (2010). Mammary gland growth factors: roles in normal development and in cancer. Cold Spring Harbor Perspectives in Biology 2:a003186–a003186.

Incassati, A., Chandramouli, A., Eelkema, R. and Cowin, P. (2010). Key signaling nodes in mammary gland development and cancer: β-catenin. Breast Cancer Research 12:213.

Jardé, T. and Dale, T. (2011). Wnt signalling in murine postnatal mammary gland development. Acta Physiologica 204:118–127.

Jardé, T.J., Evans, R.J., McQuillan, K.L., Parry, L., Feng, G.J., Alvares, B., Clarke, A.R., et al. (2012). In vivo and in vitro models for the therapeutic targeting of Wnt signaling using a Tet-OΔN89β-catenin system. :1–11.

Jardé, T., Lloyd-Lewis, B., Thomas, M., Kendrick, H., Melchor, L., Bougaret, L., Watson, P.D., *et al.* (2016). Wnt and Neuregulin1/ErbB signalling extends 3D culture of hormone responsive mammary organoids. *Nature Communications* **7**:13207.

Joshi, P.A., Jackson, H.W., Beristain, A.G., Di Grappa, M.A., Mote, P.A., Clarke, C.L., Stingl, J., et al. (2010). Progesterone induces adult mammary stem cell expansion. Nature 465:803–807.

Joshi, P.A., Waterhouse, P.D., Kannan, N., Narala, S., Fang, H., Di Grappa, M.A., Jackson, H.W., et al. (2015). RANK Signaling Amplifies WNT-Responsive Mammary Progenitors through R-SPONDIN1. Stem cell reports 5:31–44.

Kabiri, Z., Greicius, G., Madan, B., Biechele, S., Zhong, Z., Zaribafzadeh, H., Edison, et al. (2014). Stroma provides an intestinal stem cell niche in the absence of epithelial Wnts. Development 141:2206–2215.

Kamalati, T., Niranjan, B., Yant, J. and Buluwela, L. (1999). HGF/SF in mammary epithelial growth and morphogenesis: in vitro and in vivo models. Journal of Mammary Gland Biology and Neoplasia 4:69–77.

Karthaus, W.R., Iaquinta, P.J., Drost, J., Gracanin, A., van Boxtel, R., Wongvipat, J., Dowling, C.M., et al. (2014). Identification of Multipotent Luminal Progenitor Cells in Human Prostate Organoid Cultures. Cell 159:163–175.

Khramtsov, A.I., Khramtsova, G.F., Tretiakova, M., Huo, D., Olopade, O.I. and Goss, K.H. (2010). Wnt/β-Catenin Pathway Activation Is Enriched in Basal-Like Breast Cancers and Predicts Poor Outcome. The American journal of pathology 176:2911–2920.

Kim, S., Goel, S. and Alexander, C.M. (2011). Differentiation generates paracrine cell pairs that maintain basaloid mouse mammary tumors: proof of concept. Oshima, R. (ed.). PLoS ONE 6:e19310.

Kim, S., Xu, X., Hecht, A. and Boyer, T.G. (2006). Mediator is a transducer of Wnt/beta-catenin signaling. Journal of Biological Chemistry 281:14066–14075.

Kordon, E.C. and Smith, G.H. (1998). An entire functional mammary gland may comprise the progeny from a single cell. Development 125:1921–1930.

Kostadinova, R., Boess, F., Applegate, D., Suter, L., Weiser, T., Singer, T., Naughton, B., et al. (2013). A long-term three dimensional liver co-culture system for improved prediction of clinically relevant drug-induced hepatotoxicity. Toxicology and applied pharmacology 268:1–16.

Kurosawa H. Application of Rho-associated protein kinase (ROCK) inhibitor to human pluripotent stem cells. J Biosci Bioeng. 2012 Dec;114(6):577-81. PubMed PMID: 22898436.

Lau, T., Chan, E., Callow, M., Waaler, J., Boggs, J., Blake, R.A., Magnuson, S., et al. (2013). A novel tankyrase small-molecule inhibitor suppresses APC mutation-driven colorectal tumor growth. Cancer Research 73:3132–3144.

Lee GY, Kenny PA, Lee EH, Bissell MJ. Three-dimensional culture models of normal and malignant breast epithelial cells. Nat Methods. 2007 Apr;4(4):359-65. PubMed PMID: 17396127; PubMed Central PMCID: PMC2933182.

Lehtiö, L., Chi, N.-W. and Krauss, S. (2013). Tankyrases as drug targets. FEBS Journal 280:3576–3593.

Levenson, A.S. and Jordan, V.C. (1997). MCF-7: the First Hormone-Responsive Breast Cancer Cell Line.

Li, M L, Aggeler, J., Farson, D.A., Hatier, C., Hassell, J. and Bissell, M.J. (1987). Influence of a reconstituted basement membrane and its components on casein gene expression and secretion in mouse mammary epithelial cells. Proceedings of the National Academy of Sciences 84:136–140.

Li, Yi, Welm, B., Podsypanina, K., Huang, S., Chamorro, M., Zhang, X., Rowlands, T., et al. (2003). Evidence that transgenes encoding components of the Wnt signaling pathway preferentially induce mammary cancers from progenitor cells. Proceedings of the National Academy of Sciences 100:15853–15858.

Li, Yonghe, Lu, W., King, T.D., Liu, C.-C., Bijur, G.N. and Bu, G. (2010). Dkk1 stabilizes Wnt co-receptor LRP6: implication for Wnt ligand-induced LRP6 down-regulation. PLoS ONE 5:e11014.

Liao, M.-J., Zhang, C.C., Zhou, B., Zimonjic, D.B., Mani, S.A., Kaba, M., Gifford, A., et al. (2007). Enrichment of a population of mammary gland cells that form mammospheres and have in vivo repopulating activity. Cancer Research 67:8131–8138.

Lim, E., Vaillant, F., Wu, D., Forrest, N.C., Pal, B., Hart, A.H., Asselin-Labat, M.-L., et al. (2009). Aberrant luminal progenitors as the candidate target population for basal tumor development in BRCA1 mutation carriers. Nature Medicine 15:907–913.

Lindvall, C., Evans, N.C., Zylstra, C.R., Li, Y., Alexander, C.M. and Williams, B.O. (2006). The Wnt signaling receptor Lrp5 is required for mammary ductal stem cell activity and Wnt1-induced tumorigenesis. Journal of Biological Chemistry 281:35081–35087.

Linnemann, J.R., Miura, H., Meixner, L.K., Irmler, M., Kloos, U.J., Hirschi, B., Bartsch, H.S., et al. (2015). Quantification of regenerative potential in primary human mammary epithelial cells. Development 142:3239–3251.

Liu, B.Y., McDermott, S.P., Khwaja, S.S. and Alexander, C.M. (2004). The transforming activity of Wnt effectors correlates with their ability to induce the accumulation of mammary progenitor cells. Proceedings of the National Academy of Sciences 101:4158–4163.

Liu, C.-C., Prior, J., Piwnica-Worms, D. and Bu, G. (2010). LRP6 overexpression defines a class of breast cancer subtype and is a target for therapy. Proceedings of the National Academy of Sciences of the United States of America 107:5136–5141.

Liu, J., Pan, S., Hsieh, M.H., Ng, N., Sun, F., Wang, T., Kasibhatla, S., et al. (2013). Targeting Wnt-driven cancer through the inhibition of Porcupine by LGK974. Proceedings of the National Academy of Sciences of the United States of America 110:20224–20229.

Lu, W. and Li, Yonghe (2014). Salinomycin suppresses LRP6 expression and inhibits both Wnt/β-catenin and mTORC1 signaling in breast and prostate cancer cells. Journal of cellular biochemistry 115:1799–1807.

Luetteke, N.C., Qiu, T.H., Fenton, S.E., Troyer, K.L., Riedel, R.F., Chang, A. and Lee, D.C. (1999). Targeted inactivation of the EGF and amphiregulin genes reveals distinct roles for EGF receptor ligands in mouse mammary gland development. Development 126:2739–2750.

MacDonald, B.T., Tamai, K. and He, X. (2009). Wnt/beta-catenin signaling: components, mechanisms, and diseases. Developmental Cell 17:9–26.

Mallepell, S., Krust, A., Chambon, P. and Brisken, C. (2006). Paracrine signaling through the epithelial estrogen receptor alpha is required for proliferation and morphogenesis in the mammary gland. Proceedings of the National Academy of Sciences 103:2196–2201.

Mallinger, A., Crumpler, S., Pichowicz, M., Waalboer, D., Stubbs, M., Adeniji-Popoola, O., Wood, B., et al. (2015). Discovery of potent, orally bioavailable, small-molecule inhibitors of WNT signaling from a cell-based pathway screen. Journal of medicinal chemistry 58:1717–1735.

Mastroianni, M., Kim, S., Kim, Y.C., Esch, A., Wagner, C. and Alexander, C.M. (2010). Wnt signaling can substitute for estrogen to induce division of ERα-positive cells in a mouse mammary tumor model. CANCER LETTERS 289:23–31.

Matano, M., Date, S., Shimokawa, M., Takano, A., Fujii, M., Ohta, Y., Watanabe, T., et al. (2015). Modeling colorectal cancer using CRISPR-Cas9-mediated engineering of human intestinal organoids. Nature Medicine 21:256–262.

Maupin, K.A., Droscha, C.J. and Williams, B.O. (2013). A Comprehensive Overview of Skeletal Phenotypes Associated with Alterations in Wnt/β-catenin Signaling in Humans and Mice. Bone research 1:27–71.

Meyer, K.B., Maia, A.-T., O'Reilly, M., Teschendorff, A.E., Chin, S.-F., Caldas, C. and Ponder, B.A.J. (2008). Allele-specific up-regulation of FGFR2 increases susceptibility to breast cancer. PLOS Biology 6:e108.

Molyneux, G., Geyer, F.C., Magnay, F.-A., McCarthy, A., Kendrick, H., Natrajan, R., Mackay, A., et al. (2010). BRCA1 basal-like breast cancers originate from luminal epithelial progenitors and not from basal stem cells. Cell Stem Cell 7:403–417.

Mulac-Jericevic, B., Mullinax, R.A., DeMayo, F.J., Lydon, J.P. and Conneely, O.M. (2000). Subgroup of reproductive functions of progesterone mediated by progesterone receptor-B isoform. Science 289:1751–1754.

Nandi, S., Imagawa, W., Tomooka, Y., McGrath, M.F. and Edery, M. (1984). Collagen gel culture system and analysis of estrogen effects on mammary carcinogenesis. Archives of toxicology 55:91–96.

Nardulli, A.M. and Katzenellenbogen, B.S. (1988). Progesterone receptor regulation in T47D human breast cancer cells: analysis by density labeling of progesterone receptor synthesis and degradation and their modulation by progestin. 122:1532–1540.

Nelson, C.M., Vanduijn, M.M., Inman, J.L., Fletcher, D.A. and Bissell, M.J. (2006). Tissue geometry determines sites of mammary branching morphogenesis in organotypic cultures. Science 314:298–300.

Neve, R.M., Chin, K., Fridlyand, J., Yeh, J., Baehner, F.L., Fevr, T., Clark, L., *et al.* (2006). A collection of breast cancer cell lines for the study of functionally distinct cancer subtypes. *Cancer cell* **10**:515–527.

Niranjan, B., Buluwela, L., Yant, J., Perusinghe, N., Atherton, A., Phippard, D., Dale, T., et al. (1995). HGF/SF: a potent cytokine for mammary growth, morphogenesis and development. Development 121:2897–2908.

Nusse, R. and Varmus, H.E. (1982). Many tumors induced by the mouse mammary tumor virus contain a provirus integrated in the same region of the host genome. Cell 31:99–109.

Obr, A.E., Grimm, S.L., Bishop, K.A., Pike, J.W., Lydon, J.P. and Edwards, D.P. (2013). Progesterone receptor and Stat5 signaling cross talk through RANKL in mammary epithelial cells. Molecular endocrinology (Baltimore, Md.) 27:1808–1824.

Ohkawara, B., Glinka, A. and Niehrs, C. (2011). Rspo3 Binds Syndecan 4 and Induces Wnt/PCP Signaling via Clathrin-Mediated Endocytosis to Promote Morphogenesis. Developmental Cell 20:303–314.

OncoMed Pharmaceuticals, (2016). *OncoMed Presents Phase 1b Data for First-in-Class Treatments in Ovarian, Breast and Lung Cancer at the 2016 ASCO Annual Meeting*. [online] Available at: http://investor.shareholder.com/oncomed/releasedetail.cfm?ReleaseID=974305 [Accessed 2 Dec. 2016].

Panchal, H., Wansbury, O., Parry, S., Ashworth, A. and Howard, B. (2007). Neuregulin3 alters cell fate in the epidermis and mammary gland. BMC developmental biology 7:105.

Parsa, S., Ramasamy, S.K., De Langhe, S., Gupte, V.V., Haigh, J.J., Medina, D. and Bellusci, S. (2008). Terminal end bud maintenance in mammary gland is dependent upon FGFR2b signaling. 317:121–131.

Pasic, L., Eisinger-Mathason, T.S.K., Velayudhan, B.T., Moskaluk, C.A., Brenin, D.R., Macara, I.G. and Lannigan, D.A. (2011). Sustained activation of the HER1-ERK1/2-RSK signaling pathway controls myoepithelial cell fate in human mammary tissue. Genes & Development 25:1641–1653.

Pegram, M.D., Konecny, G.E., O'Callaghan, C., Beryt, M., Pietras, R. and Slamon, D.J. (2004). Rational combinations of trastuzumab with chemotherapeutic drugs used in the treatment of breast cancer. Journal of the National Cancer Institute 96:739–749.

Piccin, D. and Morshead, C.M. (2011). Wnt signaling regulates symmetry of division of neural stem cells in the adult brain and in response to injury. STEM CELLS 29:528–538.

Pinto, D., Gregorieff, A., Begthel, H. and Clevers, H. (2003). Canonical Wnt signals are essential for homeostasis of the intestinal epithelium. Genes & Development 17:1709–1713.

Prenzel, N. et al., 2001. The epidermal growth factor receptor family as a central element for cellular signal transduction and diversification. *Endocrine-related cancer*, 8(1), pp.11–31.

Proffitt, K.D., Madan, B., Ke, Z., Pendharkar, V., Ding, L., Lee, M.A., Hannoush, R.N., et al. (2013). Pharmacological inhibition of the Wnt acyltransferase PORCN prevents growth of WNT-driven mammary cancer. Cancer Research 73:502–507.

Richert, M.M., Schwertfeger, K.L., Ryder, J.W. and Anderson, S.M. (2000). An atlas of mouse mammary gland development. Journal of Mammary Gland Biology and Neoplasia 5:227–241.

Rijsewijk, F., Schuermann, M., Wagenaar, E., Parren, P., Weigel, D. and Nusse, R. (1987). The Drosophila homolog of the mouse mammary oncogene int-1 is identical to the segment polarity gene wingless. Cell 50:649.

Rios-Esteves, J., Haugen, B. and Resh, M.D. (2014). Identification of key residues and regions important for porcupine-mediated Wnt acylation. The Journal of biological chemistry 289:17009–17019.

Rios, A.C., Fu, N.Y., Lindeman, G.J. and Visvader, J.E. (2014). In situ identification of bipotent stem cells in the mammary gland. Nature 506:322–327.

Rock, J.R., Onaitis, M.W., Rawlins, E.L., Lu, Y., Clark, C.P., Xue, Y., Randell, S.H., *et al.* (2009). Basal cells as stem cells of the mouse trachea and human airway epithelium. *Proceedings of the National Academy of Sciences of the United States of America* **106**:12771–12775.

Dasti, A., Huyghe, M., Lafkas, D., Laurent, C., Reyal, F. and Fre, S. (2015). Luminal Progenitors Restrict Their Lineage Potential during Mammary Gland Development Eaves, C. J. (ed.). PLOS Biology 13:e1002069–24.

Roelink, H., Wagenaar, E., Lopes da Silva, S. and Nusse, R. (1990). Wnt-3, a gene activated by proviral insertion in mouse mammary tumors, is homologous to int-1/Wnt-1 and is normally expressed in mouse embryos and adult brain. Proceedings of the National Academy of Sciences of the United States of America 87:4519–4523.

Romanov, S.R., Kozakiewicz, B.K., Holst, C.R., Stampfer, M.R., Haupt, L.M. and Tlsty, T.D. (2001). Normal human mammary epithelial cells spontaneously escape senescence and acquire genomic changes. *Nature* **409**:633–637.

Russo, J., Ao, X., Grill, C. and Russo, I.H. (1999). Pattern of distribution of cells positive for estrogen receptor alpha and progesterone receptor in relation to proliferating cells in the mammary gland. Breast Cancer Research and Treatment 53:217–227.

Santos, dos, C.O., Rebbeck, C., Rozhkova, E., Valentine, A., Samuels, A., Kadiri, L.R., Osten, P., *et al.* (2013). Molecular hierarchy of mammary differentiation yields refined markers of mammary stem cells. *Proceedings of the National Academy of Sciences of the United States of America* **110**:7123–7130.

Sasaki, M., Nishio, M., Sasaki, T. and Enami, J. (1994). Identification of mouse mammary fibroblast-derived mammary growth factor as hepatocyte growth factor. Biochemical and Biophysical Research Communications 199:772–779.

Sato, T., Stange, D.E., Ferrante, M., Vries, R.G.J., Van Es, J.H., van den Brink, S., van Houdt, W.J., et al. (2011). Long-term Expansion of Epithelial Organoids From Human Colon, Adenoma, Adenocarcinoma, and Barrett's Epithelium. YGAST 141:1762–1772.

Sato, T., van Es, J.H., Snippert, H.J., Stange, D.E., Vries, R.G., van den Born, M., Barker, N., et al. (2011). Paneth cells constitute the niche for Lgr5 stem cells in intestinal crypts. Nature 469:415–418.

Sato, T., Vries, R.G., Snippert, H.J., van de Wetering, M., Barker, N., Stange, D.E., van Es, J.H., et al. (2009). Single Lgr5 stem cells build crypt-villus structures in vitro without a mesenchymal niche. Nature 459:262–265.

Seewaldt, V.L., Mrózek, K., Sigle, R., Dietze, E.C., Heine, K., Hockenbery, D.M., Hobbs, K.B., et al. (2001). Suppression of p53 function in normal human mammary epithelial cells increases sensitivity to extracellular matrix-induced apoptosis. The Journal of Cell Biology 155:471–486.

Shackleton, M., Vaillant, F., Simpson, K.J., Stingl, J., Smyth, G.K., Asselin-Labat, M.-L., Wu, L., et al. (2006). Generation of a functional mammary gland from a single stem cell. Nature 439:84–88.

Shehata, M., Teschendorff, A., Sharp, G., Novcic, N., Russell, I.A., Avril, S., Prater, M., et al. (2012). Phenotypic and functional characterisation of the luminal cell hierarchy of the mammary gland. Breast Cancer Research 14:R134.

Silberstein, G.B., Van Horn, K., Hrabeta-Robinson, E. and Compton, J. (2006). Estrogen-triggered delays in mammary gland gene expression during the estrous cycle: evidence for a novel timing system. The Journal of endocrinology 190:225–239.

Sleeman, K.E., Kendrick, H., Ashworth, A., Isacke, C.M. and Smalley, M.J. (2006). CD24 staining of mouse mammary gland cells defines luminal epithelial, myoepithelial/basal and non-epithelial cells. Breast Cancer Research 8:R7.

Sleeman, K.E., Kendrick, H., Robertson, D., Isacke, C.M., Ashworth, A. and Smalley, M.J. (2007). Dissociation of estrogen receptor expression and in vivo stem cell activity in the mammary gland. The Journal of Cell Biology 176:19–26.

Smalley, M.J. (2010). Isolation, Culture and Analysis of Mouse Mammary Epithelial Cells. In: *Progenitor Cells*. Totowa, NJ: Humana Press, pp. 139–170.

Smith, G.H. (1996). Experimental mammary epithelial morphogenesis in an in vivo model: evidence for distinct cellular progenitors of the ductal and lobular phenotype. Breast Cancer Research and Treatment 39:21–31.

Smith, G.H. and Boulanger, C.A. (2003). Mammary epithelial stem cells: transplantation and self-renewal analysis. Cell proliferation 36 Suppl 1:3–15.

Snippert, H.J., van der Flier, L.G., Sato, T., van Es, J.H., van den Born, M., Kroon-Veenboer, C., Barker, N., et al. (2010). Intestinal crypt homeostasis results from neutral competition between symmetrically dividing Lgr5 stem cells. Cell 143:134–144.

Sokol, E.S., Miller, D.H., Breggia, A., Spencer, K.C., Arendt, L.M. and Gupta, P.B. (2016). Growth of human breast tissues from patient cells in 3D hydrogel scaffolds. Breast Cancer Research 18:19.

Spencer-Dene, B., Dillon, C., Fantl, V., Kerr, K., Petiot, A. and Dickson, C. (2001). Fibroblast growth factor signalling in mouse mammary gland development. Endocrine-related cancer 8:211–217.

Spike, B.T., Engle, D.D., Lin, J.C., Cheung, S.K., La, J. and Wahl, G.M. (2012). A mammary stem cell population identified and characterized in late embryogenesis reveals similarities to human breast cancer. *Cell Stem Cell* **10**:183–197.

Sternlicht MD, Sunnarborg SW, Kouros-Mehr H, Yu Y, Lee DC, Werb Z. Mammary ductal morphogenesis requires paracrine activation of stromal EGFR via ADAM17-dependent shedding of epithelial amphiregulin. Development. 2005 Sep;132(17):3923-33. PubMed PMID: 16079154; PubMed Central PMCID: PMC2771180.

Sternlicht MD. Key stages in mammary gland development: the cues that regulate ductal branching morphogenesis. Breast Cancer Res. 2006;8(1):201. PubMed PMID: 16524451; PubMed Central PMCID: PMC1413974.

Stingl, J. (2009). Detection and analysis of mammary gland stem cells. The Journal of Pathology 217:229–241.

Stingl, J., Eirew, P., Ricketson, I., Shackleton, M., Vaillant, F., Choi, D., Li, H.I., et al. (2006). Purification and unique properties of mammary epithelial stem cells. Nature 439:993–997.

Sørlie, T., Perou, C.M., Tibshirani, R., Aas, T., Geisler, S., Johnsen, H., Hastie, T., *et al.* (2001). Gene expression patterns of breast carcinomas distinguish tumor subclasses with clinical implications. *Proceedings of the National Academy of Sciences* **98**:10869–10874.

Tao, L., van Bragt, M.P.A., Laudadio, E. and Li, Z. (2014). Lineage tracing of mammary epithelial cells using cell-type-specific cre-expressing adenoviruses. Stem cell reports 2:770–779.

Theodorou, V., Boer, M., Weigelt, B., Jonkers, J., van der Valk, M. and Hilkens, J. (2004). Fgf10 is an oncogene activated by MMTV insertional mutagenesis in mouse mammary tumors and overexpressed in a subset of human breast carcinomas. Oncogene 23:6047–6055.

Thorn, C.F., Oshiro, C., Marsh, S., Hernandez-Boussard, T., McLeod, H., Klein, T.E. and Altman, R.B. (2011). Doxorubicin pathways: pharmacodynamics and adverse effects. Pharmacogenetics and genomics 21:440–446.

Tiede B, Kang Y. From milk to malignancy: the role of mammary stem cells in development, pregnancy and breast cancer. Cell Res. 2011 Feb;21(2):245-57. PubMed PMID: 21243011; PubMed Central PMCID: PMC3193434.

Tsukamoto, A.S., Grosschedl, R., Guzman, R.C., Parslow, T. and Varmus, H.E. (1988). Expression of the int-1 gene in transgenic mice is associated with mammary gland hyperplasia and adenocarcinomas in male and female mice. Cell 55:619–625.

Usary J, Zhao W, Darr D, Roberts PJ, Liu M, Balletta L, Karginova O, Jordan J, Combest A, Bridges A, Prat A, Cheang MC, Herschkowitz JI, Rosen JM, Zamboni W, Sharpless NE, Perou CM. Predicting drug responsiveness in human cancers using genetically engineered mice. Clin Cancer Res. 2013 Sep 1;19(17):4889-99. PubMed PMID: 23780888; PubMed Central PMCID: PMC3778918.

van Amerongen, R., 2012. Alternative Wnt Pathways and Receptors. Cold Spring Harbor Perspectives in Biology, 4(10), pp.a007914–a007914.

van Amerongen, R., Bowman, A.N. and Nusse, R. (2012). Developmental Stage and Time Dictate the Fate of Wnt/β-Catenin-Responsive Stem Cells in the Mammary Gland. Cell Stem Cell 11:387–400.

van de Wetering, M., Francies, H.E., Francis, J.M., Bounova, G., Iorio, F., Pronk, A., van Houdt, W., et al. (2015). Prospective derivation of a living organoid biobank of colorectal cancer patients. Cell 161:933–945.

van Genderen, C., Okamura, R.M., Fariñas, I., Quo, R.G., Parslow, T.G., Bruhn, L. and Grosschedl, R. (1994). Development of several organs that require inductive epithelial-mesenchymal interactions is impaired in LEF-1-deficient mice. Genes & Development 8:2691–2703.

Van Keymeulen, A., Rocha, A.S., Ousset, M., Beck, B., Bouvencourt, G., Rock, J., Sharma, N., et al. (2011). Distinct stem cells contribute to mammary gland development and maintenance. Nature 479:189–193.

Veltmaat, J.M., Van Veelen, W., Thiery, J.P. and Bellusci, S. (2004). Identification of the mammary line in mouse by Wnt10b expression. Developmental Dynamics 229:349–356.

Visvader, J.E. (2009). Keeping abreast of the mammary epithelial hierarchy and breast tumorigenesis. Genes & Development 23:2563–2577.

Visvader, J.E. and Stingl, J. (2014). Mammary stem cells and the differentiation hierarchy: current status and perspectives. Genes & Development 28:1143–1158.

Walen, K.H. and Stampfer, M.R. (1989). Chromosome analyses of human mammary epithelial cells at stages of chemical-induced transformation progression to immortality. Cancer genetics and cytogenetics 37:249–261.

Wang F, Scoville D, He XC, Mahe MM, Box A, Perry JM, Smith NR, Lei NY, Davies PS, Fuller MK, Haug JS, McClain M, Gracz AD, Ding S, Stelzner M, Dunn JC, Magness ST, Wong MH, Martin MG, Helmrath M, Li L. Isolation and characterization of intestinal stem cells based on surface marker combinations and colony-formation assay. Gastroenterology. 2013 Aug;145(2):383-95.e1-21. PubMed PMID: 23644405; PubMed Central PMCID: PMC3781924.

Wansbury, O., Panchal, H., James, M., Parry, S., Ashworth, A. and Howard, B. (2008). Dynamic expression of Erbb pathway members during early mammary gland morphogenesis. The Journal of investigative dermatology 128:1009–1021.

Watanabe, K., Ueno, M., Kamiya, D., Nishiyama, A., Matsumura, M., Wataya, T., Takahashi, J.B., et al. (2007). A ROCK inhibitor permits survival of dissociated human embryonic stem cells. Nature biotechnology 25:681–686.

Wuidart, A., Ousset, M., Rulands, S., Simons, B.D., Van Keymeulen, A. and Blanpain, C. (2016). Quantitative lineage tracing strategies to resolve multipotency in tissue-specific stem cells. :1–18.

Xiang, T., Li, L., Yin, X., Zhong, L., Peng, W., Qiu, Z., Ren, G., et al. (2013). Epigenetic silencing of the WNT antagonist Dickkopf 3 disrupts normal Wnt/β-catenin signalling and apoptosis regulation in breast cancer cells. Journal of Cellular and Molecular Medicine 17:1236–1246.

Xu, W.-H., Liu, Z.-B., Yang, C., Qin, W. and Shao, Z.-M. (2012). Expression of dickkopf-1 and beta-catenin related to the prognosis of breast cancer patients with triple negative phenotype. PLoS ONE 7:e37624.

Yang, L., Wu, X., Wang, Y., Zhang, K., Wu, J., Yuan, Y.-C., Deng, X., et al. (2011). FZD7 has a critical role in cell proliferation in triple negative breast cancer. Oncogene 30:4437–4446.

Yant, J., Buluwela, L., Niranjan, B., Gusterson, B. and Kamalati, T. (1998). In vivo effects of hepatocyte growth factor/scatter factor on mouse mammary gland development. Experimental cell research 241:476–481.

Yin X, Farin HF, van Es JH, Clevers H, Langer R, Karp JM. Niche-independent high-purity cultures of Lgr5+ intestinal stem cells and their progeny. Nat Methods. 2014 Jan;11(1):106-12. PubMed PMID: 24292484; PubMed Central PMCID: PMC3951815.

Yoda, A., Kouike, H., Okano, H. and Sawa, H. (2005). Components of the transcriptional Mediator complex are required for asymmetric cell division in C. elegans. Development 132:1885–1893.

Zeng, Y.A. and Nusse, R. (2010). Wnt proteins are self-renewal factors for mammary stem cells and promote their long-term expansion in culture. Cell Stem Cell 6:568–577.

Zhang M, Behbod F, Atkinson RL, Landis MD, Kittrell F, Edwards D, Medina D, Tsimelzon A, Hilsenbeck S, Green JE, Michalowska AM, Rosen JM. Identification of tumor-initiating cells in a p53-null mouse model of breast cancer. Cancer Res. 2008 Jun 15;68(12):4674-82. PubMed PMID: 18559513; PubMed Central PMCID: PMC2459340.

Zhang, M., Atkinson, R.L. and Rosen, J.M. (2010). Selective targeting of radiation-resistant tumor-initiating cells. Proceedings of the National Academy of Sciences 107:3522–3527.

Zhang, M., Tsimelzon, A., Chang, C.H., Fan, C., Wolff, A., Perou, C.M., Hilsenbeck, S.G., et al. (2015). Intratumoral Heterogeneity in a Trp53-Null Mouse Model of Human Breast Cancer. Cancer Discovery 5:520–533.

Zhou, S.-J., Zhuo, S.-R., Yang, X.-Q., Qin, C.-X. and Wang, Z.-L. (2014). Serum Dickkopf-1 expression level positively correlates with a poor prognosis in breast cancer. Diagnostic pathology 9:161.

9 Appendices

9.1 Appendix I: Additional figures from Jardé et al. (2016)

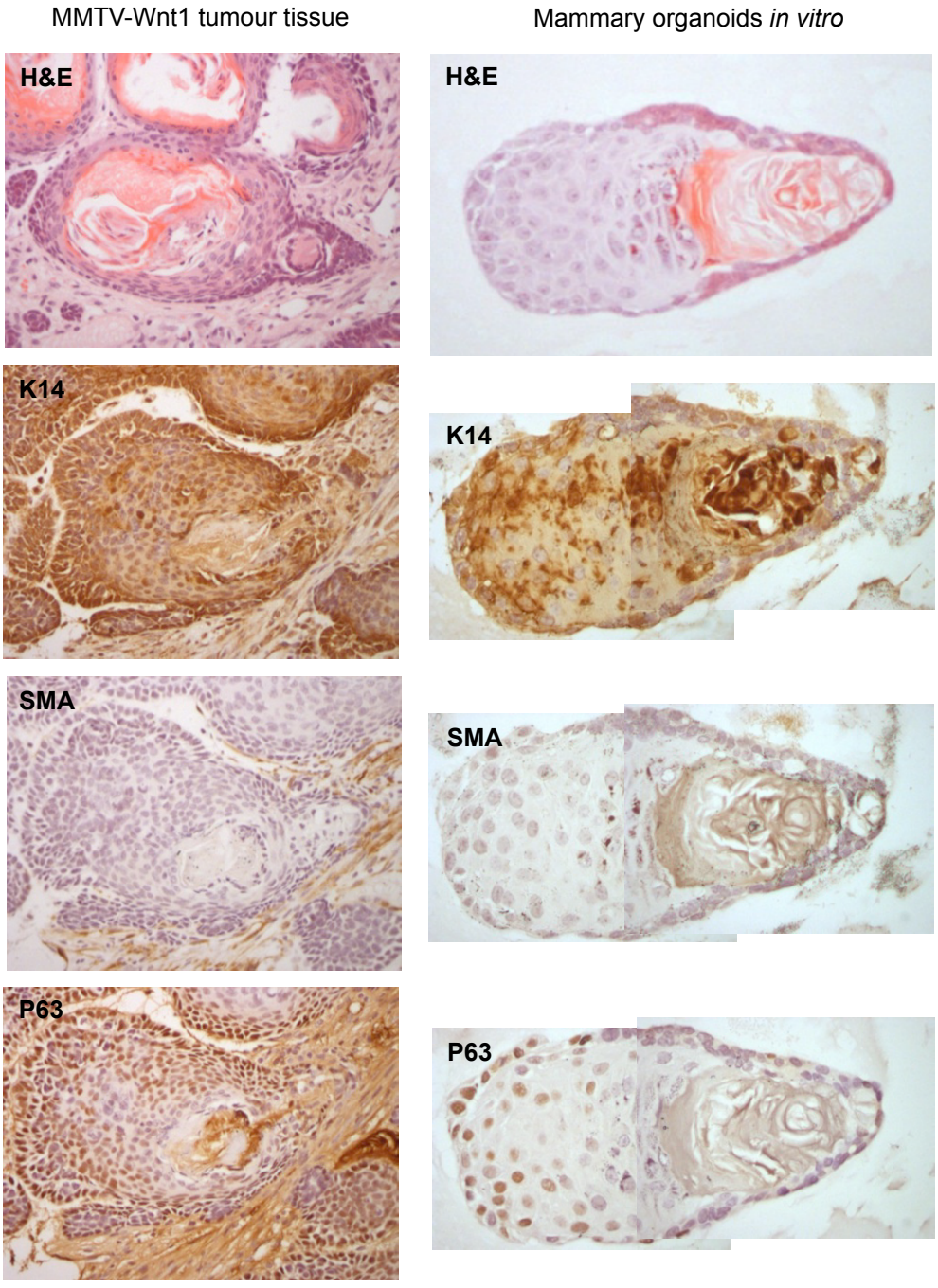

Appendix I-1 R-spondin-1 treated mammary organoids recapitulate MMTV-Wnt1 tumour tissue histology.

Mammary epithelial cells were cultured with 600 ng/ml R-spondin-1(R&D systems), 50 ng/ml EGF and 100 ng/ml noggin for 21 days. Organoids were fixed, embedded in paraffin and sectioned. Sections were stained for Hematoxylin and Eosin (H&E) and basal markers (keratin-14, K14; p63; smooth muscle actin, SMA). In parallel, MMTV-Wnt1 driven mammary gland tumours were fixed, embedded in paraffin, sectioned and stained.

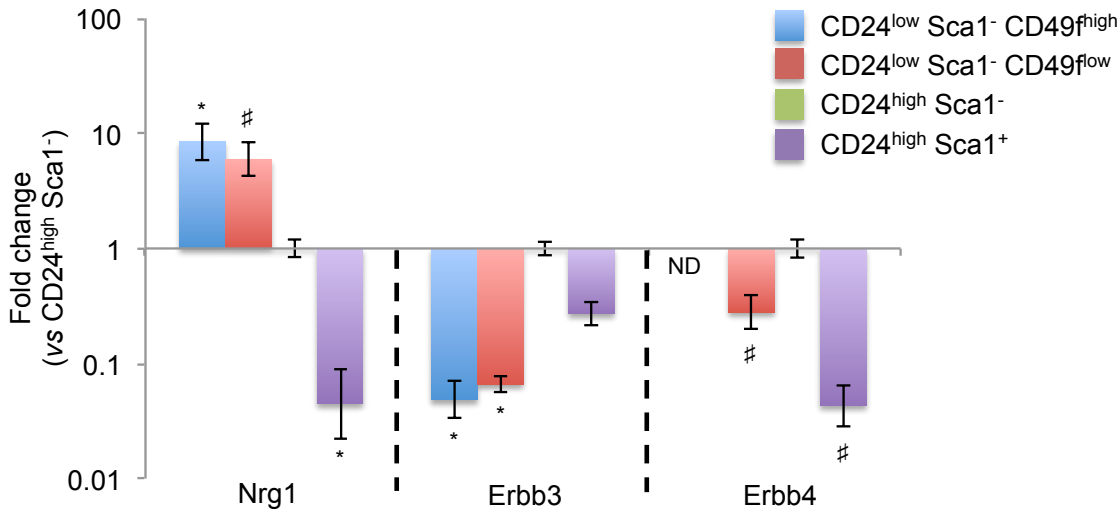

Appendix I-2 Neuregulin 1 and its receptors Erbb3 and Erbb4 are expressed in distinct mammary cell populations.

Mammary epithelial cell populations were FACS sorted using a panel of antibodies: $CD24^{low}$ Sca-1^{-} $CD49f^{high}$ (stem cell enriched fraction), $CD24^{low}$ Sca-1^{-} $CD49f^{low}$ (myoepithelial cell population), $CD24^{high}$ Sca-1^{-} (luminal estrogen receptor negative cells) and $CD24^{high}$ Sca-1^{+} (luminal estrogen receptor positive cells). Expression of Neuregulin 1, Erbb3 and Erbb4 was evaluated by quantitative RT-PCR (n=3 independent experiments). Fold expression±95% confidence over the comparator population ($CD24^{high}Sca1^{-}$). ND, no expression of Erbb4 detected. *, $p < 0.05$; ♯, $0.05 < p < 0.1$ (vs $CD24^{high}$ $Sca1^{-}$), unpaired Student T test.

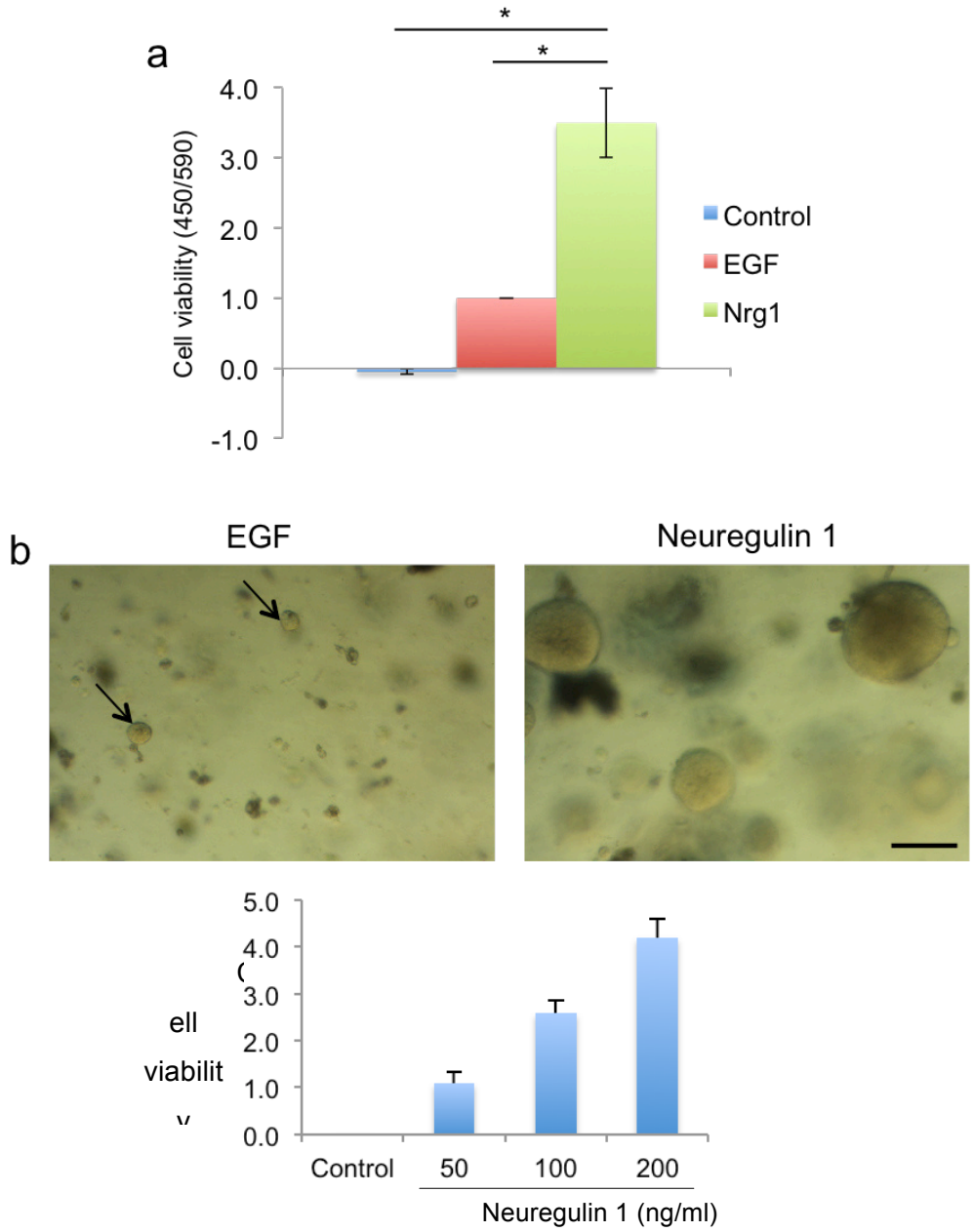

Appendix I-3 Neuregulin 1 increases the growth of mammary organoids compared to EGF.

(a) Mammary epithelial cells were freshly isolated, embedded in matrigel and exposed to culture medium containing Noggin (100ng/ml), EGF (100 ng/ml) or Neuregulin 1 (100ng/ml) for 15 days. The number of viable cells (Wst assay) was evaluated (n=3, means±standard deviation.). *, $p < 0.05$, paired Student T test. (b) Representative pictures of mammary organoids treated with culture medium containing Noggin (100ng/ml), EGF (100 ng/ml) or Neuregulin 1 (100ng/ml) for 15 days. Scale bar, 50 µm. (c) The number of viable cells (Wst assay) was evaluated (n=3, means ±standard deviation) under increasing concentrations of Nrg1 in culture. *, $p< 0.05$, paired student T-test.

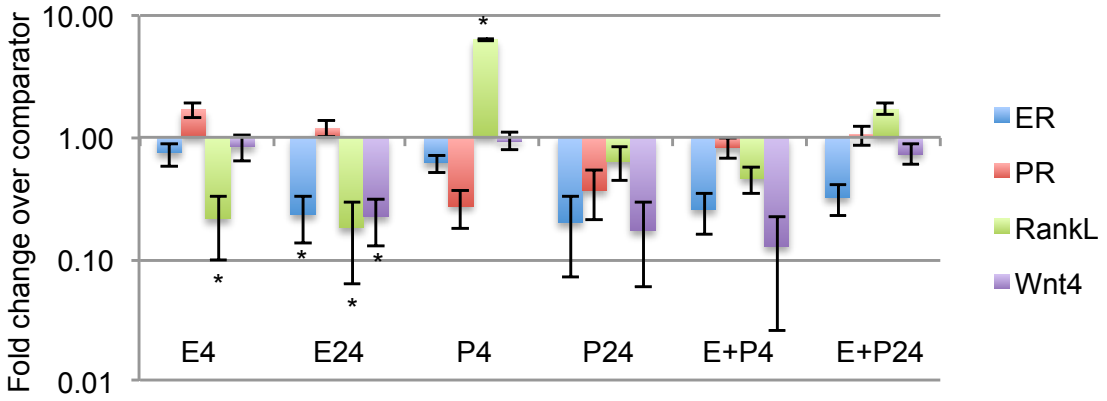

Appendix I-4 Mammary organoids exhibit normal responses to steroid hormones after 30 days in culture.

Expression of ER, PR, RankL and Wnt4 following treatment with progesterone (P, 40ng/ml), estrogen (E, 4ng/ml) or both hormones. Mammary organoids cultured for 30 days were treated for 4 and 24 hours and gene expression evaluated by quantitative RT-PCR. Data are expressed as fold change (*vs* untreated, n=3, means±standard deviation.). *, $p < 0.05$, paired Student T test.

9.2 Appendix II: Single Wnt inhibitor titration studies

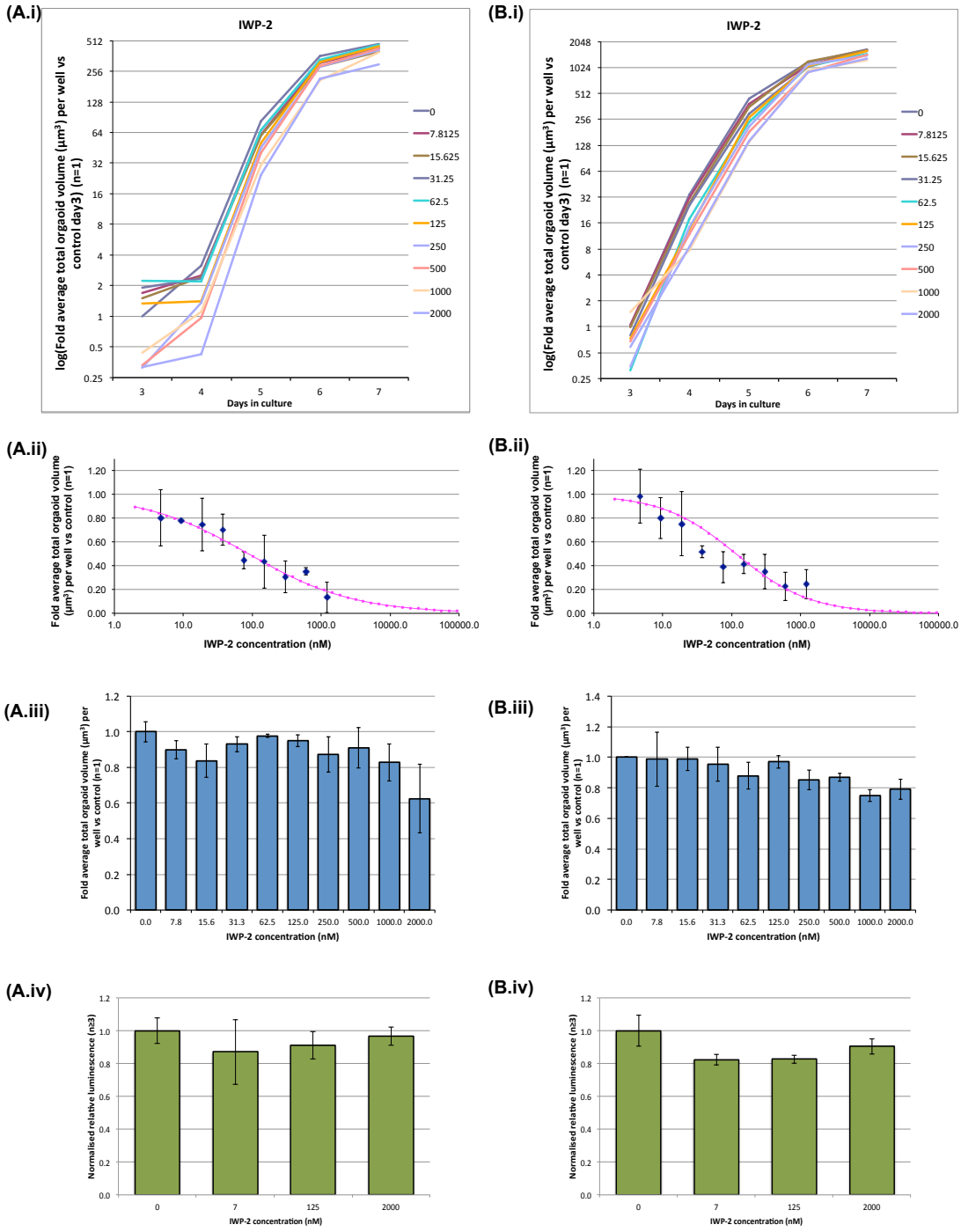

Appendix II-1 Analysis of the effects of IWP-2 on T1 tumour organoid growth.

Freshly trypsinised T1 tumour cells were seeded at 1000 per µl Matrigel and overlaid with media containing **(A)** Neuregulin (100 ng/ml), Noggin (100 ng/ml) and R-Spondin (2.65625 ng/ml); or **(B)** EGF (50 ng/ml), Noggin (100 ng/ml) and R-Spondin (42.5 ng.ml), supplemented with either a set concentration of IWP-2 from a two fold titration range (7.8nM – 2000 nM), or a matched DMSO control.

(i) Growth curves from days 3 to 7 in culture. Organoid volume was measured daily using GelCountTM analysis software under the IWP-2 titration range, expressed here as log fold vs control at day 3 values (n=1). **(ii)** IC_{50} best fit curves were generated at day 4 of culture, and **(iii)** Fold total organoid volume (vs control) graphs at day 7 (mean ±standard deviation, NRL n=1, ERH n=1). **(iv)** Endpoint Cell Titer Glo 3D viability (mean ± standard deviation, n=1) measurements.

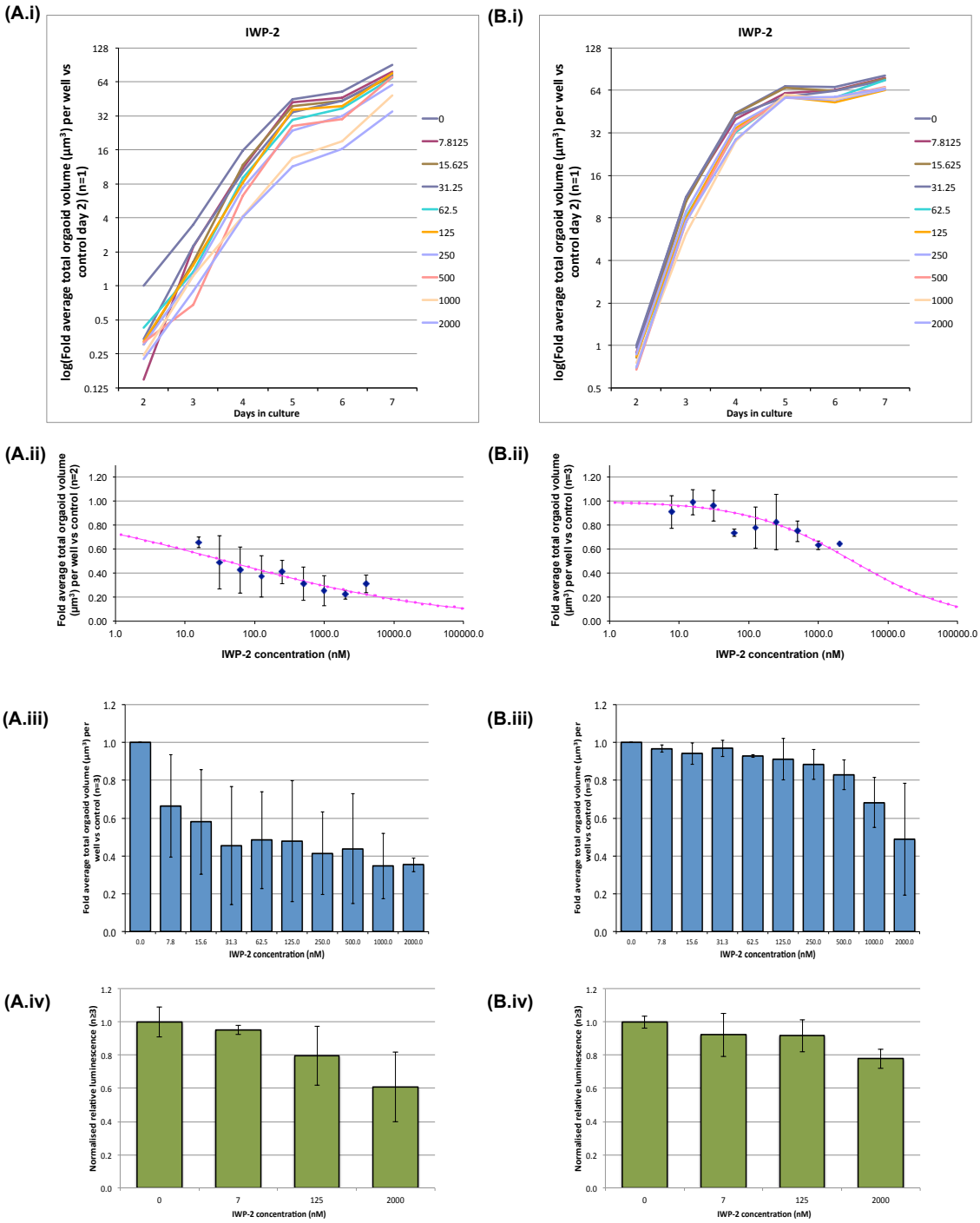

Appendix II-2. Analysis of the effects of IWP-2 on MMTV-Wnt1 tumour organoid growth.

Freshly trypsinised MMTV-Wnt1 tumour cells were seeded at 750 per µl Matrigel and overlaid with media containing **(A)** Neuregulin (100 ng/ml), Noggin (100 ng/ml) and R-Spondin (2.65625 ng/ml); or **(B)** EGF (50 ng/ml), Noggin (100 ng/ml) and R-Spondin (42.5 ng.ml), supplemented with either a set concentration of IWP-2 from a two fold titration range (7.8nM – 2000 nM), or a matched DMSO control.

(i) Growth curves from days 2 to 7 in culture. Organoid volume was measured daily using GelCountTM analysis software under the IWP-2 titration range, expressed here as log fold vs control at day 2 values (n=1). **(ii)** IC_{50} best fit curves were generated at day 4 of culture, and **(iii)** Fold total organoid volume (vs control) graphs at day 7 (mean ±standard deviation, NRL n=3, ERH n=3). **(iv)** Endpoint Cell Titer Glo 3D viability (mean ± standard deviation, n=1) measurements.

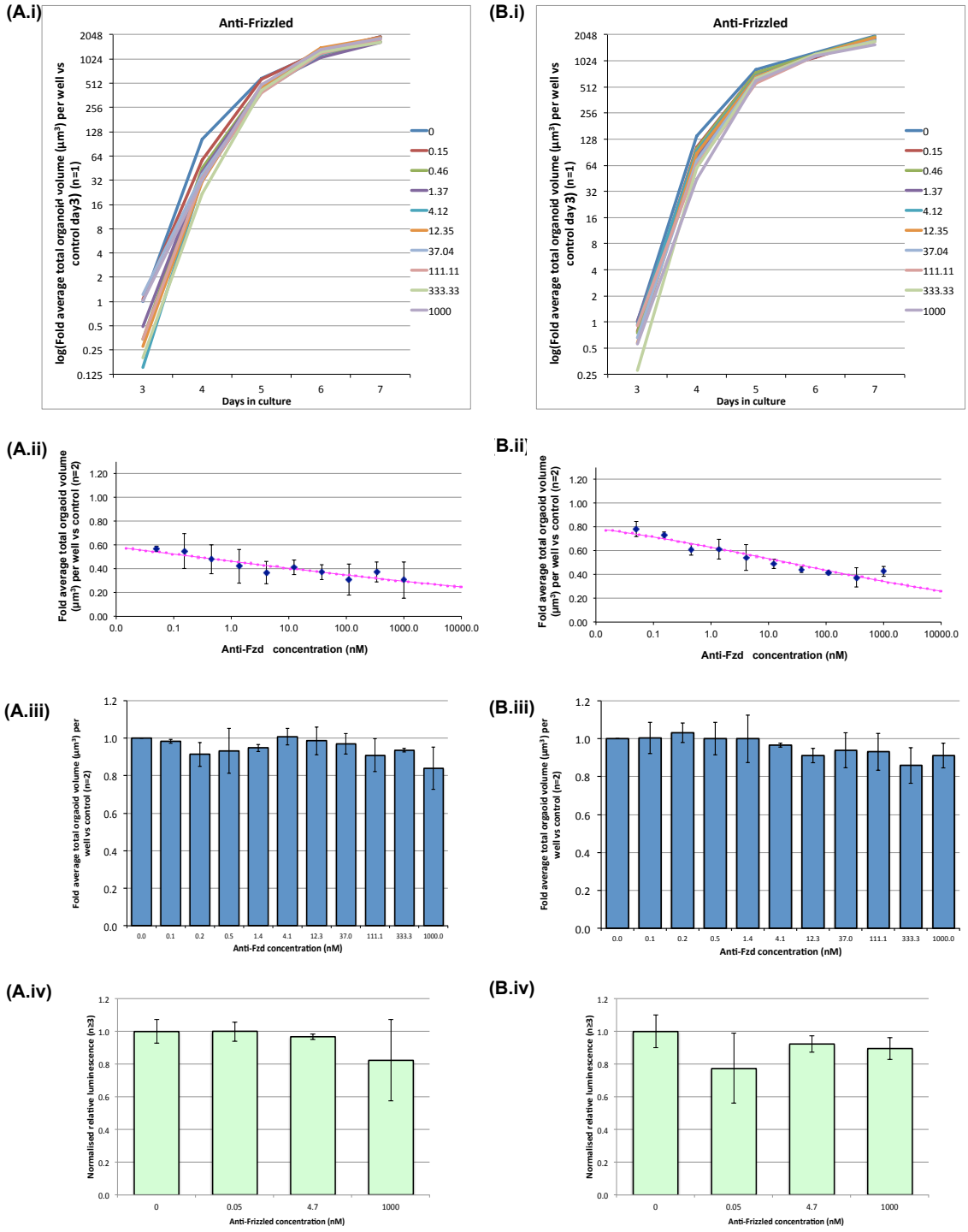

Appendix II-3. Analysis of the effects of Anti-Fzd on T1 tumour organoid growth.

Freshly trypsinised T1 tumour cells were seeded at 1000 per µl Matrigel and overlaid with media containing **(A)** Neuregulin (100 ng/ml), Noggin (100 ng/ml) and R-Spondin (2.65625 ng/ml); or **(B)** EGF (50 ng/ml), Noggin (100 ng/ml) and R-Spondin (42.5 ng.ml), supplemented with either a set concentration of Anti-Fzd antibody from a two fold titration range (0.05 nM – 1000 nM), or a matched PBS control.

(i) Growth curves from days 3 to 7 in culture. Organoid volume was measured daily using GelCountTM analysis software under the Anti-Fzd titration range, expressed here as log fold vs control at day 3 values (n=1). **(ii)** IC_{50} best fit curves were generated at day 4 of culture, and **(iii)** Fold total organoid volume (vs control) graphs at day 7 (mean ±standard deviation, NRL n=2, ERH n=2). **(iv)** Endpoint Cell Titer Glo 3D viability (mean ± standard deviation, n=1) measurements.

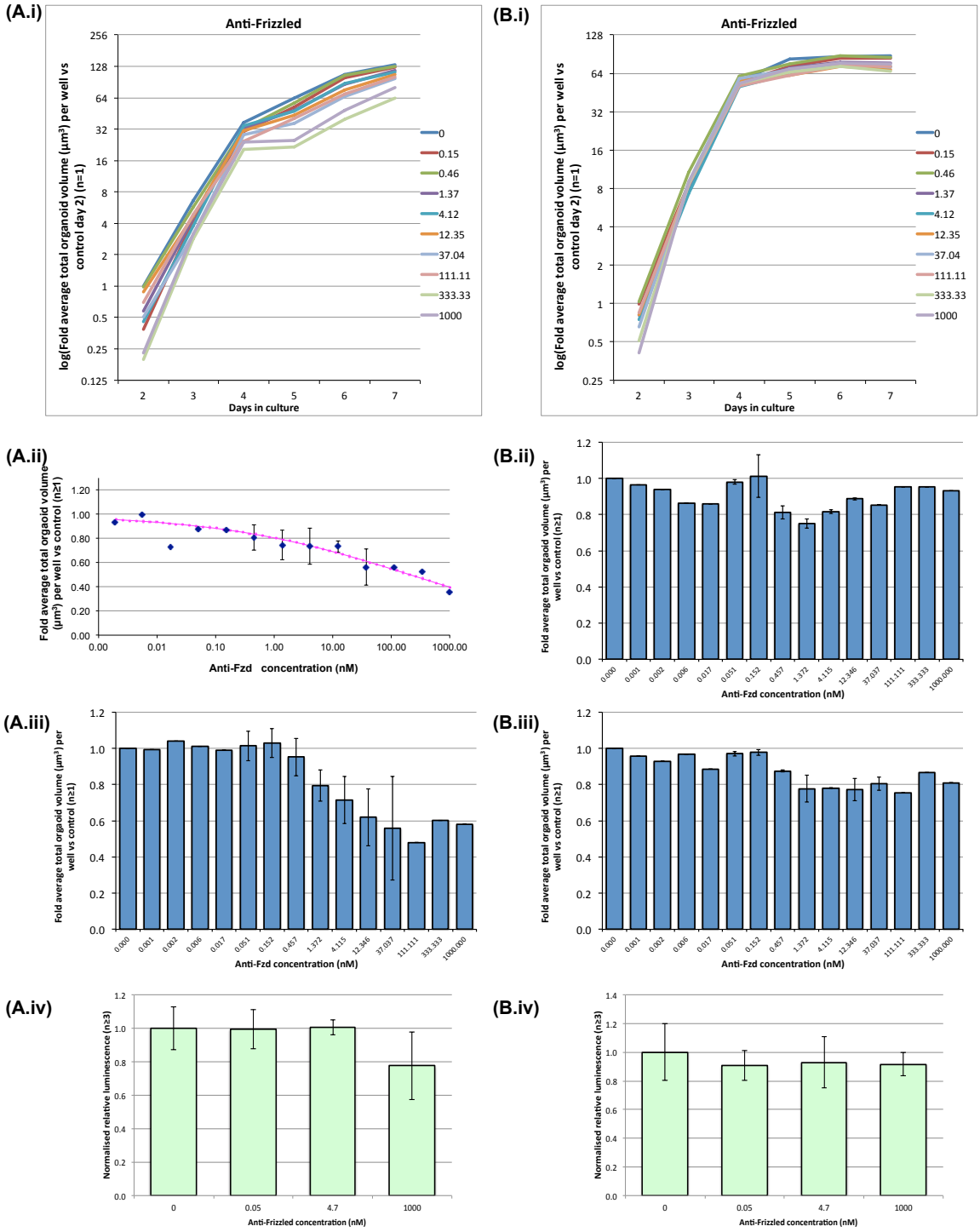

Appendix II-4. Analysis of the effects of Anti-Fzd on MMTV-Wnt1 tumour organoid growth.

Freshly trypsinised MMTV-Wnt1 tumour cells were seeded at 750 per µl Matrigel and overlaid with media containing **(A)** Neuregulin (100 ng/ml), Noggin (100 ng/ml) and R-Spondin (2.65625 ng/ml); or **(B)** EGF (50 ng/ml), Noggin (100 ng/ml) and R-Spondin (42.5 ng.ml), supplemented with either a set concentration of Anti-Fzd antibody from a two fold titration range (0.05nM – 1000 nM), or a matched PBS control.

(i) Growth curves from days 2 to 7 in culture. Organoid volume was measured daily using GelCountTM analysis software under the Anti-Fzd titration range, expressed here as log fold vs control at day 2 values (n=1). **(ii)** IC_{50} best fit curves were generated at day 4 of culture, and **(iii)** Fold total organoid volume (vs control) graphs at day 7 (mean ± standard deviation, NRL n=2, ERH n=2). **(iv)** Endpoint Cell Titer Glo 3D viability (mean ± standard deviation, n=1) measurements.

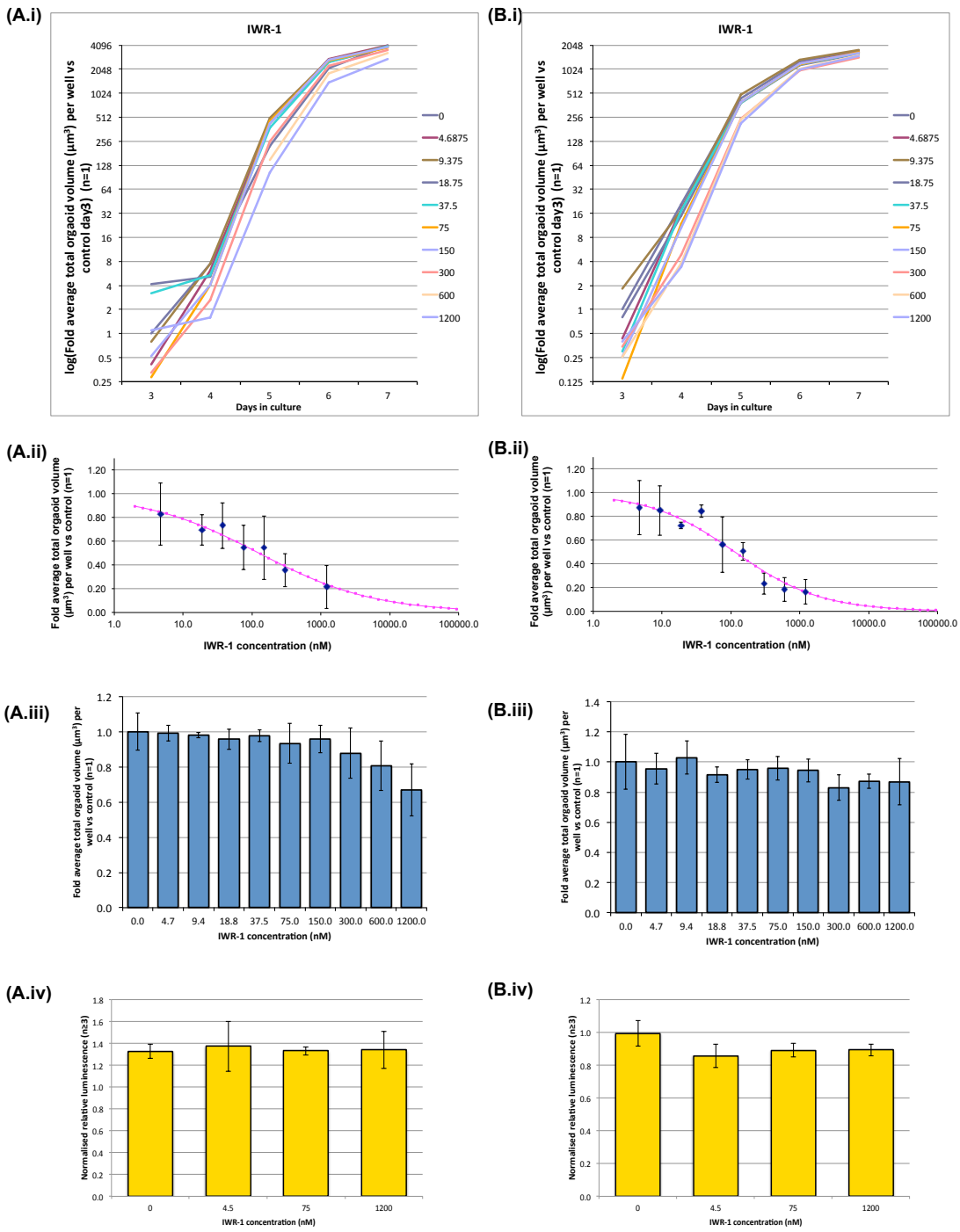

Appendix II-5 Analysis of the effects of IWR-1 on T1 tumour organoid growth.

Freshly trypsinised T1 tumour cells were seeded at 1000 per µl Matrigel and overlaid with media containing **(A)** Neuregulin (100 ng/ml), Noggin (100 ng/ml) and R-Spondin (2.65625 ng/ml); or **(B)** EGF (50 ng/ml), Noggin (100 ng/ml) and R-Spondin (42.5 ng.ml), supplemented with either a set concentration of IWR-1 from a two fold titration range (4.7 – 1200 nM), or a matched DMSO control.

(i) Growth curves from days 3 to 7 in culture. Organoid volume was measured daily using GelCountTM analysis software under the IWR-1 titration range, expressed here as log fold vs control at day 3 values (n=1). **(ii)** IC_{50} best fit curves were generated at day 4 of culture, and **(iii)** Fold total organoid volume (vs control) graphs at day 7 (mean ±standard deviation, NRL n=1, ERH n=1). **(iv)** Endpoint Cell Titer Glo 3D viability (mean ± standard deviation, n=1) measurements.

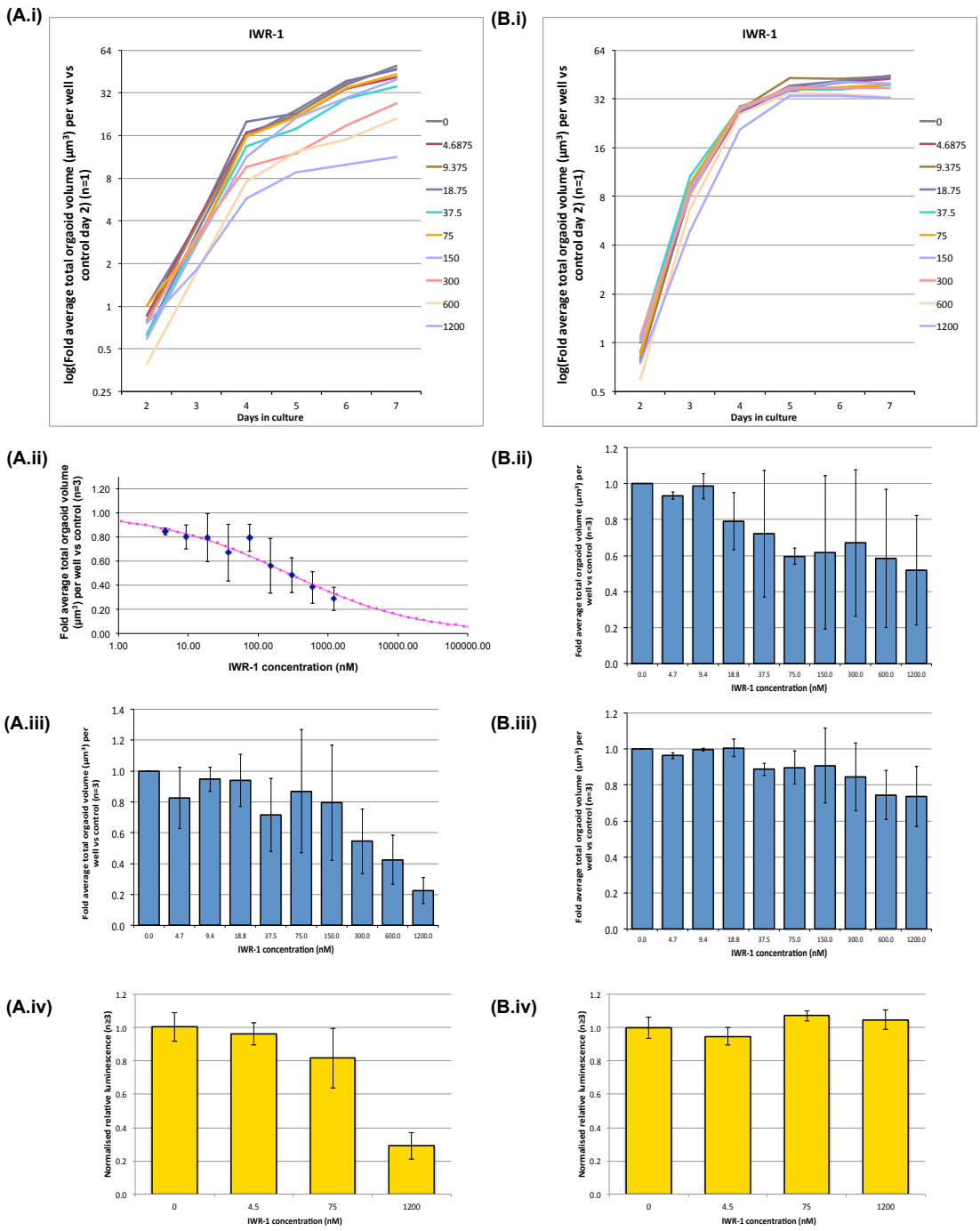

Appendix II-6 Analysis of the effects of IWR-1 on MMTV-Wnt1 tumour organoid growth.

Freshly trypsinised MMTV-Wnt1 tumour cells were seeded at 750 per µl Matrigel and overlaid with media containing **(A)** Neuregulin (100 ng/ml), Noggin (100 ng/ml) and R-Spondin (2.65625 ng/ml); or **(B)** EGF (50 ng/ml), Noggin (100 ng/ml) and R-Spondin (42.5 ng.ml), supplemented with either a set concentration of IWR-1 from a two fold titration range (4.7nM-1200 nM), or a matched DMSO control.

(i) Growth curves from days 2 to 7 in culture. Organoid volume was measured daily using GelCountTM analysis software under the IWR-1 titration range, expressed here as log fold vs control at day 2 values (n=1). **(ii)** IC_{50} best fit curves or fold total organoid volume (vs control) graphs were generated at day 4 of culture, and **(iii)** Fold total organoid volume (vs control) graphs at day 7 (mean ±standard deviation, NRL n=3, ERH n=3). **(iv)** Endpoint Cell Titer Glo 3D viability (mean ± standard deviation, n=1) measurements.

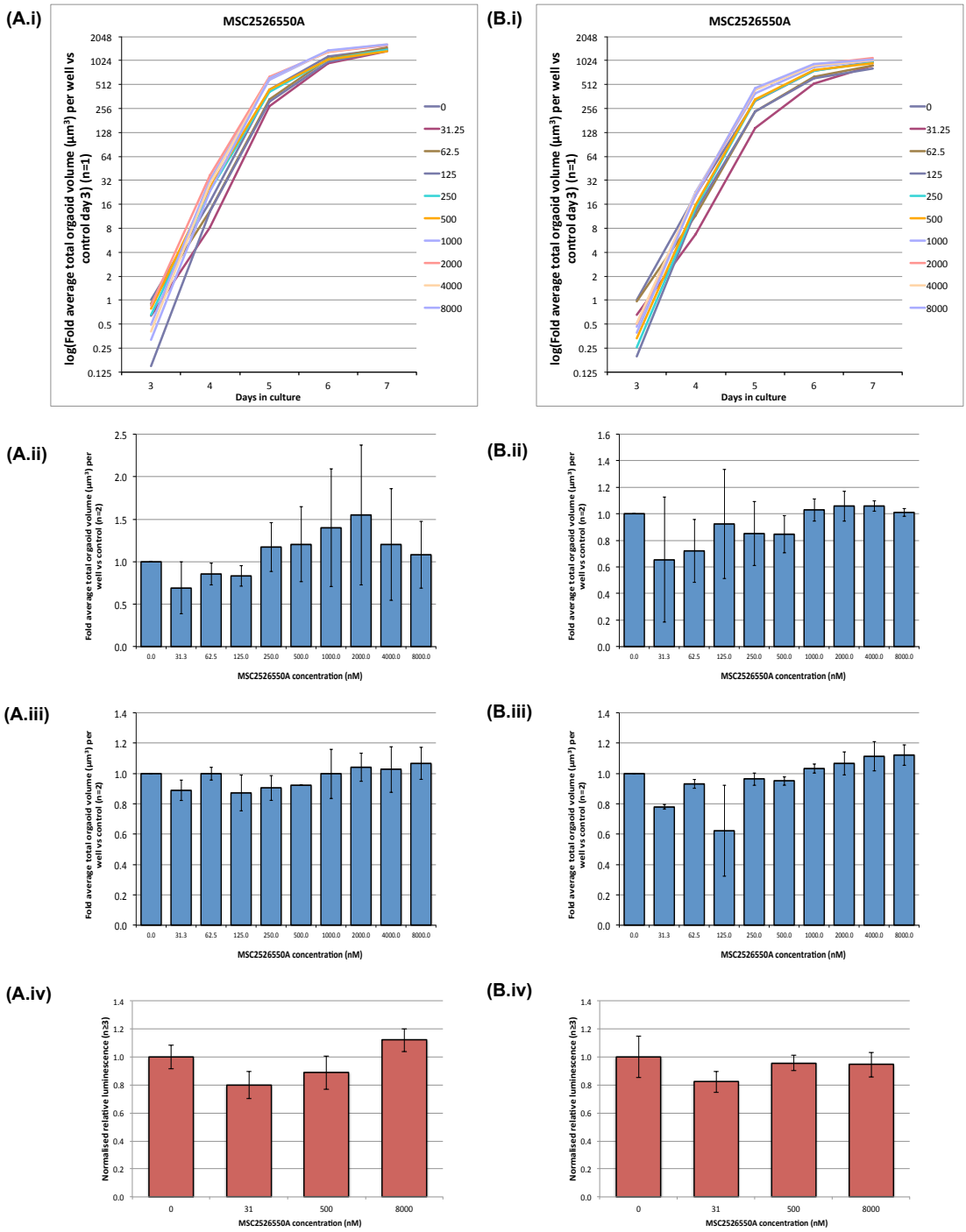

Appendix II-7 Analysis of the effects of MSC2526550-A on T1 tumour organoid growth.

Freshly trypsinised T1 tumour cells were seeded at 1000 per µl Matrigel and overlaid with media containing **(A)** Neuregulin (100 ng/ml), Noggin (100 ng/ml) and R-Spondin (2.65625 ng/ml); or **(B)** EGF (50 ng/ml), Noggin (100 ng/ml) and R-Spondin (42.5 ng.ml), supplemented with either a set concentration of MSC2526550-A from a two fold titration range (31.25nM – 8000 nM), or a matched DMSO control.

(i) Growth curves from days 3 to 7 in culture. Organoid volume was measured daily using GelCountTM analysis software under the MSC2526550-A titration range, expressed here as log fold vs control at day 3 values (n=1). **(ii)** Fold total organoid volume (vs control) graphs were generated at day 4 of culture, and **(iii)** at day 7 (mean ±standard deviation, NRL n=2, ERH n=2). **(iv)** Endpoint Cell Titer Glo 3D viability (mean ± standard deviation, n=1) measurements.

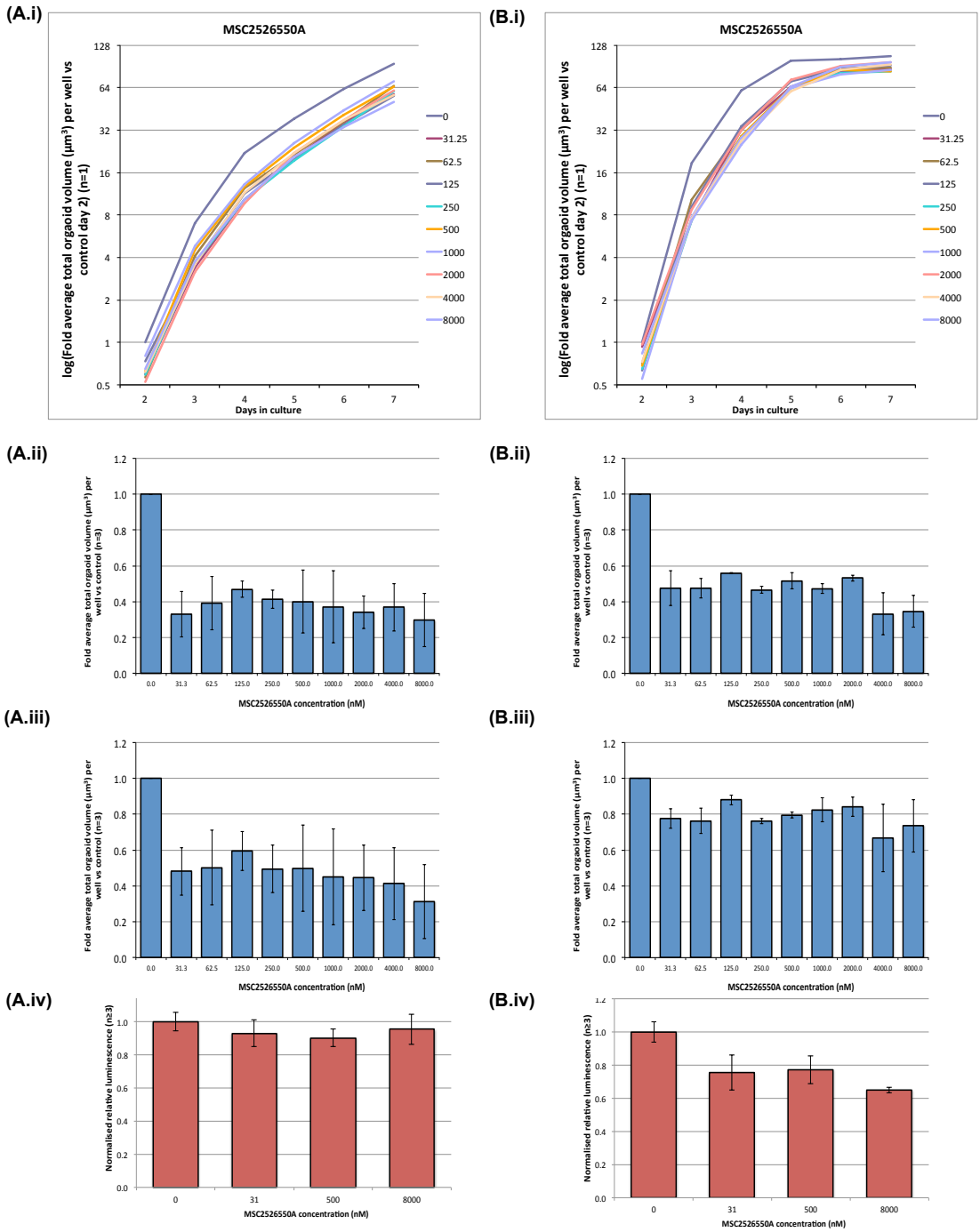

Appendix II-8 Analysis of the effects of MSC2526550-A on MMTV-Wnt1 tumour organoid growth.

Freshly trypsinised MMTV-Wnt1 tumour cells were seeded at 750 per µl Matrigel and overlaid with media containing **(A)** Neuregulin (100 ng/ml), Noggin (100 ng/ml) and R-Spondin (2.65625 ng/ml); or **(B)** EGF (50 ng/ml), Noggin (100 ng/ml) and R-Spondin (42.5 ng.ml), supplemented with either a set concentration of MSC2526550-A from a two fold titration range (32.5nM-8000 nM), or a matched DMSO control.
(i) Growth curves from days 2 to 7 in culture. Organoid volume was measured daily using GelCountTM analysis software under the MSC2526550-A titration range, expressed here as log fold vs control at day 2 values (n=1). **(ii)** Fold total organoid volume (vs control) graphs were generated at day 4 of culture and **(iii)** at day 7 (mean ±standard deviation, NRL n=3, ERH n=3). **(iv)** Endpoint Cell Titer Glo 3D viability (mean ± standard deviation, n=1) measurements.

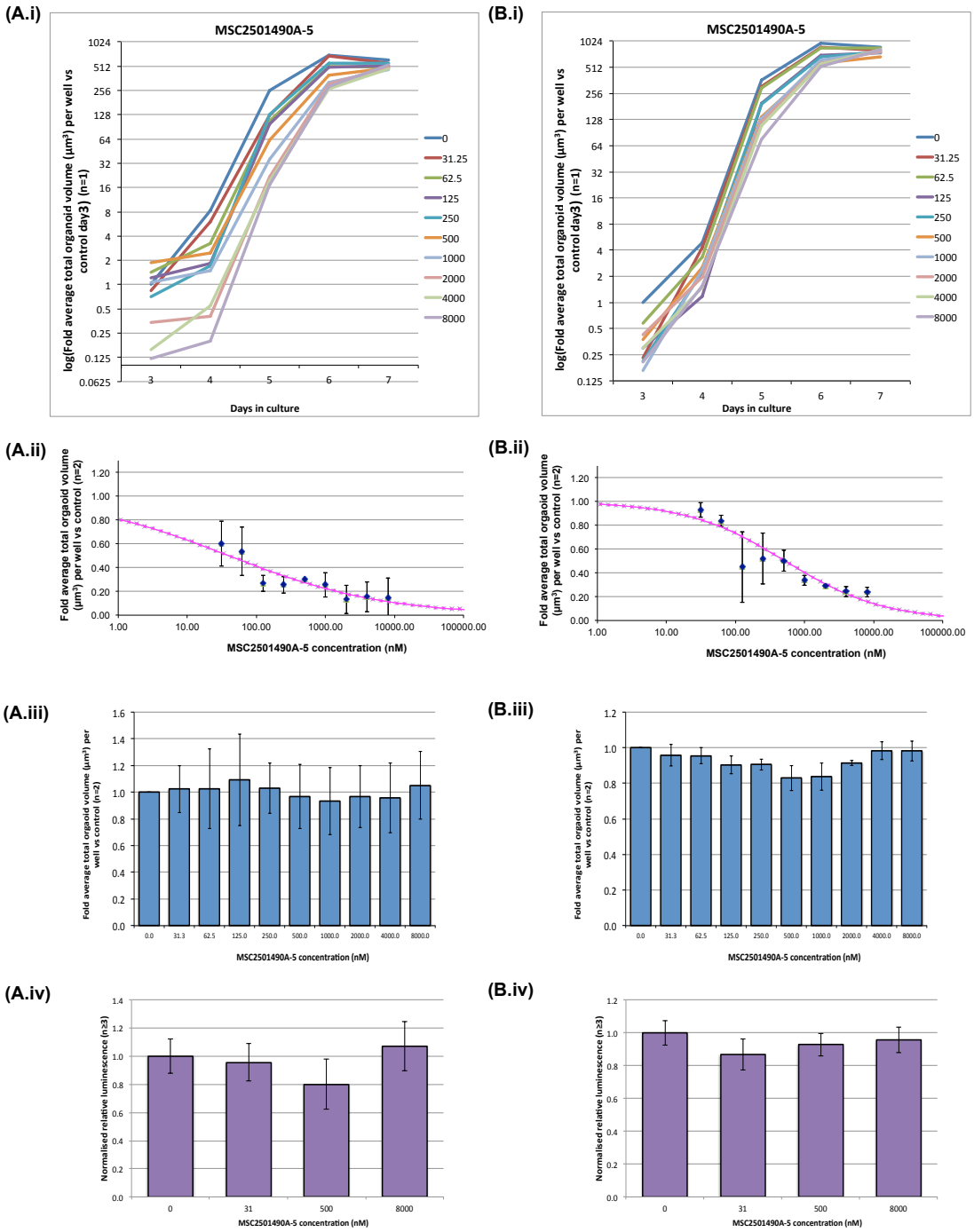

Appendix II-9 Analysis of the effects of MSC2501490A-5 on T1 tumour organoid growth.

Freshly trypsinised T1 tumour cells were seeded at 1000 per µl Matrigel and overlaid with media containing **(A)** Neuregulin (100 ng/ml), Noggin (100 ng/ml) and R-Spondin (2.65625 ng/ml); or **(B)** EGF (50 ng/ml), Noggin (100 ng/ml) and R-Spondin (42.5 ng.ml), supplemented with either a set concentration of MSC2501490A-5 from a two fold titration range (31.25nM – 8000 nM), or a matched DMSO control.
(i) Growth curves from days 3 to 7 in culture. Organoid volume was measured daily using GelCountTM analysis software under the MSC2501490A-5 titration range, expressed here as log fold vs control at day 3 values (n=1). **(ii)** IC_{50} best fit curves were generated at day 4 of culture and **(iii)** Fold total organoid volume (vs control) graphs at day 7 (mean ±standard deviation, NRL n=2, ERH n=2). **(iv)** Endpoint Cell Titer Glo 3D viability (mean ± standard deviation, n=1) measurements.

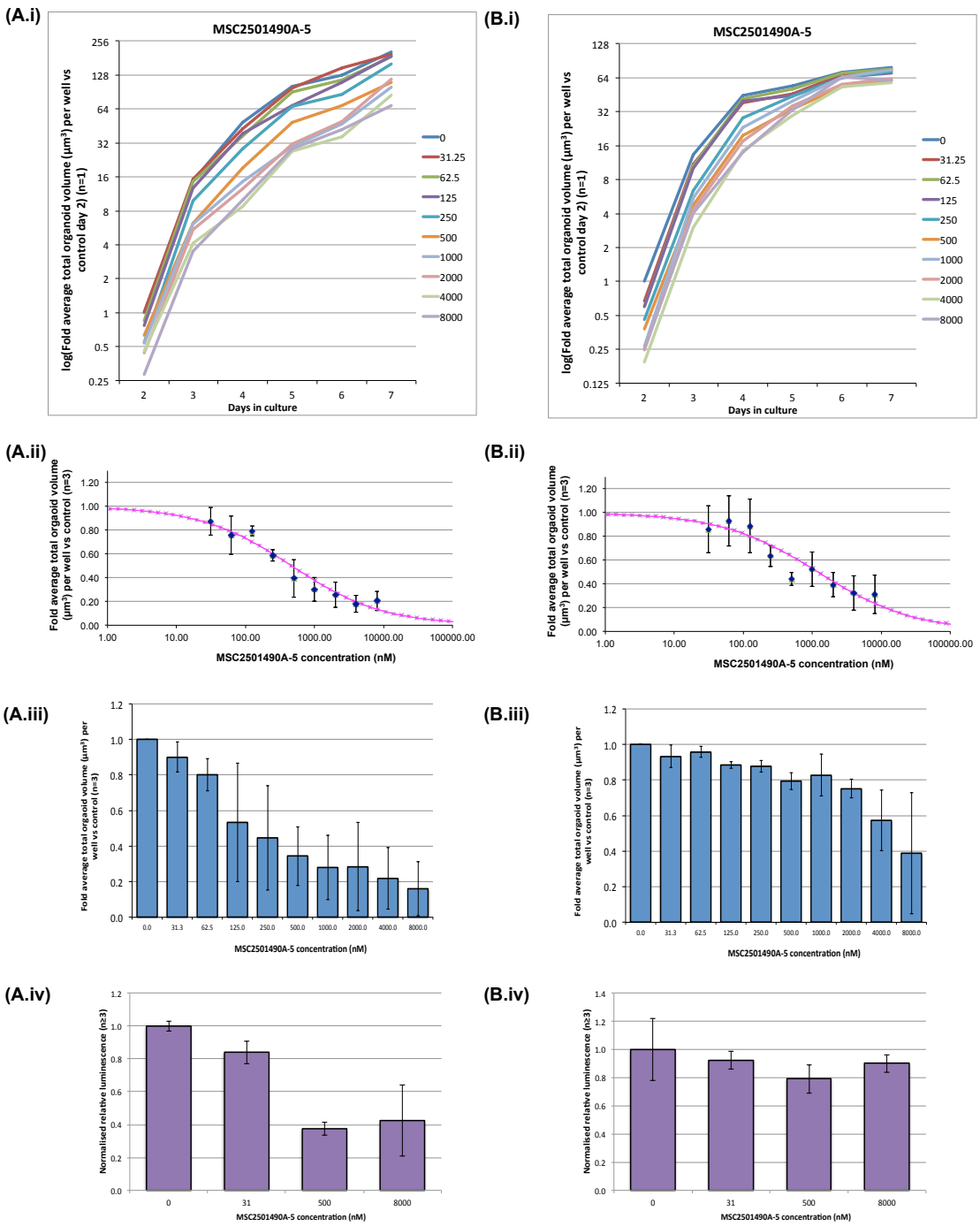

Appendix II-10 Analysis of the effects of MSC2501490A-5 on MMTV-Wnt1 tumour organoid growth.

Freshly trypsinised MMTV-Wnt1 tumour cells were seeded at 750 per µl Matrigel and overlaid with media containing **(A)** Neuregulin (100 ng/ml), Noggin (100 ng/ml) and R-Spondin (2.65625 ng/ml); or **(B)** EGF (50 ng/ml), Noggin (100 ng/ml) and R-Spondin (42.5 ng.ml), supplemented with either a set concentration of MSC2501490A-5 from a two fold titration range (32.5nM-8000 nM), or a matched DMSO control.
(i) Growth curves from days 2 to 7 in culture. Organoid volume was measured daily using GelCountTM analysis software under the MSC2501490A-5 titration range, expressed here as log fold vs control at day 2 values (n=1). **(ii)** IC_{50} best fit curves were generated at day 4 of culture and **(iii)** Fold total organoid volume (vs control) graphs at day 7 (mean ±standard deviation, NRL n=3, ERH n=3). **(iv)** Endpoint Cell Titer Glo 3D viability (mean ± standard deviation, n=1) measurements.

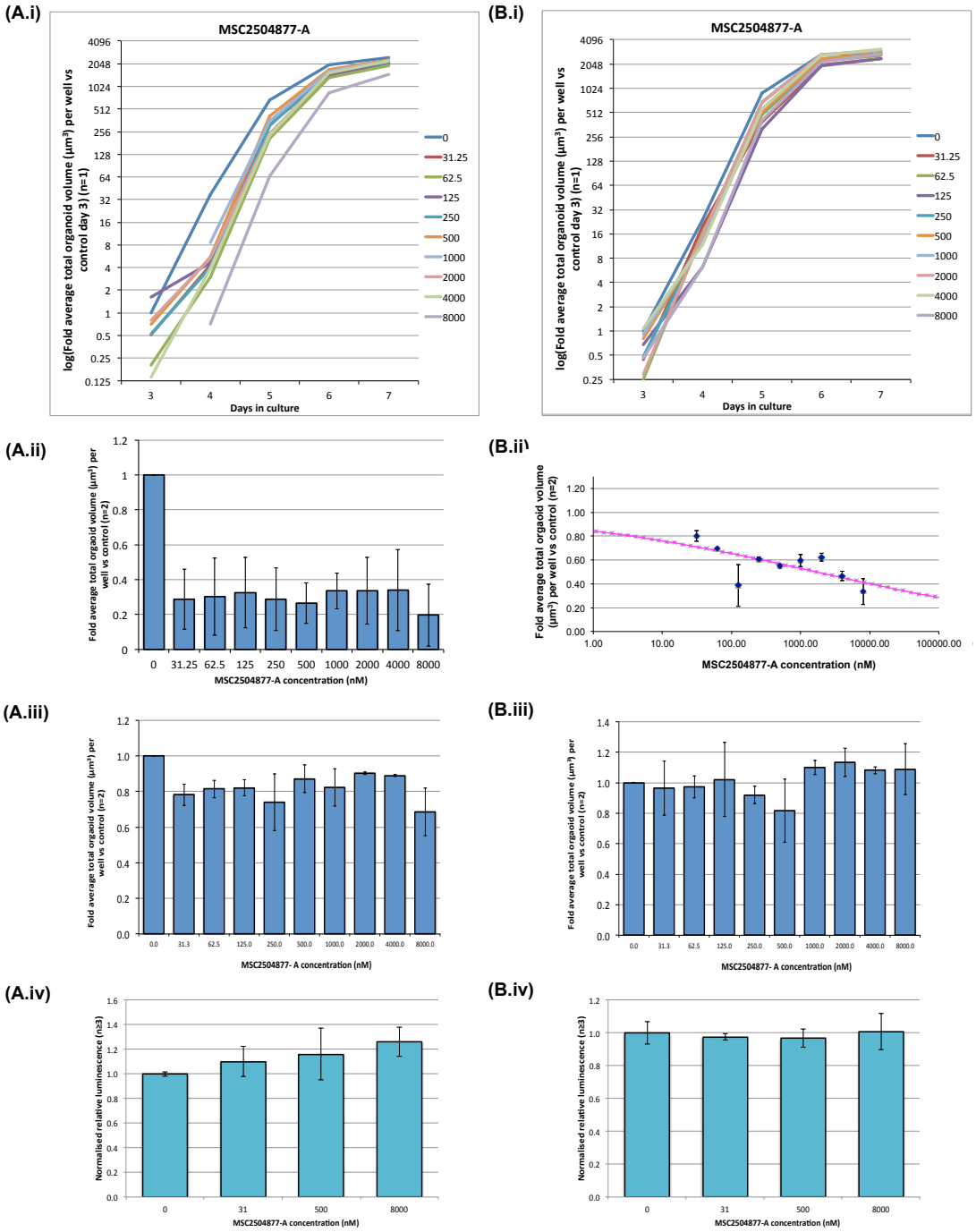

Appendix II-11 Analysis of the effects of MSC2504877-A on T1 tumour organoid growth.

Freshly trypsinised T1 tumour cells were seeded at 1000 per µl Matrigel and overlaid with media containing **(A)** Neuregulin (100 ng/ml), Noggin (100 ng/ml) and R-Spondin (2.65625 ng/ml); or **(B)** EGF (50 ng/ml), Noggin (100 ng/ml) and R-Spondin (42.5 ng.ml), supplemented with either a set concentration of MSC2504887-A from a two fold titration range (31.25nM – 8000 nM), or a matched DMSO control.

(i) Growth curves from days 3 to 7 in culture. Organoid volume was measured daily using GelCountTM analysis software under the MSC2504877-A titration range, expressed here as log fold vs control at day 3 values (n=1). **(ii)** Fold total organoid volume (vs control) graphs or IC_{50} best fit curves were generated at day 4 of culture and **(iii)** Fold total organoid volume (vs control) graphs at day 7 (mean ±standard deviation, NRL n=2, ERH n=2). **(iv)** Endpoint Cell Titer Glo 3D viability (mean ± standard deviation, n=1) measurements.

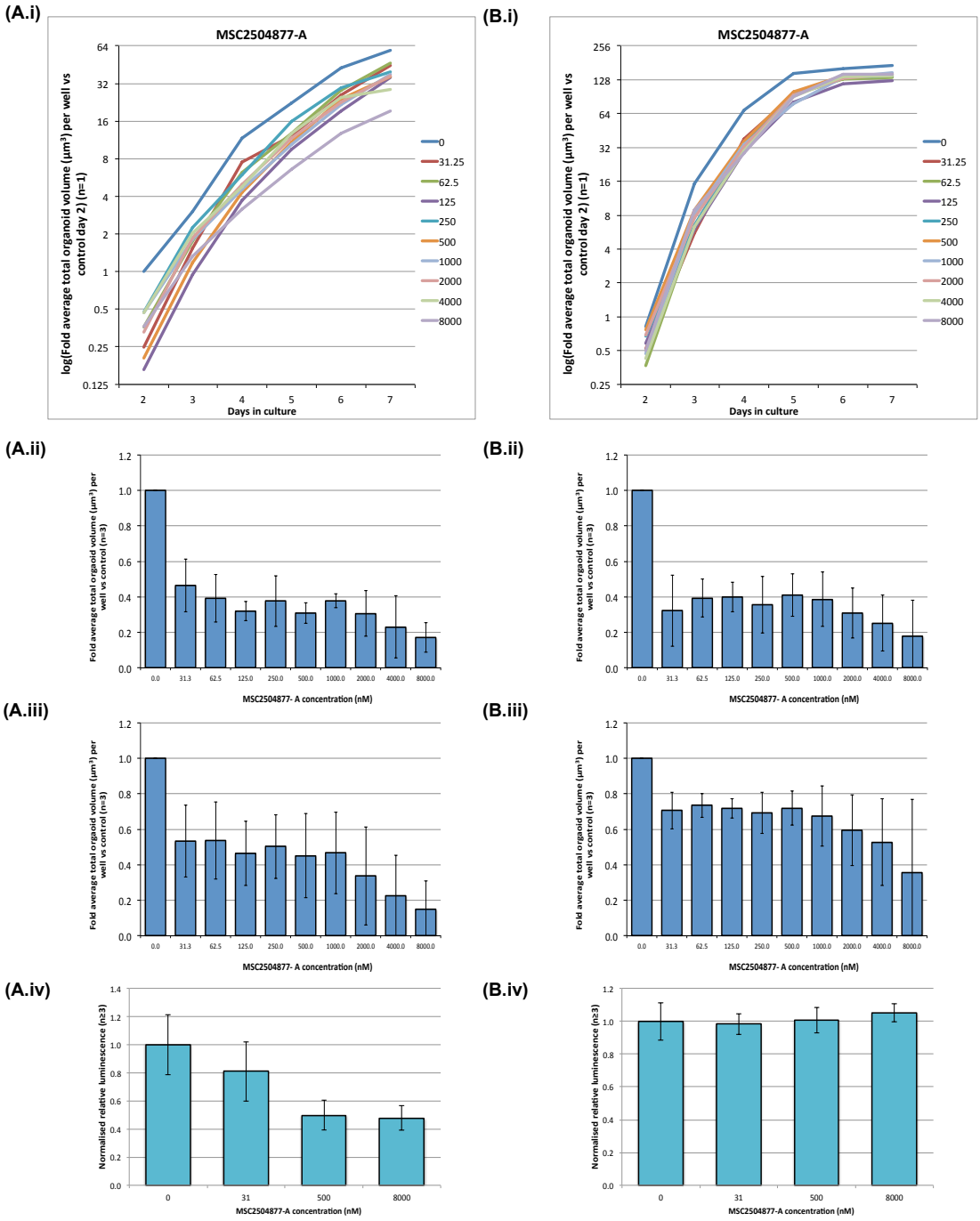

Appendix II-12 Analysis of the effects of MSC2504877-A on MMTV-Wnt1 tumour organoid growth.

Freshly trypsinised MMTV-Wnt1 tumour cells were seeded at 750 per µl Matrigel and overlaid with media containing **(A)** Neuregulin (100 ng/ml), Noggin (100 ng/ml) and R-Spondin (2.65625 ng/ml); or **(B)** EGF (50 ng/ml), Noggin (100 ng/ml) and R-Spondin (42.5 ng.ml), supplemented with either a set concentration of MSC2504877-A from a two fold titration range (32.5nM-8000 nM), or a matched DMSO control.
(i) Growth curves from days 2 to 7 in culture. Organoid volume was measured daily using GelCountTM analysis software under the MSC2504877-A titration range, expressed here as log fold vs control at day 2 values (n=1). **(ii)** Fold total organoid volume (vs control) graphs were generated at day 4 of culture and **(iii)** at day 7 (mean ±standard deviation, NRL n=3, ERH n=3). **(iv)** Endpoint Cell Titer Glo 3D viability (mean ± standard deviation, n=1) measurements.

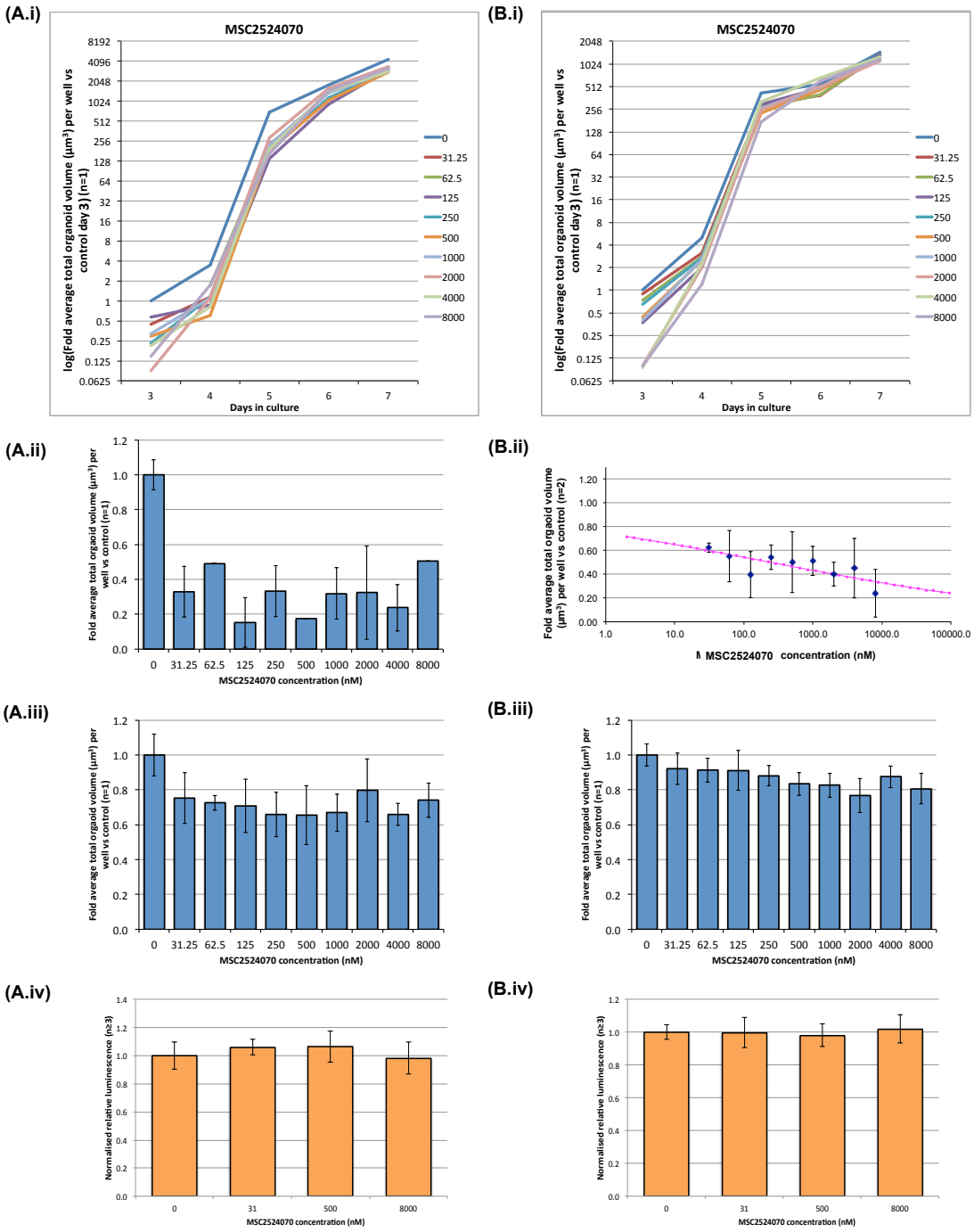

Appendix II-13 Analysis of the effects of MSC2524070 on T1 tumour organoid growth.

Freshly trypsinised T1 tumour cells were seeded at 1000 per µl Matrigel and overlaid with media containing **(A)** Neuregulin (100 ng/ml), Noggin (100 ng/ml) and R-Spondin (2.65625 ng/ml); or **(B)** EGF (50 ng/ml), Noggin (100 ng/ml) and R-Spondin (42.5 ng.ml), supplemented with either a set concentration of MSC2524070 from a two fold titration range (31.25nM – 8000 nM), or a matched DMSO control.

(i) Growth curves from days 3 to 7 in culture. Organoid volume was measured daily using GelCountTM analysis software under the MSC2524070 titration range, expressed here as log fold vs control at day 3 values (n=1). **(ii)** Fold total organoid volume (vs control) graphs or IC_{50} best fit curves were generated at day 4 of culture and **(iii)** Fold total organoid volume (vs control) graphs at day 7 (mean ±standard deviation, NRL n=1, ERH n=1). **(iv)** Endpoint Cell Titer Glo 3D viability (mean ± standard deviation, n=1) measurements.

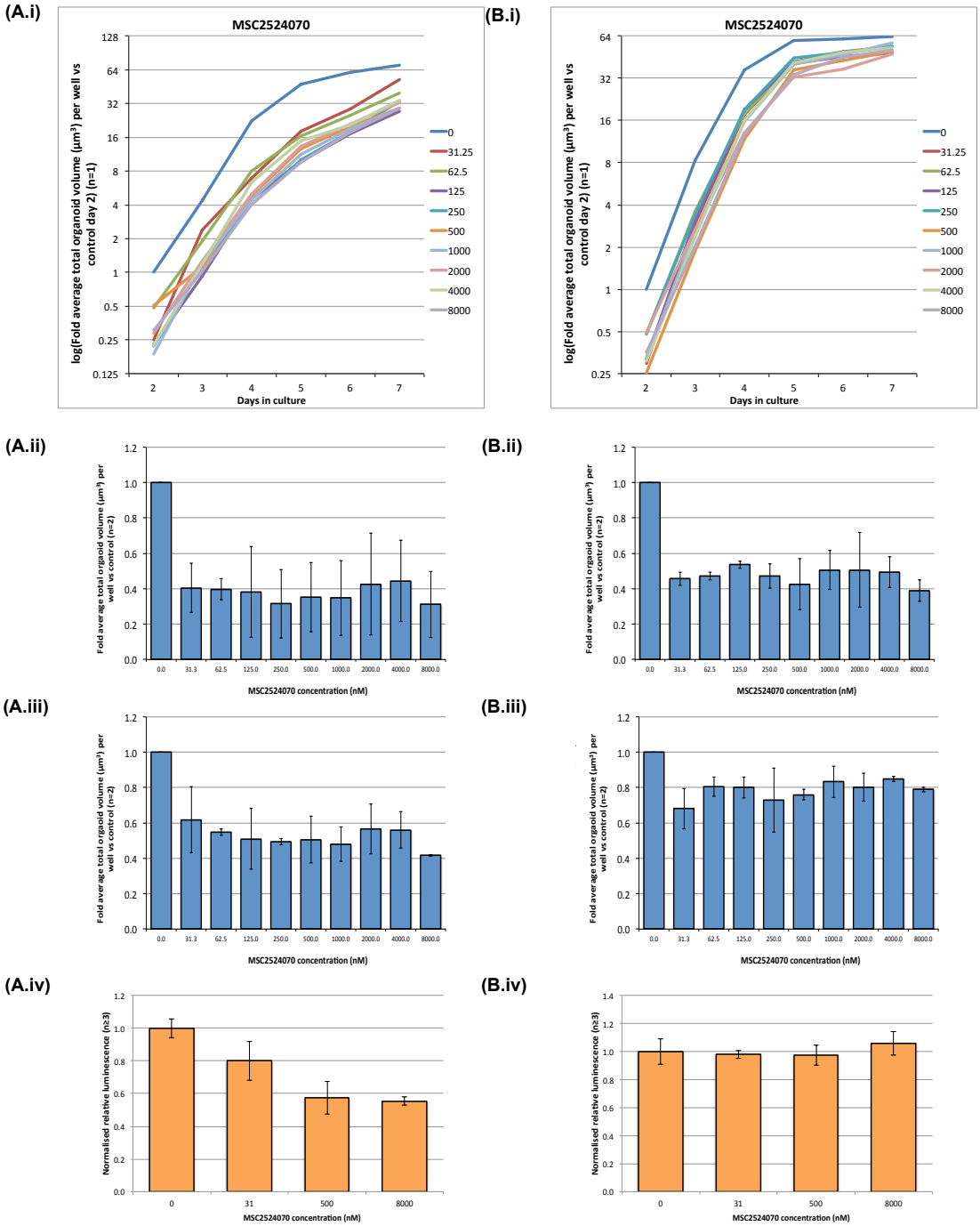

Appendix II-14 Analysis of the effects of MSC2524070 on MMTV-Wnt1 tumour organoid growth.

Freshly trypsinised MMTV-Wnt1 tumour cells were seeded at 750 per µl Matrigel and overlaid with media containing **(A)** Neuregulin (100 ng/ml), Noggin (100 ng/ml) and R-Spondin (2.65625 ng/ml); or **(B)** EGF (50 ng/ml), Noggin (100 ng/ml) and R-Spondin (42.5 ng.ml), supplemented with either a set concentration of MSC2524070 from a two fold titration range (32.5nM-8000 nM), or a matched DMSO control.

(i) Growth curves from days 2 to 7 in culture. Organoid volume was measured daily using GelCountTM analysis software under the MSC2524070 titration range, expressed here as log fold vs control at day 2 values (n=1). **(ii)** Fold total organoid volume (vs control) graphs were generated at day 4 of culture and **(iii)** at day 7 (mean ±standard deviation, NRL n=3, ERH n=3). **(iv)** Endpoint Cell Titer Glo 3D viability (mean ± standard deviation, n=1) measurement.